Modeling of packed bed membrane reactors: Impact of oxygen distribution on conversion and selectivity in partial oxidation systems

Samenstelling promotiecommissie:

Prof.dr. T. Reith, voorzitter	Universiteit Twente
Prof.dr.ir. J.A.M. Kuipers, promotor	Universiteit Twente
Prof.dr.ir. G.F. Versteeg, promotor	Universiteit Twente
Dr.ir. M. van Sint Annaland, assistent-promotor	Universiteit Twente
Prof.dr.ir. L.Lefferts	Universiteit Twente
Prof.dr.ir. M.M.C.G. Warmoeskerken	Universiteit Twente
Prof.dr. F. Kapteijn	TU Delft

The research in this thesis was funded by the Netherlands Organisation for Scientific Research (N.W.O.).

U. Kürten

Modeling of packed bed membrane reactors: Impact of oxygen distribution on conversion and selectivity in partial oxidation systems

Thesis, University of Twente, The Netherlands

ISBN 90-365-1891-1

MODELING OF PACKED BED MEMBRANE REACTORS: IMPACT OF OXYGEN DISTRIBUTION ON CONVERSION AND SELECTIVITY IN PARTIAL OXIDATION SYSTEMS

PROEFSCHRIFT

ter verkrijging van
de graad van doctor aan de Universiteit Twente,
op gezag van de rector magnificus,
prof.dr. F.A. van Vught,
volgens besluit van het College voor Promoties
in het openbaar te verdedigen
op vrijdag 25 april 2003 te 16.45 uur

door

Ulrich Kürten
geboren op 12 maart 1970
te Mannheim (Duitsland)

Dit proefschrift is goedgekeurd door de promotoren

Prof.dr.ir. J.A.M. Kuipers

en

Prof.dr.ir. G.F. Versteeg

en de assistent-promotor

Dr.ir. M. van Sint Annaland

Contents

1 General introduction

In heterogeneously catalyzed partial oxidation systems where the reaction order in oxygen for the formation of the target product is lower than the reaction order in oxygen for the formation of waste products, low oxygen concentrations can significantly enhance the product selectivity. A decrease in the oxygen concentration is beneficial for the product selectivity for both consecutive and parallel reaction schemes. If the main by-product is formed via a consecutive reaction, the reactor must possess low back-mixing characteristics in order to limit the product losses. A packed bed membrane reactor (PBMR) combines the features of distributive oxygen feeding and low axial back-mixing of a packed bed reactor. For a parallel reaction scheme high conversions can be achieved with low oxygen concentrations without the application of membranes and without loss of selectivity in a well-mixed reactor (e.g. fluidized bed). Therefore, in the evaluation of the benefits and disadvantages of distributive oxygen feeding the following reaction scheme of the partial oxidation of a hydrocarbon is studied in this thesis:

target product formation: $A + \nu_1 O_2 \rightarrow P$ $\quad r_1 = k_1 c_A c^n$

waste product formation: $P + \nu_2 O_2 \rightarrow W$ $\quad r_2 = k_2 c_P c^m$

where A represents the hydrocarbon reactant, P the target product, W the waste product and ν_i the stoichiometric constants and k_i the reaction rate constants. The reaction rates of both reactions have been assumed first order in the hydrocarbons. The reaction orders of oxygen for the target product formation and for the waste product formation are indicated with n and m, respectively.

In the PBMR air or oxygen permeates through the membrane due to pressure or concentration gradients. From the membrane surface the oxygen penetrates into the packed bed perpendicular to the main flow direction of the reaction mixture, and radial concentrations profiles may emerge. These concentrations profiles can effect the performance of the PBMR.
In addition, intraparticle transport limitations can play an important role, since often in these reactors porous catalysts are employed. However, the standard approach of effectiveness factors cannot be applied for this special type of reaction system. Due to the fact that oxygen is consumed in both reactions the particle effectiveness factors of the main and consecutive reactions are correlated (for m>0). Thus, even if the consecutive reaction rate is small, the effectiveness of that reaction can be reduced by the consumption of oxygen by the primary reaction. The consecutive reaction could even be stronger effected by oxygen concentration gradients than the primary reaction due to the higher reaction order in oxygen (m>n). While in usual consecutive reactions of the type A→B→C the selectivity of the intermediate product is negatively effected by intraparticle mass transport limitations, the reaction systems

discussed in this theses show a selectivity improvement, if the oxygen concentration is small compared to the concentrations of the hydrocarbons, as is the situation in the PBMR.

The main objective of this thesis is to elucidate the effects of the oxygen distribution in PBMR's, particularly

- the axial distribution over the reactor length,
- the radial distribution from the membrane wall towards the center of the packed bed and
- intraparticle concentration gradients.

In this thesis the focus is on the effect of the oxygen distribution on the performance of the PBMR in terms of conversion and selectivities. A detailed description of the oxygen transport through the membrane is not considered in this work. Here, the membrane is considered as an ideal distributor with a fixed membrane flow, independent from the reaction conditions inside the packed bed. This assumption enables an independent discussion of the influence of the oxygen distribution on the performance of the PBMR.

In Chapter 2 a literature study is presented with two main objectives. Firstly, industrially relevant partial oxidation systems and oxidative dehydrogenations are screened, whether they could benefit from distributive oxygen feeding. Secondly, a short literature overview on experimental and modeling studies on packed bed membrane reactors is presented focusing on the incentives to study the application of PBMRs and on the type of models used to describe these reactors.

In Chapters 3 to 6, the different issues of oxygen transport are discussed based on the model reaction system presented above. In Chapter 3 the influence of the shape of the axial oxygen concentration profile on the integral reactor performance will be studied. Firstly, the yield of an idealized PBMR with an axially constant oxygen concentration will be compared with the optimum yield of fixed bed reactors (FBRs) to demonstrate the potential of PBMRs. Furthermore, the effect of different oxygen distribution patterns, including the ratio of premixed and distributive feeding and axially constant vs. linearly or exponentially decreasing membrane fluxes, will be investigated.
Chapter 4 is devoted to intrinsic effects of oxygen concentration profiles caused by mass transport limitations either in a particle or a slab of the PBMR on the conversion rate and on the product selectivity. In this chapter, the oxygen concentration is assumed to be small compared to those of the hydrocarbons, thus ignoring a possible effect of hydrocarbon concentration profiles.

In Chapter 5 the effect of intraparticle mass transfer limitations on the integral reactant conversion and selectivity of the intermediate product in a PBMR will be investigated with a one-dimensional, heterogeneous reactor model. Two opposing effects will influence the

integral selectivity of the target product. If the oxygen concentration is low, the intrinsic selectivity increases with particle size. However, due to the decreased particle effectiveness factors the oxygen concentration downstream in the PBMR increases, resulting in a selectivity loss. The extent of these effects will be quantified.

In Chapter 6 a two-dimensional, pseudo-homogeneous model will be presented to describe the radial and axial concentration and temperature profiles in the PBMR, including the 2-D velocity field induced by the distributive membrane flow and a radial porosity profile. The effects of mass transfer limitations from the membrane wall to the center of the bed on the integral performance of the PBMR will be investigated in detail, including the effect of hydrocarbon concentration profiles, that were ignored in Chapter 4.

In Chapter 7 the different effects of the distribution of oxygen in packed bed membrane reactors (PBMR) will be studied for three industrially relevant reaction systems, namely the oxidative formation of propene and ethene from propane, the oxidative dehydrogenation (ODH) of ethylbenzene to styrene and the ODH of methanol to formaldehyde. The potentials of distributive feeding of oxygen for the improvement of selectivity or yield of these processes will be explored, and possible effects of mass transfer limitations are evaluated. Two additional benefits of the PBMR, namely that the hot-spot temperature can be reduced by the distribution of oxygen and the possibility to operate the PBMR with overall feed compositions within the flammability limits will be studied for the ODH of ethylbenzene and for the ODH of methanol respectively.

2 Literature survey: short-listing of possibly interesting applications of distributive oxygen feeding and inventory of experimental and modeling studies on packed bed membrane reactors

Abstract

In this chapter industrially relevant partial oxidation systems have been shortly described in order to investigate which partial oxidation systems can benefit from distributive oxygen feeding. ODH of methanol to formaldehyde, ethylbenzene to styrene and propane to propene have been identified as attractive for further investigation of the concept of distributed oxygen addition.

Secondly, a short literature overview on experimental and modeling studies on packed bed membrane reactors has been presented focusing on the incentives to study the application of PBMRs and on the type of models used to describe these reactors.

2.1 Introduction

In partial oxidation systems the target product is an intermediate. The thermodynamic stable product is carbon dioxide. With increasing conversion - and concentration of the intermediate product - the driving force for total combustion grows. Therefore, in the field of catalysis one is usually trying to develop catalysts that activate the desired reaction already at lower temperatures.

An alternative method to improve the yield of the target product is to operate at an oxygen concentration as low as possible, provided that the rate of the total combustion reactions – that have a higher consumption of oxygen – have a higher order in oxygen (m) than the partial oxidation reactions (n).

$$C_aH_b \xrightarrow[+0.5\,O_2]{r_1 \sim [O_2]^n} C_aH_bO \xrightarrow[-(b/2)H_2O]{r_2 \sim [O_2]^m} a\,CO_2 \qquad \text{oxygenate formation}$$

or

$$C_aH_b \xrightarrow[-H_2O]{r_1 \sim [O_2]^n} C_aH_{b-2} \xrightarrow[-(b/2-1)H_2O]{r_2 \sim [O_2]^m} a\,CO_2 \qquad \text{oxidative dehydrogenation}$$

In these reaction systems a decrease in the oxygen concentration leads to improved selectivity of the intermediate. Yet, distributive addition of oxygen is required, because the yield is limited due to the total conversion of co-fed oxygen.

In this chapter, firstly, partial oxidation reaction systems are investigated that could possibly benefit from distributive oxygen feeding. Secondly, a short literature overview on experimental and modeling studies on packed bed membrane reactors is presented. The

incentives to study the application of PBMRs are outlined, and the type of models used to describe these reactors.

2.2 Applicability of controlled oxygen feeding in partial oxidation systems

Two main fields of application for the concept of distributive oxygen feeding can be distinguished. Firstly, the improvement of existing partial oxidation processes and secondly substitution for dehydrogenation processes. The conceptual advantage of oxidative dehydrogenation (ODH) is the absence of thermodynamic limitations.

In 'Ullmann's encyclopedia of industrial chemistry' (1996) a series of industrial oxidation processes is listed, of which the following concern gas-phase oxidation of hydrocarbons:

- Ethylene epoxidation ($6 \cdot 10^6$ t/a),
- Partial oxidation of benzene or butane to maleic anhydride ($2 \cdot 10^5$ t/a; $3 \cdot 10^5$ t/a),
- Partial oxidation of naphthalene or o-xylene to phthalic anhydride ($2 \cdot 10^5$ t/a; $2.5 \cdot 10^6$ t/a),
- Two-stage partial oxidation of propylene via acrolein to acrylic acid (10^6 t/a),
- Oxidative dehydrogenation of methanol to formaldehyde ($4 \cdot 10^6$ t/a),
- Oxidative dehydrogenation of ethanol to acetaldehyde (10^5 t/a; $2 \cdot 10^6$ t/a by liquid phase oxidation),
- Oxidative dehydrogenation of butane to butadiene (minor importance),
- Oxidative esterification of acetic acid and ethylene to vinyl acetate ($2 \cdot 10^6$ t/a).

In the literature oxidative dehydrogenation was also studied for ethane, propane, and ethylbenzene. In the following it will be investigated whether the product yield in these reaction systems can be enhanced using the concept of distributive oxygen feeding.

2.2.1 Ethylene epoxidation

Ethylene oxide (EO) is mainly used as intermediate for ethylene glycol (polyester and antifreezes) and surfactants, and is produced by oxidation of ethylene on silver based catalysts (Ullmann's, 1996).

The reaction scheme of the ethylene epoxidation is mainly parallel with a minor contribution of consecutive combustion (Al-Juaied, 2001).

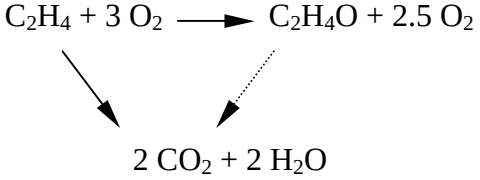

In a series of articles Varma and co-workers showed that actually high oxygen concentrations improve the EO selectivity over a cesium-doped silver catalyst (Lafarga, 2000). The EO

selectivity can be further increased in a membrane reactor under distributive addition of the ethylene to the packed bed reactor via membranes (Pena, 1998; Al-Juaied, 2001).

2.2.2 Formation of anhydrides

2.2.2.1 Partial oxidation of butane to maleic anhydride

Maleic anhydride (MA) is an intermediate for polyester and alkyd resins (fiberglass reinforced plastics), lacquers, plasticizers, copolymers (with styrene for engineering plastics, with acrylic acid in the detergent industry), and lubricants (Ullmann's, 1996). It is produced industrially by catalytic oxidation of benzene or butane. Yields of 40-60 % are realized by the oxidation of butane. A usual gas composition is 1.5 % butane in air, which indicates the enormous excess of oxygen that is applied in this process.

The MA formation from n-butane is represented in a general, parallel-consecutive scheme as follows:

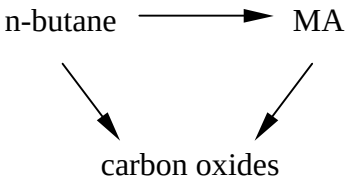

n-butane: C_4H_{10}

MA: $C_4H_2O_3$ 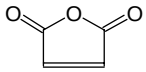

Menéndez, Santamaría and co-workers (Mallada et al., 2000; Pedernera et al., 2000) published a series of articles on this reaction system using a VPO-catalyst. They used typically a gas composition of 10 % butane in air and obtained up to 20 % yield in maleic anhydride. A dual-site Mars-van Krevelen mechanism was proposed (Pedernera et al., 2000), where the selective sites produce MA and nonselective sites carbon oxides. The MA formation showed a higher order in oxygen than the combustion reaction. The catalyst becomes more selective with increasing oxygen concentration, or in other words – the catalyst used is selective only in its oxidized state, which corresponds with the general statement in Ullmann (G. Franz and R.A. Sheldon):

'*Mixed oxide catalysts are only catalytically active and selective in their higher oxidation state. Unlike the noble metal catalysts they must be used in an excess of oxygen, i.e. in an oxidizing atmosphere.*'

This can also be interpreted as a directive for research groups in the field of catalysis to develop new catalysts that are stable and active at low oxygen concentrations.

2.2.2.2 Oxidation of o-xylene to phthalic anhydride

Phthalic anhydride (PA) is used mainly in the production of plasticizers and resins (unsaturated polyester resins and alkyd resins). On industrial scale it is mainly produced by gas-phase oxidation of o-xylene or naphthalene (Ullmann's, 1996).

The formation of PA from o-xylene over a V_2O_5-TiO_2 catalyst can be described by a parallel reaction scheme (Chandrasekharan, 1979; Papageorgiou, 1994), the consecutive combustion is insignificant:

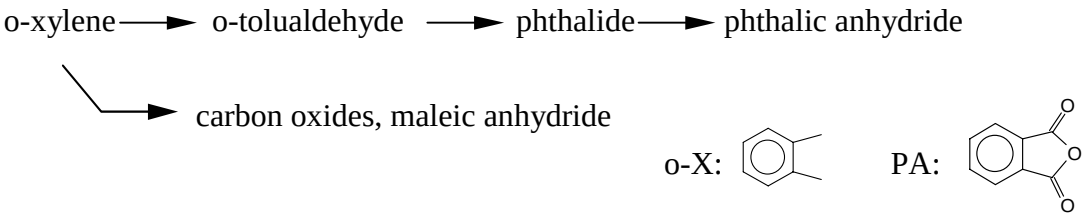

According to Papageorgiou et al. (1994) the selectivity for combustion products (CO_x and MA) is independent of the composition of the reaction mixture. However, the formation of tolualdehyde has a higher reaction order in oxygen, so that with increasing oxygen the selectivity of this intermediate increases, as well as the activity of the catalyst. At low and medium conversions a decrease of the oxygen concentrations improves the selectivity of phthalic anhydride.

In a later modeling paper Papageorgiou et al. (1996) showed that by intermediate addition of oxygen the PA selectivity is increased by about 4 % with respect to the premixed multi-tubular reactor (71 % selectivity at 99 % o-X conversion). The improvements are partially due to the reduced oxygen level in the reactor and partially due to the reduction of the temperature rise.

However, polymeric by-products can be formed at low conversion, when the surface is not highly oxidized (Bond, 1997).

2.2.3 Olefins to unsaturated aldehydes

2.2.3.1 Propylene to acrolein

The main use of acrolein is the production of D,L-methionine, an essential amino acid used as an animal feed supplement. Acrylic acid is another commercially important product derived from acrolein. It is used to make acrylates (Ullmann's, 1996).

Acrolein is produced on a large commercial scale by heterogeneously catalyzed gas-phase oxidation of propene. Modern commercial catalysts for this reaction system are multicomponent metal oxide systems (MoBiFe oxides with traces of Co, Ni, P, W, K and/or Si). The catalysts operate by a catalyst-reduction cycle (selective product formation), and a catalyst-reoxidation cycle (lattice-oxygen regeneration). Propene (5–10 vol.%) is mixed with air and steam in a molar ratio of approximately 1:8:(2–6) (Ullmann's, 1996).

The reactor is usually operated at 300–400°C and inlet pressures of 150–250 kPa. The conversion rate of propene is approximately 95 % so that there is no need to recover and recycle unreacted propene. The acrolein yield using commercial catalysts is approximately 80 %, with acrylic acid yields of 5–10 %.

Generally, the motivation to apply distributive oxygen addition is to improve the single pass yield of the product and thereby reduce the separation costs. Concluding, for this process the product selectivity is important and not the product yield, rendering distributive oxygen feeding uninteresting.

2.2.3.2 Isobutene to methacrolein

Methacrolein is an intermediate in one of the processes for the production of methyl methacrylate.

Catalysts for the oxidation of i-butene are multicomponent metal oxide systems similar to those used to produce acrolein. However, the product yields are generally somewhat lower than for acrolein. Yields of 75–85 % methacrolein and 1–5 % methacrylic acid for 90–98 % conversions in short-time laboratory experiments have been reported. For high selectivity, the methacrolein process generally requires a stronger dilution of the feed gas with steam or inert gas than is needed for propene oxidation. Impurities, such as butadiene, often oligomerize on the oxidation catalyst causing serious deterioration of its activity (Ullmann's, 1996).

The same conclusions as for the production of acrolein hold for the production of methacrolein.

2.2.4 Oxidative dehydrogenation of alcohols to aldehydes

2.2.4.1 Methanol to formaldehyde

Formaldehyde is one of the most versatile chemicals and is employed by the chemical and other industries to produce a virtually unlimited number of indispensable products used in daily life. It is irreplaceable as a C1 building block and as an intermediate in the manufacture of e.g. polyurethane and polyester plastics, resins, resin coatings, dyes, tanning agents, dispersion and plastics precursors, and so on (Ullmann's, 1996).

Formaldehyde is produced by partial oxidation of methanol either catalyzed by MoO_3/Fe_2O_3 (250-400°C) at excess of oxygen, or by silver (600-720°C) under oxygen deficiency.

Although, the Ag-catalyst seems more attractive to test the concept of distributive oxygen addition, Varma and co-workers (Diakov, 2001) chose the mixed oxide catalyst for an experimental study of the ODH of methanol in a membrane reactor. In commercial processes low methanol concentrations (and thus excess of oxygen) are selected in order to avoid flammable mixtures.

The authors found that high methanol concentration and low oxygen concentrations are favorable for the formaldehyde selectivity at a fixed conversion of 90 %. Consequently, the reactor performance improved in a membrane reactor with distributed oxygen addition compared to the (premixed) fixed bed reactor.

2.2.4.2 Ethanol to acetaldehyde

Acetaldehyde is an important intermediate in the production of acetic acid, acetic anhydride, ethyl acetate, butanol, and other chemicals.

Acetaldehyde is mainly produced by oxidation of ethylene, and to a smaller amount by oxidation of ethanol in a liquid phase process or in a silver catalyzed (450-550°C) gas phase process under oxygen deficiency.

In the production of acetaldehyde, the separation costs are not an important issue as far as the Veba-Chemie process is concerned. Here, the acetaldehyde and alcohol (50-70 % conversion, >97 % selectivity) are separated from the product mixture by washing with cold alcohol (Ullmann's, 1996). Again, the product selectivity is the key factor, not the product yield.

2.2.5 Oxidative dehydrogenation of alkanes to olefins

2.2.5.1 ODH of ethane and propane

Ethene is produced mainly by thermal cracking of hydrocarbons in the presence of steam, and by recovery from refinery cracked gas, and propene is produced almost entirely as a byproduct because it is obtained in sufficient amounts in ethylene production by steam cracking and in some refinery processes. Polyethylene (1993: 56 %; 7 % was used for ethylbenzene.) and polypropylene are the largest consumer of ethene and propene respectively (Ullmann's, 1996).

Predictions of increasing demands for propene were driving intensive research activities in the field of ODHP. A countless number of catalysts was tested for ODHE and especially ODHP. A common problem of all the tested catalysts was the strong decrease in the selectivity at high conversions. As an example the V/MgO catalysts, widely investigated by Kung (see e.g. Kung and Kung, 1997 or Kung, 1994), is mentioned here. The propene selectivity decreases from 70-80 % at low conversions to about 20–30 % at 50 % conversion. The reaction mechanism is still under discussion. Creaser et al. (2000) tested several Mars-van Krevelen models with dual CO_x production paths with better results than a simple redox model with one type of surface oxygen for CO_X formation. Hou et al. (2001), however, present a single-site Mars-van Krevelen model.

In a review paper Cavani and Trifirò (1995a) compared the performances of different catalysts showing a maximum ethene yield of about 50 % and a maximum propene yield of just above 30 %.

Landau *et al.* (1996) investigated the production of mixed olefins from LPG over rare earth-alkali-halogen catalysts. The propene yield is comparable to the maximum propene yield found for the oxidative propane dehydrogenation over Mg-V-O catalyst, however ethene is formed to a large extent over rare earth-alkali-halogen catalysts. Olefin yields of about 50 % were obtained. According to Buyevskaya et al. (2000) the same olefin yield is obtained from pure propane at a maximum contribution of propene of 17 %.

Leveles (2002) investigated this catalyst group. His kinetic investigation on a halogen free catalyst indicates the benefit of distributive feeding of oxygen, showing low orders in the oxygen concentration for the formation of ethene and propene and higher orders for the formation of carbon oxides (see also Chapter 7 of this thesis).

2.2.5.2 ODH of ethylbenzene to styrene

Styrene monomer is used as a feedstock in a variety of polymer products: thermoplastics, elastomers, dispersions, and thermoset plastics. Approximately 65 % of the styrene produced is used for the production of polystyrene (Ullmann's, 1996). World capacity for styrene was about $17 \cdot 10^6$ t in 1993, of which 85 % was produced by direct dehydrogenation of ethylbenzene in the presence of steam. Commercial units operate at typical conversion levels of 50–70 wt.%, with process yields of 88–95 mol %. The reaction temperature ranges in commercial processes from 540 to 650°C with a steam-to-hydrocarbon ratio from 4 to 20 (Cavani and Trifirò, 1995b).

In a review paper Cavani and Trifirò (1995b) discuss alternative processes for the styrene production with integrated hydrogen combustion (parallel or in series) or oxidative dehydrogenation. The commercial SMART process is based on intermediate hydrogen combustion. By this equilibrium shift a single-pass conversion of 80 % can be reached in three reactors (oxygen addition before the second and third reactor, both containing oxidation catalyst in a first layer with dehydrogenation catalyst in series). For the selectivity values between 90 and 95 % have been reported.

For the oxidative dehydrogenation of ethylbenzene to styrene the investigated oxide catalysts are only the 'carrier' of the active component. The actual catalyst is the 'active coke', which is formed in the first hours of reaction reaching a stationary amount on the surface (Cavani and Trifirò, 1995b). Due to the conversion of oxygen the conversions on these catalysts are usually not higher than 70 %.

Shakhnovich et al. (1984) investigated the kinetics of the ODH of ethylbenzene on a zinc oxide modified vanadia/magnesia catalyst in the presence of steam. They investigated the catalyst in steady state after the initial coke formation. The following parallel-consecutive scheme is presented:

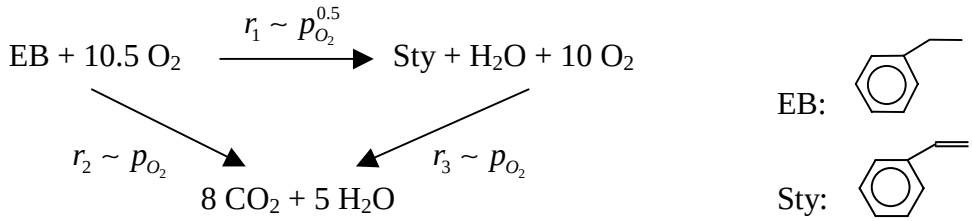

Because both combustion reactions show a higher order in oxygen than the styrene formation, a low oxygen concentration improves the selectivity of the target product.

2.2.6 Vinyl acetate

Vinyl acetate is used mainly for the production of polymers and copolymers, e.g., for paints (mainly dispersions), adhesives, textile and paper processing, chewing gum, and for the production of poly(vinyl alcohol) and polyvinylbutyral (Ullmann's, 1996). The commercial catalyzed gas phase process operates at temperatures between 150 and 250°C at pressures up to 10 bar. Due to oxygen deficiency in the reactor feed the conversions are limited to 10 % for ethylene and 25 % for acetic acid.

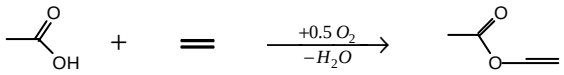

More specific information was not available in the open literature for this reaction system.

2.2.7 Discussion and conclusions

Remarkably, only a few industrially relevant partial oxidation systems can benefit from distributive oxygen feeding. From the investigated partial oxidation systems only the ODH of methanol to formaldehyde, ethylbenzene to styrene and of propane to propene are attractive for further investigation of the concept of distributed oxygen addition. In all these cases the new concept has to compete with industrial processes that can already realize high product selectivities at high conversions. However, small improvements in the product yield are still very important due to the very large scale of production.

2.3 PBMR-literature

Membrane reactors are widely investigated in literature either for the in-situ removal of one of the reaction products, for example hydrogen to shift the equilibrium of a dehydrogenation reaction, or the distributive addition of one of the reactants, in most cases oxygen. For a general review on high-temperature membrane reactors the interested reader is referred to the book of Hsieh (1996) and the article of Saracco et al. (1999). In this chapter the literature review is restricted to packed bed membrane reactor (PBMR) studies for the distributive addition of oxygen in partial oxidation systems. Published experimental and modeling studies will be classified according to the incentives of the authors to study the application of packed bed membrane reactors.

2.3.1 Pros and contras of PBMR

Four main advantages are driving the investigation of PBMRs as an alternative reactor for partial oxidation systems.

1. Separation costs

Application of oxygen selective membranes can reduce the costs for the separation of nitrogen either before or after the reactor. In-situ application of membrane separation is more cost effective, because firstly the driving force for the transmembrane transport is

higher and secondly because the oxygen selective membranes require - up to now – very high operating temperatures to achieve acceptable permeabilities. In this context synthesis gas formation from methane is the major research field.

2. Reactor safety and controllability

Temperature control is an important issue for the reactor design. Partial oxidation reactions are often operated in wall-cooled tubular reactors, where the tube diameter is determined by the maximum allowed temperature rise. This temperature rise is sensitive to changes in the reactant concentrations or cooling temperature, causing packed bed tubular reactors to have a tendency to show run-away behavior when the reactions accelerate uncontrollably resulting in fast total consumption of the reactants. By staged or distributive addition of oxygen to the reaction zone run-away behavior is avoided by the early consumption of oxygen, which is present only in a low concentration. The PBMR therefore shows more stable reactor behavior and is less sensitive to changes of the process parameters. On the other hand, breakage of the membranes should be carefully considered as a possible safety risk.

3. Wider operating range resulting in higher productivities

a) If the reaction rates depend on the oxygen concentration, distributive addition of oxygen results in a better distribution of the reactivity over the length of the packed bed. The temperature rise is reduced compared with the FBR of the same tube size. The PBMR has a higher degree of freedom concerning the choice of the reactor temperature. The cooling temperature can be increased, without the risk of a runaway, which improves the productivity of the reactor.

b) Furthermore, partial oxidation reaction mixtures often show a high degree of dilution, that is required both to avoid explosive (or flammable) mixtures and to reduce the temperature rise. In a PBMR an exit product gas composition can be achieved, that would fall within the explosion limits, if all the reactants would have been added premixed to the packed bed.

4. Improved product selectivity

a) If the product selectivity is temperature sensitive, selectivity improvements can be expected from the application of PBMR, because the reactor can overall be operated closer to the optimal reaction temperature due to the smaller temperature gradients compared to the FBR.

b) If the reaction order in oxygen is smaller for the desired primary reaction than for undesired consecutive (or parallel) reactions, a low oxygen concentration is favorable for the selectivity of the target product. Via continuous axial feeding of oxygen via a membrane to the packed bed high reactant conversions can be realized while keeping the oxygen concentration small. Alternatively, a series of FBR with intermediate oxygen feeding can be applied, or a series a PBMR with membrane flows of different magnitude as suggested by Thomas and Seidel-Morgenstern (2002).

On the other hand, the use of membranes can bring some disadvantages, which are shortly outlined below:

A. Counter-diffusion

Counter-diffusion of the hydrocarbons can occurs in non-selective, porous membranes, and depends on the relative magnitude of the reverse, diffusive (molecular or Knudsen) flow driven by the concentration gradients of the hydrocarbons compared to the viscous flow driven by the pressure gradient over the membrane. Next to product losses, counter-diffusion could bring about the formation of an explosive mixture on the oxygen-rich side of the membrane.

B. Reactivity of the membrane

Unwanted reactions catalyzed by the membrane could result in additional product losses. For this reason membranes with good permeability properties can often not be applied, as for example selective membranes from metal silver or dense ceramic membranes (see Lu et al., 2000), which are good combustion catalyst, or membranes from sintered stainless steel, which have good processing properties, but also catalyze combustion at high temperatures.

C. Investment costs

The application of membranes on industrial scale will increase the investment costs for the reactor, especially in combination with a possible heat removal problem. Multi-tubular reactors are required for highly exothermic partial oxidation systems, which are very cost intensive, even without the membranes. However, if the distributive addition of oxygen has a strong effect on the maximal local heat production, a less cost intensive reactor type can be chosen, reducing the investment costs somewhat.

Finally, the reduced oxygen concentration level can result in a reduction of the catalyst activity, and thus increase the reactor size.

The systematic investigation of selectivity improvements in PBMR is the main objective of this thesis, in particular the effect of the quality of the distribution of oxygen on the realized selectivity improvement. Most literature in the field of PBMRs for selectivity improvements in partial oxidation reactions has been published by the universities of Zaragoza in Spain (Coronas, Menéndez, Santamaría, et al.) and Notre Dame in the USA (Varma, Lafarga, Al-Juaied, Diakov et al.).

2.3.2 Experimental PBMR studies

Some of the literature of experimental studies on PBMRs in this field are short-listed in Table 1. Next to the authors and the reaction system and catalyst investigated, the main incentive of the authors to study PBMRs is given in the third column according to the classification presented in the previous section.

A repeated problem of the experimental studies is that FBR and PBMR experiments are executed in the same setup with the same range of contact times. However, the reduced

oxygen level in the PBMR results in a reduced activity, such that the product selectivities are improved, but the gain in product yield is small. For some systems, as the ODHP on V/MgO, the realized improved product yield is still far away from the economical requirement. The question arises, whether a further improvement is possible for higher contact times and lower oxygen concentrations. One possible reason why it was not tried to clarify this point is, that for a larger reactor a membrane with an even smaller permeation flow is required, which is difficult to create with the used porous membranes. The trans-membrane pressure drop should not be decreased too far, in order to prevent counter-diffusion. Therefore, membranes with different permeability properties are required.

Table 1 Experimental studies.

reference	*Reaction system; catalyst*	*incentives*	*results*
Veldsink et al., 1992		2	Better controllability, greater protection with respect to thermal runaway
Lafarga et al., 1994	OCM;	4	Commercial α-alumina microfiltration membrane. Permeability reduced by depositing silica in the porous alumina structure, impregnation with Li_2CO_3 solution to reduce acidity. Sealing between tube and shell by means of graphite gaskets. Description of the effect of the deposit on the membrane permeability.
Coronas et al, 1994	OCM; Li/MgO	4	Further development of the membrane modification by silica sol described in Lafarga et al. (1994) by creating four membrane sections with different amounts of deposit. Thus, a pattern of decreasing permeability was created in the direction of flow along the membrane length giving rise to an important increase in the conversion of methane and selectivity of ethene at a given concentration. Max. yield of 23 %.
Coronas et al, 1995a	OCM; Li/MgO	2	Gradual feeding of oxygen avoids and limits the formation of hot spots, improves the controllability and decreases the chance on a run-away. Additionally, error/failure tolerance of the membrane reactor is higher.
Coronas et al, 1995b	ODHE; Li/MgO	4	Mixed membrane reactor (second half or last quarter of membrane impervious) results in higher selectivities than PBMR; at high conversions better than FBR
Tonkovich et al., 1996 Tonkovich et al., 1995	ODHE; Li/Sm/ MgO	4	The membrane flux is reduced by partial coating of the membrane surface letting only four 1 mm strips free of glaze. The catalyst was packed outside the membrane. Lots of data, but no clear results for high conversions.
Téllez et al., 1997	ODHB; V/MgO	2 4	Higher selectivities than FBR

Ramos et al., 2000	ODHP; 4 V/MgO	Silica modified alumina membrane (preparation method as in Coronas et al., 1994); For the conversion range of 28 - 65 % it was shown that the propene selectivity is increased compared to the co-feed packed bed reactor. The maximum yield of 18 % was realized at 575°C. Alfonso et al. (2000) presented studies on different CMRs, but the propene yield did not exceed 15 %.
Lu et al., 2000	OCM; 2 La/MgO 4	Oxygen selective perovskite membranes; For conversions below 40 % improved selectivities have been reported, however the selectivities for higher conversions are presented only for the conventional co-feed quartz tube reactor. Problems arise because of the combustion activity of the membranes. The maximal yield reported was 16.5 %.
Diakov et al., 2001	ODH of 4 methanol ; Fo-Mo oxide	The catalyst was packed around a porous stainless steel tube. They showed that at a conversion level of 90 % in the packed bed the formaldehyde selectivity increases with decreasing oxygen concentration. Consequently, the selectivities in the PBMR were considerably improved compared to the co-feed PBR.

2.3.3 Model studies of PBMR

In Table 2 the most important contributions on PBMR modeling are listed, where next to the reaction and catalyst system investigated, the type of model used is indicated, along with some keywords on the aspects investigated with the model. As can be concluded from this table, most studies on PBMR reported in the open literature make use of a pseudo-homogeneous, one-dimensional reactor model. This simplification may be justified because in most studies the model is used to describe a laboratory-scale reactor.

For highly exothermic partial oxidation processes with a significant contribution of an undesired consecutive reaction multi-tubular, wall-cooled reactors are used in industrial practice to remove the reaction heat, which are very cost intensive. With decreasing size of the tubular packed beds to increase the heat exchanging area the required number of the tubes and thus the reactor costs increases. Therefore, the diameter of the membrane tubes is a key factor in the design of an industrial scale PBMR, which demands for two-dimensional modeling.

Hou et al. (2001) and Assabumrungrat et al. (2002) used two-dimensional modeling of PBMRs. The 2D-model by Hou et al. (2001) for the ODHP uses a Mars-van Krevelen model to describe the kinetics, with the same dependency on the oxygen concentration for all reactions. Still, propane conversion and propene selectivity decrease as the reactor radius increases (at constant contact time, length-diameter ratio and feed composition). The drawback to be paid for lower cost of membrane, as they put it. They explain the effect with

the radial oxygen concentration profiles, but it is more the combinatorial effect of the oxygen and hydrocarbons concentration profiles.
Assabumrungrat et al. (2002) used a 2D-model of a PBMR for the ODHB, where the catalyst is packed on the shell-side. The authors determined the optimal shell diameter. However, with the increase of the shell diameter, the contact time increases, which complicates the comparison of the results. The calculated optimum reactor size is thus more the result of an optimized catalyst mass, rather than a measure of the quality of the radial oxygen transport.
In both articles by Hou et al. and Assabumrungrat et al., the reactor design is optimized for a given reaction system. However, they do not give a guideline for other developers of PBMR for partial oxidation systems.

Another important issue in packed bed reactor design is the pressure drop, which determines the minimal catalyst size. PBMRs should be operated under low, at times even very low oxygen concentrations, which can result in an increased risk of intra-particle transport limitations, provided that the order of the overall oxygen consumption is below unity.
No reference was found in the open literature in PBMR-modeling that account for intraparticle mass transport limitations and their effect on the reactor performance.

Table 2 Model studies.

reference	*reaction system catalyst*	*incentives*	*Dimension of packed bed Membrane flux*	*Results*
Cheng and Shuai, 1995	OCM; lead oxide	4	Pseudo-homogeneous 1-D; Uniform oxygen flux through membrane;	Despite the title, the model describes a PBMR better. Yield is strongly improved.
Al-Sherehy et al., 1998	ODHE; Mo-V-Nb	2, 4	1-D: heterogeneous or with pellet efficiency accounting for external mass and heat transport; packed-bed reactor with injection points for oxygen.	Effect on the number of injection points on the hot-spot temperature, the runaway behavior and ethene yield (max. 21 % with 200 injection points).
Hou et al., 2001	ODHP; V/MgO	-	Pseudo-homogeneous 2-D with diffusive and convec-tive radial transport; Fixed membrane flow with constant or linear profile.	Propane conversion and propene selectivity decrease as reactor radius increases; Linear increased oxygen flow has negative effect on conversion, but is positive for propene yield .
Al-Juaied et al., 2001	ethylene epoxi-dation; Cs-doped Ag	4	Pseudo-homogeneous 1-D Gas transport through membrane modeled by EFM or DGM.	Comparison of experimental and model results for distributed oxygen and distributed ethylene (n>m); Model deviations particularly at low oxygen / ethylene ratios.

M. Alonso et al., 2001	Partial oxidation of butane to maleic anhydride; VPO	3, 4	Pseudo-homogeneous 1-D; Fixed membrane flow with constant profile.	Fluidized-bed cooled membrane reactor; Wider operating range with respect to temperature and inlet gas composition, thus higher product rates. Reduced hotspot temperature has secondary effect on the reactor performance. Intrinsic MA selectivity increases with temperature, but catalyst stability limits process temperature. Reactor can be operated closer to maximum temperature, if hot spot temperature is lower; higher productivity and MA selectivity.
Assaburngrat et al., 2002	ODHB; V/MgO	4	Pseudo-homogeneous 2-D; "Membralox" membrane with Knudsen and viscous flow.	Reduced hot spot temperature in PBMR; optimal Air/n-butane ratio for FBR and PBMR; PBMR better at high ratios.
Diakov et al., 2002ab	ODHM; Fe-Mo-O	2, 4	Pseudo-homogeneous 1-D; Fixed membrane flow with constant profile.	a: Improved reactor stability in PBMR; b: Improved selectivity.
Thomas and Seidel-Morgenstern, 2002	Power law kinetics	4	Pseudo-homogeneous 1-D; Series of PBMR with different, but each axially constant membrane fluxes	Optimization of the oxygen distribution pattern

2.3.4 Summary and conclusions

Most models used in literature to describe PBMRs are 1D-pseudo-homogeneous models. In order to describe industrial scale PBMRs 2D-models need to be developed in order to investigate the effect of the quality of the oxygen distribution on the overall reactor performance. Especially the effect of radial oxygen concentration profiles from the membrane surface to the core of the packed bed and the effect on intraparticle concentration profiles on the intrinsic and overall product yield need to be investigated, which are the main topics of the next chapters of this thesis.

NOTATION

CMR catalytic membrane reactor

DGM dusty gas model

EB ethylbenzene

EFM extended Fick model

FBR fixed bed reactor
EO ethylene oxide
MA maleic anhydride
m reaction order in oxygen of reaction forming the waste product
n reaction order in oxygen of reaction forming the target product
OCM oxidative coupling of methane
ODH oxidative dehydrogenation of methanol (M), ethane (E), propane (P), butane (B) or ethylbenzene (EB)
o-X o-xylene
PA phthalic anhydride
PBMR packed bed membrane reactor
p_i partial pressure of component i [bar]
r_i rate of reaction i [mol / m^3 s]
Sty styrene

References

M.J. Alfonso, A. Julbe, D. Farrusseng, M. Menéndez, J. Santamaría, 1999, Oxidative dehydrogenation of propane on V/Al_2O_3 catalytic membranes. Effect of the type of membrane and reactant feed configuration, *Chemical Engineering Science 54*, 1265-1272

M.J. Alfonso, M. Menéndez, J. Santamaría, 2000, Vanadium-based catalytic membrane reactors for the oxidative dehydrogenation of propane, *Catalysis Today 56*, 247-252

M. Alonso, M.J. Lorences, M.P. Pina, G.S. Patience, 2001, Butane partial oxidation in an externally fluidized bed-membrane reactor, *Catalysis Today 67*, 151-157

F.A. Al-Sherehy, A.M. Adris, M.A. Soliman and R. Hughes, 1998, Avoidance of flammability and temperature runaway during oxidative dehydrogenation using a distributed feed, *Chemical Engineering Science 53*, 3965-3976

M.A. Al-Juaied, D. Lafarga, A. Varma, 2001, Ethylene epoxidation in a catalytic packed-bed membrane reactor: experiments and model, *Chemical Engineering Science 56*, 395-402

S. Assabumrungrat, T. Rienchalanusarn, P. Praserthdam, S. Goto, 2002, Theoretical study of the application of porous membrane reactor to oxidative dehydrogenation of n-butane, *Chem. Eng. Journal 85*, 69-79

G.C. Bond, 1997, What limits the selectivity attainable in the catalysed oxidation of o-xylene to phthalic anhydride, *Journal of Chemical Technology and Biotechnology 68*, 6-13

O.V. Buyevskaya, D. Wolf, M. Baerns, 2000, Ethylene and propene by oxidative dehydrogenation of ethane and propane 'Performance of rare-earth oxide based catalysts and development of redox-type catalytic materials by combinatorial methods', *Catalysis today 62*, 01-99

K. Chandrasekharan, P.H. Calderbank, 1978, Prediction of packed-bed catalytic reactor performance for a complex reaction (oxidation of o-xylene to phthalic anhydride*), Chemical Engineering Science 34*, 1323-1331

F. Cavani, F. Trifirò, 1995a, The oxidative dehydrogenation of ethane and propane as an alternative way for the production of light olefins, *Catalysis Today 24*, 307-313

F. Cavani, F. Trifirò, 1995b, Review Alternative processes for the production of styrene, *Applied Catalysis A 133*, 219-239

S. Cheng, X. Shuai, 1995, Simulation of a catalytic membrane reactor for oxidative coupling of methane, *AIChE journal 41*, 1598-1601

J. Coronas, M. Menéndez, J. Santamaría, 1994, Development of ceramic membrane reactors with a non-uniform permeation pattern. Application to methane oxidative coupling, *Chemical Engineering Science 49*, 4749-4757

J. Coronas, M. Menéndez, J. Santamaría, 1995a, The porous-wall ceramic membrane reactor: inherently safer contacting device for gas-phase oxidation of hydrocarbons, *J. Loss Prev. Process Ind. 8*, 97-101

J. Coronas, M. Menéndez, J. Santamaría, 1995b, Use of a ceramic membrane reactor for the oxidative dehydrogenation of ethane to ethylene and higher hydrocarbons, *Ind. Eng. Chem. Res. 34*, 4229-4234

J. Coronas, J. Santamaría, 1999, Catalytic reactors based on porous ceramic membranes, *Catalysis Today 51*, 377-389

D.C. Creaser, B. Andersson, R.R. Hudgins, P.L. Silveston, 2000, Kinetic modeling of oxygen dependence in oxidative dehydrogenation of propane, *The Canadian Journal of Chemical Engineering 78,*182-193

V. Diakov, D. Larfarga, A. Varma, 2001, Methanol oxidative dehydrogenation in a catalytic packed-bed membrane reactor, *Catalysis Today* 67, 159 - 167

V. Diakov, A. Varma, 2002a, Reactant distribution by inert membrane enhances packed-bed reactor stability, *Chem. Eng. Sci.* 57, 1099 - 1105

V. Diakov, B. Blackwell, A. Varma, 2002b, Methanol oxidative dehydrogenation in a catalytic packed-bed membrane reactor: experiments and model, *Chem. Eng. Sci.* 57, 1563 - 1569

G. Franz, R.A. Sheldon, Oxidation – Heterolytic Oxidation in W. Gerhartz, Y. S. Yamamoto, F. T. Campbell, R. Pfefferkorn, J. F. Rounsaville, 1985-1996, Ullmann's encyclopedia of industrial chemistry, VHC, Weinheim

K. Hou, R. Hughes, R. Ramos, M. Menéndez, J. Santamaría, 2001, Simulation of a membrane reactor for oxidative dehydrogenation of propane, incorporating radial concentration and temperature profiles, *Chemical Engineering Science 56*, 57-67

H.P. Hsieh, 1996, Inorganic membranes for separation and reaction, Elsevier, Amsterdam

A. Julbe, D. Farrusseng, C. Guizard, 2001, Porous ceramic membranes for catalytic reactors – overview and new ideas, *Journal of Membrane Science 181*, 3-20

H.H. Kung, 1994, Oxidative dehydrogenation of light (C_2 to C_4) alkanes, *Advances in catalysis 40*, 1-37

H.H. Kung, M.C. Kung, 1997, Oxidative dehydrogenation of alkanes over vanadium-magnesium-oxides, *Applied Catalysis A: General 157*, 105-116

D. Lafarga, J. Santamaría, M. Menéndez, 1994, Methane oxidative coupling using porous ceramic membrane reactors – I. reactor development, *Chemical Engineering Science 49*, 2005-2013

D. Lafarga, M. A. Al-Juaied, C.M. Bondy, A. Varma, 2000, Ethylene epoxidation on Ag-Cs/α-Al_2O_3 catalyst: experimental results and strategy for kinetic parameter determination, *Industrial and Engineering Chemistry Research 39*, 2148-2156

Landau, M.V., van den Oosterkamp, P.F., Kaliya, M.L., Bocqué, P.S.G. and Herskowitz, M., 1996, Produce light olefins from parafins by catalytic oxidation, *Chemtech 26*, 24-29

L. Leveles, 2002, 'Oxidative conversion of lower alkanes to olefins', Doctoral Thesis, Twente University, Enschede, the Netherlands

Y. Lu, A.G. Dixon, W.R. Moser, Y.H. Ma, 2000, Oxidative coupling of methane using oxygen-permeable dense membrane reactors, *Catalysis Today 56*, 297-305

R. Mallada , M. Menéndez, J. Santamaría, 2000, Use of membrane reactors for the oxidation of butane to maleic anhydride under high butane concentrations, *Catalysis Today 56*, 191-197

J.N. Papageorgiou, M.C. Abello, G.F. Froment, 1994, Kinetic modeling of the catalytic oxidation of o-xylene over an industrial V_2O_5-TiO_2 (anatase) catalyst, *Applied Catalysis A 120*, 17-43

J.N. Papageorgiou, G.F. Froment, 1996, Phthalic anhydride synthesis, reactor optimization aspects, *Chemical Engineering Science 51*, 2091-2098

M. Pedernera, R. Mallada, M. Menéndez, J. Santamaría, 2000, Simulation of an inert membrane reactor for the synthesis of maleic anhydride, *AIChE Journal 46*, 2489-2498

R. Ramos, M. Menéndez, J. Santamaría, 2000, Oxidative dehydrogenation of propane in an inert membrane reactor, *Catalysis Today 56*, 239-245

M.A. Pena, D.M. Carr, K.L. Yeung, A. Varma, 1998, Ethylene epoxidation in a catalytic packed-bed membrane reactor, *Chemical Engineering Science 53*, 3821-3834

G. Saracco, H.W.J.P. Neomagus, G.F. Versteeg, W.P.M. van Swaaij, 1999, High-temperature membrane reactors: potential and problems, *Chemical Engineering Science 54*, 1997-2017

G.V. Shakhnovich, I.P. Belomestnykh, N.V. Nekrasov, M.M. Kostyukovsky, S.L. Kiperman, 1984, 'Kinetics of ethylbenzene oxidative dehydrogenation to styrene over vanadia/magnesia catalyst', *Applied Catalysis 12*, 23-34

C. Téllez, M. Menéndez, J. Santamaría, 1997, Oxidative dehydrogenation of butane using membrane reactors, *AIChE Journal 43*, 777-784

S. Thomas, A. Seidel-Morgenstern, 2002, Improved performance of parallel-series reactions in fixed-bed and membrane reactors by stagewise reactant dosing, *submitted to ISCRE 17, august 25-28, Hong Kong*

A.L.Y. Tonkovich, R.B. Secker, E.L. Reed, G.L. Roberts, J.L. Cox, 1995, Membrane reactor/separator: a design for bimolecular reactant addition, *Separation Science and technology 30*, 1609-1624

A.L.Y. Tonkovich, J.L. Zilka, D.M. Jimenez, G.L. Roberts, J.L. Cox, 1996, Experimental Investigations of inorganic membrane reactors: a distributed feed approach for partial oxidation reactions, *Chemical Engineering Science 51*, 789-806

W. Gerhartz, Y.S. Yamamoto, F.T. Chambell, R. Pfefferkorn, J.F. Rounsaville, 1985-1996, Ullmann's encyclopedia of industrial chemistry, 5^{th} edition, VHC, Weinheim

3 Axial distribution of oxygen: premixed vs. distributive feeding

Abstract

The optimization of the product yield in partial oxidation systems was investigated through controlling of the axial concentration profile of oxygen. A consecutive reaction scheme with power law kinetics was used showing a higher reaction order (m) in the oxygen concentration for the undesired consecutive reaction compared to the reaction order (n) of the primary reaction. In this reaction system a reduction of the oxygen concentration results an improved product selectivity. By distributive feeding of oxygen, e.g. in a packed bed membrane reactor (PBMR), high conversions can be realized keeping the oxygen concentrations low.

Firstly, potential yields improvements of PBMRs have been identified by comparing the maximal product yield in a PBMR with a constant oxygen concentration level with the optimal yield of a FBR with premixed oxygen feed. The influence of the difference in the oxygen reaction orders (m-n) and the ratio of the reaction rates of consecutive and primary reaction (k_2/k_1) were demonstrated.

Secondly, the optimal axial oxygen concentration profile in a PBMR with a given catalyst mass was investigated. The extent of premixed and distributed oxygen feed were varied, and the effect of different axial profiles for the oxygen distribution were compared. For small catalyst masses it was found that premixed feeding can produce the maximum product yield. With further increase of the catalyst mass, an increasing part of the oxygen should be added distributively to the PBMR to achieve the maximum product yield. For medium catalyst masses the combination of premixed and constant distributed oxygen feeding is best, but for high catalyst masses membranes with an axially decreasing permeation profile produce better results.

3.1 Introduction

In partial oxidation systems the formation rates for the target product and the waste product often differ in their dependency on the oxygen concentration. Thus, the oxygen concentration can be used to influence the ratio of the reaction rates of these two reactions in order to optimize the product selectivity or yield. For example, for some partial oxidation processes, like ethylene epoxidation (Larfarga et al., 2000) or selective oxidation of butane to maleic anhydride (Pedernera et al., 2000), the product formation shows a higher reaction order in oxygen than the sequential or parallel formation rate of the waste products and are thus operated with an excess of oxygen. In the opposite case, where the oxygen dependency of the target product formation is less pronounced, the waste product formation rate (e.g. oxidative dehydrogenation (ODH) of ethylbenzene to styrene (Shakhnovich et al., 1984) or ODH of

methanol to formaldehyde (Diakov et al., 2002)) can be suppressed by operating under oxygen deficiency, leading, however, to a low single-pass conversion. By means of distributive addition of oxygen to the reaction mixture along the axial coordinate of the reactor high conversions can be obtained at a low oxygen level.

A decrease in the oxygen concentration is beneficial for the product selectivity for both consecutive and parallel reaction schemes, provided that the reaction order in oxygen is lower in the target product formation reaction.

For a parallel reaction scheme, however, high conversions can also be achieved with low oxygen concentrations without the application of membranes and without loss of selectivity in a well-mixed reactor (e.g. fluidized bed). Because of the reduced reactant concentrations, a well-mixed reactor requires a considerably larger reactor volume. The application of a PBMR could decrease the required reactor volume.

In the evaluation of the benefits and disadvantages of distributive oxygen feeding the following reaction scheme of the partial oxidation of a hydrocarbon has been selected:

target product formation: $A + \nu_1 O_2 \rightarrow P$ $r_1 = k_1 c_A c^n$ (1)

waste product formation: $P + \nu_2 O_2 \rightarrow W$ $r_2 = k_2 c_P c^m$ (2)

where A represents the hydrocarbon reactant, P the target product, W the waste product and ν_i the stoichiometric constants and k_i the reaction rate constants.

The reaction rates of both reactions have been assumed first order in the hydrocarbons. The reaction orders of oxygen for the target product formation and for the waste product formation are indicated with n and m, respectively.

In this chapter it is shown for a consecutive reaction scheme to what extent improvements in the product yield can be achieved when operating with a distributed oxygen feed in a packed bed membrane reactor (PBMR), in comparison with premixed oxygen feed. The possible increase in product yield is investigated for reactions with different reaction orders and relative reaction rates.

However, at lower oxygen concentrations possible mass transfer limitations, both from the membrane wall to the core of the bed and from bulk of the gas phase into the catalyst particle, become increasingly important. In this chapter, it is discussed under what conditions mass transport limitations can be expected, and how the local activity of the catalyst bed and the (intrinsic) selectivity are effected.

3.2 Product yield improvement and activity losses due to the reduction of the oxygen concentration level

3.2.1 Product yield improvement via reduced oxygen level

For a consecutive reaction scheme the product selectivity can be increased up to almost 100 % when decreasing the oxygen concentration. The degree of selectivity improvement that accompanies a specific reduction in the oxygen concentration depends on the ratio of the reaction rate constants (k_2/k_1) and the difference in the reaction orders of oxygen (m-n). To elucidate this effect a constant oxygen concentration has been assumed in the entire PBMR, assuming that the oxygen flow through the membrane equals the oxygen consumption rate in the reactor. The effect of a reduction of the constant oxygen concentration is evaluated below. In case of a constant oxygen concentration the reaction rates reduce to pseudo-first order, for which the maximum product yield (Y_{max}) is given by (Westerterp et al., 1984):

$$Y_{max} = \kappa^{\kappa/(1-\kappa)} \quad \text{with} \quad \kappa = \left(k_2/k_1\right) c^{m-n} \tag{3}$$

A reduction of the oxygen concentration by a factor $f = c/c_0$ results in a decreased value of $\kappa = \kappa_0 f^{m-n}$ (defining κ_0 as a base case value) and an increase of Y_{max} as shown in Fig. 1a.

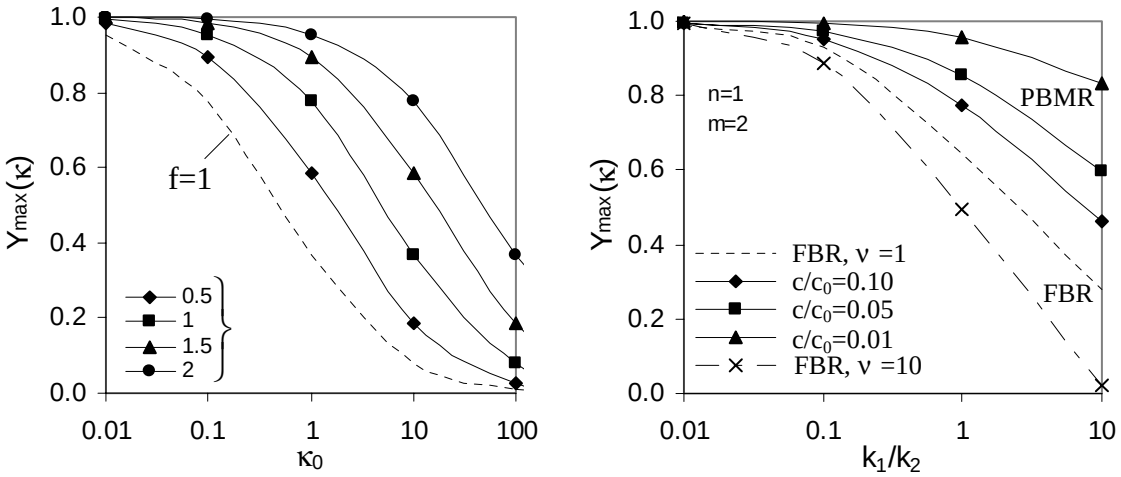

Fig. 1 Effect of a decrease of the oxygen concentration on the maximum product yield. (a) for a factor f=0.1 and order differences m-n from 0.5 to 2; (b) comparison of FBR (dashed line; ν_2=1) with PBMR with constant oxygen concentrations of 0.1, 0.05 and 0.01 of the initial concentration of the FBR, maximum FBR-yield for reaction scheme with ν_2=10.

For κ=1 the maximum yield is about 37 % (indicated with the dashed line for which f=1). By a reduction of the constant oxygen concentration with a factor 10 (f=0.1) the value of κ is decreased so that the maximum yield increases to 59 % if the reaction orders differ by m-n=0.5 and even to 77 % if m-n=1. The yield improvement by decreasing the oxygen concentration by a factor 10 is illustrated in Fig. 1a as a function of the κ-value of a reference

case (κ_0, calculated with the oxygen concentration before the reduction) for different reaction order differences (m-n).

Fig. 1b shows the comparison of PBMRs with different, constant oxygen concentrations and a FBR (dashed line) for the reaction orders n=1 and m=2 ($\nu_1=\nu_2=1$). The initial oxygen concentration of the FBR was optimized for maximum product yield. The calculated maximum yield for the FBR is compared with the maximum yield for three different PBMR operating at 1/10, 1/20 and 1/100 of the initial oxygen concentration of the FBR.

The consecutive reaction often represents the combustion of the intermediate product to CO or CO_2. The relative consumption of oxygen by a consecutive reaction can exceed that of the primary reaction tremendously. For example, in the oxidative dehydrogenation of ethyl benzene to styrene the ratio ν_2/ν_1 is 20. In this case, the inlet oxygen concentration to a FBR has to be increased in order to achieve the required conversions at the expense of a decrease in the maximum product yield (see FBR, $\nu_2=10$ in Fig. 1b). The difference in maximum product yields between the FBR and the PBMR at the same constant oxygen concentration is even higher when ν_2/ν_1 is higher as also shown in Fig. 1b. However, the oxygen consumption rate and thus the risk of local oxygen depletion also increases.

Finally, yield improvements via distributive oxygen dozing also increase with the reaction order difference m-n.

3.2.2 Activity losses via a reduced oxygen level

The reduction of the concentration level obviously results in a lower reactivity for n>0. The relative increase of the required residence time due to the reduced oxygen concentration is expressed by the following expression (adapted from Westerterp et al., 1984):

$$F_\tau = \frac{\tau_f}{\tau_0} = \frac{1}{f^n}\frac{\kappa_0 - 1}{\kappa_0 f^{m-n} - 1}\ln\left(\kappa_0 f^{m-n}\right)/\ln\kappa_0 \qquad (4)$$

The effect of the decrease in oxygen concentration on the required residence time is shown in Fig. 2 for different reaction orders of the target and waste product formation. The hydrocarbon conversion with the maximum product yield is higher the more selective the reaction system is, and thus increases with a decreasing oxygen concentration. The effect thereof on the residence time is included in Fig. 2.

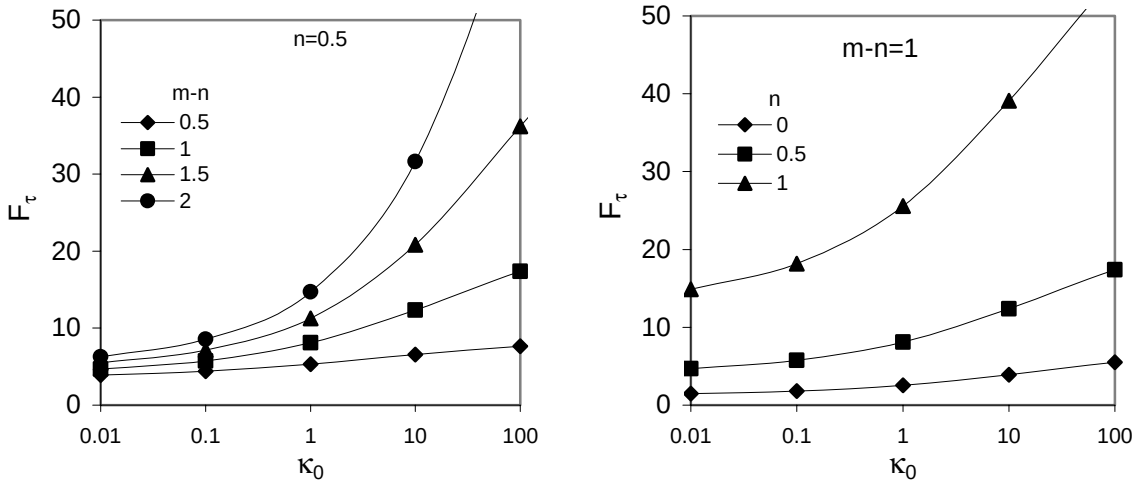

Fig. 2 Effect of a decrease in the oxygen concentration by a factor of 10 (f=0.1) on the residence time corresponding to the optimum conditions.

For example, a yield improvement from 64 % (FBR) to 95 % (PBMR; c/c_0=0.01) shown in Fig. 1b for k_2/k_1 = 1 (n=1/m=2) is accompanied by an increase of the required residence time (reactor size) by a factor of 18, while a yield improvement to 77 % (PBMR; c/c_0=0.1) is achieved without an increase in residence time.

The economical incentive to use a PBMR in a certain process depends on the difference between the saved separation (operational and investment) costs and the increased reactor costs compared to a FBR. In some cases, it could even be preferred to operate with an excess of oxygen despite the lower product selectivities. For instance, for κ=0.1 a 10 % excess of oxygen results in a loss of only 0.1 % in product yield, while the required residence time is reduced by a factor of 8 (n=1).

Most industrially interesting reaction systems for application of distributive oxygen dozing have κ-values in the range of 0.01-0.2, but show for the product formation reaction orders on oxygen between 0 and 0.5, in which case the activity loss is limited.

3.3 Effect of the axial profile of oxygen distribution

For the calculations presented above an axially constant oxygen concentration was assumed. This can only be realized by a selective, diffusive membrane with a very high permeability. With many common membranes, an axial oxygen concentration profile is established, because the local consumption rate of oxygen shows a strong axial profile.

The permeation fluxes of common porous, inorganic membranes show a mixed diffusive and convective transport. However, in the following is will be assumed that the convective transport is dominating – the membrane works as a distributor without the typical features of a membrane.

The axially decreasing activity of the catalyst bed could be accounted for by the development of membranes with an axial permeability profile or via an axial membrane thickness profile. For porous membranes this can be realized by a segment wise reduction of the porosity, as for example done by Coronas et al. (1994) in a further development of the membrane modification by silica sol described in Lafarga et al. (1994). They produced four membrane sections with different amounts of deposit for the oxidative coupling of methane. Thus, a pattern of (discrete) decreasing permeability was created in the direction of flow along the membrane length giving rise to an increase in conversion of methane and selectivity of ethene at a given concentration.

Julbe at al. (2001) present a membrane that continuously adjusts its permeability controlled by the re/ox properties of the gas phase. This so called 'chemical valve' membrane has the highest permeability near the reactor inlet, where the hydrocarbon concentration is maximal and no oxygen is present (all is added distributively), and the permeability decreases along the membrane length.

In a theoretical study Thomas and Seidel-Morgenstern (2002) investigated the selectivity enhancement in parallel-consecutive reaction systems by optimized reactant dozing. The results presented in their paper are limited to a series of either (a) packed bed reactors with variable (discrete) dozing of oxygen at the feed of each of the segments or (b) PBMR (continuous feeding) with different membrane flows but no intermediate, discrete feeding (see Fig. 3).

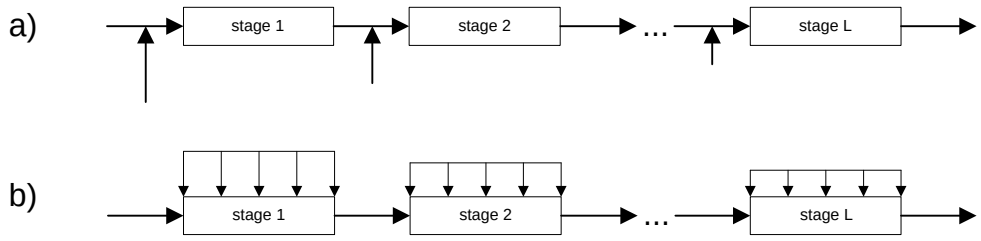

Fig. 3 Schematic illustration of the two main reactor concepts discussed in Thomas and Seidel-Morgenstern (2002).

For the case of a single section, the PBMR clearly results in a higher product yield. Unfortunately, a comparison with an optimized mixed system employing discrete and continuous feeding was not carried out.

With increasing number of stages the performance of both reactor systems improves, and the differences between the two reactor concepts gradually vanish. The amount of oxygen that should be added gradually reduces from section to section. Finally, they show that a series of 10 PBMRs with optimized membrane flows outperforms one reactor with the optimal constant oxygen concentration (n=1/m=2), however with a small difference. From the study by Thomas and Seidel-Morgenstern it can be concluded, that for high catalyst masses an axial constant oxygen concentration is close to, but not exactly equal to the optimum concentration profile. For all calculations presented the reaction rates were chosen such that conversions

and selectivities were above 80 %. Therefore, the validity of these conclusions should be verified for conditions of lower selectivities and conversions (i.e. catalyst masses), as also encountered in industrial practice.

In this paragraph two alternative methods are investigated that account for the decreasing activity of the packed bed in axial direction. Firstly, part of the oxygen can simply be added premixed to the PBMR, resulting in a relatively high oxygen concentration near the reactor inlet and decreasing oxygen concentrations along the length of the reactor. Secondly, membranes with a continuous, axial permeation profile could be applied.

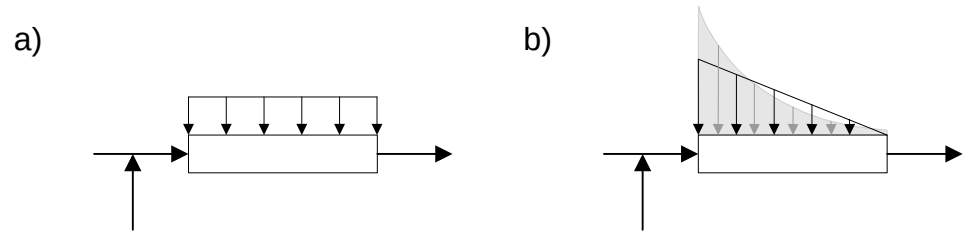

Fig. 4 Schematic illustration of the reactor concepts discussed in this chapter: oxygen fed in the premixed feed and by (a) axial constant or (b) steadily decreasing membrane flux.

Selectivity improvements realized in a PBMR are the main issue of this thesis. However, the optimization of the process selectivity for a given reaction system with power law kinetics simply results in 100 % selectivity and 100 % conversion, if catalyst mass and oxygen concentration can be chosen freely, i.e. at high catalyst masses and low oxygen concentration. Therefore, in this paragraph it is aimed at an optimization of the process parameters for a fixed catalyst mass searching for the maximal product yield. The steering variables are the amount of premixed and distributed oxygen, which are gradually varied. The optimum obtained within this parameter space is sufficient for the present analysis. First, the effect of the ratio of oxygen in premixed and distributive feed on the yield is studied. Then, it is investigated whether an axial profile for the distributive flow can yield a further improvement.

The consecutive reaction scheme described in Section 3.1 is used with methane (A), formaldehyde (P) and carbon dioxide (W) as hydrocarbons, such that all stoichiometric coefficients are $\nu = \pm 1$. The rate constants and other model parameters are listed in Table 1. As distributive feed, pure oxygen was chosen in order to exclude the dilution effect on the results. Dilution by nitrogen results in lower contact times, i.e. lower conversions and product yields. If air is distributed, the optimum reduces and shifts to slightly larger amounts of distributively added oxygen.

The PBMR is modeled as a plug flow reactor without axial dispersion.

$$\frac{d}{dz}\Phi_{m,i} = s_i + \omega_i \frac{d}{dz}\Phi_{m,distr} \text{ or (as } \sum_{i=1}^{nc} \nu_{ij} = 0\text{): } \frac{d}{dz}\Phi_{V,i} = \frac{m_{cat}}{L} r'_i + y_i \frac{d}{dz}\Phi_{V,distr} \qquad (5)$$

$$\text{with } s_i = M_i \frac{m_{cat}}{L} R'_i,\ R'_i = \sum_{j=1}^{nr} \nu_{ij} r'_j \text{ and } R'_j = \frac{mol}{g_{cat} s}. \qquad (6),(7),(8)$$

Table 1 Model parameters used to assess the influence of the axial profile of distributive oxygen feeding.

Rate constants: n=0.5/m=1.0		k_1	0.015 mol / (g s bar^{1+n})
		k_2	0.045 mol / (g s bar^{1+m})
Rate constants: n=1.0/m=2.0		k_1	0.150 mol / (g s bar^{1+n})
		k_2	4.500 mol / (g s bar^{1+m})
Catalyst mass		m_{cat}	0.001-1 g
Reactor pressure and temperature		p, T	1.013 bar, 550 K
Premixed feed:	volumetric flow rate	$\Phi_{V,0}$	100 ml(STP)/min
	mole fraction of reactant A	$y_{A,0}$	0.1
	mole fraction of oxygen	$y_{O2,0}$	0.0 ÷ 0.13
Distributed feed:	volumetric flow rate	$\Phi_{V,distr}$	0 ÷ 15 ml(STP)/min
	mole fraction of oxygen	$y_{O2,distr}$	1.0

STP: 1.013 bar and 298 K

3.3.1 Ratio of premixed and distributive oxygen addition

In Fig. 5 the effect of the distributive feed on the yield is presented for different catalyst masses ranging from 0.001 to 1 g at two different initial oxygen concentrations, $y_{O2,0}$=0 and $y_{O2,0}$=0.03.

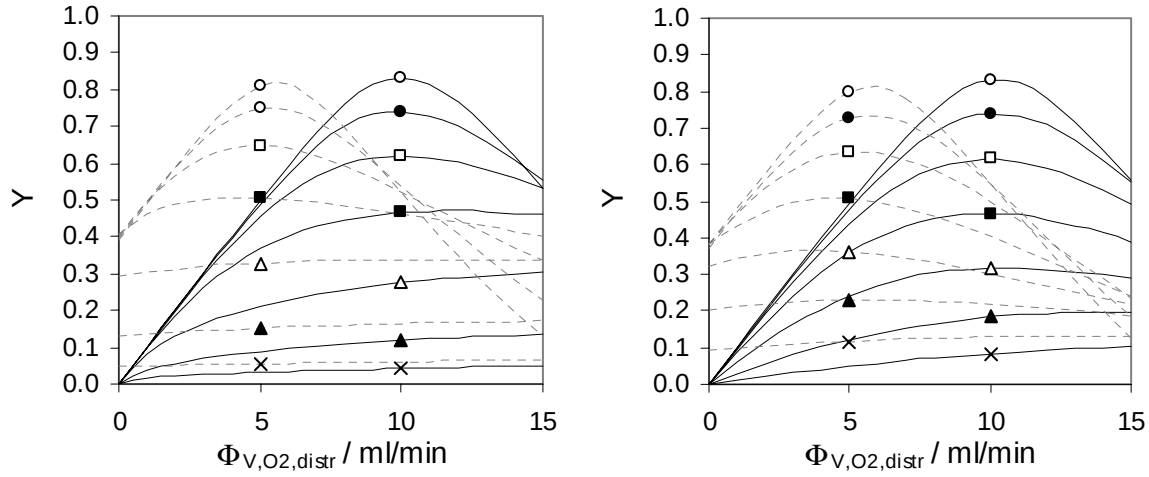

Fig. 5 Yield as function of the catalyst mass and the amount of distributively added oxygen for $\Phi_{V,O2,0}$=0 (full lines) and $\Phi_{V,O2,0}$=3 ml/min (dashed lines) and the reaction orders (a) n=0.5/m=1 and (b) n=1/m=2. Catalyst mass: ○=1000, ●=316, □=100, ■=31.6, Δ=10, ▲=3.2, ×=1 mg.

At constant flow rate of reactant A the chosen catalyst mass determines to a very large extent the maximal product yield and the optimal distribution pattern of oxygen. For very small

catalyst masses, the product yield increases with the amount of oxygen added in the premixed and the distributive feed (within the investigated limits).

At somewhat increased, but still small, catalyst mass a very remarkable situation emerges, which is illustrated in Fig. 6 for the reaction orders (n=0.5/m=1 and n=1/m=2). For a given small range of catalyst masses, the maximal product yield is achieved with complete premixed feeding of oxygen without any distributive feeding!

This observation clearly indicates, that it is not possible to conclude from a simple comparison of experimental FBR and PBMR results with small to medium conversions, if the reduction of the oxygen concentration level results in an improvement of the product selectivity (n<m) or not (n>m).

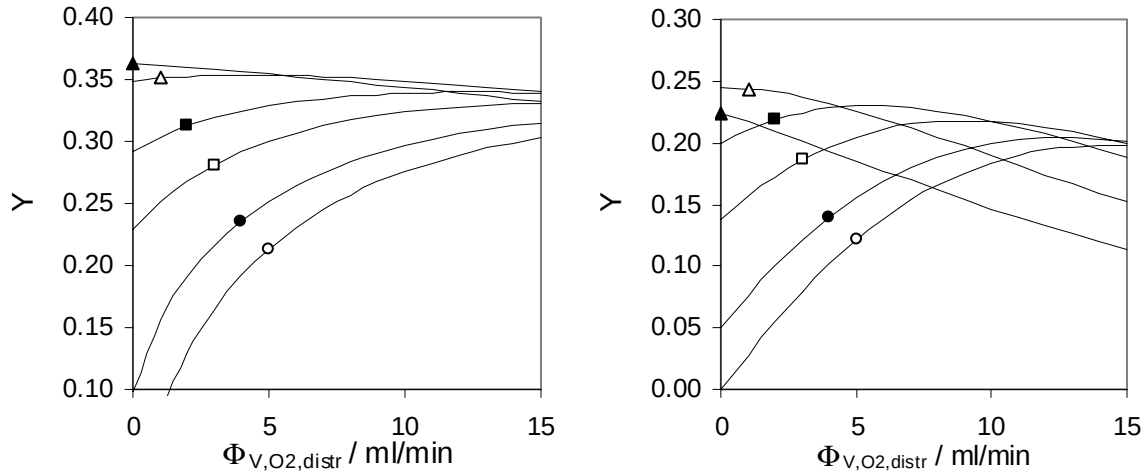

Fig. 6 Yield as function of the amount of premixed ($\Phi_{V,O2,0}$) and distributively ($\Phi_{V,O2,distr}$) added oxygen for the reaction orders (a) n=0.5/m=1 on 10 mg catalyst and (b) n=1/m=2 on 3.2 mg catalyst. $\Phi_{V,O2,0}$: ○=1, ●=1, □=3, ■=5, Δ=9, ▲=13 ml/min.

With a further increase of the catalyst mass an increasing part of the oxygen must be added distributively to optimize the product yield. However, for the calculations shown in Fig. 7 the optimal yield is achieved when between 50 and 30 % of the total oxygen addition is fed premixed.

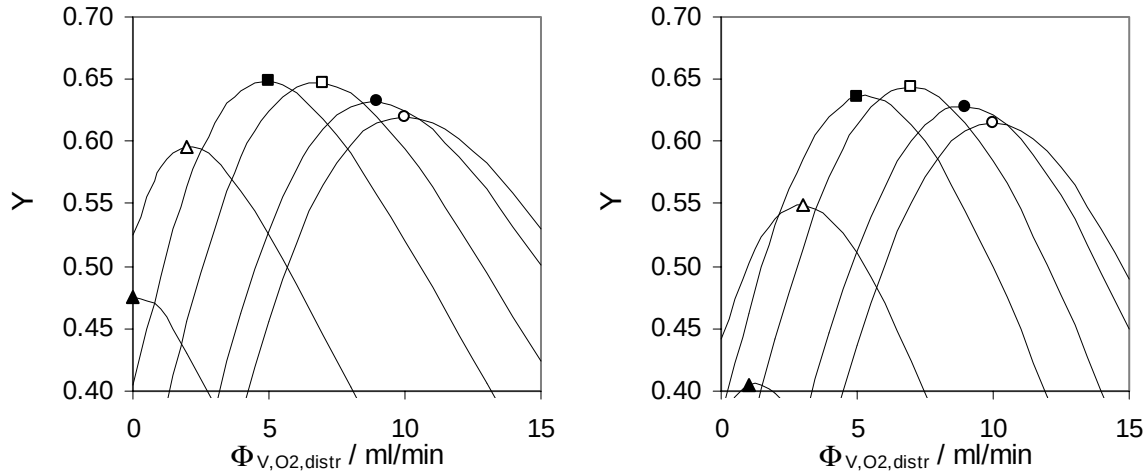

Fig. 7 Yield on 0.1g catalyst as function of the amount of premixed ($\Phi_{V,O2,0}$) and distributively ($\Phi_{V,O2,distr}$) added oxygen for the reaction orders (a) n=0.5/m=1 and (b) n=1/m=2. $\Phi_{V,O2,0}$: ○=1, ●=1, □=3, ■=5, Δ=9, ▲=13 ml/min.

For very high catalyst masses, obviously, high conversions can be realized at very low oxygen concentrations and the part of oxygen that should be added in the premixed feed approaches zero. The stoichiometric coefficient ν_1 determines the optimal amount of oxygen to be added to the PBMR – all in the distributive feed. If more oxygen is added, the yield decreases due to selectivity losses.

3.3.2 Axial distribution profile

In this section the case where the membrane flows continuously decrease is compared with the case of a membrane with a constant oxygen flow rate. Since the amount of oxygen added premixed, that is required for optimized product yield, is expected to become lower for the latter case, this variable is kept as a parameter for optimization.

To facilitate the comparison a few functions were chosen to describe the axial membrane flux:

Constant:

$$\left(\mathrm{d}\Phi_{V,distr,const}/\mathrm{dz}\right)(z) = \Phi_{V,distr}/L \qquad (9)$$

Linear:

$$\left(\mathrm{d}\Phi_{V,distr,lin}/\mathrm{dz}\right)(z) = 2\left(\Phi_{V,distr}/L\right)(1-z/L) \qquad (10)$$

Exponential:

$$\left(\mathrm{d}\Phi_{V,distr,exp}/\mathrm{dz}\right)(z) = C\left(\Phi_{V,distr}/L\right)\frac{\exp(-Cz/L)}{1-\exp(-C)}$$

$$C = 3 \text{ or } 5 \qquad (11)$$

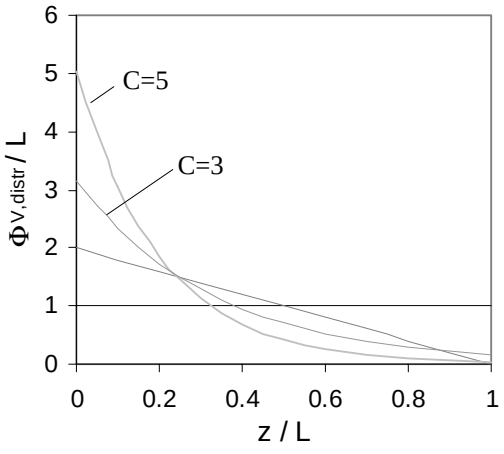

Fig. 8 Representation of three different axial patterns for the distributive feed.

These three functions are plotted in Fig. 8 as a function of the dimensionless length z/L.

In Table 2 the maximal product yields for the different permeation profiles with optimized premixed and distributive oxygen feed are listed.

Table 2 Maximum product yields for the different distribution pattern as function of the catalyst mass. In brackets the oxygen flows in premixed and distributed feed are given ($\Phi_{V,O2,0}$/ $\Phi_{V,O2,distr}$).

n=0.5/m=1

m_{cat} / mg	constant	linear	C=3	C=5
3	0.203 (13/15)	0.205 (13/15)	0.206 (13/15)	0.207 (13/15)
10	0.362 (13/0)	0.362 (13/0)	0.362 (13/0)	0.362 (13/0)
32	0.507 (5/4)	0.506 (5/5)	0.505 (5/4)	0.503 (9/0)
100	0.648 (5/4)	0.647 (3/7)	0.643 (1/8)	0.618 (0/9)
316	0.760 (3/7)	0.770 (1/10)	0.774 (1/9)	0.749 (0/10)
1000	0.841 (3/7)	0.863 (1/9)	0.870 (1/9)	0.857 (0/10)

n=1/m=2

m_{cat} / mg	constant	linear	C=3	C=5
3	0.246 (9/0)	0.246 (9/0)	0.246 (9/0)	0.246 (9/0)
10	0.365 (5/4)	0.364 (5/3)	0.364 (5/3)	0.362 (5/3)
32	0.506 (5/5)	0.505 (3/6)	0.501 (3/6)	0.488 (3/6)
100	0.644 (3/7)	0.648 (3/7)	0.643 (1/9)	0.623 (1/8)
316	0.756 (3/7)	0.772 (1/9)	0.775 (1/9)	0.756 (1/9)
1000	0.840 (1/9)	0.865 (1/9)	0.870 (1/9)	0.859 (1/9)

For low and medium catalyst masses, an axially varying membrane flow does not result in a further improvement of the maximal product yield for the investigated sets of reaction orders and membrane flux profile functions.

In Fig. 9 the axial oxygen concentration profiles and the selectivity-conversion-plot are compared for one of the situations listed in Table 2 (100 mg catalyst; n=0.5/m=1).

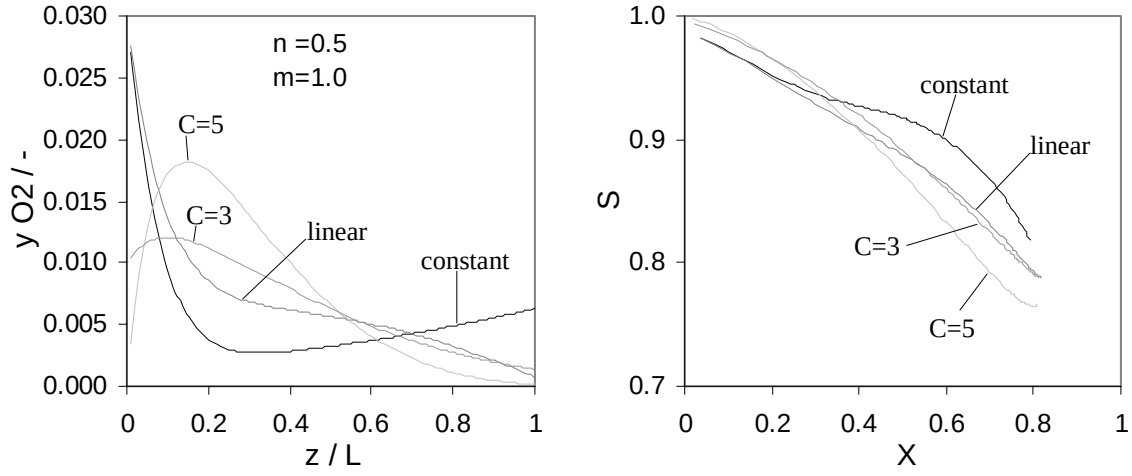

Fig. 9 Comparison of the axial oxygen concentration profile and the selectivity-conversion plot of the three distribution patterns with optimal ratio of premixed and distributive flow: constant ($\Phi_{V,O2,0}$/ $\Phi_{V,O2,distr}$ = 3/7), linear (3/7) and exponential (C=3: 1/9; C=5: 0/10); n=0.5/m=1. Catalyst mass: 0.1g.

The overall amount of oxygen added is the same for all cases, but the part added premixed varies from 30 % (constant and linear) to 0 % (C=5). The axial oxygen profiles, which result in almost the same product yield (except C=5), are quite different. Moreover, the constant feeding profile results in a higher selectivity (but lower conversions), while the linear and exponential feeding show improved conversions (at slightly lower selectivities). For high catalyst masses, feeding with an axially decreasing membrane flow is advantageous, and the exponential profile with C=3 is the best of the investigated alternatives for the conditions studied. However, it should be noted that in this selected case the oxygen concentrations are very low (for m_{cat}=1 g one order of magnitude smaller than for m_{cat}=0.1 g). Obviously it should be verified, whether the assumed reaction orders are also valid at these low oxygen concentrations.

3.3.3 Optimization of the axial oxygen profile

In the preceding section it was shown that application of the tested axial membrane flux profiles did not result in substantial yield improvements, except for very high catalyst masses. However, it was not yet investigated, whether the tested profiles are close to the optimal profile. Therefore, in this last section the local oxygen mass flow was assumed as a direct control variable to optimize the final product flow. The optimum has been determined using Pontryagin's maximization principle (Appendix A).

The optimized oxygen profile shows very high initial oxygen concentrations with a strong decrease near the reactor inlet (see Fig. 10). The initial decrease is too strong to be caused by the reactive conversion of oxygen, indicating that oxygen should actually be removed from the reaction mixture to create the optimal oxygen concentration profile! Because the oxygen mass flux is the control variable, the volumetric flow rate at the reactor entrance is not anymore fixed to 100 ml/min.

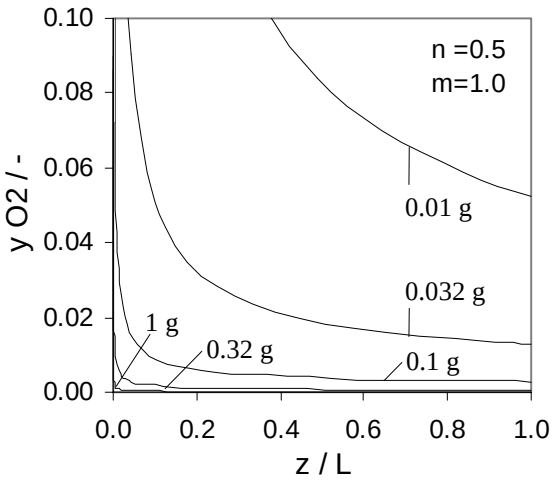

Fig. 10 Optimal axial concentration profiles for the different catalyst masses.

The oxygen profiles shown in Fig. 10 are derived for a nitrogen flow of 90 ml/min, which results in a higher dilution and reduced contact times compared to the optima presented in Sections 3.3.1 and 3.3.2, with negative effect on the total conversion. However, if the nitrogen flow is adjusted to obtain an initial flow of 100 ml/m, the removal of oxygen from the system results in the opposite effect. Therefore, the reduction of the nitrogen flow was chosen such that the concentrations of A did not exceed y_A=0.1 in the reactor. In Table 3 the optimal product yields are listed for both the high and the reduced nitrogen flow case.

Table 3 Maximum product yield for the optimized oxygen concentration profile. Between brackets the volumetric flow rate of nitrogen is given (ml/min).

m_{cat} /mg	n=0.5/m=1		n=1/m=2	
10	0.347 (90)	0.376 (70)	0.362 (90)	0.373 (80)
32	0.502	0.522 (75)	0.504	0.514 (82)
100	0.650	0.662 (80)	0.650	0.656 (85)
316	0.777	0.782 (85)	0.777	0.779 (88)
1000	0.872 (90)	0.874 (88)	0.872 (90)	0.872 (89)

Finally, it can be seen that a PBMR with a constant membrane flux can achieve product yields close to the optimum, if the correct premixed and distributed oxygen flows are chosen. The resulting axial oxygen concentration profile closely follows the optimal oxygen concentration profile (see Fig. 11a).

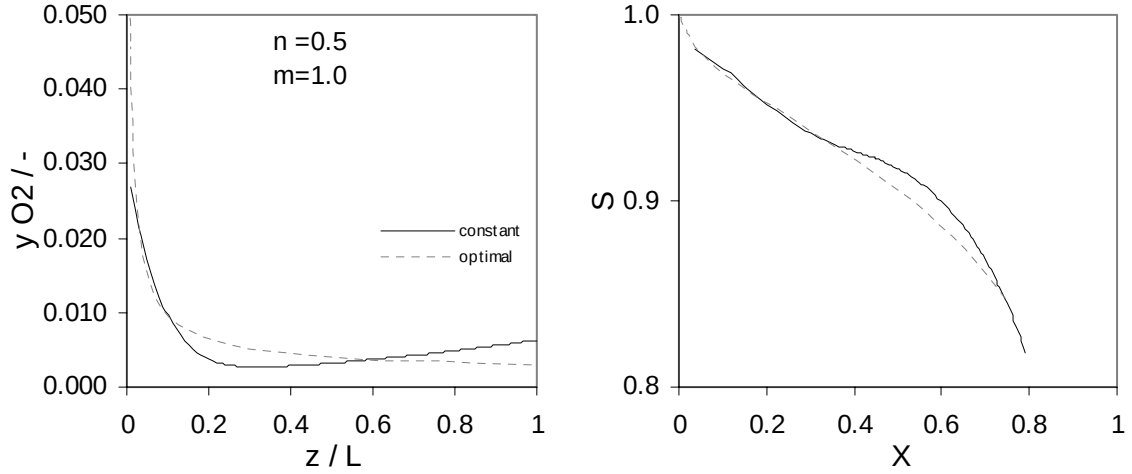

Fig. 11 Comparison of the axial oxygen concentration profile and the selectivity-conversion plot of the optimized oxygen concentration profile and the constant membrane flux with the optimal ratio of premixed and distributive flow ($\Phi_{V,O2,0}/\Phi_{V,O2,distr}$ = 3/7); n=0.5/m=1, catalyst mass 0.1 g.

3.3.4 Effect of the stoichiometric coefficients

The results presented before in this chapter were based on an equimolar reaction scheme ($\nu_1 = \nu_2 = 1$). The effect of the stoichiometric coefficients will now be briefly demonstrated for the coefficients $\nu_1 = \nu_2 = 0.5$ and $\nu_1 = 0.5/\nu_2 = 10$ and for the reaction orders n=0.5/m=1.

If half a mole of oxygen is consumed for one mole of hydrocarbon in both primary and secondary reaction, the same ratio of oxygen and hydrocarbon reactant has to be added to the PBMR for the optimum product yield, except for very low catalyst masses. The obtained optimum and the distribution between premixed and even distributed feed is approximately the same (Table 4). The small deviations between the values of $\nu_1 = \nu_2 = 1$ and $\nu_1 = \nu_2 = 0.5$ are most likely caused by a too large step-wise change in the variation of the premixed and distributed oxygen flow.

For $\nu_1 = 0.5 / \nu_2 = 10$ the oxygen consumption in the consecutive reaction is much larger than in the primary reaction. Because of the large amount of oxygen consumed in the consecutive reaction, the distributive flow is increased. Furthermore, the oxygen consumption rate is distributed more evenly over the length of the reactor. For the optimum of premixed and constant distributed flow, the axial oxygen concentration profile does not show the increase towards the end of the reactor that was shown for $\nu_1 = \nu_2 = 1$ in Fig. 9. Therefore, for high catalyst masses the optimal axial oxygen concentration profiles is approached best with the constant transmembrane flow, the exponential (C=3) distribution shows no further improvement.

Table 4 Effect of the stoichiometric coefficients on the maximum product yields as function of the catalyst mass for the reaction orders n=0.5/m=1. In brackets the oxygen flows in premixed and distributed feed are given ($\Phi_{V,O2,0}$/ $\Phi_{V,O2,distr}$).

n=0.5/m=1

m_{cat} / mg	$\nu_1=\nu_2=1$ constant	$\nu_1=\nu_2=0.5$ constant	$\nu_1=0.5/\nu_2=10$ constant	$\nu_1=0.5/\nu_2=10$ C=3
3	0.203 (13/15)	0.203 (13/15)	0.201 (13/15)	0.203 (13/15)
10	0.362 (13/0)	0.357 (13/0)	0.356 (13/6)	0.356 (13/5)
32	0.507 (5/4)	0.507 (5/0)	0.499 (9/11)	0.486 (5/13)
100	0.648 (5/4)	0.650 (3/2)	0.645 (3/14)	0.626 (1/15)
316	0.760 (3/7)	0.759 (1/4)	0.772 (1/14)	0.760 (0/15)
1000	0.841 (3/7)	0.845 (1/4)	0.866 (1/11)	0.863 (0/12)

3.4 Summary and conclusions

In partial oxidation systems in which the formation rate for the target product shows a lower dependency on the oxygen concentration than the formation rate of the waste product, the product selectivity can be increased by reducing the oxygen concentration in the reactor.

For the simple consecutive reaction scheme with power low kinetics, the improvement of the product selectivity is unlimited and reaches 100 %, when the oxygen concentration throughout the reactor approaches zero, and with a large amount of catalyst high conversions are reached. Therefore, in an optimization either the oxygen concentration or the catalyst mass should be kept constant.

Firstly, potential yields improvements of PBMRs were found by comparing the maximal product yield in a PBMR with a constant oxygen concentration level with the optimal yield of a FBR with premixed oxygen feed. The influence of the difference in the oxygen reaction orders (m-n) and the ratio of the reaction rates of consecutive and primary reaction (k_2/k_1) were demonstrated.

Secondly, the optimal axial oxygen concentration in a PBMR of a given catalyst mass was also investigated. Four different axial oxygen distribution patterns were tested to approach the optimum. Obviously, for very small catalyst masses the yield improves with the amount

of oxygen added to the reactor (either premixed or distributive), but this case is not of practical interest. For an increased, but still small catalyst mass it was found that the all premixed feeding results the maximum product yield. With further increase of the catalyst mass, an increasing part of the oxygen should be added distributively to the PBMR for the maximum product yield. For medium catalyst masses the combination of premixed and constant distributed oxygen feeding is best, but for high catalyst masses a membrane with an axially decreasing permeation profile produce better results (if $\nu_1 = \nu_2$; if $\nu_2 >> \nu_1$, the even distribution is optimal for high catalyst masses as well).

NOTATION

Latin letters

A,P,W	hydrocarbon reactant, target and waste product
c	concentration [mol / m^3]
f	factor by which oxygen concentration is reduced
F	factor by which e.g. a reaction rate or selectivity is increased
FBR	fixed bed reactor
k	rate constant [mol / m^3 s bar^{1+n}], [mol / m^3 s bar^{1+m}]
R'_i	rate of reactive consumption of component i in nr reactions ($= \sum_{j=1}^{nr} \nu_{ij} r'_j$) [mol / g_{cat} s]
r'_j	rate of reaction j [mol / g_{cat} s]
L	reactor length [m]
M_i	molecular mass of component i [kg / mol]
m_{cat}	catalyst mass [g]
m	reaction order in oxygen of reaction forming the waste product
n	reaction order in oxygen of reaction forming the target product
p	pressure
PBMR	packed bed membrane reactor
s_i	source term: mass of component i formed per reactor length [kg / m s]
S	selectivity [-]
T	temperature [K]
Y	yield [-]
y	molar fraction [-]
z	axial coordinate of the reactor [m]

Greek letters

κ	ratio of the rate constants of consecutive and primary reaction (both first order)

ν	stoichiometric coefficient
τ	residence time
Φ_V	volumetric flow [m^3 / s] or [ml / min]
Φ_m	mass flow [kg / s]

Subscripts

0	at the reactor inlet / base case
A,P,W	hydrocarbon reactant, target and waste product
distr	distributed
max	maximum value
O_2	oxygen

References

R.B. Bird, W.E. Stewart, E.N. Lightfoot, Transport phenomena, John Wiley & Sons, New York, 1960

J. Coronas, M. Menéndez, J. Santamaría, 1994, Development of ceramic membrane reactors with a non-uniform pemeation pattern. Application to methane oxidative coupling, *Chemical Engineering Science 49*, 4749-4757

V. Diakov. B. Blackwell, A. Varma, 2002, Methanol oxidative dehydrogenation in a catalytic packed-bed membrane reactor: experiments and model, *Chem. Eng. Sci. 57*, 1563-1569

G. Follmer, L.Lehmann, M. Baerns, 1989, Effect of transport limitations on C_{2+} selectivity in the oxidative methane coupling reaction using a NaOH/CaO catalyst, *Catalysis Today 4*, 323-332

A. Julbe, D. Farrusseng, C. Guizard, 2001, Porous ceramic membranes for catalytic reactors – overview and new ideas, *Journal of membrane science 181*, 3-20

D. Lafarga, J. Santamaría, M. Menéndez, 1994, Methane oxidative coupling using porous ceramic membrane reactors – I. reactor development, *Chemical Engineering Science 49*, 2005-2013

D. Lafarga, M. A. Al-Juaied, C.M. Bondy, A. Varma, 2000, Ethylene epoxidation on Ag-Cs/α-Al_2O_3 catalyst: experimental results and strategy for kinetic parameter determination, *Industrial and Engineering Chemistry Research 39*, 2148-2156

M. Pedernera, R. Mallada, M. Menéndez, J. Santamaría, 2000, Simulation of an inert membrane reactor for the synthesis of maleic anhydride, *AIChE Journal 46*, 2489-2498

S.C. Reyes, C.P. Kelkar, E. Iglesia, 1993, Kinetic-transport models and design of catalysts and reactors for the oxidative coupling of methane, *Catalysis Letters 19*, 167-180

G.W. Roberts, 1972, The selectivity of porous catalysts: parallel reactions, *Chem. Eng. Sci. 27*, 1409-1420

G.V. Shakhnovich, I.P. Belomestnykh, N.V. Nekrasov, M.M. Kostyukovsky, S.L. Kiperman, 1984, Kinetics of ethylbenzene oxidative dehydrogenation to styrene over vanadia/magnesia catalyst, *Applied Catalysis 12*, 23-34

M. van Sint Annaland, 2000, A novel reverse flow reactor coupling endothermic and exothermic reactions, Doctoral Thesis, Twente University, Enschede, the Netherlands

S. Thomas, A. Seidel-Morgenstern, 2002, Improved performance of parallel-series reactions in fixed-bed and membrane reactors by stagewise reactant dosing, *submitted to ISCRE 17, august 25-28, Hong Kong*

K.R. Westerterp, W.P.M. van Swaaij, A.A.C.M. Beenackers, 1984, Chemical Reactor Design and Operation – 2nd ed., John Wiley & Sons, Chichester, Chapter III.4

Appendix A Determination of the optimal axial oxygen mass flow profile using Pontryagin's maximization principle

The program written by M. van Sint Annaland (Chapter 8 of his thesis, 2000) was adjusted from the optimization of the temperature profile to the optimization of the oxygen flow profile.

The aim is to determine the axial oxygen mass flux $\Phi_{m,O_2}(z)$ such that

$$S\left(\bar{\Phi}_m\big|_{z=L}\right)+\int_{z=0}^{L} F\left(\bar{\Phi}_m,\Phi_{m,O2},z\right)dz \qquad (A.1)$$

is maximized for a process described by a system of ordinary differential equations given by

$$\frac{d}{dz}\bar{\Phi}_m=\bar{f}\left(\bar{\Phi}_m,\Phi_{m,O2},z\right) \qquad \bar{\Phi}_m\big|_{z=0}=\bar{\Phi}_{m,in} \qquad (A.2, A.3)$$

with $f_i=M_i\frac{m_{cat}}{L}R'_i$, $R'_i=\sum_{j=1}^{nr}\nu_{ij}r'_j$ and $r'_j=\frac{mol}{g_{cat}s}$.

The process equations consist of differential mass balances describing the axial profiles of the mass fluxes of all components besides oxygen.

Applying Pontryagin's maximization principle the optimal oxygen mass flux profile is determined via optimization of the Hamilton function H as a function of the oxygen mass flux for all axial positions

$$\left.\frac{\partial H}{\partial\Phi_{m,O_2}}\right|_z=0\left(\text{and}\quad\left.\frac{\partial^2 H}{\partial\Phi_{m,O_2}{}^2}\right|_z\le 0\right) \qquad (A.4)$$

where the Hamilton function H and the adjungated functions are defined as

$$H=F+\bar{p}\cdot\bar{f} \qquad (A.5)$$

$$\frac{d}{dz}\bar{p}=-\frac{\partial}{\partial\bar{\Phi}_m}H= \qquad \bar{p}\big|_{z=L}=\frac{\partial}{\partial\bar{\Phi}_m}S \qquad (A.6, A.7)$$

With $F=\frac{d}{dz}\Phi_{m,P}$ and S=0 the product yield is optimized.

4 Intrinsic effects of insufficient distribution of oxygen

Abstract

In partial oxidation systems in which the formation rate for the target product shows a lower dependency on the oxygen concentration than the formation rate of the waste product, the product selectivity can be increased by reducing the oxygen concentration in the reactor. By distributive addition of oxygen to the reaction mixture along the axial coordinate of the reactor, for example in a packed bed membrane reactor (PBMR), high conversions can be achieved at a low oxygen level.

However, at lower oxygen concentrations possible problems with the distribution of oxygen from the membrane wall to the centerline of the packed bed as well as from the bulk of the gas phase to the inside the particle might emerge. If the reaction order in oxygen of the main reaction is smaller than 1, mass transfer limitations become increasingly more important when reducing the oxygen concentration level. The effect of mass transfer limitations on the intrinsic product selectivity and the intrinsic activity of a catalyst particle and a slab of the PBMR were investigated.

If the oxygen concentration is small compared to that of the hydrocarbons, intraparticle mass transport limitations will result in an increase in the intrinsic product selectivity. This effect has been illustrated for different combinations of reaction orders of target and waste product formation rates as a function of the characteristic numbers ϕ' and p_{nm}, representing the modified Thiele-modulus for oxygen transport and consumption and the ratio of primary and consecutive reaction rates.

In contrast, transport limitations from the membrane at the tube wall to the center of the packed bed will decrease the intrinsic product selectivities for most sets of relevant reaction orders, especially at high values of the modified Thiele-modulus ϕ''. Here a constant permeation has been assumed. Oxygen depletion in the center of the packed bed further decreases the product selectivity. In lab-scale PMBRs transport limitations from the membrane wall to the center of the packed bed may prevail. In PBMR of industrial scale for high Reynolds-numbers the intraparticle transport limitations may become more severe.

On the basis of the results on the intrinsic activity and selectivity of a catalyst particle and a slab of the PBMR the effects on the integral activity and selectivity will be studied in Chapters 5,6 and 7.

4.1 Introduction

In partial oxidation systems the formation rates for the target product and the waste product often differ in their dependency on the oxygen concentration. Thus, the oxygen concentration can be used to influence the ratio of the reaction rates of these two reactions, by which

product selectivity or yield can be improved. For example, for some partial oxidation processes, like ethylene epoxidation (Larfarga et al., 2000) or selective oxidation of butane to maleic anhydride (Pedernera et al., 2000), the product formation shows a higher reaction order in oxygen than the sequential or parallel formation rate of the waste products and are thus operated with an excess of oxygen. In the opposite case, where the oxygen dependency of the target product formation is less pronounced than the waste product formation rate (e.g. oxidative dehydrogenation (ODH) of ethylbenzene to styrene (Shakhnovich et al., 1984) or ODH of methanol to formaldehyde (Diakov et al., 2002)), the process should be operated under oxygen deficiency for optimal product yield, what results, however, in a low single-pass conversion. By means of distributive addition of oxygen to the reaction mixture along the axial coordinate of the reactor high conversions can be obtained at a low oxygen level.

A packed bed membrane reactor can realize this concept. Oxygen is added to the packed bed along the axial coordinate of the reactor via a membrane and is dispersed from the wall to the center of the packed bed perpendicular to the main flow direction. Radial oxygen concentration gradients from the membrane wall to the center of the packed bed can emerge, that depend on the ratio of radial transport and the local consumption rates. The radial oxygen profiles can influence the conversion and product distribution of a PBMR.
Moreover, if the concentration of oxygen in the PBMR is small compared with those of the hydrocarbons, the effectiveness of the catalyst particles can be determined by intraparticle oxygen concentration gradients, thus influencing the effective product selectivity of the catalyst particle.
In this chapter it is investigated how the performance of an intrinsic part of the PBMR – a slab of the reactor or a single catalyst particle - is influenced by the extent of the radial oxygen distribution in the packed bed and inside the catalyst particles.
To elucidate the effects of the oxygen profiles the following reaction scheme of the partial oxidation of a hydrocarbon with power law kinetics has been selected:

target product formation: $A + \nu_1 O_2 \rightarrow P \qquad r_1 = k_1 c_A c^n$ (1)

waste product formation: $P + \nu_2 O_2 \rightarrow W \qquad r_2 = k_2 c_P c^m$ (2)

where A represents the hydrocarbon reactant, P the target product, W the waste product and ν_i the stoichiometric constants and k_i the reaction rate constants.
The reaction rates of both reactions have been assumed first order in the hydrocarbons. The reaction orders of oxygen for the target product formation and for the waste product formation are indicated with n and m, respectively.

4.2 Intraparticle oxygen transport limitations and their effect on the reactor performance

Due to the decreased oxygen concentration level in a PBMR intraparticle diffusion limitations may emerge. Two opposing effects will determine the change in product selectivity due to intraparticle transport limitations.

On one side, the concentration of reactant A decreases towards the particle center, while that of the intermediate product increases - as long as the product formation exceeds its consumption. This results in a selectivity loss. On the other side, the decrease in the oxygen concentration towards the particle center favors the product selectivity.

In most part of the PBMR, the oxygen concentration is small compared to those of the hydrocarbons.

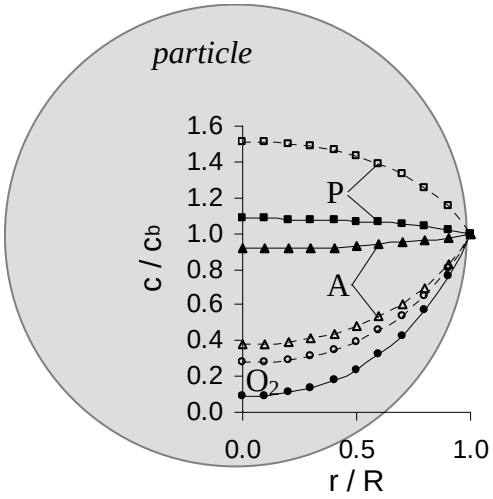

Fig. 1 Concentration profiles in the catalyst particle for $c_b/c_{Ab}= c_b/c_{Pb}=0.1$ (full lines) and $c_b/c_{Ab}=c_b/c_{Pb}=1$ (dashed lines); n=0.5/m=1, ϕ'=1, $p_{nm}=0.1$.

Therefore, the relative oxygen concentration gradients within the catalyst particles are much larger than the relative hydrocarbon concentration gradients (see full lines in Fig. 1), and have consequently a larger effect on the local reaction rates.

The effect of intraparticle mass transfer limitations on the particle effectiveness η and product selectivity ratio, defined as

- particle effectiveness $\eta = \dfrac{\text{actual conversion rate of catalyst particle}}{\text{conversion rate corresponding to bulk concentrations}}$ (3) and

- selectivity ratio $F = \dfrac{\text{actual selectivity of catalyst particle}}{\text{selectivity corresponding to bulk concentrations}}$ (4)

will be analyzed as function of the particle Thiele-modulus for different sets of reaction orders. To calculate the particle effectiveness and product selectivity ratio, firstly the intraparticle concentration profiles are calculated, subsequently the integral conversion rates are determined and put in ratio with those corresponding to the bulk concentrations.

The concentration profiles are calculated under the following model assumptions:

- The concentration of oxygen in the gas phase is small compared to the hydrocarbon concentrations A and P ($c_b/c_{Ab}=c_b/c_{Pb}=0.1$).
- The particle is assumed isobaric and isothermal, so that the pressure and temperature are radially uniform (which allows the use of the concentration gradient notation),

- The effective diffusion coefficient is constant and the same for all species (which allows a Fickian description of the molecular mass transport inside the particle).

If the particle performance is indeed dominated by the oxygen concentration profile, the characteristic Thiele-modulus should refer to the conversion rate and mass transfer of oxygen. Because oxygen is consumed in parallel by both reactions, the following modified Thiele-modulus is suggested:

$$\phi' = \frac{R}{3}\sqrt{\frac{\frac{n+1}{2}\nu_1 k_1 c_{Ab} c_b^{n-1} + \frac{m+1}{2}\nu_2 k_2 c_{Pb} c_b^{m-1}}{D}} \tag{5}$$

After substitution of the dimensionless variables

$$\gamma = \frac{c}{c_b}, \quad \rho = \frac{r}{R}, \quad p_{nm} = \frac{k_2 c_{Pb}}{k_1 c_{Ab}} c_b^{m-n} = \frac{\text{rate of unwanted reaction}}{\text{rate of wanted reaction}} \tag{6),(7),(8)}$$

the radial concentration profiles is numerically calculated from the following set of equations:

$$\frac{1}{\rho^2}\frac{d}{d\rho}\left(\frac{\rho^2}{\phi'^2}\frac{d\gamma_A}{d\rho}\right) = \frac{9}{\frac{n+1}{2}\nu_1 + \frac{m+1}{2}\nu_2 p_{nm}} \frac{c_b}{c_{Ab}} \gamma_A \gamma^n \tag{9}$$

$$\frac{1}{\rho^2}\frac{d}{d\rho}\left(\frac{\rho^2}{\phi'^2}\frac{d\gamma_P}{d\rho}\right) = -\frac{9}{\frac{n+1}{2}\nu_1 + \frac{m+1}{2}\nu_2 p_{nm}} \frac{c_b}{c_{Pb}} \gamma_A \gamma^n + \frac{9 p_{nm}}{\frac{n+1}{2}\nu_1 + \frac{m+1}{2}\nu_2 p_{nm}} \frac{c_b}{c_{Pb}} \gamma_P \gamma^m \tag{10}$$

$$\frac{1}{\rho^2}\frac{d}{d\rho}\left(\frac{\rho^2}{\phi'^2}\frac{d\gamma}{d\rho}\right) = \frac{9\nu_1}{\frac{n+1}{2}\nu_1 + \frac{m+1}{2}\nu_2 p_{nm}} \gamma_A \gamma^n + \frac{9 p_{nm}\nu_2}{\frac{n+1}{2}\nu_1 + \frac{m+1}{2}\nu_2 p_{nm}} \gamma_P \gamma^m \tag{11}$$

with the boundary conditions $\gamma_i\big|_{\rho=1} = 1$ and $\left(\partial\gamma_i/\partial\rho\right)\big|_{\rho=0} = 0$.

From the resulting concentration profiles the effect of intraparticle mass transport limitations on the effectiveness of the oxygen consumption and the product selectivity can be calculated, under the conditions listed above.

4.2.1 Effect on particle effectiveness for oxygen consumption $(\nu_1 = \nu_2 = 1)$

The particle effectiveness concerning the consumption of oxygen is given by:

$$\eta_{O_2} = \frac{\nu_1\langle r_1\rangle + \nu_2\langle r_2\rangle}{r_{1b} + \nu_2 r_{2b}} = \frac{\int_0^R 4\pi r^2 \nu_1 k_1 c_A c^n \, dr + \int_0^R 4\pi r^2 \nu_2 k_2 c_P c^m \, dr}{\frac{4\pi}{3}R^3\left(\nu_1 k_1 c_{Ab} c_b^n + \nu_2 k_2 c_{Pb} c_b^n\right)}$$

$$= 3\frac{\nu_1\int_0^1 \rho^2 \gamma_A \gamma^n \, d\rho + \nu_2 p_{nm}\int_0^1 \rho^2 \gamma_P \gamma^m \, d\rho}{\nu_1 + \nu_2 p_{nm}} = \frac{\nu_1\langle \gamma_A \gamma^n\rangle + \nu_2 p_{nm}\langle \gamma_P \gamma^m\rangle}{\nu_1 + \nu_2 p_{nm}} \tag{12}$$

$\langle x\rangle$ represents the spatial average of variable x.

Fig. 2 shows the particle effectiveness factor concerning the consumption of oxygen for two sets of reaction orders and p_{nm} ranging from 0.01 to 2.

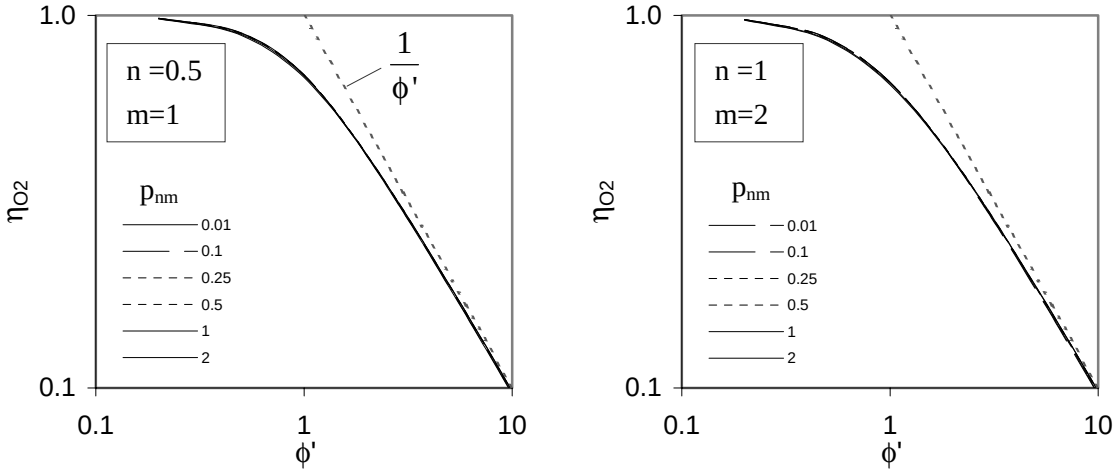

Fig. 2 Particle effectiveness concerning consumption of oxygen (η_{O2}) as a function of the modified Thiele-modulus for different values of p_{nm} ($c_b/c_{Ab}=c_b/c_{Pb}=0.1$). (a) n=0.5/m=1 and (b) n=1/m=2.

The effectiveness factor η_{O2} is virtually independent (for n,m ≥ 0.5) of the ratio of the reaction rates of the primary and secondary reaction p_{nm} (≤2) (see Fig. 2), and can very well be described by:

$$\eta_{O_2} = \frac{1}{3\phi'^2}\left(\frac{3\phi'}{\tanh(3\phi')} - 1\right) \qquad (13)$$

which is the analytical solution for a single, first order reaction (Bird, Steward, Lightfoot, 1960). Only for reaction orders close to n,m=0 the numerically calculated particle effectiveness is slightly higher than that predicted with the above equation at intermediate values of the Thiele-modulus ϕ' (e.g. $\phi'=1$ and n=0.1: $\eta_{O2}=0.74$ instead of 0.67).

Nevertheless, the used definition of the Thiele-modulus gives a very good approximation of the particle effectiveness factor η_{O2} for all relevant reaction orders and all ratios of the reaction rates of the consecutive and primary reaction p_{nm}.

It should be noted, that the consumption of A and the production of W are generally effected differently by the formed concentration profiles. This effect can neither be described by the presented modified Thiele-modulus of the oxygen consumption, nor by moduli defined for the single reactions (Appendix A).

4.2.2 Effect on particle selectivity $(\nu_1 = \nu_2 = 1)$

The selectivity with respect to the bulk concentration is directly correlated to p_{nm} and takes the value of zero, if the rates of wanted and unwanted reaction are equal:

$$\sigma_b = \frac{k_1 c_{Ab} c_b^n - k_2 c_{Pb} c_b^m}{k_1 c_{Ab} c_b^n} = 1 - p_{nm} \tag{14}$$

The actual product selectivity is given by:

$$\langle\sigma\rangle = \frac{\int_0^R 4\pi r^2 k_1 c_A c^n \, dr - \int_0^R 4\pi r^2 k_2 c_P c^m \, dr}{\int_0^R 4\pi r^2 k_1 c_A c^n \, dr} = 1 - \frac{\int_0^1 \rho^2 \frac{k_1 c_{Pb} c_b^m}{k_1 c_{Ab} c_b^n} \gamma_p \gamma^m \, d\rho}{\int_0^1 \rho^2 \gamma_A \gamma^n \, d\rho}$$

$$= 1 - p_{nm} \frac{\langle \gamma_P \gamma^m \rangle}{\langle \gamma_A \gamma^n \rangle} \tag{15}$$

The effect of intraparticle mass transfer is indicated by the differences in σ_b and $\langle\sigma\rangle$. In analogy to the effectiveness factor, a ratio F_σ of selectivity with and without transport limitation could be defined as,

$$F_\sigma = \frac{\langle\sigma\rangle}{\sigma_b} = \left(1 - p_{nm} \frac{\langle \gamma_P \gamma^m \rangle}{\langle \gamma_A \gamma^n \rangle}\right) \Big/ \left(1 - p_{nm}\right) \tag{16}$$

However, this ratio of the product selectivities is not very illustrative, and is impractical if p_{nm} approaches 1. Furthermore, for p_{nm} values above unity, F_σ takes values below 1, since $<\sigma>$ is less negative than $\sigma_b = 1 - p_{nm} < 0$, as illustrated in Fig. 3.

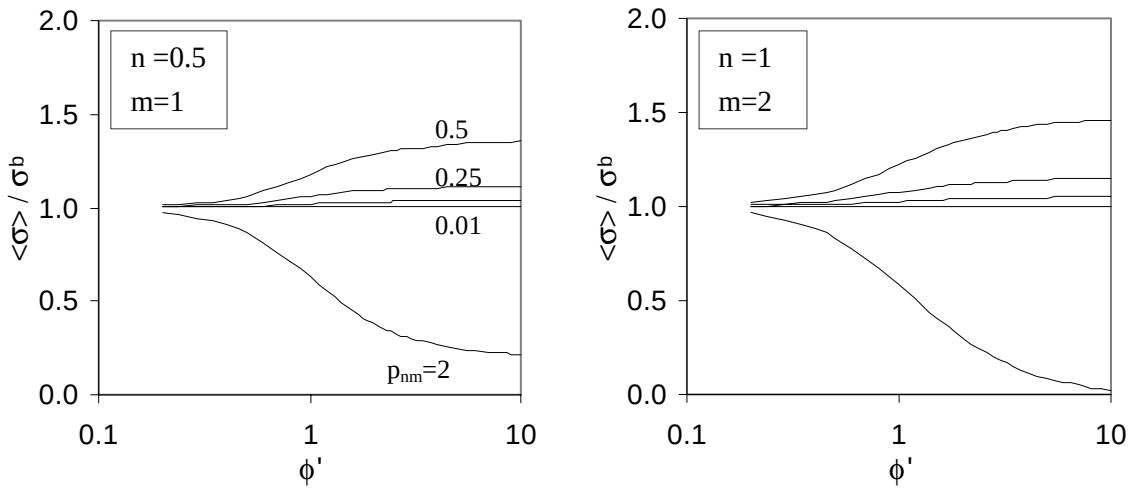

Fig. 3 Influence of intraparticle transport limitations on the average product selectivity as function of the modified Thiele-modulus for different values of p_{nm} (c_b/c_{Ab}=0.1 and c_b/c_{Pb}=0.1). (a) n=0.5/m=1 and (b) n=1/m=2.

Therefore, the following definition is chosen to elucidate the effect of intraparticle diffusion limitations on the product selectivity:

$$F_{1-\sigma} = \frac{1 - \langle\sigma\rangle}{1 - \sigma_b} = \frac{\langle \gamma_P \gamma^m \rangle}{\langle \gamma_A \gamma^n \rangle} \tag{17}$$

The effect of intraparticle mass transfer limitations on the product selectivity is shown in Fig. 4 as a function of the modified Thiele-modulus for two sets of reaction orders. The figure clearly shows that the selectivity calculated with the bulk concentrations underpredicts the actual selectivity that takes the concentration profile inside the particle into account. Due to the higher oxygen dependency of the consecutive reaction, the reaction rate of this undesired reaction is stronger decreased than the main reaction, resulting in improved product selectivity.

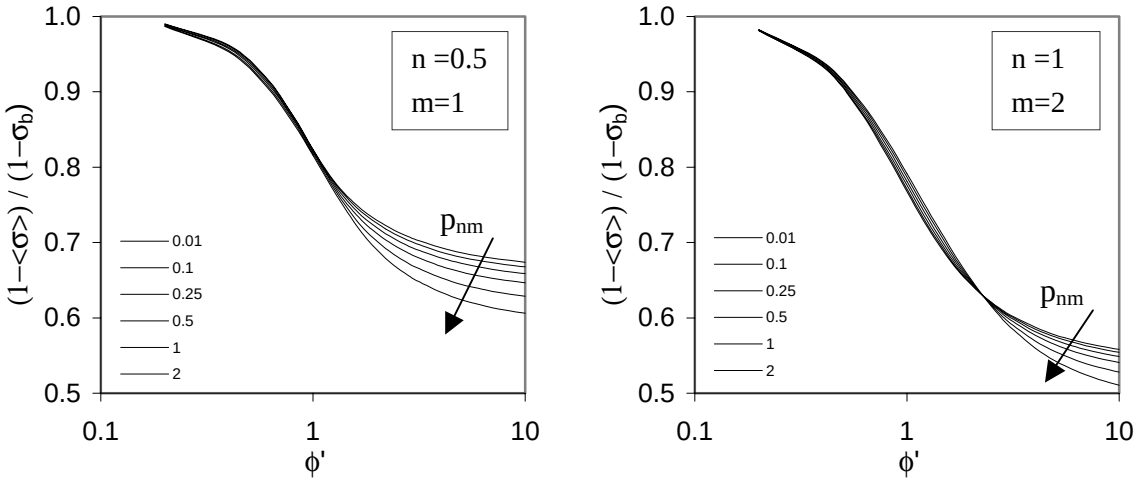

Fig. 4 Influence of intraparticle transport limitations on the average product selectivity as function of the modified Thiele-modulus for different values of p_{nm} (c_b/c_{Ab}=0.1 and c_b/c_{Pb}=0.1). (a) n=0.5/m=1 and (b) n=1/m=2.

As can be concluded from Fig. 4, the selectivity gain caused by the oxygen profile inside the particle is larger for higher values of ϕ' and p_{nm}, i.e. at higher oxygen concentration gradients and at relatively higher reaction rates of the consecutive reaction.

The increase of the catalyst particle size (with a corresponding increase of ϕ') thus results in an improvement of the product selectivity as long as the oxygen concentration in the gas phase is small compared to the concentrations of A ($c_b < \nu_1 c_{Ab}$) and P. This effect has been reported in the literature for the oxidative coupling of methane both as a result of model calculations (Reyes et al., 1993; *intrapellet oxygen sieving*) and as experimental result (Follmer et al., 1989). Reyes et al. conclude that low oxygen concentrations permit the use of larger pellets. They also show that the oxygen concentration has to be low compared to that of the hydrocarbons.

Follmer et al. found in a packed bed reactor for the same oxygen conversion increased product selectivities for larger catalyst pellets. But, their reaction scheme shows a parallel route of coupling (n=0.8) and combustion (m=1.6). In case of a consecutive reaction scheme, however, the concentration of the intermediate product is low near the inlet of the packed bed reactor, and thus the intraparticle mass transport limitations have a negative influence on the

product selectivity. In Chapter 5, therefore, the effect of the particle size on the product selectivity will be investigated as an integral result over the reactor length.

If the oxygen concentration is of the same order of magnitude of the hydrocarbon concentrations, transport limitations in the particle resulting in a decreased concentration of A and an increased concentration of P (see Fig. 1) can however effect a selectivity loss especially at high selectivities. This is illustrated in Fig. 5 by comparing for two different concentration ratios (a) c_b/c_{Ab}=0.1 (full lines) and (b) c_b/c_{Ab}=1 (dashed lines).

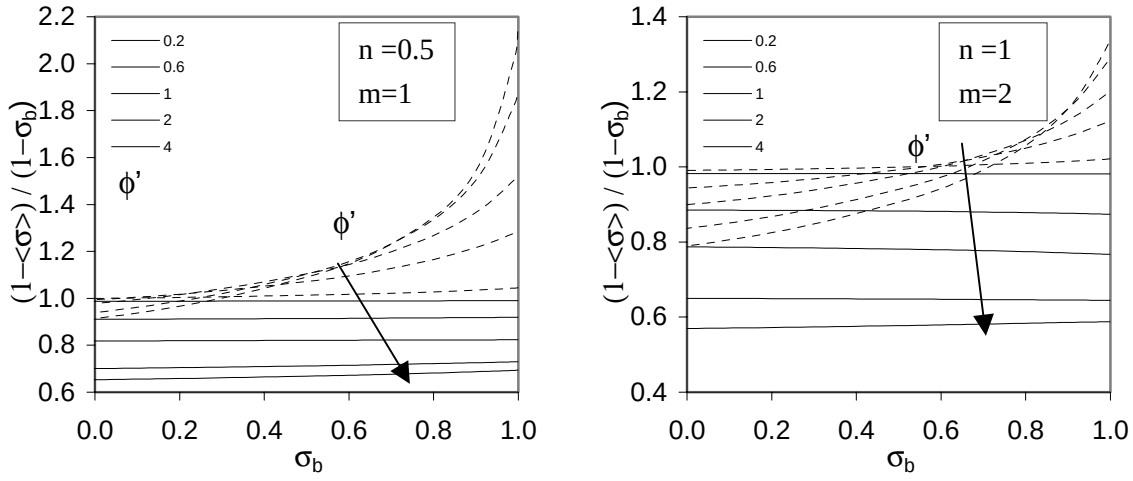

Fig. 5 Effect of radial oxygen profile inside the particle on the product selectivity as a function of the selectivity at bulk concentrations and the modified Thiele-modulus. Comparison of $c_b/c_{Ab}=c_b/c_{Pb}$=0.1 (full lines) and $c_b/c_{Ab}=c_b/c_{Pb}$=1 (dashed lines). (a) n=0.5/m=1 and (b) n=1/m=2.

For the model calculations in Fig. 5 stoichiometric constants $\nu_1 = 1$ and $\nu_2 = 1$ were chosen. In case of an oxidative dehydrogenation reaction system ($\nu_1 = 0.5$) the molar conversion rate of oxygen in primary reaction is only half of that of the conversion of A and the formation of P. Therefore, the c_b/c_{Ab}- ratio reduces below which the effect of the oxygen gradients exceeds that of the hydrocarbon concentration gradients, and the following correlation may serve as a guideline: $\max\left\{c_b/(\nu_1 c_{Ab}), c_b/(\nu_1 c_{Pb}), c_b/(\nu_2 c_{Pb})\right\} \le 0.1$

Furthermore, the effective diffusion coefficients have to be taken into account, if they differ for the molecules: $\max\left\{(c_b D)/(\nu_1 c_{Ab} D_A), (c_b D)/(\nu_1 c_{Pb} D_P), (c_b D)/(\nu_2 c_{Pb} D_P)\right\} \le 0.1$

4.2.3 Effect on particle selectivity for $\nu_{1,2} \neq 1$

If the oxygen concentration is small as defined by the above given criterion, the particle efficiency towards oxygen is independent of the stoichiometric coefficients $\nu_{1,2} \neq 1$. Furthermore, the effect on the product selectivity is as it was shown in Fig. 4, if $\nu_1 = \nu_2$,

which was tested for $\nu_{1,2} = 0.5$ ($c_b/c_{Ab}=c_b/c_{Pb}=0.05$) and $\nu_{1,2} = 2$ ($c_b/c_{Ab}=c_b/c_{Pb}=0.2$) for n=0.5/m=1 and n=1/m=2.

However, especially for Thiele-moduli above unity the effect of intraparticle mass transfer limitations on the product selectivity is influenced by the stoichiometric coefficients. This is shown for the reaction orders n=1/m=2 in Fig. 7 and for n=0.5 and m=1 in Fig. 6.

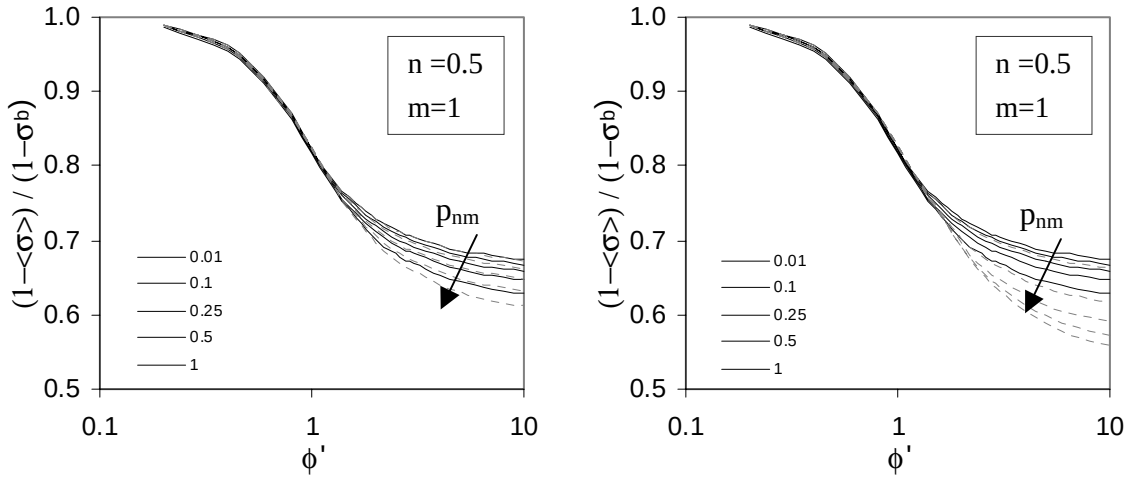

Fig. 6 Influence of the stoichiometric factors $\nu_{1,2}$. Full lines $\nu_1=\nu_2=1$ and $c_b/c_{Ab}=c_b/c_{Pb}=0.1$. Dashed lines (a) $\nu_1=0.5/\nu_2=1$ / $c_b/c_{Ab}=c_b/c_{Pb}=0.05$ and (b) $\nu_1=0.5/\nu_2=10$ / $c_b/c_{Ab}=c_b/c_{Pb}=0.05$.

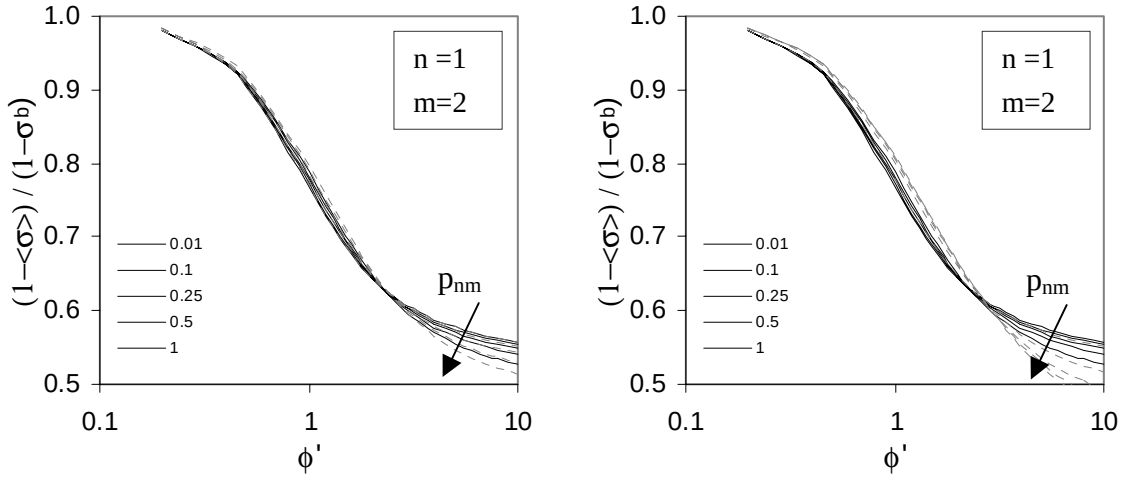

Fig. 7 Influence of the stoichiometric factors $\nu_{1,2}$. Full lines: $\nu_1=\nu_2=1$ and $c_b/c_{Ab}=c_b/c_{Pb}=0.1$. Dashed lines: (a) $\nu_1=1/\nu_2=2$ / $c_b/c_{Ab}=c_b/c_{Pb}=0.1$ and (b) $\nu_1=0.5/\nu_2=10$ / $c_b/c_{Ab}=c_b/c_{Pb}=0.05$.

For smaller values of ν_1 (Fig. 6a) as well as for higher values of ν_2 (Fig. 7a) the effect of intraparticle mass transfer limitations on the product selectivity is larger compared to $\nu_1=\nu_2=1$, especially for higher values of p_{nm}. Here, $\nu_1=0.5/\nu_2=1$ and $\nu_1=1/\nu_2=2$ (same ratio ν_1/ν_2) result in the same curves.

In a PBMR an axial concentration profile of the target product P will prevail. Near the reactor entrance the concentration of the target product is very low, and a strong concentration profile inside the particle is easily formed with negative consequences for the intrinsic selectivity of a catalyst particle. A reduction of the oxygen concentration helps to reduce this selectivity loss. Consequently, it should be advised to add all oxygen distributively to the packed bed to keep the zone where the oxygen concentration exceeds that of the hydrocarbons (A or P) as small as possible. However, the effect of the initial drop of the intrinsic selectivity near the reactor entrance on the integral reactor selectivity has to be evaluated in order to find the optimal inlet oxygen concentration (see Chapter 5). The low oxygen level in the PBMR requires an increased reactor volume (n>0) compared to the FBR and, possibly, an increase of the size of the catalyst particles (pressure drop). Yet, in contrast to the FBR an increase of the particle diameter will not result in a selectivity loss.

4.3 Oxygen profiles over the reactor radius and its effect on the reactor performance

In a PBMR most of the oxygen is added via the membrane to the tubular packed bed. If the radial mass transport of oxygen from the membrane wall to the center of the bed is insufficient compared to the local oxygen consumption rate, radial concentration profiles can emerge. The membrane fluxes are driven by different transport mechanisms depending on the kind of membrane used, as for example atomar or ionic diffusion in case of selective membranes or combinations of molecular diffusion and convection in case of porous membranes. The permeation flow will usually be influenced by the radial transport in the packed bed. However, for two limiting situations the membrane flow can be assumed to be independent, such that the effect of the radial transport on the performance of the PBMR can be discussed here separately.

The first, perhaps hypothetical case, considers a diffusive membrane with a very high permeability that realizes an almost complete assimilation of the oxygen concentration on both sides of the membrane. Provided that the oxygen concentration in the packed bed close to the membrane is known and independent of the radial transport to the centerline of the packed bed and neglecting the effect of radial concentration gradients of the hydrocarbons, the situation is congruent with that of the catalyst particle in a bulk of known composition discussed in Section 4.2.

For the second case, that forms the basis for the further discussion in this section, it will be assumed that the transmembrane flow is dominated by convection and determined by the pressure drop between tube and shell side of the PBMR. Therefore, it can be assumed that the membrane permeation flow is independent of the oxygen concentration within the packed bed, and thus not influenced by radial transport limitations. In this case, the average oxygen concentration in a slab of the PBMR is in first instance not effected by the rate of the radial

mass transport. Only if the average oxygen consumption rate differs from the reaction rate of the averaged oxygen concentration, the average oxygen concentration is altered.
The effect of mass transfer limitations from the membrane wall to the centerline of the packed bed on the relative conversion $F_{R,n}$ and the relative selectivity $F_{1-\sigma}$ will be analyzed.

- conversion of A $$F_{R,n} = \frac{\text{spatially averaged consumption rate of A}}{\text{rate corresponding to spatially averaged concentration}} \quad (18)$$ and

- selectivity $$F_{1-\sigma} = \frac{\text{spatially averaged selectivity of W}}{\text{selectivity corresponding to spatially averaged concentration}} \quad (19)$$

Two situations can be distinguished, depending on whether radial transport limitations result in oxygen depletion in the center of the packed bed. Firstly, the effect of oxygen profiles over the reactor radius without oxygen depletion is studied assuming a parabolic radial oxygen profile to allow an easy analysis. Subsequently, the analysis is extended calculating the oxygen profile numerically, which also allows to study the effect of oxygen depletion.

4.3.1 Analytical evaluation of the effect of a parabolic radial oxygen profile

If oxygen is not depleted in the center, the effect on the performance of the PBMR can be evaluated analytically, assuming that the radial oxygen concentration profile can be approximated with a parabolic function. The ratio of the wall to the centerline concentration is denoted by $x=c_R/c_0$.

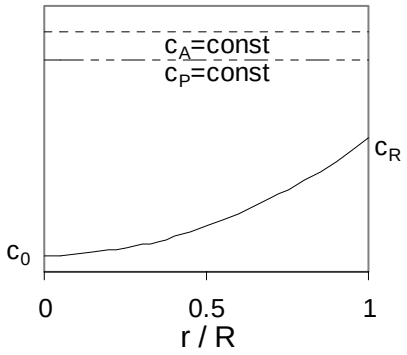

Fig. 8 Assumed radial concentration profiles for oxygen and the hydrocarbons.

The average concentration over the parabolic profile equals the arithmetic average of the wall and centerline concentrations, as is easily found via:

$$\langle c \rangle = \frac{1}{\pi R^2} \int_0^R 2\pi r \left(c_0 + \frac{c_R - c_0}{R^2} r^2 \right) dr = \frac{c_R + c_0}{2} \quad (20)$$

The hydrocarbon concentrations c_A and c_P are assumed to be constant and can therefore be included in the kinetic rate constants, according to $k^* = (1-\varepsilon) k_{1,2} c_{A,P}$.

For an n^{th}-order reaction the reaction rate at the average concentration R(<c>) is given by:

$$R(\langle c \rangle) = k^* \langle c \rangle^n = k^* \left(\frac{c_R + c_0}{2} \right)^n \quad (21)$$

Which is compared with the average reaction rate <R(c)>:

$$\left\langle R(c)\right\rangle = \frac{\int_0^R 2\pi r k^* \left(c_0 + \frac{c_R - c_0}{R^2} r^2\right)^n dr}{\pi R^2} \tag{22}$$

Using substitution of $\xi = c_0 + \frac{c_R - c_0}{R^2} r^2$ and $\frac{d\xi}{dr} = 2\frac{c_R - c_0}{R^2} r$ the integration results in:

$$\left\langle R(c)\right\rangle = \frac{\int_{c_0}^{c_R} k^* \xi^n d\xi}{c_R - c_0} = k^* \frac{{c_R}^{n+1} - {c_0}^{n+1}}{(n+1)(c_R - c_0)} \tag{23}$$

An influence factor F_R is defined as the ratio of the above two reaction rates, which indicates the extent the average reaction rate in a slab of the PBMR changes when oxygen added via the membrane is not uniformly distributed over the tube radius.

$$F_{R,n} = \frac{\left\langle R(c)\right\rangle}{R\left(\langle c\rangle\right)} = \frac{2^n}{(n+1)} \frac{{c_R}^{n+1} - {c_0}^{n+1}}{(c_R - c_0)(c_R + c_0)^n} = \frac{2^n}{(n+1)} \frac{x^{n+1} - 1}{(x-1)(x+1)^n} \tag{24}$$

The influence of the reaction order n and the steepness of the oxygen concentration profile x on F_R is shown in Table 1.

Table 1 Influence factor F_R as a function of concentration ratio $x=c_R/c_0$ and reaction order n.

x \ n	*0.25*	*0.5*	*0.75*	*1*	*1.5*	*2*	*3*
2	0.996	0.995	0.996	1.000	1.014	1.037	1.111
4	0.988	0.984	0.988	1.000	1.046	1.120	1.360
8	0.977	0.971	0.979	1.000	1.078	1.202	1.605
∞	0.951	0.943	0.961	1.000	1.131	1.333	2.000

For a first order reaction –as well as for a zeroth order reaction – the average reaction rate is identical to the reaction rate evaluated at the average concentration. In this case, the one-dimensional model ignoring radial concentration profiles and calculating only average concentrations is sufficient to determine the correct integral conversions and product selectivities.

For $0<n<1$ the presence of a radial profile due to mass transport limitations over the tube radius results in a lower value of F_R, which means that the average reaction rate is smaller than the reaction rate at the average concentration. However, this effect is quite small, at maximum ~5 %, even for steep gradients ($x \rightarrow \infty$). The maximum decrease is observed at about $n_{min}=0.5$ (for x=8: $n_{min}=0.48$). For higher reaction orders, for $n>1$, the reaction rate is underpredicted when the reaction rate is evaluated with the average concentration.

For two consecutive reactions with different orders in oxygen, the presence of a radial oxygen profile effects the intrinsic selectivity. The intrinsic selectivity of a slab of the catalyst bed is the ratio of the rate of net product formation to the rate of reactant consumption. As

before, the difference in intrinsic selectivity using the average concentration σ(<c>) and the average intrinsic selectivity <σ(c)> is investigated. The intrinsic selectivity is expressed by the rate of the average oxygen concentration $\sigma(\langle c\rangle)$ or by the radially averaged rates $\langle\sigma(c)\rangle$:

$$\sigma(\langle c\rangle)=\frac{R_1(\langle c\rangle)-R_2(\langle c\rangle)}{R_1(\langle c\rangle)}=1-\frac{R_2(\langle c\rangle)}{R_1(\langle c\rangle)} \tag{25}$$

$$\langle\sigma(c)\rangle=\frac{\langle R_1(c)\rangle-\langle R_2(c)\rangle}{\langle R_1(c)\rangle}=1-\frac{F_{R,m}}{F_{R,n}}\frac{R_2(\langle c\rangle)}{R_1(\langle c\rangle)} \tag{26}$$

The average selectivity <σ> is a function of the rate influence factors F_R for the two reactions and the selectivity of the average oxygen concentration.

The intrinsic selectivity σ(<c>) can take all values of the range [-∞,1], where negative values represent the situation that the product consumption rate exceeds its formation rate. In practice, this situation is avoided, because it represents a loss of product yield, and the reactor length should be reduced.

The effect of a radial parabolic concentration profile on the intrinsic selectivity is as before indicated with:

$$F_{1-\sigma}=\frac{1-\langle\sigma(c)\rangle}{1-\sigma(\langle c\rangle)}=\frac{F_{R,m}(x,n)}{F_{R,n}(x,m)} \tag{27}$$

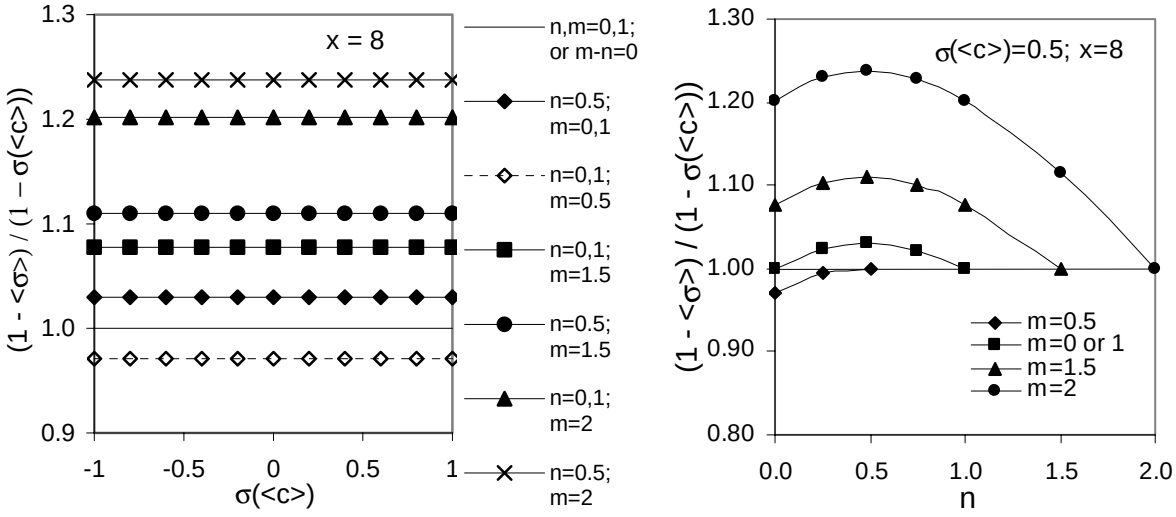

Fig. 9 Influence of a parabolic oxygen concentration profile (x=8) on the consecutive reaction scheme (a) as a function of the average concentration selectivity σ(<c>) for different sets of reaction orders m and n, (b) for different orders m as a function of order n at σ(<c>)=50 %.

The effect of calculating the intrinsic selectivity with the average concentration instead of the average reaction rate taking a parabolic concentration profile into account for x=8 is given in

Fig. 9, showing that this ratio $F_{1-\sigma}$ is indeed independent of the selectivity of the average concentration as opposed to F_{σ}[1].

For the reaction schemes that are interesting for distributive oxygen addition (m-n>0) several cases with different reaction orders for target and waste product formation rates have been included in the study of the effect of a radial profile on the product selectivity. Calculation of the intrinsic selectivity with the average concentration will overpredict the product selectivity compared to the selectivity where the radial profile has been taken into account for all m>1. The overprediction is stronger if the difference between the reaction orders is larger. Yet, a small selectivity underprediction could result if n and m $\in$ [0,0.5], respectively in the range $0 \leq n,m \leq 1$, if $|n-n_{min}|>|m-n_{min}|$ with a maximum deviation for n=0 and $m=n_{min}$ (see Fig. 9b).
For n=0.5 and m=1 the selectivity loss (i.e. overprediction of $\sigma(<c>)$ compared with $<\sigma(c)>$) caused by a radial profile (x=8) is however only 1.5 % at $\sigma(<c>)$=50 %. Other orders of the range $0 \leq n,m \leq 1$, which includes most of the reaction orders described in literature, result in even smaller selectivity losses.
In case of a consecutive reaction scheme, the intrinsic product selectivity is 100 % at the reactor inlet and decreases as the conversion proceeds and the intermediate product concentration increases. The strongest influence of a radial profile is therefore observed at the end of the PBMR. The effect on the reactor selectivity is calculated as an integral over the entire reactor length.
Finally, it is noted that the presented approach assuming a parabolic concentration profile is not applicable to situations in which oxygen depletion occurs in the center of the tube. This will be considered in the next paragraph.

4.3.2 Numerical calculation of the effect of a radial oxygen profile

In a second approach, the oxygen profile is no longer assumed *a priori*, but calculated by solving the diffusion equation for a slab of a PBMR. The amount of oxygen added to the slab of the packed bed is independent of the concentration inside the reactor. A radial concentration profile is established from the membrane wall to the center of the packed bed, where the gradients depend on the relative rates of mass transfer and reaction. The radial concentration profile is determined by two dimensionless parameters, the modified Thiele-modulus ϕ'' defined as

$$\phi'' = \frac{R}{2}\sqrt{\frac{\frac{n+1}{2}\nu_1 k_1^* \langle c\rangle^{n-1} + \frac{m+1}{2}\nu_2 k_2^* \langle c\rangle^{m-1}}{D}} \qquad (28)$$

[1] In Appendix B the corresponding graph is given for $F_{\sigma} = \langle\sigma(c)\rangle / \sigma(\langle c\rangle)$, which demonstrates that this definition is not useful in this study.

and the ratio of the oxygen consumption rates in the secondary and the primary reaction

$$p_{nm} = \frac{k_2 \langle c_P \rangle}{k_1 \langle c_A \rangle} \langle c \rangle^{m-n} \quad \text{with } k_1^* = (1-\varepsilon) k_1 \langle c_A \rangle,\ k_2^* = (1-\varepsilon) k_2 \langle c_P \rangle \tag{29}$$

and the reaction orders n and m. Concentration gradients of the hydrocarbons are neglected here. Furthermore, pressure and temperature are assumed radially constant, which allows rewriting radial dispersion in terms of the concentration gradient. The radial profile can be calculated from:

$$\frac{D}{r} \frac{d}{dr} \left(r \frac{dc}{dr} \right) = \nu_1 k_1^* c^n + \nu_2 k_2^* c^m \tag{30}$$

with the boundary conditions $c\big|_{r=R} = c_R$ and $(dc/dr)\big|_{r=0} = 0$

Here, the radial dispersion coefficient D is assumed constant, which is indeed true for the core of the bed, where the bed porosity and the gas velocity are constant. Only close to the wall increased values for the radial dispersion coefficient are expected due to slip flow along the wall. The effect of the porosity function on the radial dispersion will be discussed in Chapter 6.

Introducing new dimensionless variables $\gamma = \frac{c}{\langle c \rangle}$ and $\rho = \frac{r}{R}$ yields

$$\frac{1}{\rho} \frac{d}{d\rho} \left(\frac{\rho}{\phi''^2} \frac{d\gamma}{d\rho} \right) = \frac{4\nu_1}{\frac{n+1}{2}\nu_1 + \frac{m+1}{2}\nu_2 p_{nm}} \gamma^n + \frac{4\nu_2 p_{nm}}{\frac{n+1}{2}\nu_1 + \frac{m+1}{2}\nu_2 p_{nm}} \gamma^m \tag{31}$$

with the corresponding boundary conditions $\gamma\big|_{\rho=1} = \gamma_M$ and $(d\gamma/d\rho)\big|_{\rho=0} = 0$.

The dimensionless concentration at the membrane wall (γ_M) is not known beforehand, but by definition $\langle \gamma \rangle = 1$. The ordinary differential equation is solved as a partial differential equation including an accumulation term with a false time step in order to calculate γ_M using $\langle \gamma \rangle = 1$. Initially, the concentration in the particle is put to $\gamma(r) = 1$, and $\gamma_M = 1$. After every time step the actual $\langle \gamma \rangle^t$ is calculated, and the boundary condition for the next time step is corrected: $\gamma_M^{t+1} = \gamma_M^t \big/ \langle \gamma \rangle^t$

4.3.2.1 Effect on the reactivity of the packed bed

The influence factors $F_{R,n}$ are determined by integration over the calculated radial oxygen concentration profile:

$$F_{R,n} = \frac{\langle R(c) \rangle}{R(\langle c \rangle)} = \frac{\int_0^R 2\pi r k_1^* c^n dr \Big/ \pi R^2}{k_1^* \left(\int_0^R 2\pi r c\, dr \Big/ \pi R^2 \right)^n} = \frac{\int_0^1 2\rho \gamma^n d\rho}{\left(\int_0^1 2\rho \gamma d\rho \right)^n} = \frac{\langle \gamma^n \rangle}{\langle \gamma \rangle^n} = \langle \gamma^n \rangle \tag{32}$$

Fig. 10 shows $F_{R,n}$ as a function of the modified Thiele-modulus ϕ''. For $\phi''<0.9$ the difference is less than 1 % (for n=0.5 and m=1). For higher values of ϕ'' the average reaction rate is increasingly overpredicted when using the reaction rate at the average concentration ($\phi''=2$:$F_{R,n}$ = 0.9 ÷ 0.94). For higher values for p_{nm} the ratio $F_{R,n}$ increases. Towards the centerline of the packed bed the oxygen concentration decreases. This decrease is the strongest for n=0. For a higher the reaction order the oxygen concentration profile is - compared at the same Thiele-modulus - less pronounced, because the reduction of oxygen concentration results in a decreased conversion rate further inside the catalyst, and with an increase of p_{nm} the overall reaction order of the oxygen consumption increases.

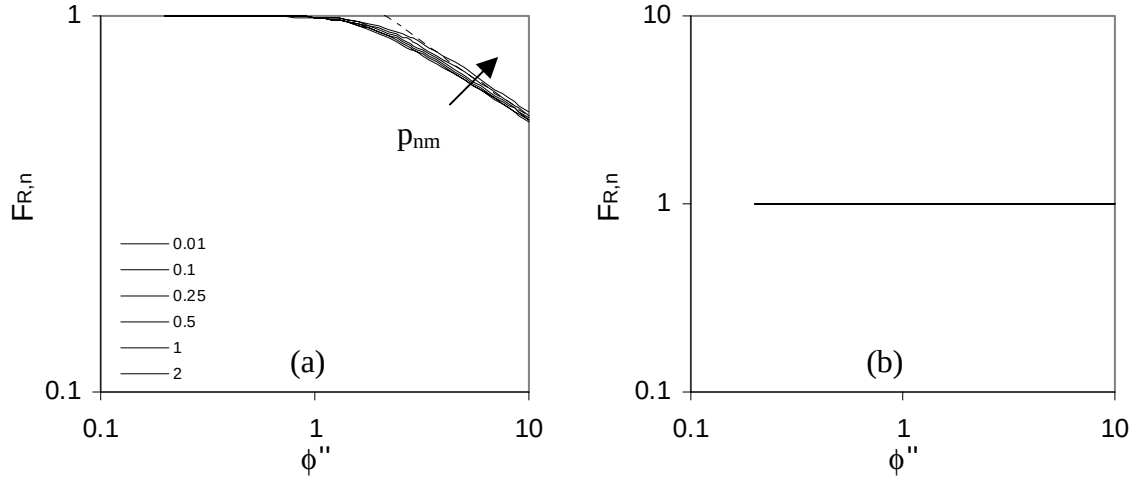

Fig. 10 Influence of transport limitations on the average rate of r_1 as a function of the modified Thiele-modulus for different ratios $p_{nm}=r_2/r_1$ for the reaction orders (a) n=0.5 and m=1 and (b) n=1 and m=2.

The dashed line in Fig. 10a represents an asymptotic solution for $p_{nm}\rightarrow 0$ (see Appendix C):

$$F_{R,n} \cong \left(\frac{1}{\phi''}\right)^{2(1-n)/(3-n)} \left(\frac{3-n}{n+1}\right)^{(n+1)/(3-n)} \qquad (33)$$

The average reaction rate of a first order reaction is not effected by transport limitations (see Fig. 10b) even in case of oxygen depletion in the center of the packed bed under the assumptions made above that the membrane flux is fixed and that the effect of the concentration gradients of the hydrocarbons is negligible.

4.3.2.2 Effect of transport limitations on the product selectivity

The effect of transport limitations on the product selectivity is indicated by ratio of the selectivity losses $F_{1-\sigma}$ of the average selectivity $\langle\sigma(c)\rangle$ and selectivity of the average concentration $\sigma(\langle c\rangle)$

$$\left\langle \sigma(c) \right\rangle = \frac{\left\langle R_1(c) \right\rangle - \left\langle R_2(c) \right\rangle}{\left\langle R_1(c) \right\rangle} = 1 - \frac{\int_0^R 2\pi r\, k_2^* c^m dr \Big/ \pi R^2}{\int_0^R 2\pi r\, k_1^* c^n dr \Big/ \pi R^2} = 1 - \frac{k_2^* \langle c \rangle^m}{k_1^* \langle c \rangle^n} \frac{\int_0^1 2\rho\, \gamma^m d\rho}{\int_0^1 2\rho\, \gamma^n d\rho} = 1 - p_{nm} \frac{\langle \gamma^m \rangle}{\langle \gamma^n \rangle} \quad (34)$$

$$\sigma\left(\langle c \rangle\right) = \frac{R_1\left(\langle c \rangle\right) - R_1\left(\langle c \rangle\right)}{R_1\left(\langle c \rangle\right)} = 1 - \frac{k_2^* \left(\int_0^R 2\pi r\, c\, dr \Big/ \pi R^2 \right)^m}{k_1^* \left(\int_0^R 2\pi r\, c\, dr \Big/ \pi R^2 \right)^n} = 1 - \frac{k_2^* \langle c \rangle^m}{k_1^* \langle c \rangle^n} \frac{\left(\int_0^1 2\rho\, \gamma d\rho \right)^m}{\left(\int_0^1 2\rho\, \gamma d\rho \right)^n} = 1 - p_{nm} \quad (35)$$

so that

$$F_{1-\sigma} = \frac{1 - \langle \sigma(c) \rangle}{1 - \sigma\left(\langle c \rangle\right)} = \frac{F_{R,m}(\phi, p_{nm}, n, m)}{F_{R,n}(\phi, p_{nm}, n, m)} = \frac{\langle \gamma^m \rangle}{\langle \gamma^n \rangle} \quad (36)$$

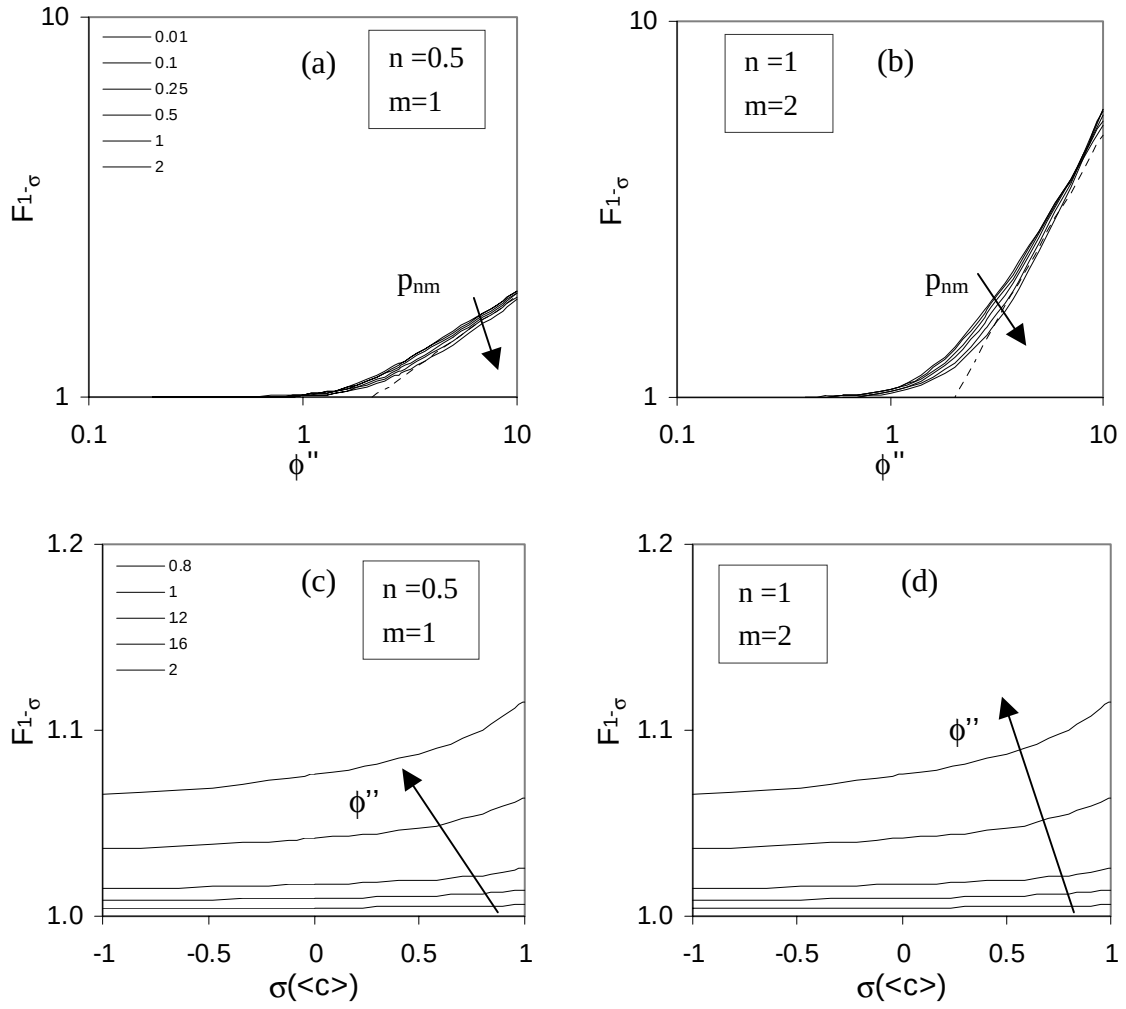

Fig. 11 Influence of transport limitations on the average product selectivity (a, b) as a function of the modified Thiele-modulus for different ratios $p_{nm}=r_2/r_1$, (c, d) as a function of the selectivity of the average concentration for different modified Thiele-moduli. For the reaction orders: (a, c) n=0.5/m=1 and (b, d) n=1/m=2.

Fig. 11 illustrates the dependence of $F_{1-\sigma}$ on the Thiele-modulus $\phi"$ and the ratio of oxygen consumption rates in the consecutive and main reaction p_{nm} for two sets of reaction orders n=0.5/m=1 and n=1/m=2.

Recalling that in Fig. 9 for a parabolic oxygen profile without oxygen depletion in the center of the tube $F_{1-\sigma}$ is not a function of $\sigma(\langle c \rangle)$, it should be noted that in Fig. 11c,d the full lines represent a constant parameter p_{nm}, while in Fig. 9a the oxygen concentration profile (ratio x) is kept constant.

As can be seen from Fig. 11 the selectivity calculated with the average concentration again overpredicts the actual average selectivity. It can be concluded from Fig. 11 that the oxygen depletion increases the selectivity overprediction.

Furthermore, with increasing Thiele-modulus and decreasing effective reaction order, which increases with the contribution of the consecutive reaction (p_{nm}), the profile in the oxygen concentration gets more pronounced and the effect on the product selectivity (i.e. overprediction) increases as shown in Fig. 11. The selectivity calculated with the average oxygen concentration <c> is directly correlated to $p_{nm}=1-\sigma(<c>)$, thus that the selectivity loss is higher at high selectivities $\sigma(<c>)$, compared at the same Thiele-modulus (see Fig. 11 c,d).

The dashed line in Fig. 11a,b represents an asymptotic solution for $p_{nm} \rightarrow 0$ (Appendix C):

$$F_{1-\sigma} \cong \frac{n+1}{2m-n+1}\left(\phi" \frac{3-n}{n+1}\right)^{2(m-n)/(3-n)} \qquad (37)$$

Only, in the range $0 \leq n,m \leq 1$, the selectivity loss calculated with the average concentration can be overpredicted, if $|n-n_{min}|>|m-n_{min}|$. Fig. 12b shows that for higher values of the Thiele-modulus this effect is turned to its opposite, which is caused by the development of depletion of oxygen in the center of the bed. The depletion results in an increased average oxygen concentration in the regions where the reactions still take place, and thus reduces the product selectivity.

Depletion influences the selectivity as well in case of the pair of reaction orders (n=0 and m=1), where originally no influence of the oxygen concentration profile was predicted (see Fig. 12a).

If the radial oxygen concentration profile has no effect on the average reactivity and product selectivity, a simple one-dimensional balance is sufficient to model the PBMR. On the other side, the above-presented graphs can give a qualitative estimation of the reliability of the 1-D model and an indication if a 2-D model is required for a better calculation of the average reactivity and product selectivity.

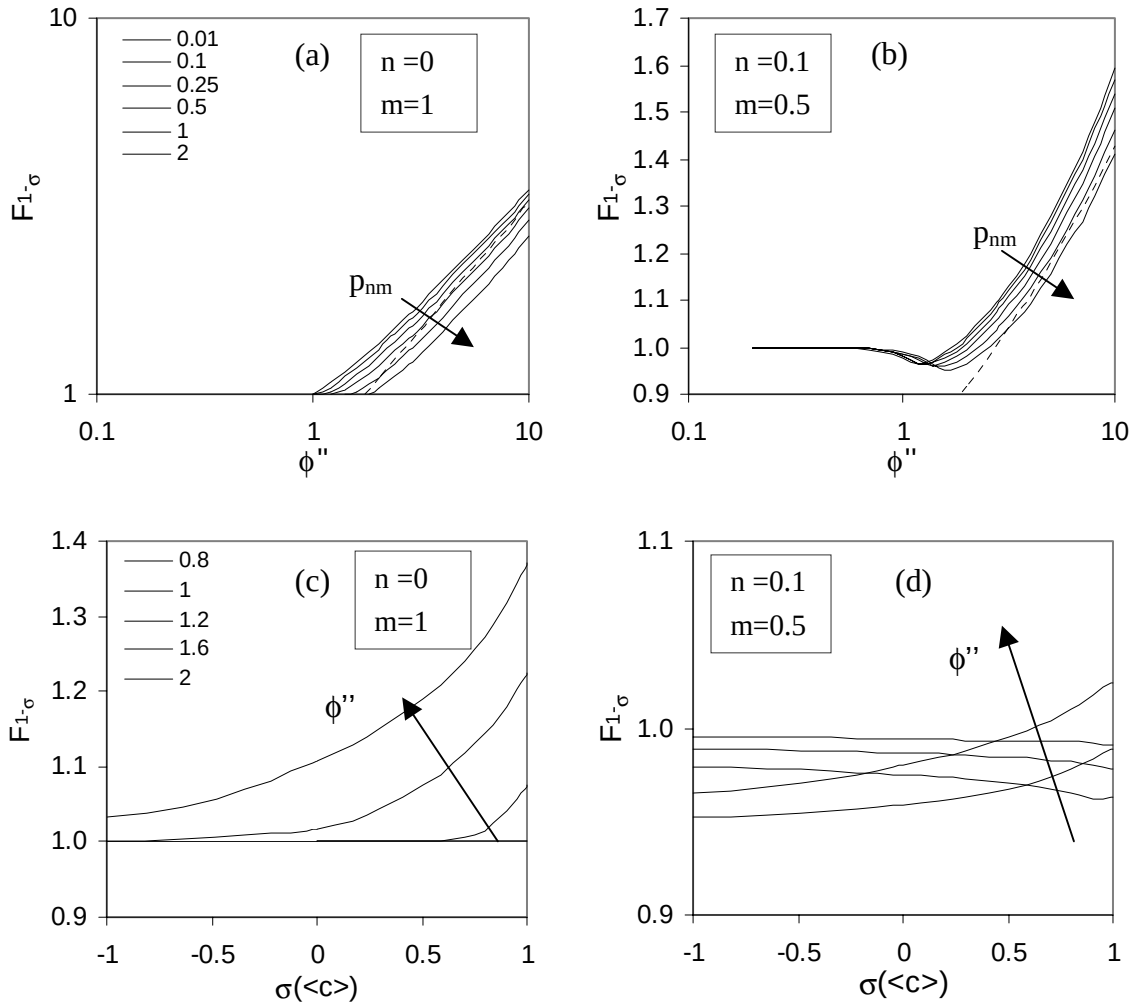

Fig. 12 Influence of transport limitations on the average product selectivity (a, b) as a function of the modified Thiele-modulus for different ratios $p_{nm}=r_2/r_1$, (c, d) as a function of the selectivity of the average concentration for different modified Thiele-moduli. For the reaction orders: (a,c) n=0 and m=1and (b,d). n=0.1 and m=0.5

4.4 Relative significance of intraparticle and membrane to centerline transport limitations

In the following the relative significance of the two transport limitations discussed in this chapter is outlined, comparing which transport limitation is more relevant, the intraparticle or that from the membrane to centerline of the packed bed.

Therefore, the ratio of the two transport moduli, $\phi"$ and ϕ', is formed:

$$\text{Tube: } \phi" = \frac{R_t}{2}\sqrt{\frac{\frac{n+1}{2}\nu_1 k_1^* \langle c\rangle^{n-1} + \frac{m+1}{2}\nu_2 k_2^* \langle c\rangle^{m-1}}{D_r}} \quad \text{with } k_1^* = (1-\varepsilon)\, k_1 \langle c_A\rangle \qquad (38)$$

With ε representing the porosity of the packed bed.

Particle: $$\phi' = \frac{R_p}{3}\sqrt{\frac{\frac{n+1}{2}\nu_1 k_1 c_{Ab} c_b^{n-1} + \frac{m+1}{2}\nu_2 k_2 c_{Pb} c_b^{m-1}}{D_{eff}}} \quad (39)$$

Starting from a pseudo-homogeneous, one-dimensional model, the concentrations agree with the bulk concentration of the heterogeneous and the average concentrations of the 2-D model: $c_i = c_{ib} = \langle c_i \rangle$

The ratio of the moduli is thus given by:

$$\frac{\phi''}{\phi'} = \frac{3}{2}\frac{d_t}{d_p}\sqrt{(1-\varepsilon)}\sqrt{\frac{D_{eff}}{D_r}} \quad (40)$$

Two limiting cases are now distinguished. Firstly, laminar flow as can be expected for usual laboratory scale reactors because of the low flow rates, and secondly, turbulent flow representing the situation in industrial scale PBMRs.

The following correlation for the dispersion in the core of the packed bed proposed by Tsotsas and Schlünder (1988) is used (see discussion on dispersive transport in packed bed in Chapter 6):

$$D_r = \left(1-\sqrt{1-\varepsilon}\right)D_m + \frac{u d_p}{8} \quad (41)$$

4.4.1 Laminar flow

The catalyst is assumed to be macro-porous, so that the effective diffusion is determined by molecular diffusion: $D_{eff} = D_{eff,m} = (\varepsilon/\tau)_p D_m$ (42)

For the porosity of the packed bed ε_{bed} a value of 0.37 is assumed, and for ratio of porosity and tortuosity of the catalyst particle $(\varepsilon/\tau)_p$=0.15.

$$\frac{\phi''}{\phi'} = \frac{3}{2}\frac{d_t}{d_p}\sqrt{(1-\varepsilon)}\sqrt{\frac{(\varepsilon/\tau)_p}{\left(1-\sqrt{1-\varepsilon}\right)}} \approx \frac{d_t}{d_p} \quad (43)$$

The transport limitations from the membrane tube to the core of the packed bed are much more important than the intraparticle transport limitations.

If the effective diffusion coefficient in the particles is determined by Knudsen diffusion ($D_{eff} = D_{eff,K}$), a very small Knudsen-coefficient of $D_K = 0.01 \cdot D_m$ is required for a diameter ratio of d_t/d_p =10. A catalyst particle characterized by such a low effective diffusion is not likely to be of commercial interest.

4.4.2 Turbulent flow

Again, the catalyst is assumed to be macro-porous. The ratio of the transport moduli is now:

$$\frac{\phi''}{\phi'} = \frac{3}{2}\frac{d_t}{d_p}\sqrt{(1-\varepsilon)}\sqrt{\frac{D_{eff}}{ud_p/8}} \approx 3.4\frac{d_t}{d_p}\sqrt{\frac{(\varepsilon/\tau)_p D_m}{ud_p}} = 1.3\frac{d_t}{d_p}\sqrt{\frac{D_m}{ud_p}} \qquad (44)$$

Reformulating using the definition of the Reynolds and the Schmidt-number,

$$\frac{\phi''}{\phi'} \approx 1.3\frac{d_t}{d_p}\sqrt{\frac{\nu}{ud_p}}\sqrt{\frac{D_m}{\nu}} = 1.3\frac{d_t}{d_p}\sqrt{\frac{1}{Re}}\sqrt{\frac{1}{Sc}} \qquad (45)$$

and assuming a value of Sc=0.8[1] results finally in

$$\frac{\phi''}{\phi'} \approx 1.5\frac{d_t}{d_p}\frac{1}{\sqrt{Re}} \qquad (46)$$

For a packed bed with diameter ratio d_t/d_p =10, the transport limitations from the membrane wall to the center of the bed is more significant up to a Reynolds-number of about 200, which is not an unrealistic value for an packed bed reactor of industrial scale.

4.5 Discussion and conclusions

In partial oxidation systems in which the formation rate for the target product shows a lower dependency on the oxygen concentration than the formation of the waste product, the product selectivity can be increased by keeping the oxygen concentration in the reactor low. If the target product is the intermediate of a series reaction, packed bed reactors are preferred due to the low back-mixing. However, a standard packed bed reactor is characterized by one premixed feed and high inlet concentrations. A PBMR offers the possibility of continuous feeding of oxygen to replace the consuming oxygen and thus combine low oxygen concentrations with high reactant conversions.

Yet, the discrete feeding of oxygen over the membrane wall and the low oxygen concentrations imply possible problems with the distribution of oxygen from the membrane wall to the centerline of the packed bed as well as from the bulk gas phase to the center of a particle. If the reaction order in oxygen of the main reaction is n<1, the mass transfer limitations become increasingly more important, when the oxygen concentration level is reduced. The effect of such mass transfer limitations on intrinsic product selectivity and intrinsic activity of a catalyst particle and a slab of the PBMR were investigated in this chapter.

In literature PBMRs usually are modeled with a pseudo-homogeneous, one-dimensional reactor model. This model, however, can only be applied, if the oxygen is well distributed

[1] For ODH of methanol at 250°C. For ODH of ethylbenzene at 277°C Sc=1.4 can be applied.

within the packed bed and the catalyst particles and if mass transfer limitations have little effect on the result.

Intraparticle mass transport limitations

When the concentration of oxygen in the gas phase is small compared to that of the hydrocarbons, the following modified Thiele-modulus can be defined using the concentrations in the gas bulk

$$\phi' = \frac{R}{3}\sqrt{\frac{\frac{n+1}{2}\nu_1 k_1 c_{Ab} c_b^{n-1} + \frac{m+1}{2}\nu_2 k_2 c_{Pb} c_b^{m-1}}{D}} \tag{47}$$

and the effectiveness of the particle towards the conversion of oxygen is well approximated by

$$\eta_{O_2} = \frac{1}{3\phi'^2}\left(\frac{3\phi'}{\tanh(3\phi')} - 1\right) \tag{48}$$

which is the analytical solution for a single, first order reaction (Bird, Steward, Lightfoot, 1960).

However, the established oxygen concentration profile reduces the reaction rate of the consecutive reaction due to the higher reaction order more than the rate of the product formation. Therefore, the product selectivity is increased as a consequence of the transport limitations. The spatially averaged selectivity over the catalyst particle is higher than the selectivity corresponding to the gas phase concentrations for $c_b < \min(\nu_2 c_{Pb}, \nu_1 c_{Ab})$.

Yet, the product selectivity is not a simple function of the above described Thiele-modulus, it depends furthermore on the ratio of the secondary to the primary reaction rates p_{nm} and on the set of reaction orders n and m.

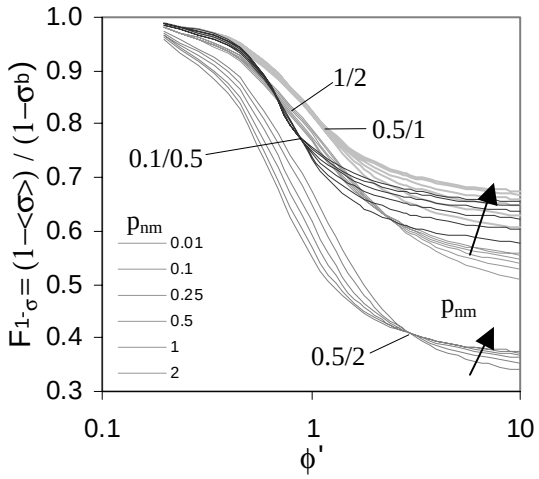

Fig. 13 Influence of intraparticle transport limitations on the average product selectivity as function of the modified Thiele-modulus for different values of p_{nm} ($c_b/c_{Ab}=c_b/c_{Pb}=0.1$, $\nu_{1,2}=1$) and orders n/m indicated in graph.

Mass transport from the membrane wall to the centerline of the packed bed

In the PBMR, oxygen is distributive added to the packed bed via a membrane. If the transport from the membrane wall to the centerline of the packed bed is insufficient compared to the local consumption rate, concentration profiles are established. Provided that the membrane

flux is independent of the concentrations at the membrane wall and that the radial transport is dominated by dispersion, the mass transport problem can be characterized by the characteristic number (disregarding the effect of radial concentration profiles of the hydrocarbon).

$$\phi'' = \frac{R}{2}\sqrt{\frac{\frac{n+1}{2}\nu_1 k_1^* \langle c\rangle^{n-1} + \frac{m+1}{2}\nu_2 k_2^* \langle c\rangle^{m-1}}{D}} \qquad (49)$$

The effect of the radial transport limitations on the average reaction rate of the primary reaction and the product selectivity, $F_{R,n}$ and $F_{1-\sigma}$, are presented in Fig. 14 as a function of ϕ'' for p_{nm}=0.01 together with the asymptotic solutions.

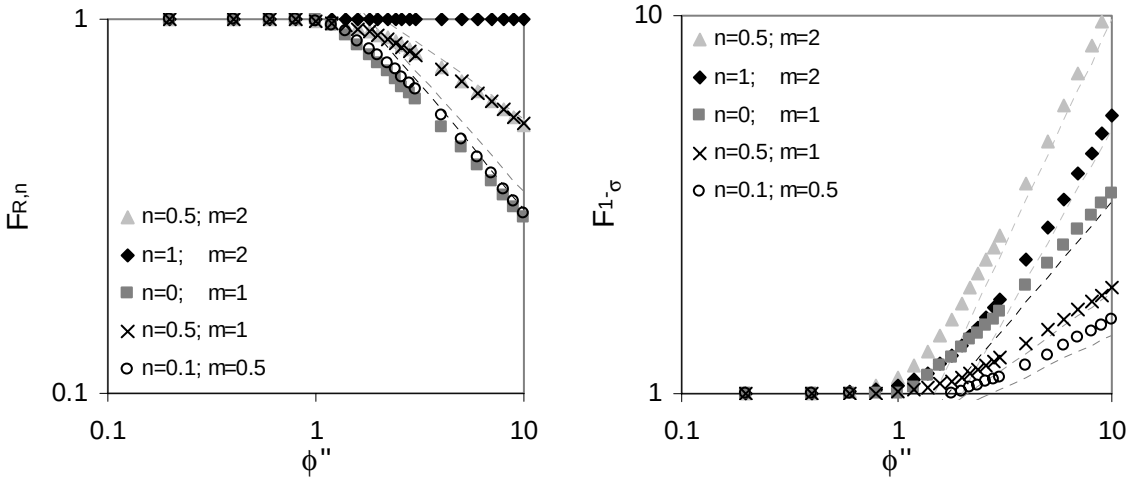

Fig. 14 $F_{R,n}$ and $F_{1-\sigma}$ as a function of the Thiele-modulus ϕ'' for p_{nm}=0.01 and the asymptotic solutions.

Fig. 14 shows that the effect of radial oxygen concentration profiles is negligible small for ϕ''<1. PBMR with higher values of ϕ'' should be modeled by a two-dimensional reactor model.

Relative significance of intraparticle and membrane to centerline transport limitations

In lab-scale PMBRs the transport limitations from the membrane wall to the center of the packed bed are prevailing. In PBMR of industrial scale the intraparticle transport limitations become more severe at high Reynolds-numbers. For a packed bed with diameter ratio d_t/d_p =10 Reynolds numbers ranging between about 100 and 200 are required, depending on the reaction system.

Intrinsic versus integral effects

In the present chapter the effect of transport limitations on the activity and product selectivity were investigated intrinsically for a single particle or a thin slab of the packed bed. The

effects are quite large and make the use of heterogeneous, two-dimensional models advisable. However, there are good reasons to expect that the integral effect of transport limitations is different.

- The intraparticle transport was discussed under the assumption that the hydrocarbon concentrations are large compared to that of oxygen. Yet, near the reactor inlet the concentration of the intermediate product is smaller than that of oxygen, with a consequently negative effect on the integral product selectivity.
- In the balance of the oxygen concentration of a slab of the PBMR, the axial transport of oxygen was neglected.
- Both reduced activity and improved selectivity of one increment of the packed bed results an increased oxygen concentration downstream of the reactor, with an opposite effect on activity and selectivity.

Therefore, in the next chapters the integral effects will be investigated.

NOTATION

Latin letters

c	concentration [mol / m^3]
D	diffusion or dispersion coefficient [m^2 / s]
f	factor by which oxygen concentration is reduced
F	factor by which a reaction rate or selectivity is increased due to mass transport limitations
k	rate constant [mol / m^3 s bar^{1+n}], [mol / m^3 s bar^{1+m}]
k^*	rate constant for the packed bed ((1-ε) k $c_{A,P}$) [mol / m^3 s bar^n], [mol / m^3 s bar^m]
m	reaction order in oxygen of reaction forming the waste product
n	reaction order in oxygen of reaction forming the target product
PBMR	packed bed membrane reactor
R	radius of catalyst particle or of membrane tube [m]
r_j	rate of reaction j [mol / m^3 s]
r	axis is radial direction [m]
x	ratio of oxygen concentrations (=c_R/c_0)

Greek letters

γ	dimensionless concentration (=c/c_R)
ε	porosity
η	yield
κ	ratio of the rate constants of consecutive and primary reaction (both first order)

ν stoichiometric coefficient

ξ substitution $\left(= c_0 + \frac{c_R - c_0}{R^2} r^2 \right)$

ρ dimensionless coordinate in radial direction (=r/R)

σ intrinsic selectivity

τ tortuosity

Subscripts

0 at the center of catalyst / at centerline of tube / base case

A,P,W hydrocarbon reactant, target and waste product

b gas bulk value

m molecular

O_2 oxygen

p particle

r radial

R at the outer radius of a catalyst particle or a tubular packed bed

t membrane tube

Dimensionless numbers

ϕ Thiele-modulus $\left(= L\sqrt{\frac{k_1 c_b^{n-1}}{D}} \right)$

ϕ' modified Thiele-modulus $\left(= L\sqrt{\left(\frac{n+1}{2} \nu_1 k_1 c_{Ab} c_b^{n-1} + \frac{m+1}{2} \nu_2 k_2 c_{Pb} c_b^{m-1} \right) \Big/ D} \right)$

with $L=R_p/3$ for spherical catalyst particle

ϕ'' modified Thiele-modulus $\left(= L\sqrt{\left(\frac{n+1}{2} \nu_1 k_1^* \langle c \rangle^{n-1} + \frac{m+1}{2} \nu_2 k_2^* \langle c \rangle^{m-1} \right) \Big/ D} \right)$

with $L = R_t/2$ for tubular packed bed

p_{nm} ratio of reaction rates in the secondary and primary reaction

sphere: $\left(= \frac{k_2 c_{Pb}}{k_1 c_{Ab}} c_b^{m-n} \right)$ tube: $\left(= \frac{k_2 \langle c_P \rangle}{k_1 \langle c_A \rangle} \langle c \rangle^{m-n} \right)$

$\langle x \rangle$ represents the spatial average of variable x

References

R.B. Bird, W.E. Stewart, E.N. Lightfoot, 1960, Transport phenomena, John Wiley & Sons, New York

V. Diakov. B. Blackwell, A. Varma, 2002, Methanol oxidative dehydrogenation in a catalytic packed-bed membrane reactor: experiments and model, *Chem. Eng. Sci. 57*, 1563-1569

G.Follmer, L.Lehmann, M. Baerns, 1989, Effect of transport limitations on C_{2+} selectivity in the oxidative methane coupling reaction using a NaOH/CaO catalyst, *Catalysis Today 4*, 323-332

D. Lafarga, M. A. Al-Juaied, C.M. Bondy, A. Varma, 2000, Ethylene epoxidation on Ag-Cs/α-Al_2O_3 catalyst: experimental results and strategy for kinetic parameter determination, *Industrial and Engineering Chemistry Research 39*, 2148-2156

M. Pedernera, R. Mallada, M. Menéndez, J. Santamaría, 2000, Simulation of an inert membrane reactor for the synthesis of maleic anhydride, *AIChE Journal 46*, 2489-2498

S.C. Reyes, C.P. Kelkar, E. Iglesia, 1993, Kinetic-transport models and design of catalysts and reactors for the oxidative coupling of methane, *Catalysis Letters 19*, 167-180

G.W. Roberts, 1972, The selectivity of porous catalysts: parallel reactions, *Chem. Eng. Sci. 27*, 1409-1420

G.V. Shakhnovich, I.P. Belomestnykh, N.V. Nekrasov, M.M. Kostyukovsky, S.L. Kiperman, 1984, Kinetics of ethylbenzene oxidative dehydrogenation to styrene over vanadia/magnesia catalyst, *Applied Catalysis 12*, 23-34

E. Tsotsas and E.U. Schlünder, 1988, Some remarks on channelling and on radial dispersion in packed beds, *Chem. Eng. Sci. 43*, 1200-1203

Appendix A Particle effectiveness of the consumption of A and the formation of W as function of different modified Thiele-moduli

In Section 4.2.1 it was shown that the particle efficiency for oxygen consumption can be described as a function of the modified Thiele-modulus ϕ'. Yet, the effect of intraparticle mass transfer limitations on the consumption of reactant A and the formation of W, η_A and η_W, cannot be described by the same analytical relation neither as a function of the same modified Thiele-modulus (Fig.- A-1, Fig.- A-2) nor by another moduli characterizing mass transfer and reaction rate of primary or consecutive reaction, ϕ'_A (Fig.- A-3) or ϕ'_W (Fig.- A-4).

A.1 Modified Thiele-modulus for oxygen consumption

Compared at the same ϕ' the radial profiles get less pronounced with increasing reaction order n, which explains, that the particle effectiveness related to the consumption of A increases with an increasing contribution of the second reaction, i.e. higher values of p_{nm} (if m>n), as can be seen in Fig.- A-1.

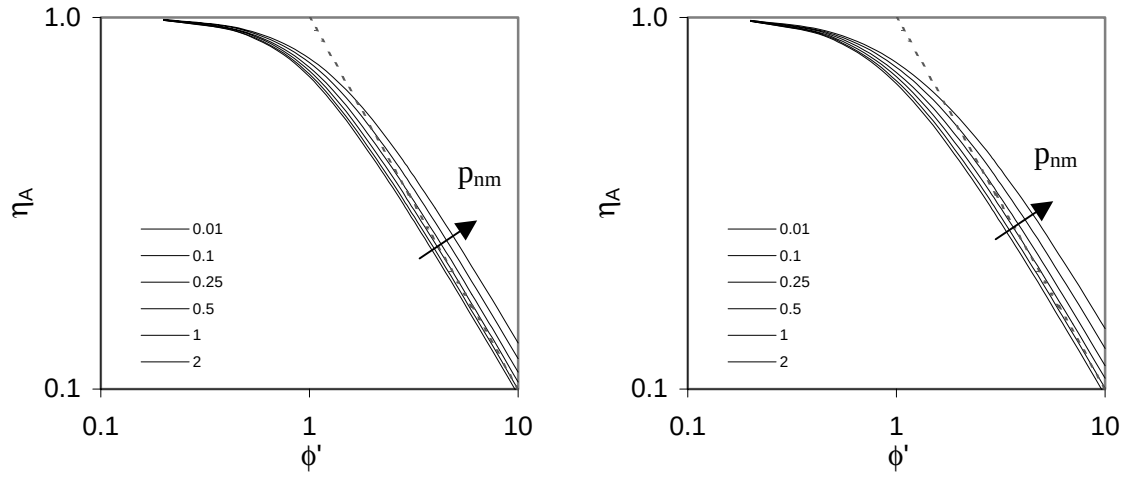

Fig.- A-1 Particle effectiveness concerning consumption of A (η_A) as function of the modified Thiele-modulus ϕ' for different values of p_{nm} (c_b/c_{Ab}=0.1 and c_b/c_{Pb}=0.1). (a) n=0.5 and m=1 and (b) n=1 and m=2.

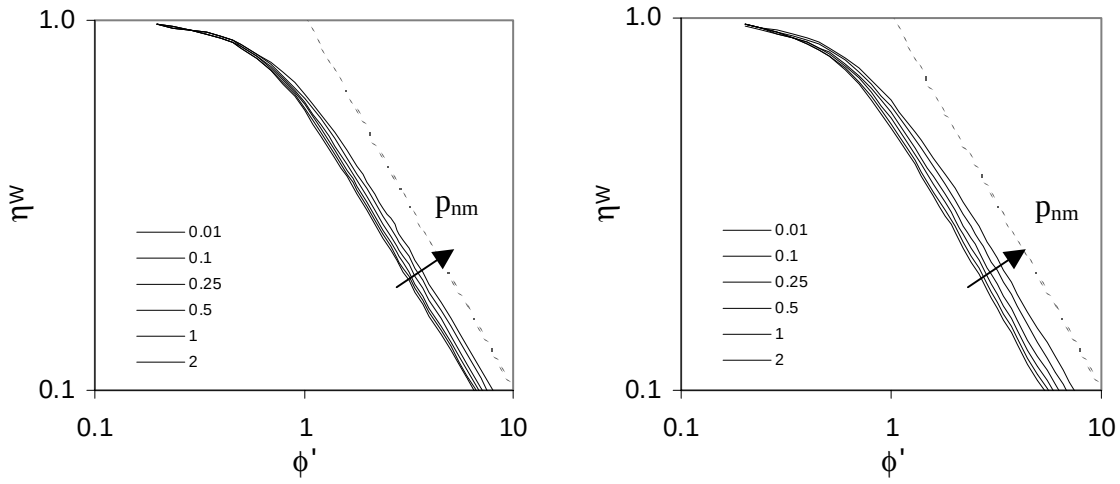

Fig.- A-2 Particle effectiveness concerning formation of W (η_W) as function of the modified Thiele-modulus ϕ' for different values of p_{nm} (c_b/c_{Ab}=0.1 and c_b/c_{Pb}=0.1). (a) n=0.5 and m=1 and (b) n=1 and m=2.

A.2 Modified Thiele-moduli for the consumption of A or the formation of W

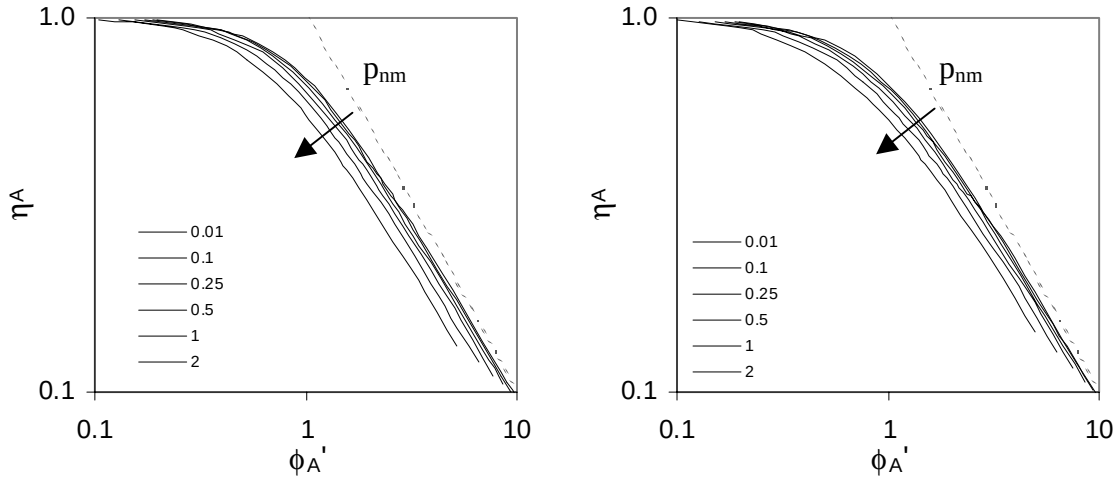

Fig.- A-3 Particle effectiveness concerning consumption of A (η_A) as function of the modified Thiele-modulus ϕ'_A for different values of p_{nm} (c_b/c_{Ab}=0.1 and c_b/c_{Pb}=0.1). (a) n=0.5 and m=1 and (b) n=1 and m=2.

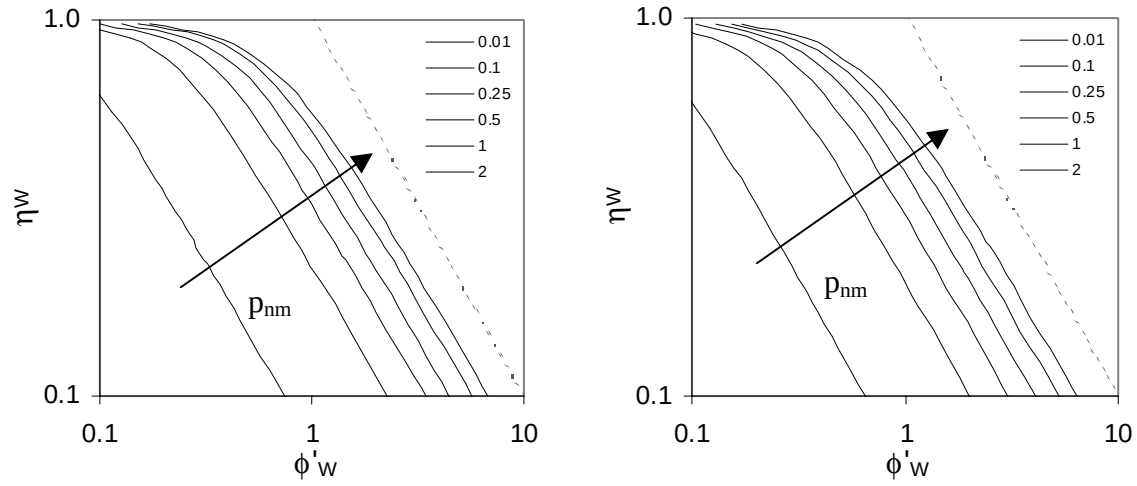

Fig.- A-4 Particle effectiveness concerning formation of W (η_W) as function of the modified Thiele-modulus ϕ'_W for different values of p_{nm} (c_b/c_{Ab}=0.1 and c_b/c_{Pb}=0.1). (a) n=0.5 and m=1 and (b) n=1 and m=2.7

Appendix B Influence factor $F_\sigma = \langle\sigma(c)\rangle / \sigma(\langle c\rangle)$ as a function of $\sigma(\langle c\rangle)$

The figure below shows the inadequacy of the influence factor F_σ, leading to the use of $F_{1-\sigma}$ instead.

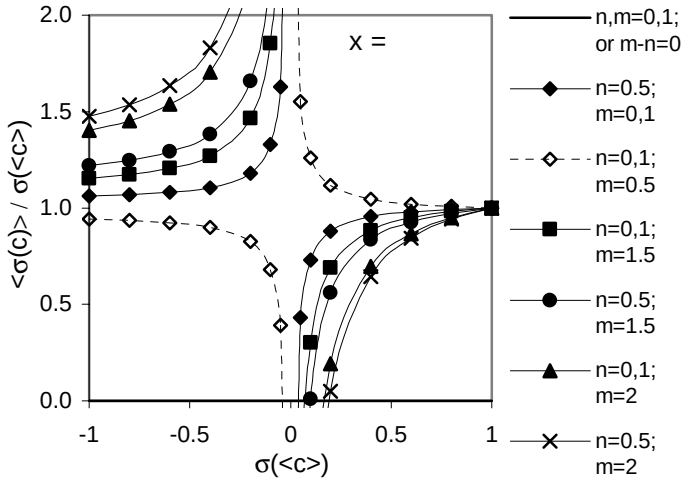

Fig.- B-1 Influence of a parabolic oxygen concentration profile (x=8) on the consecutive reaction scheme as a function of the average concentration selectivity σ(<c>) for different sets of reaction orders m and n.

Appendix C Derivation of the asymptotic solution following the procedure of G.W.Roberts, 1972

G.W. Roberts (1972) investigated the selectivity of porous catalysts for two parallel reactions. Assuming that the catalyst pellet can be represented as a semi-infinite slab of the thickness 2L, he was able to derive analytic solutions of the diffusion equation for three sets of reaction orders n=1 / m=0, n=2 / m=0 and n=2 /m=1. The solutions are expressed in cosh-functions and incomplete elliptic integrals of the first kind. Under the assumption that the concentration gradient of the hydrocarbons are small compared to that of oxygen together with the limiting situation of oxygen depletion in the center of the pellet, the reaction system discussed in this chapter reduces to the one discussed by G.W. Roberts. Therefore, his approach for the determination of asymptotic solutions for high Thiele-moduli can be applied.

Model assumptions

- catalyst pellet represented as an semi-infinite slab of thickness 2L
- effective diffusion coefficient constant inside the particle
- negligible temperature gradients inside the particle
- negligible concentration and temperature difference between gas phase and catalyst surface

$$D\frac{d^2c}{dx^2}-\left(k_n c^n + k_m c^m\right)=0 \qquad (A.1)$$

$$\text{Substitution: } p \equiv \frac{dc}{dx} \;\rightarrow\; \frac{d^2c}{dx^2}=\frac{dp}{dx}=\frac{dp}{dc}\frac{dc}{dx}=p\frac{dp}{dc} \;\rightarrow\; p\,dp=\frac{k_n c^n + k_m c^m}{D}dc \qquad (A.2)$$

Integrate (with p(a)=0) and re-substitute

$$\frac{dc}{dx}=\left(\frac{2}{D}\right)^{1/2}\left[\frac{k_n}{n+1}\left(c^{n+1}-c(a)^{n+1}\right)+\frac{k_m}{m+1}\left(c^{m+1}-c(a)^{m+1}\right)\right]^{1/2} \qquad (A.3)$$

Make dimensionless

$$\frac{d\gamma}{d\ell}=\sqrt{2}\phi_n\left[\frac{\gamma^{n+1}-\gamma(a)^{n+1}}{n+1}+p_{nm}\frac{\gamma^{m+1}-\gamma(a)^{m+1}}{m+1}\right]^{1/2} \qquad (A.4)$$

$$\text{with } \phi_n = L\sqrt{\frac{k_n c^{n-1}}{D}},\quad \ell = x/L \text{ and } \gamma=\frac{c}{c_b} \qquad (A.5\text{-}7)$$

Definitions:

(a) Effectiveness of the oxygen consumption

$$\eta_{O_2}=\frac{D\left.\frac{dc}{dx}\right|_{x=L}}{L\left(-R\left(c_R\right)\right)}=\frac{\left.\frac{d\gamma}{d\ell}\right|_{\ell=1}}{\phi_n^2\left(1+p_{nm}\right)} \qquad (A.8)$$

For the selectivity of the oxygen consumption see Roberts, 1972

(b) Selectivity of the intermediate product

$$\langle\sigma\rangle = \frac{\int_{a/L}^{1} \gamma^n d\ell - p_{nm}\int_{a/L}^{1} \gamma^m d\ell}{\int_{a/L}^{1} \gamma^n d\ell} \qquad 1-\langle\sigma\rangle = p_{nm}\frac{\int_{a/L}^{1} \gamma^m d\ell}{\int_{a/L}^{1} \gamma^n d\ell} \tag{A.9}$$

Ratio of the selectivity loss $1-\sigma_b = p_{nm}$

$$F_{1-\sigma} = \frac{1-\langle\sigma\rangle}{1-\sigma_b} = \frac{\int_{a/L}^{1} \gamma^m d\ell}{\int_{a/L}^{1} \gamma^n d\ell} \tag{A.10}$$

Asymptotic solutions for intraparticle transport:

(a) Effectiveness of the oxygen consumption: c(a)=0 $\gamma(a) = 0$

$$\eta_{O_2} \cong \frac{\sqrt{2}\left[\frac{1}{n+1} + p_{nm}\frac{1}{m+1}\right]^{1/2}}{\phi_n\left(1+p_{nm}\right)} \tag{A.11}$$

(b) Selectivity of the intermediate product

From Fig. 4 it is clear that at high ϕ' the influence of the transport limitation on the selectivity increases with p_{nm}. When $p_{nm}>>1$ and c(a)=0 then

$$\frac{d\gamma}{d\ell} = \phi_n\left(\frac{2p_{nm}}{m+1}\right)^{1/2}\gamma^{(m+1)/2} \tag{A.12}$$

Rearranging and multiplying by γ^n

$$\gamma^n d\ell = \frac{1}{\phi_n}\left(\frac{m+1}{2p_{nm}}\right)^{1/2}\gamma^{(2n-m-1)/2}d\gamma \tag{A.13}$$

The maximum effect of intraparticle mass transport limitations on the product selectivity of a catalyst pellet is expressed by:

$$F_{1-\sigma,min} = \frac{1-\langle\sigma\rangle}{1-\sigma_b} = \frac{\int_{0}^{1}\gamma^{(m-1)/2}d\gamma}{\int_{0}^{1}\gamma^{(2n-m-1)/2}d\gamma} = \frac{2n-m+1}{m+1} \tag{A.14}$$

The maximum is approached when oxygen is depleted in most of the particle, reactions find place only in a thin layer near the surface. Therefore, the asymptotic solution is the same for a plate, a tube or a pellet, and the assumption made at the beginning is fulfilled.

However, in a plug-flow reactor the p_{nm} -value of a consecutive reaction scheme is zero at the inlet and decreases with the formation of the target product. In a properly designed reactor p_{nm} reaches a maximum value of 1, which means that the product consumption by the

consecutive reaction equals the production of the primary reaction. Therefore, the asymptotic solution for $p_{nm}=0$ gives a more characteristic estimation of the influence of the concentration gradients on the selectivity, even if it is not the absolute minimum.

$$\gamma^m d\ell = \frac{1}{\phi_n}\left(\frac{n+1}{2}\right)^{1/2} \gamma^{(2m-n-1)/2} d\gamma \tag{A.15}$$

$$F_{1-\sigma,h\,min} = \frac{\int_0^1 \gamma^{(2m-n-1)/2} d\gamma}{\int_0^1 \gamma^{(n-1)/2} d\gamma} = \frac{n+1}{2m-n+1} \tag{A.16}$$

Asymptotic solutions for membrane to centerline transport:

(a) Effectiveness of the consumption of A for the limiting case: $p_{nm}\rightarrow 0$

$$F_{R,n} = \frac{\int_{a/L}^1 \gamma^n d\ell}{\left(\int_{a/L}^1 \gamma d\ell\right)^n} \cong \left(\frac{1}{\phi'}\right)^{1-n}\left(\frac{3-n}{n+1}\right)^n \tag{A.17}$$

(b) Starting from the expression for the selectivity of the intermediate product given by:

$$\sigma\left(\langle c\rangle\right) = 1 - p_{nm}\frac{\left(\int_{a/L}^1 \gamma d\ell\right)^m}{\left(\int_{a/L}^1 \gamma d\ell\right)^n} \qquad F_{1-\sigma} = \frac{1-\langle\sigma\rangle}{1-\sigma\left(\langle c\rangle\right)} = \frac{\int_{a/L}^1 \gamma^m d\ell}{\int_{a/L}^1 \gamma^n d\ell}\frac{\left(\int_{a/L}^1 \gamma d\ell\right)^n}{\left(\int_{a/L}^1 \gamma d\ell\right)^m} \tag{A.18-19}$$

the following asymptotical solution for $p_{nm}\rightarrow 0$ can be obtained

$$\gamma d\ell = \frac{1}{\phi_n}\left(\frac{n+1}{2}\right)^{1/2} \gamma^{(-n+1)/2} d\gamma \rightarrow \int_{a/L}^1 \gamma d\ell = \frac{1}{\phi_n}\frac{(2n+2)^{1/2}}{3-n} \tag{A.20-21}$$

$$\lim_{p_{nm}\rightarrow 0} \phi' = \left(\frac{n+1}{2}\right)^{1/2} \varphi_n \qquad \rightarrow \int_{a/L}^1 \gamma d\ell = \frac{1}{\phi'}\frac{n+1}{3-n} \tag{A.22-23}$$

$$F_{1-\sigma} = \frac{1-\langle\sigma\rangle}{1-\sigma\left(\langle c\rangle\right)} \cong \frac{n+1}{2m-n+1}\left(\phi'\frac{3-n}{n+1}\right)^{m-n} \tag{A.24}$$

Finally, the characteristic parameters $F_{R,n}$ and $F_{1-\sigma}$ are directly correlated with the average concentration <c>. The required Thiele-modulus is then given by:

$$\phi'' = L\sqrt{\frac{\frac{n+1}{2}k_1^*\langle c\rangle^{n-1} + \frac{m+1}{2}k_2^*\langle c\rangle^{m-1}}{D}} \tag{A.25}$$

where the ratio of the two different Thiele-moduli given by

$$\frac{\phi'}{\phi''} = \sqrt{\frac{\frac{n+1}{2}k_1^* c_R^{n-1} + \frac{m+1}{2}k_2^* c_R^{m-1}}{\frac{n+1}{2}k_1^* \langle c\rangle^{n-1} + \frac{m+1}{2}k_2^* \langle c\rangle^{m-1}}} = \sqrt{\frac{1+\frac{m+1}{n+1}p_{nm}}{\langle\gamma\rangle^{n-1} + \frac{m+1}{n+1}p_{nm}\langle\gamma\rangle^{m-1}}} \qquad \text{(A.25)}$$

can be approximated for the limiting case $p_{nm} \rightarrow 0$ by:

$$\phi' = \phi''\langle\gamma\rangle^{(1-n)/2} = \phi''\left(\frac{1}{\varphi'}\frac{n+1}{3-n}\right)^{(1-n)/2} \quad \rightarrow \quad \phi' = \phi''^{2/(3-n)}\left(\frac{n+1}{3-n}\right)^{(1-n)/(3-n)} \qquad \text{(A.26-27)}$$

Thus $F_{R,n}$ and $F_{1-\sigma}$ as a function of the new Thiele-modulus ϕ'' can be expressed by

$$F_{R,n} \cong \left(\frac{1}{\phi''}\right)^{2(1-n)/(3-n)}\left(\frac{3-n}{n+1}\right)^{(n+1)/(3-n)} \qquad \text{(A.28)}$$

$$F_{1-\sigma} \cong \frac{n+1}{2m-n+1}\left(\phi''\frac{3-n}{n+1}\right)^{2(m-n)/(3-n)} \qquad \text{(A.29)}$$

5 Integral effect of intraparticle transport limitations on the PBMR performance

Abstract

The effect of intraparticle mass transfer limitations on the integral reactant conversion and selectivity of the intermediate product in a PBMR were investigated using a one-dimensional, heterogeneous reactor model for a consecutive reaction scheme with power-law kinetics with two different reaction orders in oxygen for the primary and consecutive reaction, n and m respectively (m>n).

Two opposing effects influence the integral selectivity of the target product. The intrinsic selectivity increases with particle size for a given gas phase composition with a low oxygen concentration. However, if the inherent reduced particle effectiveness due to the lower reactivity is not compensated for by an increase of the catalyst mass, the resulting increased oxygen concentration in the PBMR will result in a selectivity loss that will exceed the gain caused by the concentration gradients within the catalyst particles. Therefore, increasing the particle diameter is not an efficient method to improve the overall product selectivities in a PBMR. Nevertheless, if the design of the PBMR necessitates the use of large catalyst particles (e.g. because of pressure drop limitations), the effect on the selectivity is not adverse, provided that the oxygen concentration is small compared to the concentrations of the hydrocarbons.

5.1 Introduction

Distributive addition of oxygen to the reaction zone is a concept used to increase the selectivity of the desired partial oxidation product. This concept is based on the condition that the formation rate of the desired product is less dependent on the oxygen concentration than the rates of the side-reactions. If the main side-reaction is consecutive, the reactor must show low back-mixing characteristics in order to limit the product losses. A packed bed membrane reactor (PBMR) combines the features of distributive reactant addition and low axial back-mixing of a packed bed reactor. Oxygen or air is added distributively via a membrane to the packed bed, that is situated either on the shell-side between membrane and the reactor wall or within the tubular membrane.

In this chapter the following simple (but showing all relevant features), consecutive reaction scheme will be investigated:

$$\begin{aligned} A + \nu_1 O_2 &\rightarrow P \qquad r_1 = k_1 c_A c^n \\ P + \nu_2 O_2 &\rightarrow W \qquad r_2 = k_2 c_P c^m \end{aligned} \quad \text{with } m>n \qquad (1),(2)$$

Product losses due to the consecutive reaction can be reduced relative to the product formation by decreasing the oxygen concentration.
Mass transfer limitations inside the catalyst particles can result in a further reduction of the oxygen concentration with consequences for both conversion and product selectivity of the PBMR. In Chapter 4 the effect of intraparticle mass transfer limitation on particle effectiveness and intrinsic product selectivity were discussed. If the oxygen concentration in the gas phase is small compared to those of the hydrocarbons, the particle effectiveness for the consumption of oxygen η_{O_2} can be described by

$$\eta_{O_2} = \frac{1}{3\phi'^2}\left(\frac{3\phi'}{\tanh(3\phi')} - 1\right) \tag{3}$$

where the modified Thiele-modulus is defined as follows:

$$\phi' = \frac{R}{3}\sqrt{\frac{\frac{n+1}{2}\nu_1 k_1 c_{Ab} c_b^{n-1} + \frac{m+1}{2}\nu_2 k_2 c_{Pb} c_b^{m-1}}{D}} \tag{4}$$

for $c_b < \min(\nu_2 c_{Pb}, \nu_1 c_{Ab})$
The product selectivity is not a simple function of the above described Thiele-modulus, since it also depends on the ratio of the secondary to the primary reaction rates p_{nm} and on the reaction orders n and m. It was shown in Chapter 4 that the spatially averaged selectivity of the catalyst particle is higher than the selectivity at the corresponding gas phase concentrations for $c_b < \min(\nu_2 c_{Pb}, \nu_1 c_{Ab})$.
However, near the reactor inlet where the concentration of the intermediate product is low ($c_b > \nu_2 c_{Pb}$), intraparticle mass transport limitations cause an selectivity loss. Furthermore, the overall oxygen profile is also determined by the consumption rate. Reduced consumption rates due to intraparticle transport limitations result in increased oxygen concentrations in the PBMR with a negative effect on the product selectivity.
Therefore, in the present chapter the effect on the integral performance of the PBMR will be discussed. The one-dimensional, heterogeneous model is used to evaluate the effect of intra-particle mass transport limitations on the performance of the PBMR with an axially unniform addition of air.

5.2 One-dimensional, heterogeneous PBMR-model

To study the effect of internal particle transport limitations on the performance of PBMRs a model describing for the transport of mass from the gaseous bulk to the particle surface and the intra-particle transport was developed. Obviously, the performance of the PBMR also depends on the overall design, as for example the tube diameter, the radial flow pattern (mainly determined by the particle to tube ratio) or the pressure drop over the length of the packed bed. To clearly elucidate the effects of the intraparticle diffusion limitations on the

integral reactor performance these effects have been ignored here. To facilitate the discussion of the effects also a constant and uniform distribution of the added flow has been assumed.
The effect of the overall design, such as the effect of the particle diameter on the hydrodynamics and thus on the gas phase mixing, is studied in Chapter 6, where the integral effect of limitations in the membrane to centerline transport is investigated.

MODEL ASSUMPTIONS:

1. One-dimensional plug flow model

The equations of change in the gas phase are based on the assumption of a one-dimensional plug flow model neglecting the axial dispersion and the pressure drop of the packed bed. Source terms of the component continuity equations are due to mass transfer between the bulk of the gas phase and the catalyst surface, and the added mass flow. Homogeneous gas phase reactions have not been considered here.
The equations of change are written in the mass average reference frame. Having neglected the pressure drop, the evaluation of the momentum balance is not required, since the local mass flow can be calculated a priori from the premixed mass flow and the part of the distributive flow that has been added via the membrane up to the given location. A uniform distribution of the distributive flow over the membrane length has been assumed here.

2. Macro-porous, symmetrical catalyst particle

The catalyst particles are assumed to be of spherical shape of constant particle diameter d_P, so that a one-dimensional model can be used to describe the profiles inside the catalyst particle. The catalyst structure is assumed to be macro-porous, so that transport mechanisms like viscous transport or Knudsen diffusion can be neglected. It is assumed that the component mass transport inside the particle is described by Fick's law of diffusion (due to the relatively low concentrations of the relevant components).

The resulting model equations with the constitutive equations for the transmembrane flux and interphase mass transport have been listed in Table 1. At the reactor inlet and outlet the standard Danckwerts' boundary conditions have been used for the gas phase mass balance, while symmetry at the particle center and continuity of the mass flux at the particle outer surface has been applied for the catalyst mass phase.
The molecular diffusion coefficients were calculated by the Wilke (1950) equation from the binary diffusion coefficients estimated by the empirical relation of Fuller et al. (1966) (Appendix A). Methane, formaldehyde and carbon dioxide were chosen for as reactant A, product P and waste product W. For the calculation of the effective diffusion coefficient a value of $\varepsilon/\tau = 0.15$ was assumed.

Table 1 Model equations for the one-dimensional, heterogeneous PBMR model.

Gas phase mass balance	Boundary conditions
$\frac{\partial}{\partial t}(\varepsilon\rho\omega_i) = -\frac{\partial}{\partial z}(\varepsilon\rho\omega_i v) - a n_{s,i} + \phi_{m,distr,i}$	$v\rho\omega_{i,0} = v\rho\omega_i\big\|_{z=0}$ $\quad \frac{\partial\omega_i}{\partial z}\Big\|_{z=L} = 0$
Catalyst phase mass balance	Boundary conditions
$\frac{\partial}{\partial t}(\rho\omega_i) = \frac{1}{r^2}\frac{\partial}{\partial r}\left(r^2 D_{eff,i} \rho \frac{\partial\omega_i}{\partial r}\right) + S_i$	$D_{eff,i}\rho\frac{\partial\omega_i}{\partial r}\Big\|_{r=R} = n_{s,i}$
$S_i = M_i \sum_{j=1}^{nrr} \nu_{ij} r_j$	$\frac{\partial\omega_i}{\partial r}\Big\|_{r=0} = 0$
Transmembrane flux	Interphase mass transport
$\phi_{m,distr,i} = \frac{\Phi_{m,distr}\omega_{distr,i}}{(\pi/4) d_t^2 L}$	$n_{s,i} = \rho k_{s,i}(\omega_i - \omega_{s,i})$

The reaction orders n=0.5/m=1 and n=1/m=2 are chosen in this chapter, and two catalyst masses of 0.1 g and 0.32 g. If not mentioned otherwise the concentration ratio in the premixed feed is y_A/y_{O2}=10/3 and 70 % of the oxygen is added in distributive mode to the PBMR, according to the optimum distribution determined in Chapter 3[1]. Contrary to Chapter 3 air is used as distributive flow, resulting in slightly lower product yields.

The reaction rates were chosen such that medium to high conversions were obtained in the model calculations. Typical parameter values used in the calculations have been listed in Table 2.

Table 2 Model parameters.

Rate constants: n=0.5/m=1.0		k'_1	0.015 mol / (g s bar^{1+n})
		k'_2	0.045 mol / (g s bar^{1+m})
Rate constants: n=1.0/m=2.0		k'_1	0.150 mol / (g s bar^{1+n})
		k'_2	4.500 mol / (g s bar^{1+m})
Stoichiometric coefficients		ν_1	1
		ν_2	1
Catalyst mass		m_{cat}	0.1-0.33 g
Catalyst density		ρ_{cat}	1000 kg / m^3
Particle diameter		d_p	0.1-3 mm
Interphase mass transfer coefficient		k_s	1 m / s
Reactor pressure and temperature		p, T	1.013 bar, 550 K
Premixed feed:	volumetric flow	$\Phi_{V,0}$	100 ml(STP) / min
	mole fraction of reactant A	$y_{A,0}$	0.1
	mole fraction of oxygen	$y_{O2,0}$	0.03
Distributed feed:	volumetric flow	$\Phi_{V,distr}$	35 ml(STP) / min
	mole fraction of oxygen	$y_{O2,distr}$	0.2

STP: 1.013 bar and 298 K

[1] For n=0.5/m=1 and 0.1 g a different optimum distribution was given in Chapter 3, but the difference in the yield is smaller than 0.1 %

To obtain the steady-state solutions of both the mass balances in the bulk of the gas phase and for the catalyst phase, the equations have been solved with accumulation terms using a finite difference technique. The two partial differential equations have been solved sequentially, where the equations are coupled via the concentration and concentration gradient at the particle outer surface. To minimize the required number of grid cells for the gas phase mass balance a second order flux-delimited ('Barton') scheme for the convection term (Centrella and Wilson, 1984) has been implemented.

Typically 100 equidistant axial grid cells for the gas phase mass balance has been used, whereas typically 50 cells on the particle radius with grid refinement towards the catalyst surface was used to solve the catalyst phase mass balance.

5.3 The effect of intraparticle mass transport limitations on the integral reactor performance

In Chapter 3 it was shown that the concentration gradients inside the particles induced by mass transport limitations in the particle could result in an improvement of the intrinsic product selectivity (m>n), provided that the oxygen concentration is the gas phase is small compared to the concentrations of the hydrocarbons. However, in Chapter 3 the change of the concentrations in the bulk of the gas phase due to the intraparticle transport limitations was not taken into account.

In the following the effect of intraparticle mass transfer limitations on the integral selectivity of a PBMR will be evaluated. Several arbitrary kinetics with different sets of reaction orders of oxygen were investigated. Model parameters and operating conditions are listed in Table 2.

Because the effects of the intraparticle transport limitation on product selectivity and activity of the catalyst interfere, in a first step the axial oxygen concentration in the PBMR will be kept constant regardless of the size of the catalyst particles. In the next step, the magnitude of the distributed oxygen flow is constant, producing different axial oxygen concentration profiles depending on the catalyst particle diameter.

5.3.1 Increase of the particle size at axially constant oxygen concentration

To facilitate comparison with the results reported in Chapter 4, a first series of calculations is presented in which the axial oxygen concentration is kept constant.

Here, the constant and uniform oxygen concentration has been chosen 20 times smaller than the inlet concentration of the hydrocarbon A. The resulting axial concentration profiles of A and product P are shown in Fig. 1. With increasing particle diameter the mass transfer limitation becomes more pronounced, as can also be seen by the increase of the Thiele-modulus (Fig. 2b).

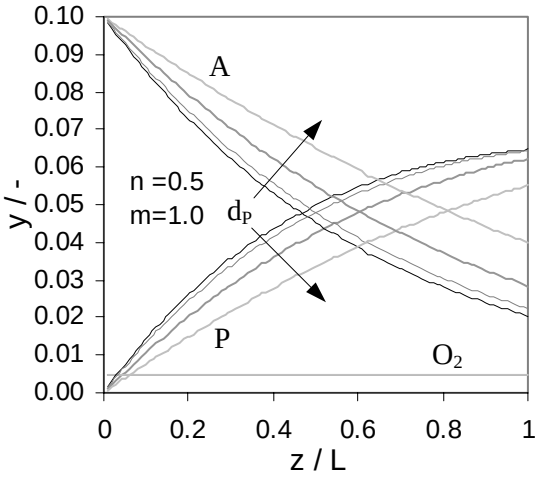

Fig. 1 Effect of particle size on the axial profiles of A and P at a constant oxygen concentration (c_0/c_{A0} = 0.05).

In regions of the PBMR where the oxygen concentration is small compared to those of the hydrocarbons, intraparticle mass transport limitations increase the product selectivity, since the rate of the consecutive reaction is stronger effected by the reduced oxygen concentration inside the particle than the primary reaction, so that the selectivity losses are reduced. This was expressed by the selectivity ratio[2] $F_{1-\sigma} = \left(1-\langle\sigma\rangle\right)/\left(1-\sigma_b\right)$. Note that $F_{1-\sigma} > 1$ means a negative effect on the average product selectivity $\langle\sigma\rangle$.

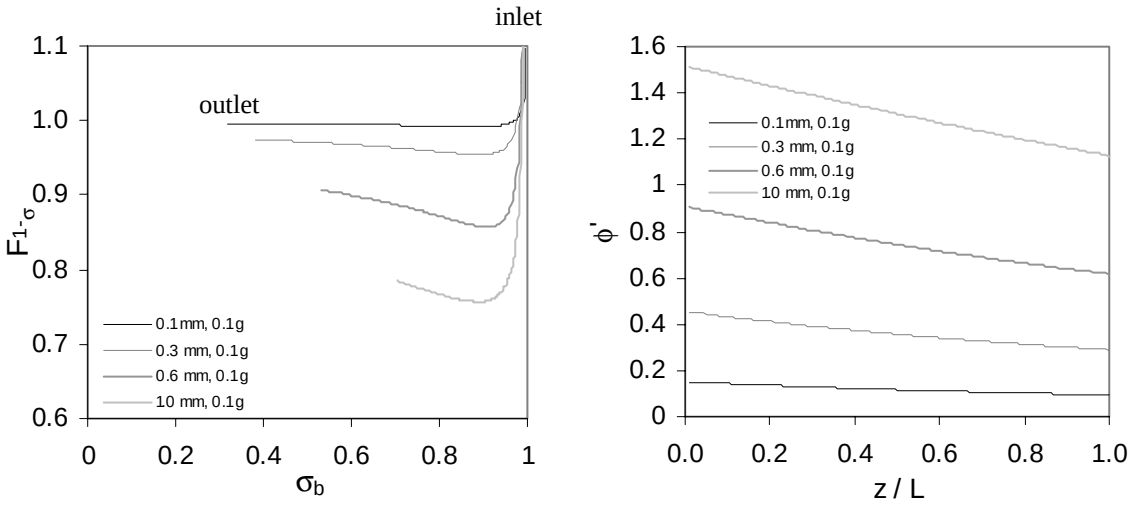

Fig. 2 Axial profile of (a) the selectivity ratio and (b) the modified Thiele-moduli for the different particle sizes.

[2] The selectivity ratio was not defined as $F_\sigma = \langle\sigma\rangle/\sigma_b$ because σ_b has a value of 0 if the primary and consecutive reaction are equal.

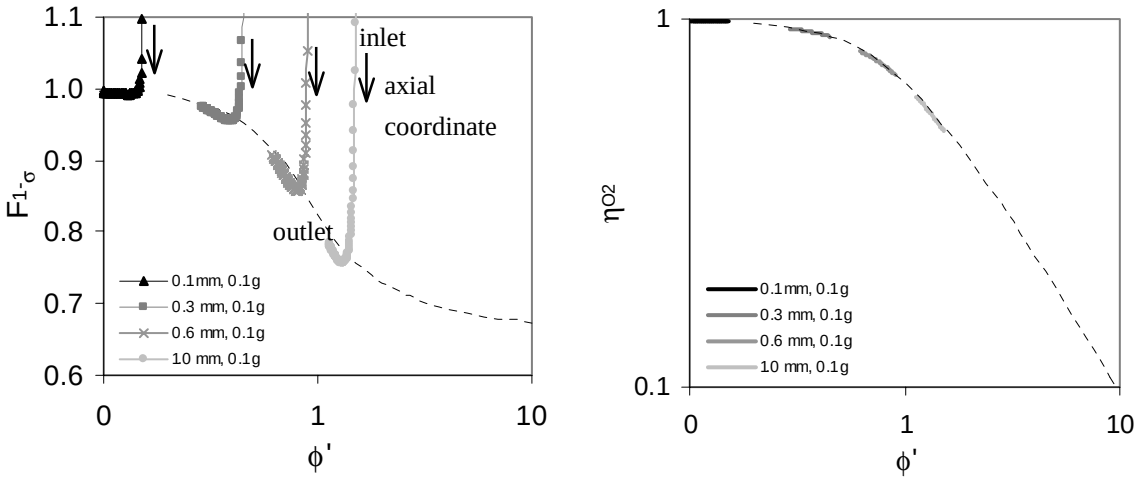

Fig. 3 Local selectivity ratio and particle effectiveness towards oxygen consumption as a function of the modified Thiele-modulus for four different particle diameters. The dashed lines correspond to $c/c_A=c/c_P=0.1$ and $p_{nm}=0.01$.

In the first 10 % of the PBMR, the concentration of P is well below that of oxygen. Thus the effect of the intraparticle mass transfer limitations on the product selectivity is therefore negative at the inlet of the PBMR (see Fig. 2a).

Fig. 3 shows a comparison of the calculated local selectivity ratios and particle efficiencies with the values determined in Chapter 3 for $c/c_A=c/c_P=0.1$ and $p_{nm}=0.01$.

The question now arises whether the positive effect of intraparticle diffusion limitations at the PBMR outlet outweighs the negative effect at the PBMR inlet.

In Fig. 4 the integral effect of the increasing particle size on conversion and selectivity is illustrated. Fig. 4 shows that for larger particles indeed higher selectivities can be achieved at the same conversion, however the overall conversion was decreased due to the intraparticle mass transport limitations.

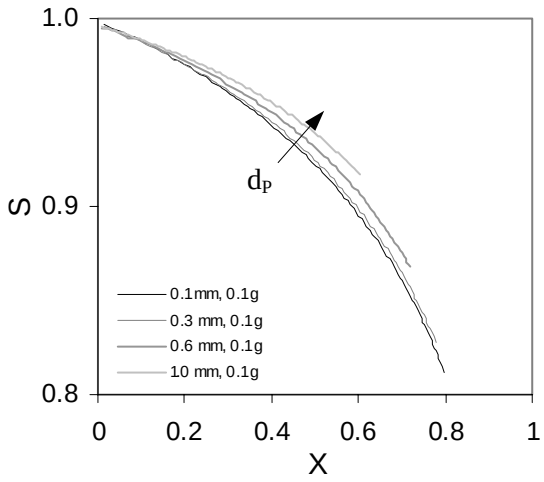

Fig. 4 Effect of the particle diameter on the selectivity – conversion plot.

To obtain the same product yield more catalyst mass is required. In these calculations it was assumed that the oxygen concentration was constant. However in most applications the membrane flux will be constant and not the oxygen concentration. This is studied in the next paragraph.

5.3.2 Increase of the particle size at axially constant oxygen transmembrane flux

If the membrane flux is independent of the reaction within the PBMR, e.g. a fixed mass flow of air is equally distributed over the length of the membrane, the reduced particle effectiveness (see Fig. 5a) causes an increase of the oxygen concentration in the gas phase further downstream in the PBMR (see Fig. 5b) with a corresponding negative effect on the product selectivity.

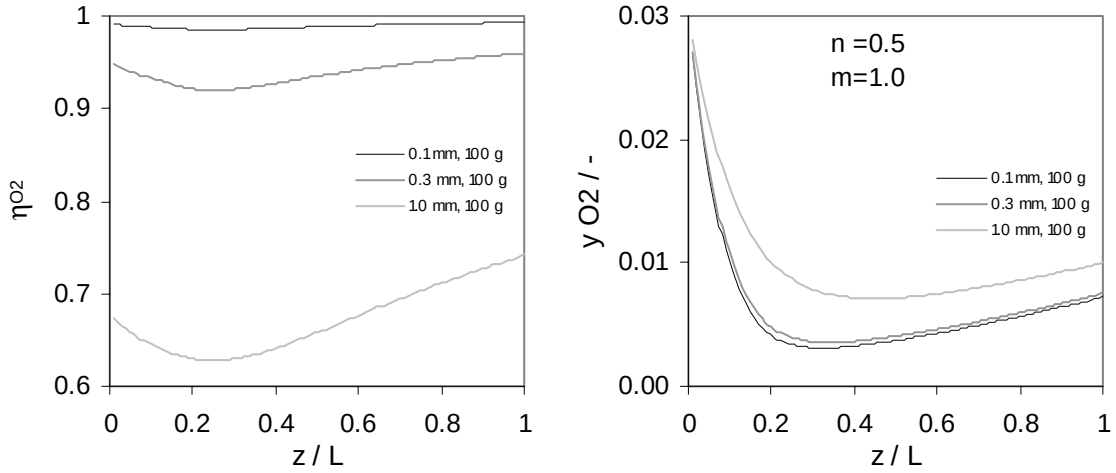

Fig. 5 Influence of the particle size on the axial profiles of (a) the particle effectiveness for oxygen consumption and (b) the oxygen concentration for a kinetic system with oxygen reaction orders n=0.5 and m=1.

The two opposing effects of increased downstream gas phase oxygen concentrations and intraparticle oxygen concentration profiles due to mass transfer limitation can cancel each for smaller particles, as is shown by the comparison of conversion versus selectivity in Fig. 6.

For larger modified Thiele-moduli the reduced particle effectiveness results in an overall selectivity loss due to the strongly increased oxygen concentrations.

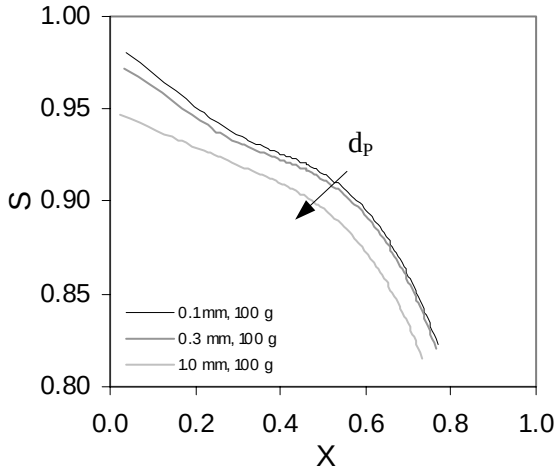

Fig. 6 Influence of the particle size on the selectivity – conversion – plot for a reaction system with oxygen reaction orders n=0.5 and m=1.

This means that the integral effect of intraparticle mass transport limitation is opposite to the intrinsic effect outlined in Chapter 4, due to its effect on the axial oxygen concentration profile.

Fig. 7a shows that the particle effectiveness can still be described by:

$$\eta_{O_2} = \frac{1}{3\phi'^2}\left(\frac{3\phi'}{\tanh(3\phi')} - 1\right) \text{ (see Chapter 4),} \qquad (5)$$

despite the fact that the oxygen concentration is not in all regions of the PBMR small compared to those of the reactant and the intermediate product. The reactant A is fed to the packed bed in a ratio of y_A/y_{O2}=10. For the case of 0.1 mm diameter particles, this ratio initially increases to a maximum value of 26 located close to the minimum oxygen concentration and subsequently slowly decreases to 1.9. The ratio of the intermediate product y_P/y_{O2} is at the inlet zero and reaches 8.4 at maximum (at about 30 % of the reactor length) and 4.3 at the reactor outlet. Near the reactor inlet the intraparticle concentration gradients of the intermediate result in a selectivity loss (y_p/y_{O2}<2 for the case of d_P=0.1 mm), respectively a smaller selectivity improvement (see values for d_P=0.3 mm in Fig. 7b; the dashed line shows the relation derived in Chapter 4 for $y_A/y_{O2}=y_P/y_{O2}$=10 and p_{nm}=0.01).

For the large particle diameter of d_P=1 mm the increased oxygen concentrations in the gas phase (i.e. decreased ratios of hydrocarbons to oxygen concentrations) result over the full length of the reactor in a negative effect of the intraparticle hydrocarbon concentration profiles on the intrinsic selectivity.

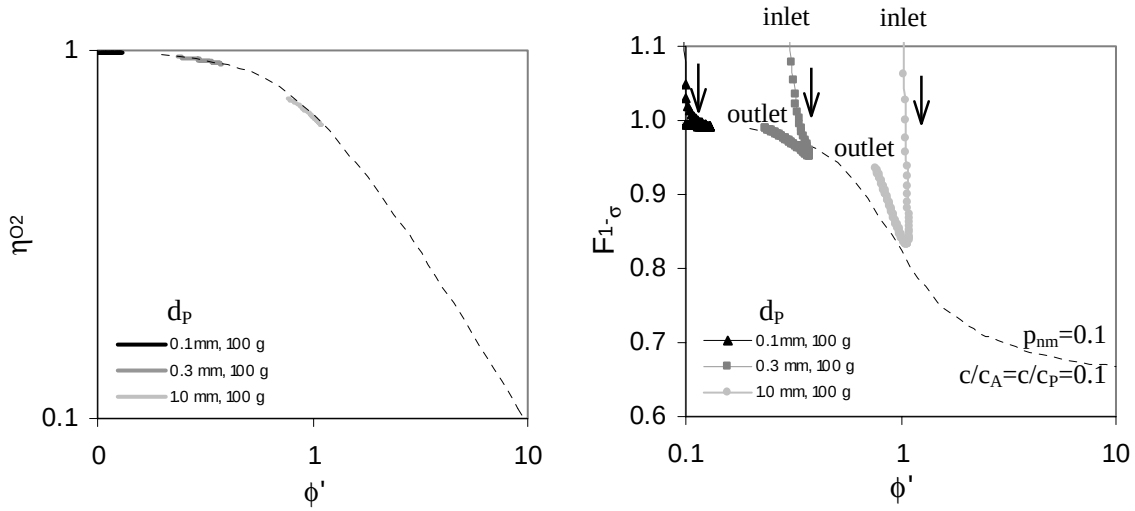

Fig. 7 Influence of the particle size on (a) the particle effectiveness for oxygen consumption and (b) the selectivity ratio as a function of the modified Thiele-modulus ϕ' for reaction kinetics with oxygen reaction orders n=0.5 and m=1.

In Appendix B the effect of intraparticle mass transport limitations on the performance of PBMR is illustrated for the other series of reaction kinetics with reaction orders n=1/m=2, and for both sets of reaction orders for a higher catalyst mass (0.32 g).

Common observations:

- For ϕ'<0.5, the effect of the effectiveness of oxygen conversion is small and the effect on product selectivity and reactant conversion is negligible.

- Further increase of the modified Thiele-modulus (ϕ'<1.1) results in an increase of the oxygen concentrations downstream in the PBMR, which results in a selectivity loss. The integral loss of product yield for the particle diameter of 1 mm is about 5 %.
- For the higher catalyst mass (lower axial oxygen concentrations), the intrinsic selectivity improvements due to intraparticle mass transfer limitations are higher. Therefore, the integral loss of product yields (d_p=1mm) decreases below 2 %. Thereby, the modified Thiele-modulus even increases for the reaction orders n=0.5/m=1 to ϕ'<1.6.

5.3.3 Increase of particle size and catalyst mass to account for the reduced activity at axially constant membrane flux

If the reduced particle effectiveness is accounted for by distributing the same total flow of oxygen over a larger amount of catalyst, the selectivity in a PBMR can be slightly improved due to the intra-particle mass transport limitations, however, at the expense of increased investment costs.

This is illustrated in Fig. 8. The increase of the particle diameter by a factor 30 is compensated for by an increase of the catalyst mass by a factor of 3.2, such that the oxygen concentration at the reactor outlet is about the same (see Fig. 8b). However, the resulting slight improvement of the selectivity, is small compared to the improvement that could have been obtained, if the catalyst mass was increased still using the smaller particle diameter. With the smaller particle diameter the oxygen concentrations downstream in the gas phase in the PBMR are much smaller with a corresponding strong increase in product selectivity.

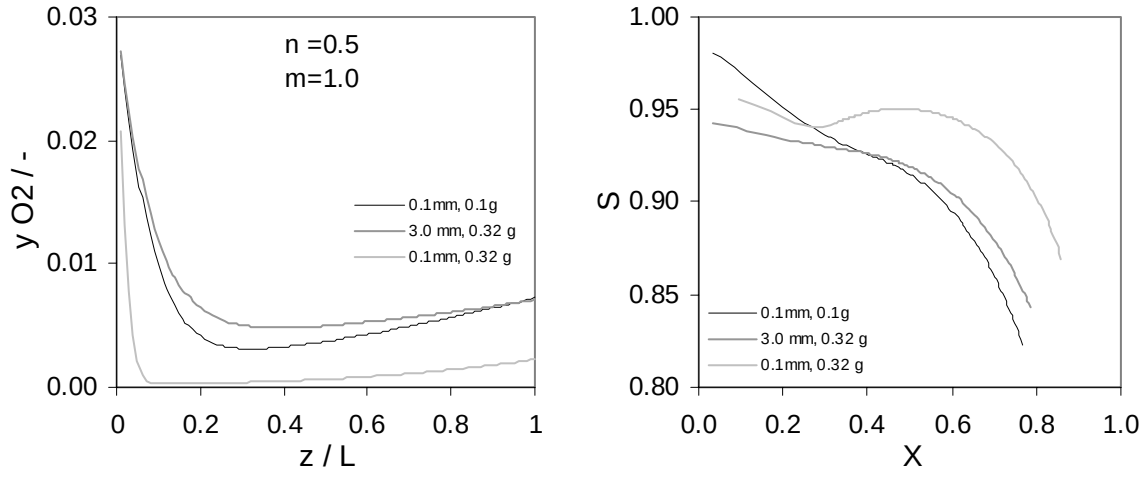

Fig. 8 Effect of an increased particle size or a reduced oxygen concentration on (a) the axial oxygen concentration profile and (b) selectivity – conversion – plot for arbitrary kinetics with oxygen reaction orders n=0.5 and m=1.

Concluding, the increase of the particle diameter is not an efficient way to improve the product selectivities in a PBMR. On the other hand, if the design of the PBMR requires the

application of large catalyst particles (e.g. because of pressure drop requirements), the effect of possible intraparticle mass transfer limitations on the selectivity is not disadvantageous, provided that the oxygen concentration is small compared to those of the hydrocarbons. Due to intraparticle diffusion limitations, larger amount of catalyst is however required to achieve the same conversion.

5.3.4 Influence of stoichiometric coefficients

As in the chapters before ν_1=0.5 and ν_2=10 were chosen to demonstrate the influence of the stoichiometric coefficients. Ethylbenzene, styrene and carbon dioxide were selected as reactant A, product P and waste product W. Opposite to Chapter 4, where the same effective diffusion coefficients were assumed for hydrocarbons and oxygen, the effect of the size of the hydrocarbon molecule on the diffusion coefficient is included in the following model calculations. The ratio of the effective molecular diffusion coefficients of reactant A and oxygen decreases with the size and the molecular weight of reactant A. For the estimation of this ratio a three-molecular mixture of reactant A (y_A=0.1), oxygen (y_{O2}=0.01) and nitrogen is assumed. Assuming that the intraparticle transport is dominated by molecular diffusion and applying the equation of Wilke (1950) the ratio is given by

$$\frac{D_{eff,A}}{D_{eff,O_2}} = \frac{D_{m,A}}{D_{m,O_2}} = \frac{1-y_A}{1-y_{O_2}} \frac{\frac{y_A}{D_{O_2A}} + \frac{y_{N_2}}{D_{O_2N_2}}}{\frac{y_{O_2}}{D_{AO_2}} + \frac{y_{N_2}}{D_{AN_2}}} = \frac{1-y_A}{1-y_{O_2}} \frac{y_A + y_{N_2} \frac{D_{AO_2}}{D_{O_2N_2}}}{y_{O_2} + y_{N_2} \frac{D_{AO_2}}{D_{AN_2}}} \qquad (6)$$

filling in the binary diffusion coefficients approximated by Fuller et al. (1966) results in

$$\frac{D_{eff,A}}{D_{eff,O_2}} = \frac{1-y_A}{1-y_{O_2}} \frac{y_A + 0.357\, y_{N_2}}{y_{O_2} + 0.965\, y_{N_2}} = 0.44 \qquad (7)$$

As a result the hydrocarbons will form stronger intraparticle concentration profiles, with a negative consequence for the intrinsic product selectivity. This is demonstrated by another series of model calculations with the stoichiometric coefficients ν_1=0.5 and ν_2=10.

Due to the higher consumption of oxygen in the consecutive reaction (despite the lower consumption in the primary reaction), the distributive flow has to be increased to $\Phi_{V,distr}$=70 ml / min. The other model parameters are as listed in Table 2.

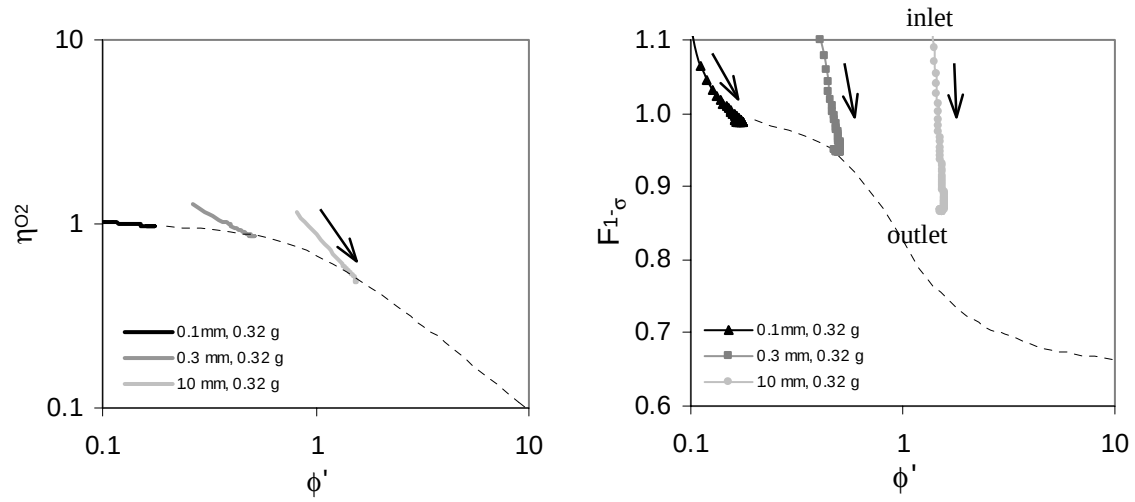

Fig. 9 Influence of the particle size on (a) the particle effectiveness for oxygen consumption and (b) the selectivity ratio as a function of the modified Thiele-modulus ϕ' for reaction kinetics with n=0.5/m=1 and ν_1 =0.5/ν_2 =10.

The effect of the decreased hydrocarbon diffusivity is illustrated in Fig. 9. The particle efficiency, η_{O_2}, and the selectivity ratio, $F_{1-\sigma}$, show strong differences from the values derived in Chapter 4, for equal effective diffusion coefficients. The particle efficiency for the oxygen consumption even takes values above unity near the reactor inlet, which shows the strong contribution of the consecutive reaction to the oxygen consumption.

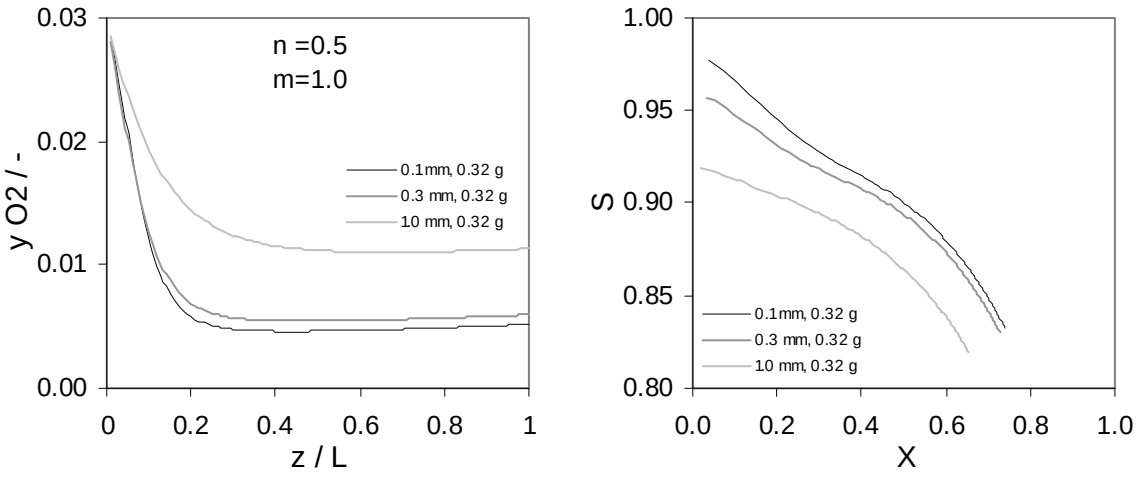

Fig. 10 Influence of the particle size on (a) the axial oxygen concentration profile and (b) the selectivity – conversion plot for arbitrary kinetics with ν_1 =0.5/ν_2 =10.

For the particle diameter of 1mm the product yield reduced by 12 % (relative value).
For a higher catalyst mass (0.32 g) and reduced initial oxygen concentration (Appendix B.4), the ratio of hydrocarbon to oxygen concentration is increased so far that the particle properties are dominated by the intraparticle concentrations of oxygen. After the first 20 % of

the reactor particle efficiency and selectivity ratio agree with the values derived in Chapter 4. The loss of product yield reduces to 5 % for d_p=1mm.

5.4 External transport limitations and temperature effects

For the model calculations presented before in this chapter, an external mass transfer coefficient for the transport from the bulk gas phase to the catalyst surface of k_s=1 m / s was assumed. This value was chosen such that the external mass transfer had a small effect on the performance of the catalyst particle.

Transport limitations from the gas bulk to the catalyst surface result in a decrease of the concentrations of oxygen and reactant A and an increase of the concentration of product P. Whether the negative effect of the change of the hydrocarbon concentrations or the positive effect of the decrease of the oxygen concentration on the intrinsic particle selectivity prevails depends on the ratio of the gas phase concentrations. In Fig. 11a it can be seen, that in the region of the PBMR, where the intraparticle mass transfer coefficients have a negative effect of the intrinsic product selectivity ($F_{1-\sigma}$ >1), this effect is further increased by the additional external mass transfer limitation (k_s=0.1 m / s). Likewise, the selectivity improvement is intensified in the region, where the positive effect of the intraparticle transport limitations prevails.

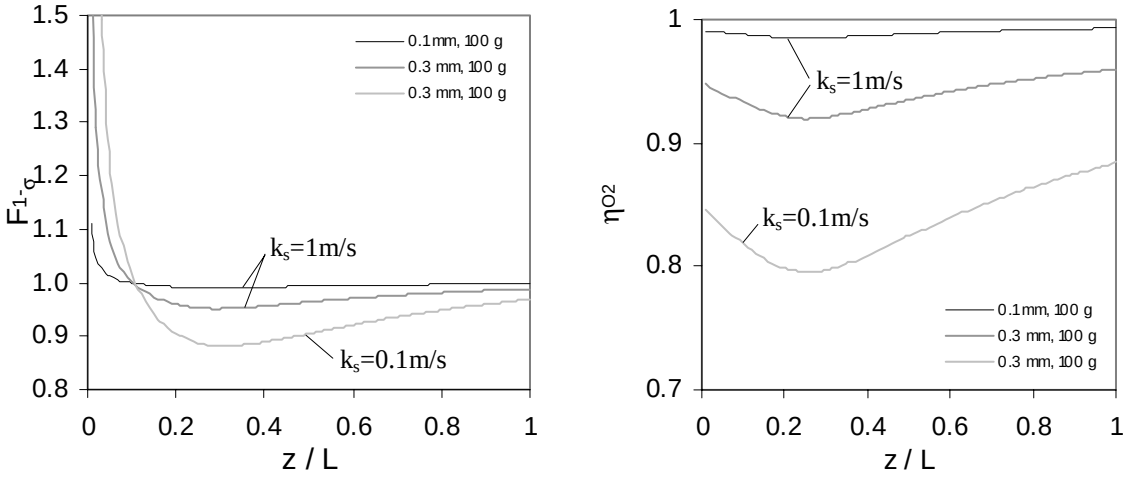

Fig. 11 Axial profiles of (a) the selectivity ratio and (b) particle effectiveness for oxygen consumption for different external mass transfer coefficients.

Obviously, external mass transfer limitations results in an activity loss, which is shown in Fig. 11b. Summarizing, it can be concluded that external mass transfer limitation intensify the effect of intraparticle mass transfer limitations.

The heat transport limitations from the bulk gas phase to catalyst surface are more significant than intraparticle heat transport limitations, especially in laboratory reactors (Mears, 1971).

The temperature within the particle is relatively uniform. The effect of the increased catalyst temperature on intrinsic selectivity of the catalyst particle depends on the difference $\Delta E_A=E_{A,2}-E_{A,1}$ between the activation energies of consecutive ($E_{A,2}$) and primary reaction ($E_{A,2}$). For $\Delta E_A>0$ the reaction rate of the consecutive reaction increases stronger with the temperature, and energy transport limitations results in additional selectivity losses. However, the increased reactivity results as well in an increase of intraparticle mass transfer limitations with possibly increasing effect on the particle selectivity. A more detailed discussion of temperature effects is beyond the scope of this thesis.

5.5 Discussion and conclusions

PBMR can be applied to improve the selectivity of an intermediate oxidation product. A low oxygen concentration throughout the entire reactor reduces product losses by the secondary combustion, provided that the oxygen dependency of the target product formation reaction rate is smaller than that of the consecutive reaction (n<m).

If the oxygen concentration is small compared to those of the hydrocarbons, the particle effectiveness and the intrinsic product selectivity are determined by the concentration gradients of oxygen inside the particle. Intraparticle mass transfer limitations result in an improvement of the selectivity over the selectivity corresponding to concentrations in the gas phase. However, the intraparticle mass transfer limitations will have their effect on the axial oxygen concentration profile, that needs to be taken into account to quantify the effect of intraparticle diffusion limitations on the integral product selectivity.

When studying the integral effect on the performance of the PBMR, two aspects have to be considered that both have a negative effect on the final product selectivity.

Firstly, in the inlet zone of the PBMR (until the concentration of the produced product P exceeds that of oxygen) the intrinsic product selectivity is decreased with increasing size of the catalyst particles.

Secondly, an even stronger loss of the integral product selectivity is caused by the reduced consumption of oxygen in large particles due to the intraparticle diffusion limitations. The increased downstream gas phase concentration counteracts the improvement of the intrinsic selectivity for larger particles.

For small modified Thiele-moduli ($\phi' < 0.5$) the effect of intraparticle mass transfer limitations can be neglected. If the modified Thiele-modulus in the PBMR is above $\phi' > 1$, the overall effect of the intraparticle mass transfer limitations is negative.

However, intraparticle mass transfer can still result in an improved integral product selectivity, if the reduced catalyst activity is counteracted, e.g. by increasing the catalyst mass. However, with the same increase of the catalyst mass still using the small catalyst

particles the product selectivity can be enhanced much more effectively due to a stronger decrease of the oxygen concentration level in the PBMR.

Nonetheless, if the design of the PBMR requires the application of large particles, for example because of pressure drop limitations, negative consequences on the product selectivity can be prevented if the catalyst mass is increased to account for the reduced particle effectiveness. To avoid negative effects of the intraparticle diffusion limitations on the integral product selectivity, the particle size should be chosen such that the modified Thiele-modulus is $\phi' < 1$.

NOTATION

Latin letters

A,P,W	hydrocarbon reactant, target and waste product
a	specific surface area per volume packed bed [m^2 / m^3]
c	concentration [mol / m^3]
d	diameter [m]
D	diffusion coefficient [m^2 / s]
F	factor by which a reaction rate or selectivity is increased due to mass transport limitations
k	rate constant [mol / m^3 s bar^{1+n}], [mol / m^3 s bar^{1+m}]
k’	rate constant [mol / g s bar^{1+n}], [mol / g s bar^{1+m}]
k_s	interphase mass transfer coefficient [m / s]
L	length of the packed bed [m]
m_{cat}	catalyst mass [kg]
m	reaction order in oxygen of reaction forming the waste product
M_i	molecular mass of component i [kg / m^3]
n	reaction order in oxygen of reaction forming the target product
n_s	interphase mass flow [kg / m^2 s]
PBMR	packed bed membrane reactor
r	length coordinate in radial direction of the packed bed [m]
r_j	rate of reaction j [mol / m^3 s]
v	superficial gas velocity [m / s]
x	length coordinate in radial direction of the spherical particle [m]
y	molar fraction
z	length coordinate in axial direction of the packed bed [m]

Greek letters

ε	porosity
η	effectiveness factor
ν	stoichiometric coefficient
ρ	density [kg / m^3]
τ	toruosity
Φ_V	volumetric flow [m^3 / s] or [ml / min]
Φ_m	mass flow [kg / s]
$\phi_{m,distr}$	specific mass flow added per volume packed bed [kg / m^3 s]
ω	mass fraction

Subscripts

0	at the reactor inlet / base case
A,P,W	hydrocarbon reactant, target and waste product
b	gas bulk value
cat	catalyst
distr	distributed
max	maximum value
O_2	oxygen
p	particle
t	tube

Dimensionless numbers

$$\phi' = \frac{R}{3}\sqrt{\frac{\frac{n+1}{2}\nu_1 k_1 c_{Ab} c_b^{n-1} + \frac{m+1}{2}\nu_2 k_2 c_{Pb} c_b^{m-1}}{D}} = \frac{R}{3}\sqrt{\frac{\frac{n+1}{2}\nu_1 R_1 + \frac{m+1}{2}\nu_2 R_2}{D c_b}}$$

References

J. Centralla, J. Wilson, 1984, Planar numerical cosmology. II. The difference equations and numerical tests, *Astrophysical J. Suppl. Ser. 54*, 229-249

E.N. Fuller, P.D. Schettler, J.C. Giddings, 1966, A new method for prediction of binary gas-phase diffusion coefficients, *Ind. Eng. Chem. 58*, 19

D.E. Mears, 1971, Tests for transport limitations in experimental catalytic reactors, *Ind. Eng. Chem. Process Des. Develop. 10*, 541-547

R.C. Reid, J.M. Prausnitz, B.E. Poling, 1988, The properties of gases and liquids, McGraw-Hill Book Company, New York, USA

C.R. Wilke, 1950, Diffusional properties of multicomponents gases, *Chemical Engineering Progess 92*, 1

Appendix A Physical properties

A.1 Diffusion coefficients

An empirical correlation for the (binary) gaseous diffusion coefficients by Fuller et al. (1966).

$$D_{ij} = 10^{-3} \frac{T^{1.75}\sqrt{1/M_i + 1/M_j}}{p\left(\sqrt[3]{\sum_k V_{ki}} + \sqrt[3]{\sum_k V_{kj}}\right)^2} \quad [m^2/s] \quad (A.1)$$

with temperature T in K, pressure p in atmosphere, molecular mass M in g/mol and the volumes of parts of the molecule V_{ij} (Table-A-1).

Table-A-1 Atomic diffusion volumes (Reid et al., 1988).

	V_{ij}		$\sum V_{ij}$
C	16.5	H_2	7.07
H	1.98	N_2	17.9
O	5.48	O_2	13.6
		CO	18.9
		CO_2	26.9
		H_2O	12.7

The molecular diffusion coefficient is approximated by the Wilke equation (Wilke, 1950)

$$D_{m,i} = (1 - y_i) \Big/ \sum_{\substack{j=1 \\ j \neq i}}^{n} \frac{y_j}{D_{ij}} \quad (A.2)$$

And finally the effective diffusion coefficient

$$D_{eff,i} = \frac{\varepsilon}{\tau} D_{m,i} \quad (A.3)$$

A.2 Viscosity, heat capacity and thermal conductivity of the gas

The gas properties are calculated using the data set of AIChE Design Institute for Physical Property Data, DIPPR, New York : AIChE

Table- A-2 Correlations for the gas physical properties.

dynamic viscosity	$\mu = \sum_{i=1}^{n} y_i \mu_i$	$\mu_i = \frac{AT^B}{1 + C/T + D/T^2}$
thermal conductivity	$\lambda = \sum_{i=1}^{n} y_i \lambda_i$	$\lambda_i = \frac{AT^B}{1 + C/T + D/T^2}$
Heat capacity	$c_p = \sum_{i=1}^{n} \omega_i \frac{\bar{c}_{p,i}}{M_i}$	$\bar{c}_{p,i} = A + B\left(\frac{C/T}{\sinh C/T}\right)^2 + D\left(\frac{E/T}{\cosh E/T}\right)^2$
	[J / kg K]	[J / mol K]

Appendix B Influence of particle size on PBMR performance for different sets of reaction orders

In this Appendix results have been summarized showing the influence of the particle size on the integral reactor performance for a higher catalyst mass of 0.32 g and for another set of reaction orders. Axial oxygen concentration profile, the overall product selectivity versus conversion, and the effectiveness for oxygen consumption, η_{O_2}, and the influence factor on the product selectivity, $F_{1-\sigma}$, as a function of the modified Thiele-modulus are given.

B.1 Reaction orders n=0.5/m=1.0 and 0.32 g catalyst

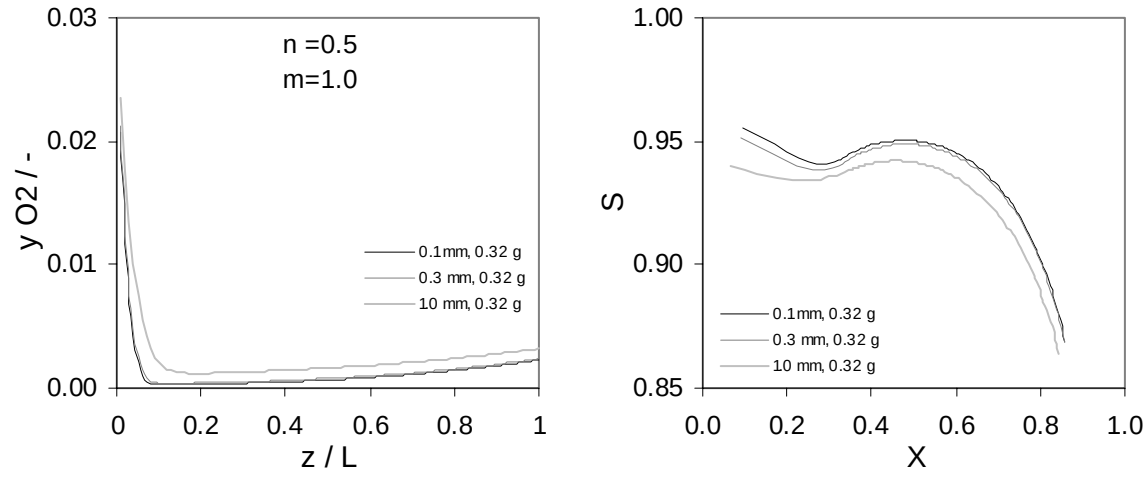

Fig.- B-1 Influence of the particle size on the (a) axial oxygen concentration profile and (b) selectivity – conversion plot for arbitrary kinetics with oxygen reaction orders n=0.5/m=1 and the catalyst mass 0.32 g.

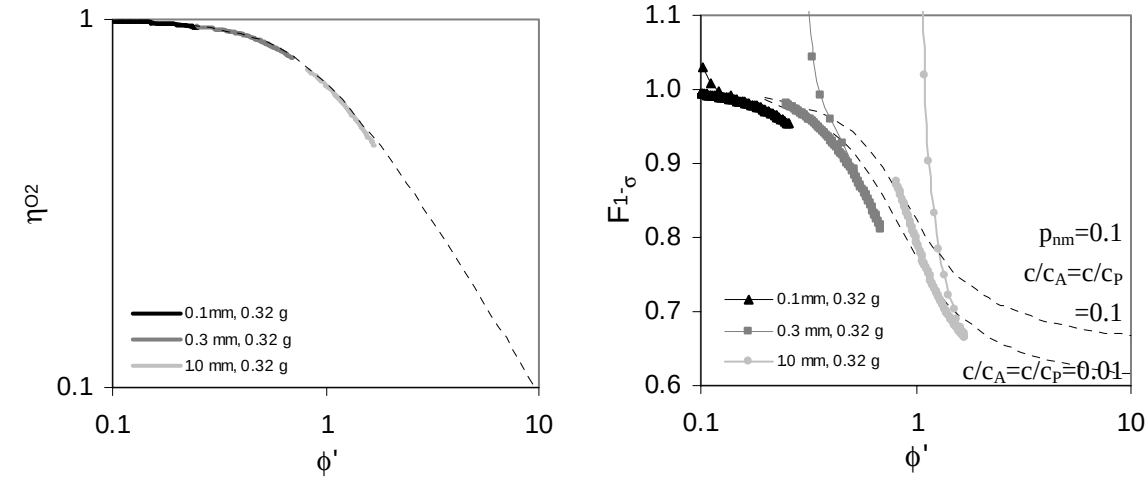

Fig.- B-2 Influence of the particle size on the (a) particle efficiency for oxygen consumption and (b) selectivity ratio as a function of the modified Thiele modulus ϕ' for arbitrary kinetics with oxygen reaction orders n=0.5/m=1 and the catalyst mass 0.32 g.

B.2 Reaction orders n=1/m=2 and 0.1 g catalyst

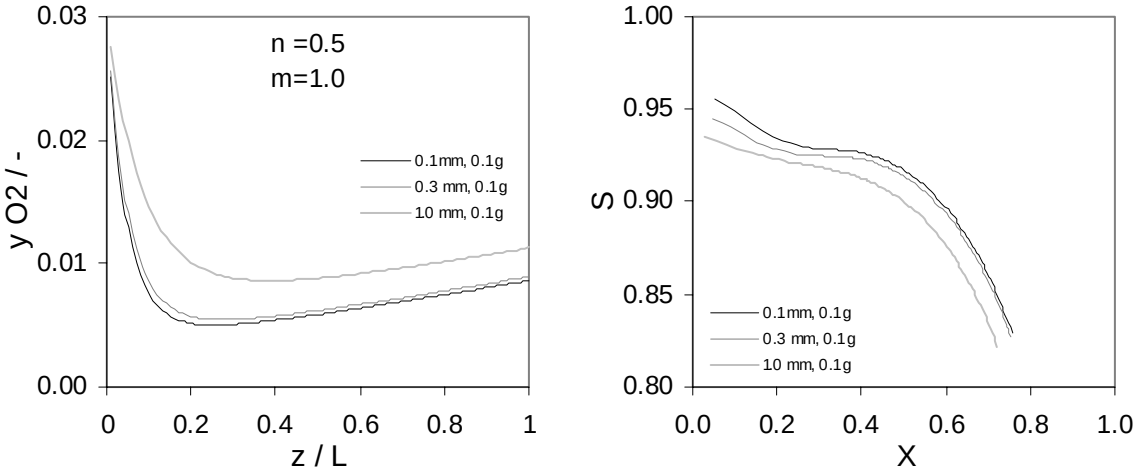

Fig.- B-3 Influence of the particle size on the (a) axial oxygen concentration profile and (b) selectivity – conversion plot for arbitrary kinetics with oxygen reaction orders n=1/m=2 and the catalyst mass 0.1 g.

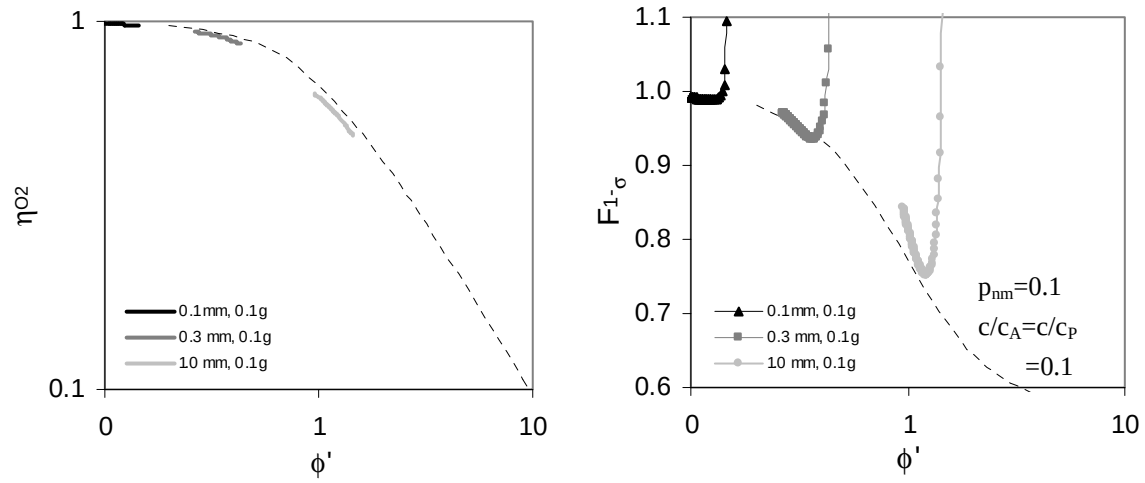

Fig.- B-4 Influence of the particle size on the (a) particle efficiency for oxygen consumption and (b) selectivity ratio as a function of the modified Thiele modulus ϕ' for arbitrary kinetics with oxygen reaction orders n=1/m=2 and the catalyst mass 0.1 g.

B.3 Reaction orders n=1/m=2 and 0.32 g catalyst

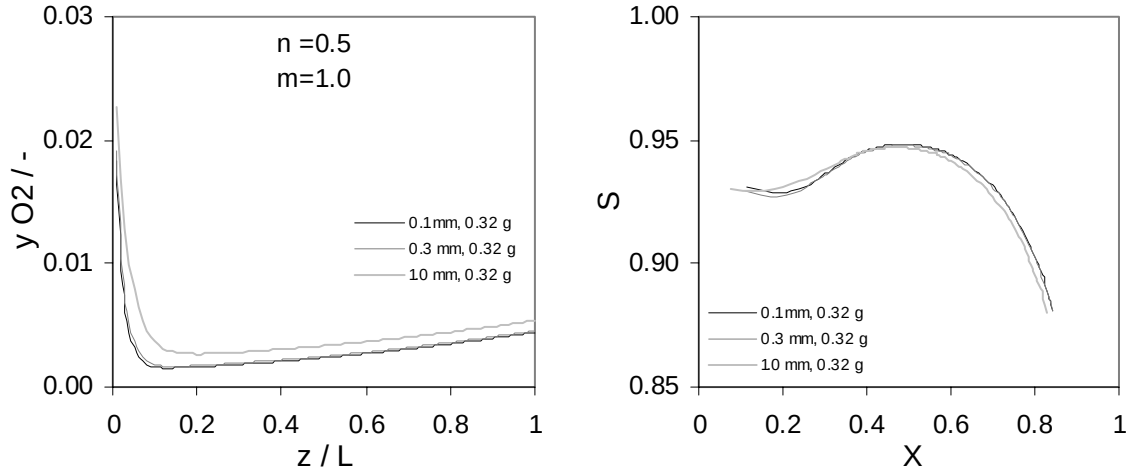

Fig.- B-5 Influence of the particle size on the (a) axial oxygen concentration profile and (b) selectivity – conversion plot for arbitrary kinetics with oxygen reaction orders n=1/m=2 and the catalyst mass 0.32 g.

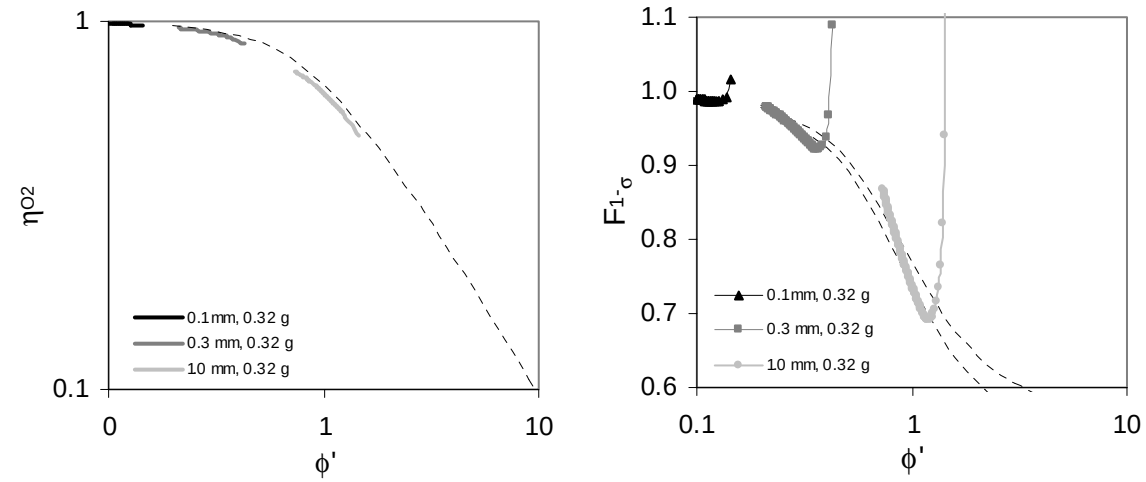

Fig.- B-6 Influence of the particle size on the (a) particle efficiency for oxygen consumption and (b) selectivity ratio as a function of the modified Thiele modulus ϕ' for arbitrary kinetics with oxygen reaction orders n=1/m=2 and the catalyst mass 0.32 g.

B.4 Reaction orders n=0.5/m=1, ν_1=0.5/ν_2=10 and 0.32 g catalyst

Finally, the effect of the stoichiometric coefficients on the reactor performance is illustrated for another catalyst mass of 0.32 g. The initial oxygen concentration is reduced to y_{O_2}=0.01 in agreement with the optimization presented in Chapter 3.

For the higher catalyst mass the loss of product yield for the particle diameter of 1 mm reduces to 5 % due to the reduces oxygen concentrations in the reactor.

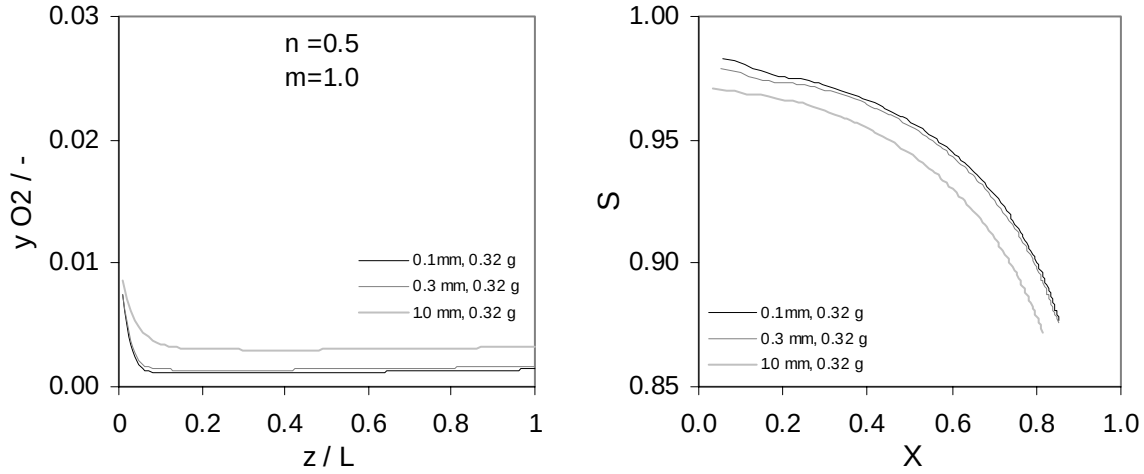

Fig.- B-7 Influence of the particle size on the (a) axial oxygen concentration profile and (b) selectivity – conversion plot for arbitrary kinetics with oxygen reaction orders n=0.5/m=1, ν_1=0.5/ν_2=10 and the catalyst mass 0.32 g.

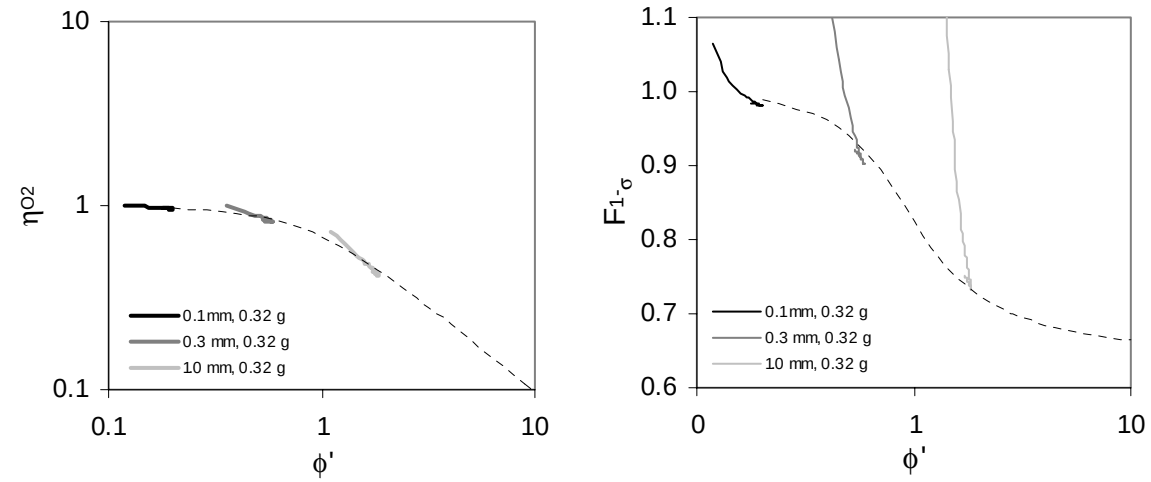

Fig.- B-8 Influence of the particle size on the (a) particle efficiency for oxygen consumption and (b) selectivity ratio as a function of the modified Thiele modulus ϕ' for arbitrary kinetics with oxygen reaction orders n=0.5/m=1, ν_1=0.5/ν_2=10 and the catalyst mass 0.32 g.

6 Integral effect of limitations in the membrane to centerline transport on the PBMR performance

Abstract

A two-dimensional, pseudo-homogeneous model has been developed to describe the radial and axial concentration and temperature profiles in the PBMR, including the 2-D velocity field induced by the distributive membrane flow and a radial porosity profile. For a consecutive reaction scheme with arbitrary reaction orders in oxygen between 0 and 2 the effects of the mass transfer limitations from the membrane wall to the center of the bed on the integral performance of the PBMR have been investigated.

The calculation results have revealed that radial mass transfer limitations deteriorate the integral conversion and selectivity of the PBMR due to its effect on both the oxygen and the hydrocarbon concentrations. For modified Thiele moduli $\phi'' > 1$ *approximately radial concentration profiles influence the integral reactor performance, but for* $\phi'' < 1$ *a one-dimensional model can sufficiently accurately describe the PBMR. Effects of a radial porosity profile need only to be taken into account, if the radial dispersion is dominated by molecular diffusion and* $\phi'' > 1$.

6.1 Introduction

Distributive addition of oxygen to the reaction zone is applied to increase the selectivity of the desired partial oxidation product, provided that the formation rate of the target product is less dependent on the oxygen concentration than the rates of the side-reactions. If the main side-reaction is a consecutive reaction, the reactor must exhibit low gas back-mixing behavior to avoid product losses (assuming positive reaction orders). A packed bed membrane reactor (PBMR) combines the features of distributive reactant addition and low axial back-mixing. Oxygen or air is added distributively via a membrane to a packed bed of particles. In this work it has been assumed that the particles are contained inside a tubular membrane. Similar trends are observed for the case where the catalyst is packed on the shell-side between the membrane and the reactor wall. The following consecutive reaction scheme will be considered:

$$\begin{aligned} A + \nu_1 O_2 &\rightarrow P \qquad r_1 = k_1 c_A c^n \\ P + \nu_2 O_2 &\rightarrow W \qquad r_2 = k_2 c_P c^m \end{aligned} \quad \text{with } m>n \qquad (1),(2)$$

Product losses due to the consecutive reaction are decreased by reducing the oxygen concentration level. However, the oxygen (either supplied as pure oxygen or as air) is added to the packed bed via the membrane and is radially distributed over the packed bed by radial

convective and dispersive transport mechanisms. In this chapter the effects of a radial oxygen concentration profile on the performance of the PBMR are investigated.

In Chapter 3 the influence of radial dispersion on the intrinsic activity and product selectivity of a slab of the PBMR was investigated. A characteristic number $\phi"$ comparable with the modified Thiele-modulus of the intraparticle mass-transport problem was formulated using radially averaged concentrations, denoting the spatially averaged oxygen concentration by <c>:

$$\phi" = \frac{R}{2}\sqrt{\frac{\frac{n+1}{2}\nu_1 k_1^* \langle c\rangle^{n-1} + \frac{m+1}{2}\nu_2 k_2^* \langle c\rangle^{m-1}}{D}} \qquad (3)$$

with $k_1^* = (1-\varepsilon)k_1\langle c_A\rangle$, $k_2^* = (1-\varepsilon)k_2\langle c_P\rangle$

Here, the concentration of the hydrocarbons were assumed constant and large compared to the oxygen concentration: $\langle c\rangle << \min\left(\nu_1\langle c_A\rangle, \nu_2\langle c_B\rangle\right)$. It was shown that under this assumption for $\phi" > 1$ radial transport limitations have a negative effect on both the activity of the packed bed and the intrinsic product selectivity.

In the present Chapter the effect on the integral performance of the PBMR will be discussed. Firstly, the concentrations of the hydrocarbons will not be large compared to the oxygen concentration at every position in the PBMR. Near the inlet where the first intermediate is formed and near the outlet in case of high reactant conversions this condition is certainly not fulfilled, and it will be investigated how this will effect the integral product selectivity. Furthermore, radial concentration profiles can be expected also for the hydrocarbons with an additional effect on the integral product selectivity.

In the characteristic number $\phi"$ presented above only radial dispersive transport is accounted for. The role of additional convective radial transport induced by the membrane flow on the radial distribution of oxygen will be discussed subsequently.

Finally, it is investigated if a by-pass effect is noticeable in a PBMR with a low particle-to-tube diameter ratio. The structure of the packing is disturbed by a solid wall, and especially if the diameter of the particles approaches that of the tube diameter a by-pass flow near the tube wall emerges. Adding oxygen via a membrane to this by-pass flow could reduce the residence time of oxygen in the PBMR with possible adverse effects on the integral performance.

Before discussing the effect of membrane to centerline mass transport limitations the reactor model and the model parameters used in this study are described.

6.2 Two-dimensional, pseudo-homogeneous PBMR-model

In order to investigate the influence of radial profiles of concentration and temperature on the integral performance of the PBMR a two-dimensional, pseudo-homogeneous reactor model was developed.

Often, a one-dimensional model is sufficiently accurate in describing the packed bed reactor, at least if temperature effects are small. In case of the PBMR, however, it is likely that a radial oxygen profile is established. If the PBMR is operated at a low oxygen concentration level with small axial concentration gradients over the length of the reactor, the local oxygen balance is (due to the high conversion rate) mainly determined by radial transport, which moreover is mainly dominated by dispersive transport driven by concentration gradients. If the consumption rate is large a radial concentration profile is to be expected.

In a packed bed with large particles relative to the tube diameter a bypass flow can emerge near the tubular wall. In a PBMR, a membrane replaces this tubular wall. Oxygen is added to the packed bed in this region of increased bed porosity and increased axial velocity reducing the residence time of oxygen in the catalyst bed. To evaluate the extent of this effect, the description of the two-dimensional flow field was included in the PBMR model. The developed PBMR model was based on the following assumptions:

1. Pseudo-homogeneous reactor model

In the model mass and heat transfer limitations from the gas bulk to the catalyst surface and inside the catalyst particle have been ignored. These effects have been investigated in Chapter 5. The reaction rates can thus be described as a direct function of the gas phase concentrations. Furthermore, the structure of the packing is characterized by a single parameter, namely the bed porosity, which can however be a function of the radial position in the tube. The bed porosity is considered here as a locally averaged value. Also axi-symmetry is assumed for the PBMR.

2. Diffusive and dispersive transport can be described with a standard dispersion model (SDM)

It is assumed that gas phase mass and energy transport in the PBMR can be modeled with a two-dimensional model with convective flow with superimposed radial and axial dispersion.

Firstly, the flow model (gas phase total continuity and Navier-Stokes equations) is described, where after the component mass balances and overall energy balance are given.

6.2.1 Flow model

Under some conditions the flow field can be calculated *a priori* independent of the reaction model. The flow field can be calculated analytically, if the following conditions are met:

1. the flow in the packed bed is fully developed,

2. the membrane flow is constant along the axial coordinate,
3. the porosity of the packed bed is assumed to be constant: $dv_z/dz \neq f(r)$,
4. the radial temperature profiles are small(otherwise deviations from plug flow can be expected due to a radial variation in density and viscosity) and
5. the influence of the reaction (change of mole number and temperature) on the volumetric flow rates is negligible.

If the membrane flow is independent of the conditions inside the packed bed – i.e. independent of the local concentrations or local membrane temperature – and if the change of the gas density due to the ongoing reactions is small, then the total flow through a cross section of the packing is known. Also if the bed porosity is constant, the axial velocity is uniform over the radius and the radial velocity is a linear function of the radial coordinate.

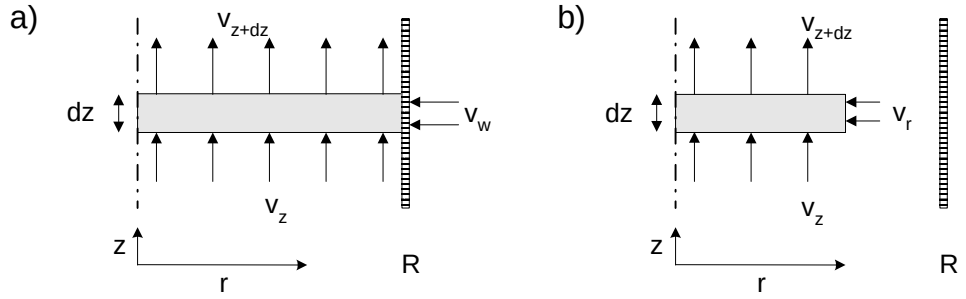

Fig. 1 a) Axial and b) radial velocity profile.

Integration of the total continuity equation over the radial coordinate (Fig. 1a) yields

$$\int_0^R 2\pi r \frac{dv_z}{dz} dr = 2\pi R|v_w| \tag{4}$$

Assuming that dv_z/dz is not a function of the radial coordinate gives

$$\pi R^2 \frac{dv_z}{dz} = 2\pi R|v_w| \text{ and } \frac{dv_z}{dz} = \frac{2|v_w|}{R} \tag{5}$$

which indeed shows that the above assumption was correct. The axial velocity profile is thus given by:

$$v_z = v_{z,0} + \frac{2|v_w|}{R} z \tag{6}$$

Making use of the fact that dv_z/dz is not a function of the radial coordinate, the total continuity equation can be integrated over the radial coordinate (Fig. 1b) to give

$$\pi r^2 \frac{dv_z}{dz} = 2\pi r|v_r| \tag{7}$$

which yields the following expression for the radial velocity profile:

$$v_r = v_w \frac{r}{R} \tag{8}$$

The two-dimensional PBMR model calculates the gas phase velocity field by solving the total continuity and momentum equations for the gas phase given respectively by:

$$\frac{\partial\left(\varepsilon\rho_g\right)}{\partial t}+\nabla\cdot\left(\varepsilon\rho_g\bar{v}\right)=0 \tag{9}$$

and:

$$\frac{\partial}{\partial t}\left(\varepsilon\rho_g\bar{v}\right)+\nabla\cdot\left(\varepsilon\rho_g\bar{v}\bar{v}\right)=-\varepsilon\nabla p-\beta\varepsilon\rho_g\bar{v}-\nabla\cdot\left(\varepsilon\bar{\bar{\tau}}_g\right)+\varepsilon\rho_g\bar{g} \tag{10}$$

where

- Friction coefficient: $\beta=150\frac{(1-\varepsilon)^2}{\varepsilon^3}\frac{\mu_g}{\rho_g d_p^{\,2}}+1.75\frac{1-\varepsilon}{\varepsilon^3}\frac{\varepsilon|\bar{v}|}{d_p}$ (11)

  (Ergun's equation) with $|\bar{v}|=\sqrt{v_r^{\,2}+v_z^{\,2}}$

- Newtonian fluid: $\bar{\bar{\tau}}_g=-\left(\lambda_g-\frac{2}{3}\mu_g\right)(\nabla\cdot\bar{v})\bar{\bar{I}}-\mu_g\left[(\nabla\bar{v})+(\nabla\bar{v})^T\right]$ (12)

  λ_g is the contribution of the bulk viscosity of the gas to the normal stress, which can be neglected for low-density gases (Bird et al., 1960).

- Ideal gas law: $\rho_g=\frac{pM_g}{RT_g}$ (13)

Although the physical properties (especially density and viscosity) are determined by the local composition and temperature, which are affected by chemical reactions, the component mass balances and the energy balance are solved sequentially after having solved the flow model. This decoupling is possible and desired because of the large differences in time scales on which the hydrodynamic phenomena and chemical reactions take place. Furthermore, the decoupling has the clear advantage that different time steps and scales can be used, speeding up the calculations tremendously.

The total continuity and Navier-Stokes equations are solved with a finite difference technique on a staggered computational mesh using a first order time discretisation and implicit treatment of the pressure gradient and linearized implicit treatment of the drag forces. The implicit treatment of the pressure gradient term requires solving a pressure correction equation (Poisson equation) derived from the mass defect of the gas phase continuity equation. The convection terms have been discretised using a first order upwind scheme, while the dispersion terms have been discretised with standard second order finite difference representations. Subsequently, the computational scheme will be discussed in more detail.

For a new time step, firstly the density field is calculated from the old pressure, temperature and concentration field data using the ideal gas law. Subsequently, the velocity field is calculated using the discretised momentum equations, followed by the calculation of the new pressure field using the pressure correction equation. Then, the density field is updated using the equation of state and the iteration-loop is repeated until all variables have converged.

Due to the explicit treatment of the convection and dispersion terms in the momentum equation the maximum allowable time step is determined by the following two stability criteria:

Viscosity stability criterion	Courant-Friedrichs-Lewy stability criterion (Courant condition)
$\frac{\mu_g \Delta t}{\rho_g \Delta x^2} < 0.5$	$\sqrt{\left(\frac{\lvert v_r \rvert \Delta t}{\Delta r}\right)^2 + \left(\frac{\lvert v_z \rvert \Delta t}{\Delta z}\right)^2} < 1$ (14),(15)

For small-scale reactors (d_t= 0.008 m) the viscosity criterion is usually limiting, however for larger reactors the Courant condition (d_t= 0.05 m) may become decisive for the permissible time step.

The minimum time step required was $2 \cdot 10^{-5}$ s when using 80 radial grid cells of $5 \cdot 10^{-5}$ m.

6.2.2 Component mass balances and energy balance

The radial and axial concentration profiles in the PBMR are calculated from component mass balances accounting for two-dimensional, instationary convective and dispersive transport including a non-linear source term:

$$\frac{\partial \rho_g \varepsilon \omega_i}{\partial t} = -\frac{1}{r}\frac{\partial r \rho_g \varepsilon v_r \omega_i}{\partial r} - \frac{\partial \rho_g \varepsilon v_z \omega_i}{\partial z} + \frac{1}{r}\frac{\partial}{\partial r}\left(\rho_g D_{r,i} r \frac{\partial \omega_i}{\partial r}\right) + \frac{\partial}{\partial z}\left(\rho_g D_{z,i} \frac{\partial \omega_i}{\partial z}\right) + S_i \qquad (16)$$

Here ω_i represents the mass fractions of all components but one. The concentration of the component present in excess is calculated from the equation: $\sum_{i=1}^{nc} \omega_i = 1$ (17)

In Equation (16) $D_{r,i}$ and $D_{z,i}$ represent the effective radial and axial dispersion coefficients, whereas the source terms are given by: $S_i = (1-\varepsilon)\rho_{cat} M_i \sum_{j=1}^{nrr} \nu_{ij} r'_j$ (18)

The energy balance for the pseudo-homogeneous PBMR describing the temperature distribution reads:

$$\left(\varepsilon \rho_g c_{p,g} + (1-\varepsilon)\rho_s c_{p,s}\right)\frac{\partial T}{\partial t} = -c_{p,g}\frac{1}{r}\frac{\partial r \rho_g \varepsilon v_r T}{\partial r} - c_{p,g}\frac{\partial \rho_g \varepsilon v_z T}{\partial z} + \lambda_r \frac{1}{r}\frac{\partial}{\partial r}\left(r\frac{\partial T}{\partial r}\right) + \lambda_z \frac{\partial^2 T}{\partial z^2} + S_h$$

with $S_h = (1-\varepsilon)\rho_{cat} \sum_{j=1}^{nrr} r'_j \Delta H_j$ (19),(20)

Again, a finite difference technique is used to discretise the equations employing the same computational mesh as used in the flow model. Convection is discretised with first order upwind, and for diffusion terms standard second order central differences are used. The *alternating direction implicit* (ADI) method was applied, where a full time step is calculated via two half time steps, treating the transport in the radial direction implicitly and in the axial direction explicitly in the first half step and vice versa in the next half time step.

6.2.3 Boundary and initial conditions

The usual Danckwerts-type boundary conditions have been implemented. Boundary and initial conditions are given in Table 1.

Table 1 Boundary and initial conditions for component mass and energy balance.

	component mass balance	energy balance
left	$\left.\frac{\partial\bar{\omega}}{\partial r}\right\|_{r=0} = 0$	$\left.\frac{\partial T}{\partial r}\right\|_{r=0} = 0$
right	$-\left(D_{r,i}\rho_g\right)_{nr+1/2}\left.\frac{\partial\omega_i}{\partial r}\right\|_{r=d_t/2} + \left(v_r\rho_g\varepsilon\bar{\omega}\right)\Big\|_{r=d_t/2} = \Phi_{m,distr,i}/\left(\pi d_t L\right)$	$T\big\|_{r=0} = T_w$ or $-\lambda_r\left.\frac{\partial T}{\partial r}\right\|_{r=d_t/2} = \alpha_w\Delta T_w$
bottom	$\left.\frac{\partial\omega_i}{\partial z}\right\|_{z=L} = 0$	$T\big\|_{z=0} = T_0$
top	$-D_{z,i}\rho_g\left.\frac{\partial\omega_i}{\partial z}\right\|_{z=0} + \left(v_z\rho_g\varepsilon\omega_i\right)_{z=0} = \Phi_{m,0,i}/\left(0.25\pi d_t^2\right)$	$\left.\frac{\partial T}{\partial z}\right\|_{z=L} = 0$
initial	$\omega_i\left(r,z\right) = \omega_{i,0}$	$T\left(r,z\right) = T_0$

6.2.4 Physical properties

The gas phase physical properties have been modeled following Reid et al. (1988) using pure component properties of the data set of AIChE Design Institute for Physical Property Data (see Appendix A in Chapter 5).

6.2.5 Combination of the flow model and the reaction balance

The calculation strategy for solving the flow field combined with the component mass balances and the energy balance (here referred to as the reaction model) has been illustrated in Fig. 2.

Since only the steady state profiles are of interest here, the flow solver is advanced for 5 consecutive time steps, after which the reaction model is solved with a time step up to 1000 times larger than the time step used in the flow solver.

The developed model was validated with the Hagen-Poiseuille law correlating the pressure drop and radial velocity profile in an empty tube, and the Nusselt-Graetz correlation describing the axial profile of the radially averaged temperature of a gas flow through a wall heated tube.

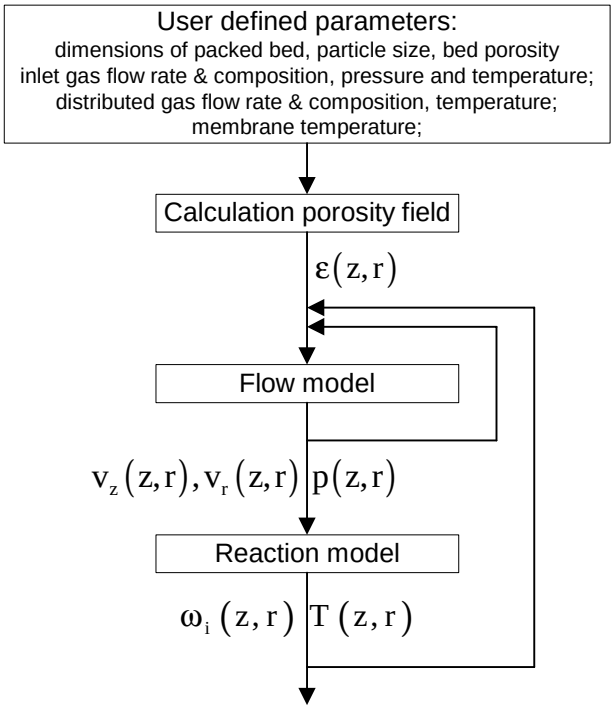

Fig. 2 Combination of flow model and reaction model in the pseudo-homogeneous, 2-dimensional PBMR model.

6.3 Model parameters

The most important constitutive equations for the 2D, pseudo-homogeneous PBMR model are the radial porosity profile (especially if the particle size approaches the tube diameter) and the effective mass and heat dispersion coefficients, which are discussed in somewhat more detail below. Despite the vast number of existing publications on packed bed reactors, these model parameters are still subject of debate and no single equation for one of these parameters is generally accepted. However, a suitable correlation presented in the literature is selected to highlight the effect of radial profiles on the integral reactor performance.

6.3.1 Porosity distribution

The porosity within a (randomly) packed bed of uniform spheres was determined by several research groups as a function of the distance from the wall, e.g. by Benenati and Brosilow (1962) and Schuster and Vortmeyer (1980).

The data points of Benenati and Brosilow formed the basis of many approaches to develop a correlation for the radial porosity distribution. Ridgway and Tarbuck (1968) started with the geometric deviation of the porosity function for a bed of regular close-packed spheres at a straight wall, which they subsequently fitted to the data of Benenati and Brosilow introducing three correction factors to account for the random character of the packing (two randomizing factors) and the cylindrical form of the bed.

The application of their method is rather cumbersome. Martin (1977) proposed the following empirical representation.

$$\varepsilon(z)=\begin{cases}\varepsilon_{min}+(1-\varepsilon_{min})z^2 & -1\le z\le 0\\ \varepsilon_0+(\varepsilon_{min}-\varepsilon_0)e^{-z/4}\cos\left(\frac{\pi}{C}z\right) & z\ge 0\end{cases} \qquad (21)$$

with $z\equiv\frac{R-r}{d_p/2}-1$ and $C=\begin{cases}0.816 & d_t/d_p=\infty\\ 0.876 & d_t/d_p=20.3\end{cases}$

The minimum porosity is in the range of ε_{min} =0.20 – 0.26 and ε_0 is the bulk porosity of the bed undisturbed by wall effects.

Several authors present approximate porosity functions, which involve only the porosity increase towards the wall without any minima in the profile or including only the first minimum. Vortmeyer and Schuster (1983) give the following equation for a circular tube:

$$\varepsilon(r)=\varepsilon_0\left\{1+C\exp\left(1-2\frac{R-r}{d_p}\right)\right\} \qquad (22)$$

where the constant C can be determined with the boundary condition for spherical particles

$$\varepsilon(R)=1:\ C=\frac{1-\varepsilon_0}{\varepsilon_0\exp(1)}$$

Reformulation results in:

$$\varepsilon(r)=\varepsilon_0+(1-\varepsilon_0)\exp\left(-2\frac{R-r}{d_p}\right) \qquad (23)$$

Hunt and Tien (1990) suggest a similar correlation replacing the constant 2 by 6 for perfect spheres and 8 for slightly irregular or non-uniform particles.

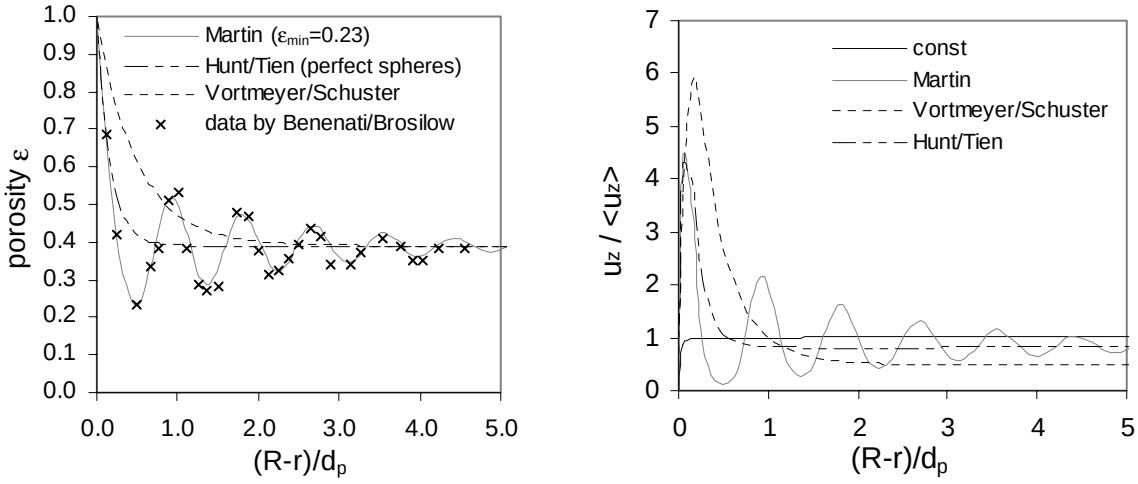

Fig. 3 (a) Porosity distribution near the wall in a bed of spherical particles. Data points by Benenati and Brosilow (1962) for d_t/d_p=20.3; ε_0 = 0.38. (b) Axial velocity profiles resulting from the different porosity distributions.

In Fig. 3a) the different porosity profiles are compared with the data points of Benenati and Brosilow, and Fig. 3b) shows the resulting dimensionless axial velocity profiles, calculated with the PBMR model with the membrane flux set to zero.

To evaluate the proposed radial porosity correlations several criteria have to be considered:

1. Average porosity
2. Pressure drop
3. Influence on velocity and concentration profiles

From Fig. 3b) it can be concluded that the porosity function of Vortmeyer and Schuster results in an overestimation of the by-pass flow, and as an consequence thereof the gas velocity in the core of the bed is predicted significantly lower than the velocities resulting from the profile of Martin, opposite to the correlation proposed by Hunt and Tien. Furthermore, a comparison of the average porosity and pressure drop (Table 2) clarifies that the correlation of Hunt and Tien is to be preferred.

Table 2 Comparison of the predictions for the average porosity, pressure drop and maximum axial velocity by the different porosity distribution models (d_t/d_p=20.3; ε_0=0.38).

Porosity model	$\langle\varepsilon\rangle$	Δp / *Pa*	$u_{max}/\langle u\rangle$
Martin	0.399	504	4.31
Hunt and Tien	0.409	470	4.96
Vortmeyer and Schuster	0.447	215	6.99

Moreover, if the particles have small deviations from the spherical form, the porosity function shows only one oscillation (Vortmeyer and Schuster, 1983). Therefore, the correlation by Hunt and Tien was selected for the porosity profile in the PBMR model.

6.3.2 Dispersive transport

An other important model parameter is the radial dispersion coefficient. Despite the addition of a distributive convective flow via the membrane tube wall, dispersion is the main driving force for radial transport. Therefore, the correlation for the radial dispersion must be carefully chosen.

The radial dispersion is often expressed in a form in which the contribution by molecular diffusion and turbulent mixing effects are separated.

$$D_r = D_r^m + D_r^t \tag{24}$$

The following correlation for the dispersion in the core of the packed bed was proposed by Tsotsas and Schlünder (1988):

$$D_r = \left(1-\sqrt{1-\varepsilon_0}\right) D_i^m + \frac{u_0 d_p}{PE_\infty \left(d_t/d_p \to \infty\right) f\left(d_t/d_p\right)} \qquad \text{or} \tag{25}$$

$$\frac{1}{Pe_r} = \frac{1-\sqrt{1-\varepsilon_0}}{Re\,Sc} + \frac{1}{PE_\infty f\left(d_t/d_p\right)} \tag{26}$$

Where d_p is the particle diameter and d_t the tube diameter, $PE_\infty\left(d_t/d_p \to \infty\right)$ is the limiting value of the Péclet number in an unconfined bed, which is about 8, and $f\left(d_t/d_p\right)$ is a correction factor accounting for the influence of the tube wall and the resulting flow maldistribution. Near the tube wall the porosity of the bed and consequently the gas velocity is increased, so that in the bed center the velocity is below the average. This results in a lower dispersion in the core of the bed.

$$D_r^t = \frac{u_0 d_p}{8\left(2-\left(1-2\left(d_p/d_t\right)\right)^2\right)} \tag{27}$$

where u_0 is the average superficial velocity.
Alternatively, the superficial velocity in the core of the bed u_c can be used, which avoids the correction term.

$$D_r^t = \frac{u_c d_p}{8} \tag{28}$$

The correlations presented above were derived from measurements, where a tracer was injected at the axis of the tube. In most cases the profiles did not reach the tube wall. So, the dispersion was determined in an area of nearly constant porosity and velocity profiles. Therefore, the equations are based on average values of the velocity and bed porosity, and do not include radial dependencies.
In case of a membrane reactor, however, the oxygen is added through the membrane wall. Near the wall the gas velocity is distinctly higher than in the core, and therefore the influence of the radius on the dispersion should be included.

$$D_r = \left(1-\sqrt{1-\varepsilon}\right)D_i^m + \frac{u d_p}{8} \tag{29}$$

where the local values are used for the bed porosity and superficial velocity.
For the axial dispersion coefficient the same correlation was used, however with a 4 times larger contribution of the turbulent dispersion.

Gunn (1987) presented different correlations for both the molecular and the turbulent contribution of the effective dispersion coefficient.

$$\frac{1}{Pe_r} = \frac{1}{Pe_r^m} + \frac{1}{Pe_r^t} = \frac{\varepsilon}{\tau Re\,Sc} + \frac{1}{40-29\exp(-7/Re)} \quad \text{or} \tag{30}$$

$$D_r = \frac{\varepsilon}{\tau} D_i^m + \frac{u d_p}{40-29\exp(-7/Re)} \tag{31}$$

where τ equals 1.2 for spheres with.

Unfortunately, Gunn did not make clear, whether the Re number should be calculated with the local or the average superficial velocity, i.e. whether the correlation can be used to calculate a local dispersion coefficient. However, the fact that Gunn advises a constant value of $\tau = 1.2$ indicates that the correlation is probably derived for the core of the packed bed with constant bed porosity and gas velocity.

The tortuosity in a packed bed depends on the bed porosity and should decrease with increasing porosity (Punčochář and Drahoš, 1993). Punčochář and Drahoš (1993) discuss the tortuosity in packed beds and give the following relation for randomly packed beds:

$$\tau = \frac{1}{\sqrt{\varepsilon}} \qquad (\ \tau(\varepsilon = 0.4) = 1.58\ ) \tag{32}$$

Obviously, this equation is strictly not valid near the wall of a packed bed due to the order induced by the wall. Nevertheless, it is used here to compare different correlations for the molecular dispersion (= effective molar diffusion).

From Fig. 4 it can be concluded that the correlations proposed by Tsotsas and Schlünder (1988) and Gunn (1987) predict comparable contributions of the effective molecular dispersion, especially when using the tortuosity relation proposed by Punčochář and Drahoš (1993) in Gunn's correlation.

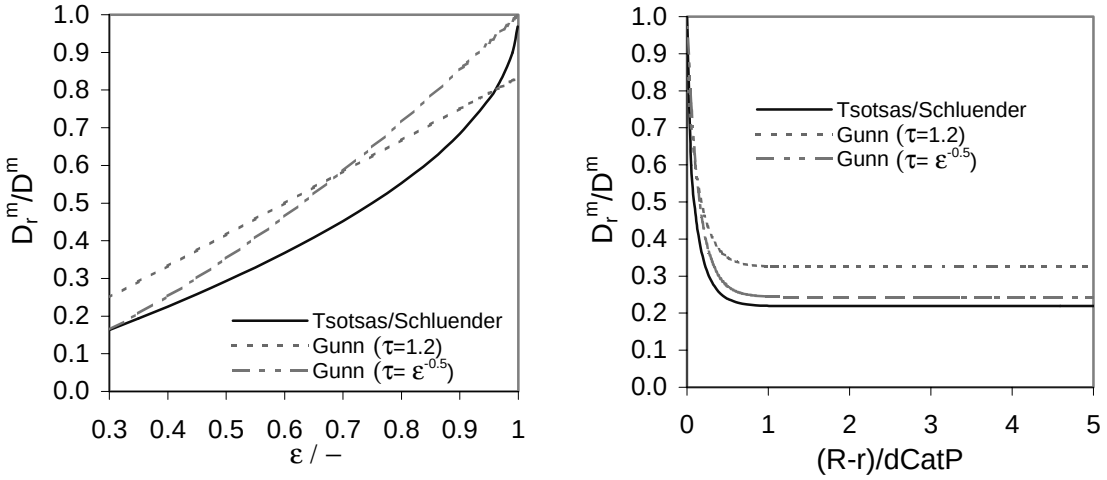

Fig. 4 Effectiveness factor for the molecular diffusion in the packed bed a) as a function of the bed porosity; b) near the tube wall applying the porosity function of Hunt and Tien (1990).

Wen and Fan (1975) have developed the following empirical correlation for the effective radial dispersion coefficient:

$$\frac{1}{Pe_r} = \frac{0.09}{1 + \dfrac{10}{Re\,Sc}} + \frac{0.4}{[Re\,Sc]^{0.8}} \quad \text{or} \quad D_r = \frac{0.09\,u\,d}{1 + \dfrac{10\,D_i^m}{u\,d}} + 0.4\left[u\,d_p\right]^{0.2} D_i^{m\,0.8} \tag{33),(34}$$

for the range of 0.4<Re<500, 0.77<Sc<1.2 .

The equation is based on fitting of measurements carried out by several research groups, where tracer was injected in the center of the bed. The radial dispersion coefficient was assumed to be constant everywhere in the bed.

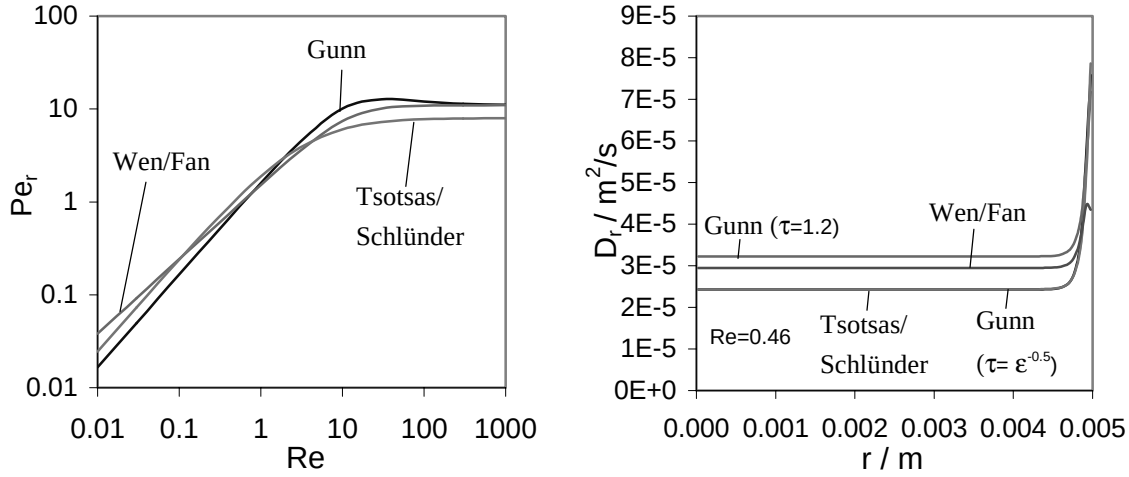

Fig. 5 Correlations for radial Peclet-number a) as function of the Re-number; b) as function of the radius in a packed bed (porosity profile of Hunt and Tien) with Re=0.46 in the core of the bed.

In Fig. 5a the different correlations for the effective radial Pe-number are plotted as a function of the Reynolds number, showing that Pe_r reaches a constant value of about 10 for Re-number exceeding about 10. The correlation of Gunn actually shows a maximum in the Pe_r-number at Re≈10, which was observed experimentally by various authors. Tsotsas and Schlünder (1988) showed, that they could also reproduce this maximum, if they use the equations proposed by Vortmeyer and Schuster (1983) for the calculation of the velocity profile in a packed bed to calculate the velocity in the core of the bed.

Axial and radial dispersion coefficients are treated separately in literature, due to the fact that in a tubular packed bed the dispersive transport is axially in line with and radially perpendicular to the main convective transport. This is, however, not true in a PBMR near the membrane wall where the distributive convective flow is added radially to the packed bed. However, near the centerline of the bed the radial velocity diminishes.
In the PBMR model the correlations by Tsotsas and Schlünder (1988) have been selected, where the local porosity and gas velocity is used. The actual differences between the proposed correlations are not very large and not very important for elucidating the effects of radial profiles on the reactor performance. Thus, the turbulent contribution to the radial dispersion increases near the membrane wall in case of a radial porosity profile.

6.3.3 Effective heat dispersion

For the description of the radial heat dispersion in a packed bed the Zehner formula extended by Bauer (VDI-Wärmeatlas, 1984) is used:

$$\frac{\lambda_r}{\lambda_g} = \frac{\lambda_{bed}}{\lambda_g} + \frac{Pe_x}{K_\infty f\left(d_t/d_p\right)} \tag{35}$$

which is a superposition of the effective heat conductivity in a packed bed without gas flowing through the bed (first term) and by convective mixing due to the gas stream (second term). In the axial direction the contribution of the convective term is generally a factor of 5 larger than in radial direction. Thus, for the axial direction

$$\frac{\lambda_z}{\lambda_g} = \frac{\lambda_{bed}}{\lambda_g} + 5\frac{Pe_x}{K_\infty f\left(d_t/d_p\right)} \tag{36}$$

Corresponding to the dispersion of mass K_∞ has a value of 8 (for a packing with infinite dimension). $f\left(d_t/d_p\right) = \left[2-\left(1-2d_p/d_t\right)^2\right]$ is again the correction of the velocity in the core of the bed in case of a significant by-pass flow, which is not needed in the model of the PBMR, because the actual flows are calculated.

The Peclet-number is here defined as $Pe_x = \frac{u_{sup}\rho_g c_{p,g}}{\lambda_g} x_F$ with the effective mixing length x_F $=F\cdot d_p$ (F=1.15 for spherical particles). In other articles e.g. Martin and Nilles,1993, the factor F is neglected, or sometimes added to the formula of the mass dispersion.

The thermal conductivity of the packed bed at zero flow is calculated by formulas summarized by Zehner and Schlünder (1970).

$$\frac{\lambda_{bed}}{\lambda_g} = \left(1-\sqrt{1-\varepsilon}\right)\left(1+\frac{\lambda_{rad}}{\lambda_g}\right) + \sqrt{1-\varepsilon}\left\{\frac{2}{1-\frac{\lambda_g}{\lambda_{cat}}B}\left[\frac{\left(1-\frac{\lambda_g}{\lambda_{cat}}\right)B}{\left(1-\frac{\lambda_g}{\lambda_{cat}}B\right)^2}\ln\frac{\lambda_{cat}}{\lambda_g B} - \frac{B+1}{2} - \frac{B-1}{1-\frac{\lambda_g}{\lambda_{cat}}B}\right] + \frac{1}{\frac{\lambda_g}{\lambda_{rad}}+\frac{\lambda_g}{\lambda_{cat}}}\right\}$$

$$\lambda_{rad} = \frac{0.23}{\frac{2}{\varepsilon_{rad}}-1}\left(\frac{T}{100}\right)^3 d_p \tag{37),(38}$$

$B = C\left(\frac{1-\varepsilon}{\varepsilon}\right)^{10/9}$; derived from experiments C (pellets)=1.25, C(broken particles)=1.4

Experimental measurements of the radial temperature profile show a temperature jump at the wall (see references in Martin and Nilles, 1993). Usually, this jump is modeled applying the

following the boundary condition at the wall, especially if the porosity of the bed is supposed to be constant:

$$-\lambda_r \frac{\partial T}{\partial r} = \alpha_w \left(T_w - T\right) \tag{39}$$

Martin and Nilles (1993) present the following set of correlations for the estimation of the wall heat transfer coefficient:

$$Nu_w = Nu_{w0} + 0.19\,Pe^{0.75}\,Pr^{-0.42} \tag{40}$$

$$Nu_{w0}\left(d_R/d_p \approx 10, \text{glas, ceramic}\right) = 17 \pm 30\%$$

$$Nu_{w0} = \left(1.3 + 5\,d_p/d_R\right)\frac{\lambda_{bed}}{\lambda_f}$$

They showed that they are able to model experimental results from literature with good agreement assuming plug flow behavior of the gas, and with very good agreement using the velocity profile of Vortmeyer. In both cases a constant radial dispersion coefficient was applied.

An alternative model without wall resistance ($1/\alpha_w=0$) and therefore radially variable λ_r also showed good agreement. The small deviation could be explained with the fact that the porosity profile of Vortmeyer was used, which overestimates the porosity drop towards the wall and therefore the heat transfer resistance.

Recently wave models have been developed based on a physically more sound description of the dispersion processes in a packed bed and provide a more fundamental description of the wall-temperature jump (Kronberg, 1997).

In this work, the heat transfer models with the porosity profile of Hunt and Tien (1990) and no wall heat transfer resistance will be applied.

6.4 The effect of membrane to centerline mass transport limitations on the integral reactor performance

In this section the effect of radial concentration profiles, extending from the membrane wall towards the centerline of the packed bed, on the performance of the PBMR will be discussed. Firstly, the effects of radial profiles in the hydrocarbon concentrations are investigated and compared with the results of Chapter 3, where the hydrocarbon concentrations were assumed constant. Unless otherwise stated, the membrane flux has been assumed constant over the entire length of the reactor.

In Table 3 the model parameters as given for the standard membrane tube diameter of d_t=0.01 m. For the evaluation of the influence of the rate of radial transport on the integral reactor performance, the membrane tube diameter is increased. Because of the laminar flow in the reactor with the standard dimensions, an increase of the membrane tube diameter results in an increase of the modified Thiele-modulus ϕ''. The flow rate of premixed and

distributive flow and the catalyst mass in the reactor have to be adjusted together with the tube diameter $d_{t,i}$ in order to keep the contact time in the reactor constant.
The new values result from

$$\Phi_{V,0,i} = \left(d_{t,i}/d_t\right)^2 \Phi_{V,0}, \Phi_{V,distr,i} = \left(d_{t,i}/d_t\right)^2 \Phi_{V,distr} \text{ and } m_{cat,i} = \left(d_{t,i}/d_t\right)^2 m_{cat}. \quad (41)$$

The other model parameters remain the same.

Table 3 Model parameters for the standard diameter of the membrane tube of d_1=0.01 m.

Rate constants: n=0.5/m=1.0		k'_1	0.015 mol / (g s bar^{1+n})
		k'_2	0.045 mol / (g s bar^{1+m})
Rate constants: n=1.0/m=2.0		k'_1	0.150 mol / (g s bar^{1+n})
		k'_2	4.500 mol / (g s bar^{1+m})
Stoichiometric coefficients		ν_1	1
		ν_2	1
Reactor length		L	0.1 m
Membrane tube diameter		d_t	0.01 m
Catalyst mass		m_{cat}	0.1 g or 0.32 g
Particle diameter		d_t/d_p	20
Bed porosity		ε	0.389
Reactor pressure and temperature		p, T	1.013 bar at outlet, 550 K
Premixed feed:	volumetric flow	$\Phi_{V,0}$	100 ml / min
	mole fraction of reactant A	$y_{A,0}$	0.1
	mole fraction of oxygen	$y_{O2,0}$	0.03
Distributed feed:	volumetric flow	$\Phi_{V,distr}$	35 ml / min
	mole fraction of oxygen	$y_{O2,distr}$	0.2

100 grid cells are used in axial and 40 in radial direction, and the time step size is $5 \cdot 10^{-5}$ s for the flow model and $5 \cdot 10^{-2}$ s for the reaction model.

6.4.1 Influence of the membrane tube diameter for a constant average concentration of oxygen along the reactor length

In Chapter 3 the influence of radial diffusive transport on the conversion rate and the product selectivity in a slab of a PBMR was investigated. It was assumed that the radial concentration gradients of the hydrocarbons can be neglected. This assumption will be re-examined by means of the 2-dimensional PBMR model assuming isothermal PBMR operation without a radial porosity profile. To reduce the interaction of conversion rate and product selectivity in a first approach the radially averaged oxygen concentration is kept constant by local adjustment of the flux of added oxygen.
The concentration ratio of oxygen and the reactant A in the model feed is $y_{O2,0}/y_{A,0}$=0.05, and the modulus ϕ" varies between 2.0 and 1.2. The resulting axial concentration profiles of the 2-D model are compared in Fig. 6a with that of a (pseudo) 1-D model, and clearly show the influence of the radial mass transport.

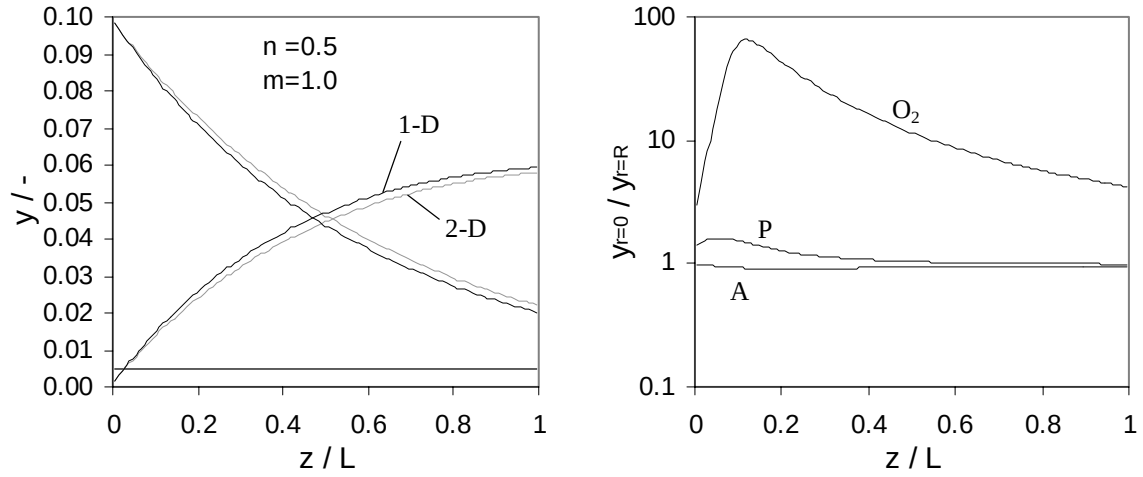

Fig. 6 Axial concentration profile: (a) comparison of 2-D and 1-D calculations and (b) ratio of concentration at the centerline ($y_{r=0}$) and close to the membrane ($y_{r=R}$).

In Fig. 6b the ratios of concentrations at the centerline ($y_{r=0}$) and close to the membrane ($y_{r=R}$) are presented for oxygen and the hydrocarbons A and P. The relative oxygen concentration gradients are the largest, and except at the reactor inlet ($z/L<0.02$) at least 4 times larger than those of the hydrocarbons.

However, the effect of the radial concentration profiles of A and P cannot be neglected for the assumed kinetics, where the reaction rates depend linearly on the concentration of either A or P. Near the membrane wall, where the oxygen concentration and the reaction rates are the highest, the concentration of reactant A and hence the formation rate of product P are relatively small, while the concentration of product P and thus the loss of product are relatively large. Therefore, as can be seen in Fig. 7a, showing the dimensionless selectivity loss $F_{1-\sigma}$ as a function of a modified Thiele modulus $\phi"$, the selectivity losses due to mass transfer limitations are significantly larger (especially near the reactor inlet where the gradients in the product concentration are the strongest) than predicted in Chapter 3, where radial profiles in the hydrocarbon concentrations were disregarded (dashed line for $p_{nm}=0.1$).

The effect of radial profiles in the hydrocarbons concentrations reduces, however, if the reaction orders in the hydrocarbon are smaller than 1, or increase if they are larger than 1.

The influence factor for the conversion of reactant A, F_R, is slightly reduced by the effect of the radial concentration profile of A (Fig. 7b).

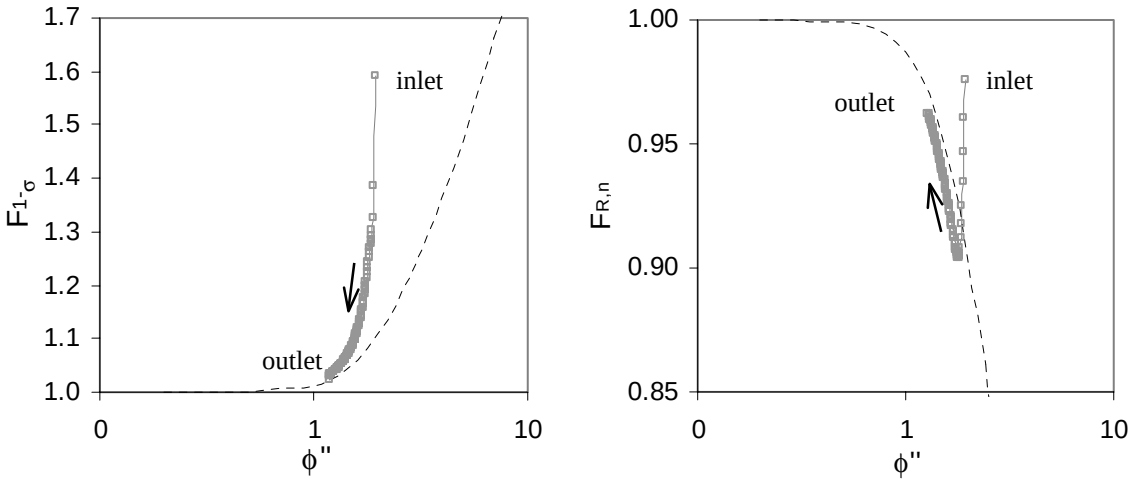

Fig. 7 (a) The selectivity loss and (b) the average reaction rate of the primary reaction for arbitrary kinetics with oxygen reaction orders n=0.5 and m=1. The dashed lines represents the results of Chapter 3 under disregard of the hydrocarbon concentrations for p_{nm}=0.1.

Finally, in Fig. 8 the selectivity-conversion plots are given. A comparison of average values of $(F_{1-\sigma})_{av}$=1.11 and $(F_{R,n})_{av}$= 0.94 with the integral effect on the product selectivity F_{1-S} (X=0.75)=1.07 and the final conversion F_X=0.98 shows that the integral effect of radial concentration profiles on the reactor performance is relatively small. The reduced axial concentrations of product P and the increased concentrations of reactant A have an opposite effect on the reactor performance compared to the effect of the radial concentration profiles.

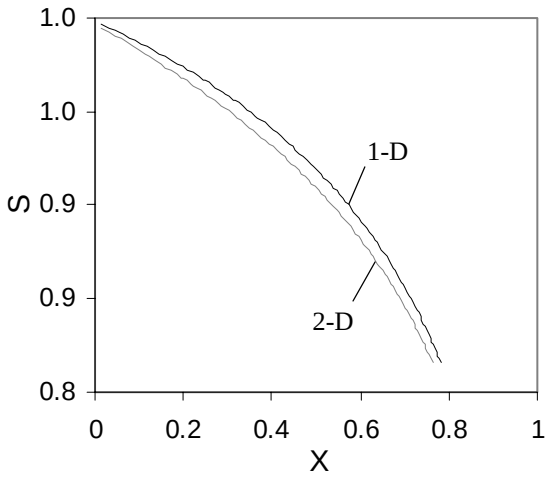

Fig. 8 Selectivity – conversion plot for 1-D and 2-D model.

6.4.2 Influence of the membrane tube diameter for equally distributed air flow

The calculations of the 2-dimensional model are compared for a computed concentration field (2-D) and constant radial concentrations (pseudo 1-D) for an equally distributed membrane flow of air. Stronger radial profiles result through the increase of the tubular diameter (factor 2 and 4). The volumetric flow rates of premixed and distributive feed are increased proportionally (factor 4 and 16) to keep the residence time constant.

Fig. 9a shows that accounting for radial concentration profiles results in an increase of the oxygen concentrations over the entire reactor length. Mass transfer limitations for the oxygen transport from the membrane wall to the center of the bed reduce the oxygen consumption rate, because the overall reaction order in oxygen is smaller than 1, which increases the

oxygen concentration level when the oxygen membrane flux is fixed. The average reaction rate is smaller when correctly accounting for radial concentration profiles.

The opposite effect can be observed, if the overall order is larger than 1 (see Appendix A.2, n=1, m=2) and a relatively small tube diameter is chosen. In case of a large tube diameter the effect of gradients in the hydrocarbon concentrations (as described in the previous section 6.4.1) can exceed the effect of an increased oxygen concentration due to radial mass transfer limitations.

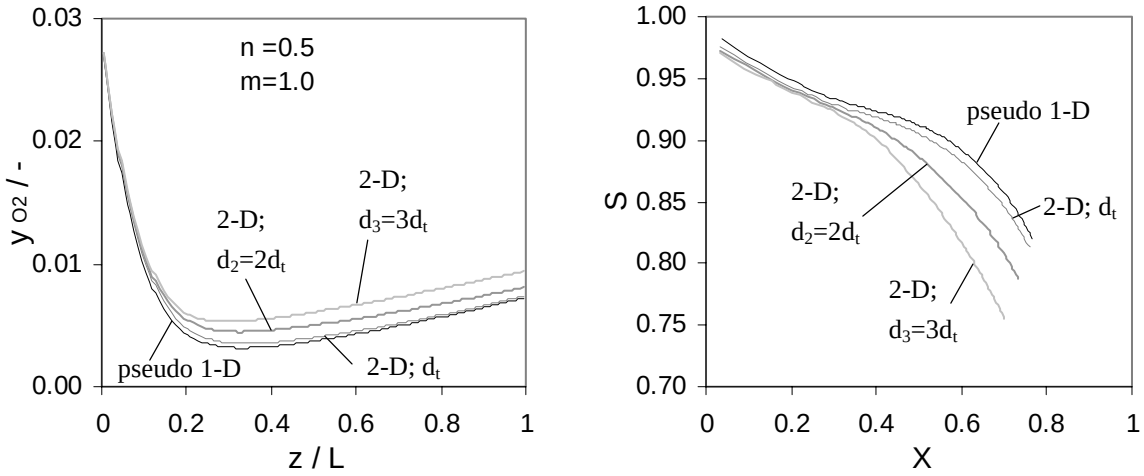

Fig. 9 Influence of the membrane tube diameter on the (a) the axial oxygen concentration profile and (b) selectivity – conversion – plot for arbitrary kinetics with oxygen reaction orders n=0.5/m=1 and m_{cat}=0.1 g.

The limitation of the radial mass transport, with its adverse effect on both the oxygen and the hydrocarbon concentration profiles, can thus have a strong negative effect on the conversion and selectivity in the PBMR (see Fig. 9b and Fig. 10). This effect is again even stronger (especially with regard to the selectivity) than calculated in Chapter 3 (dashed lines in Fig. 10) where radially constant hydrocarbon concentrations were assumed. The effect of the membrane tube diameter on the dimensionless selectivity losses and the dimensionless relative catalyst activity is shown in Fig. 10.

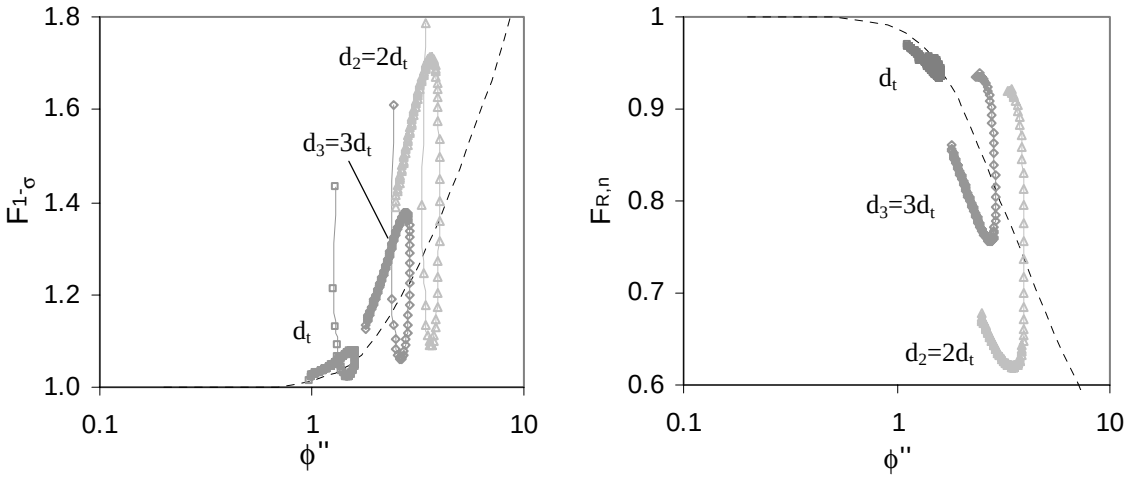

Fig. 10 Influence of the modified Thiele modulus (dimensionless membrane tube diameter) on (a) the selectivity loss and (b) the average reaction rate of the primary reaction for kinetics with oxygen reaction orders n=0.5/m=1 and m_{cat}=0.1 g.

The increase in product selectivity losses can be explained by inspecting the radial concentration profiles for oxygen, reactant A and target product P, plotted in Fig. 11, Fig. 12a and b respectively. Despite the fact that the average oxygen concentration is small compared to those of the hydrocarbons, the gradients in the hydrocarbon concentrations cannot be ignored. Even in regions of the packed bed, where no reaction takes place, strong radial profiles in the hydrocarbon mole fractions can be observed. This can be explained by the convective flow, which brings along more of reactant A and carries away more of formed product P.

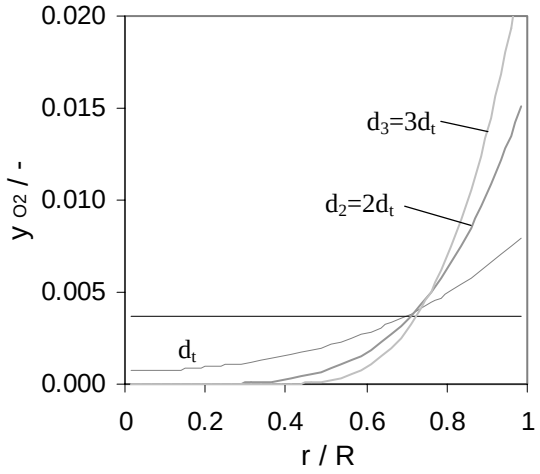

Fig. 11 Radial profile of the oxygen fraction at z/L=0.5 (for 2-D concentration field see Appendix A.1).

Especially in the presence of strong mass transfer limitations, the concentration of reactant A in the reaction zone is lower than the average whereas the concentration of the intermediate product is higher than the average, both with a negative effect on the product selectivity.

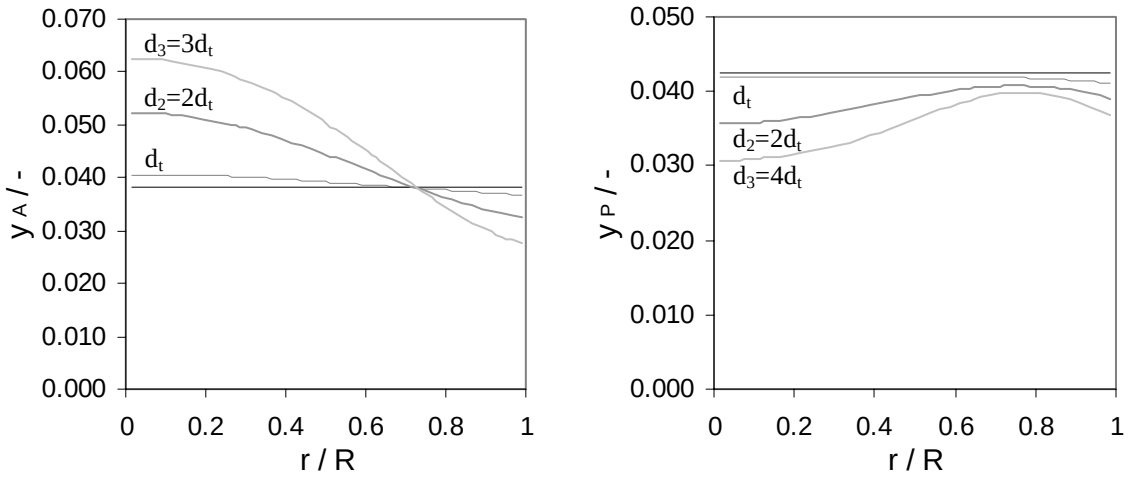

Fig. 12 Radial profile of the mole fractions of (a) reactant A and (b) intermediate product P at z/L=0.5.

For lower oxygen concentrations (increased hydrocarbon to oxygen concentration ratio), for example caused by an increased catalyst mass (Appendix A.2 and A.4), the radial gradients of the hydrocarbons and their effect on the reactor performance diminish.

Due to the radial hydrocarbon concentration profiles, the reactor performance is effected by transport limitations from the membrane wall to the center of the bed even if the reaction orders in oxygen for primary and consecutive reaction are equal (Appendix A.5). This explains the results presented by Hugh et al. (2001). They recently presented a 2-D model study based on flow fields as described in Fig. 1. The was applied to the oxidative dehydrogenation of propane on a V/MgO catalyst described by the kinetic model of Ramos et al. (2000). Propane conversion and propene selectivity decrease as the reactor radius increases (at constant contact time, length-diameter ratio and feed composition).

6.4.3 Influence of the porosity profile

The results presented in the previous paragraphs were obtained using the assumption of a radially constant porosity. However, for small ratios of the tube-to-particle diameter the increase of the bed porosity near the tube wall, which causes locally increased gas velocities, can influence the performance of the PBMR. For the evaluation of the effect of the porosity profile on the reactor performance a diameter ratio of $d_t/d_p=5$ is chosen. The reaction orders are n=1 and m=2.

In Fig. 13 the radial profiles of the velocity for an axially constant membrane flux is presented in case of radially constant porosity and in case of a radial velocity profile given by Hunt and Tien (1990) with the same radially averaged porosity.

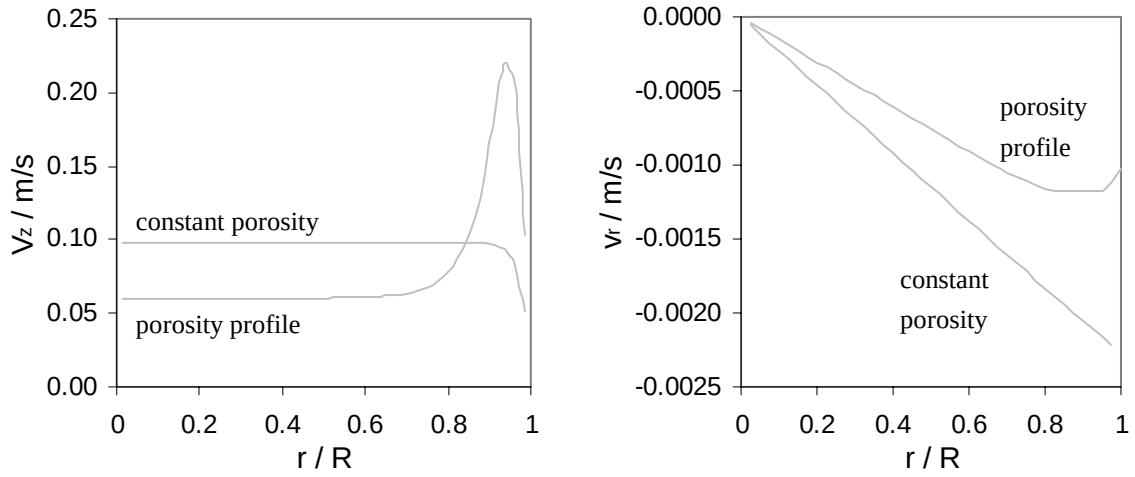

Fig. 13 Radial profile (at the position z/L=0.5) of (a) the axial and (b) the radial velocity profile for kinetics with oxygen reaction orders n=0.5/m=1; Calculations with radially constant bed porosity (ε=0.448) and a porosity profile by Hunt and Tien (1990) for d_t/d_p=5.

The radial velocities are smaller, if a radial porosity profile is accounted for. Yet, the influence on the radial concentration profiles is small, due to the small contribution of the convective flow to the radial transport.

Dispersive transport in the radial direction is negligible for $\mathrm{Bo_r} = \frac{u_r d_p}{D_r} \to \infty$

Applying the correlation of Tsotsas and Schlünder (1988) for the radial dispersion coefficient for the turbulent flow regime

$$D_r = \left(1-\sqrt{1-\varepsilon}\right) D_i^m + \frac{u d_p}{8} \geq \frac{u_z d_p}{8} \tag{42}$$

results in the following correlation for the Bodenstein number

$$\mathrm{Bo_r} \approx 8 \frac{u_r}{u_z} \tag{43}$$

The maximum radial flow is located at the membrane surface: $u_{r,max} = \Phi_{V,distr} / \left(\pi d_t L\right)$

The minimum axial flow at reactor inlet is: $u_{z,min} = \Phi_{V,0} / \left(0.25 \pi d_t^{\,2}\right)$

$$\mathrm{Bo_{r,max}} < 2 \frac{\Phi_{V,distr}}{\Phi_{V,0}} \frac{d_t}{L} \tag{44}$$

The ratio of premixed and distributive flow in the model calculations was $\Phi_{V,0} / \Phi_{V,distr}$ =100/35 (Table 3) and the minimum ratio of reactor length to tube diameter is L/d_t =10/3 (for d_3) and as a consequence

$$\mathrm{Bo_{r,max}} < 0.21$$

Due to the laminar flow in the model reactor, the radial dispersion is even increased by molecular diffusion. Therefore, it can be concluded that the radial transport is dominated by dispersive transport, and the role of radial convective transport is marginal.

For the evaluation of the effect of the porosity profiles on selectivity and conversion in the PBMR, in first instance, the radial dispersion coefficient is - artificially - limited to the molecular diffusion. Thereby, the radial dispersion coefficient is not influenced by the porosity distribution, and accounting for the radial porosity profile hardly effects the radial concentration profiles. In this case, the porosity profile has a positive influence on the selectivity of the PBMR as can be seen in Fig. 14b, in spite of the fact that the 'mixing-cup' average mole fractions (presented in Fig. 14a) are significantly increased by the porosity profile and the conversion is (slightly) decreased. Yet, near the membrane wall, where the oxygen concentration is the highest, i.e. the selectivity is the lowest, the catalyst concentration (1-ε) is strongly reduced.

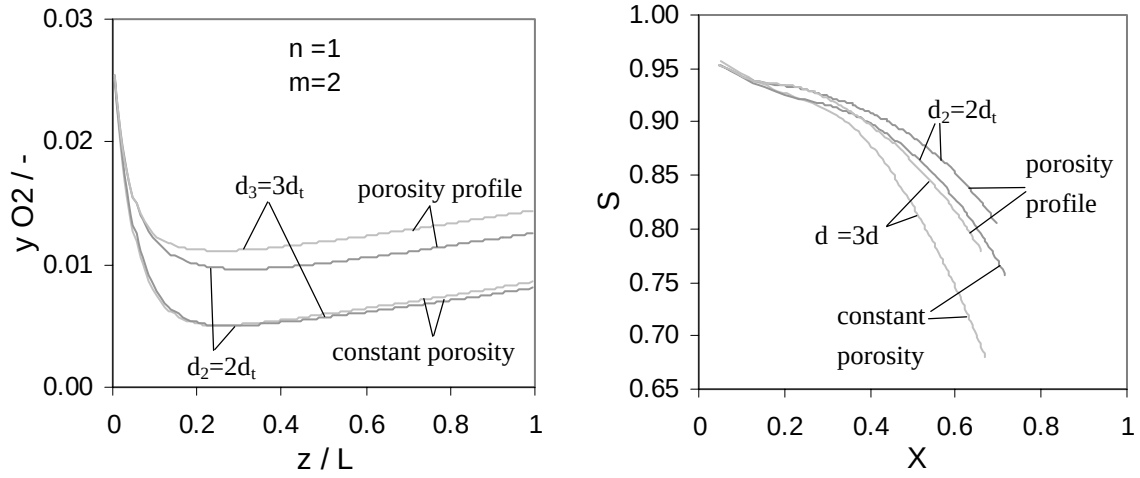

Fig. 14 Influence of the membrane tube diameter on the (a) the axial oxygen concentration profile and (b) selectivity – conversion – plot for kinetics with oxygen reaction orders n=1/m=2; Calculations with radially constant bed porosity (ε=0.448), a porosity profile by Hunt and Tien (1990) for d_t/d_p=5 and radial dispersions limited to molecular diffusion.

The mixing-cup averaged concentrations are higher, if the porosity profile is accounted for, because the porosity and thus the axial velocity is higher near (but not at) the membrane wall, where the oxygen concentrations are the highest. Therefore, in the mixing cup average the high concentrations near the membrane are weighted stronger than the lower concentrations in the core of the bed. The mixing cup average is defined by:

$$\left\langle y_{O_2} \right\rangle = \frac{1}{\pi R^2 \left\langle \varepsilon \right\rangle \left\langle v_z \right\rangle} \int_{r=0}^{R} 2\pi r\, \varepsilon(r) v_z(r)\, y_{O_2}(r)\, dr \qquad (45)$$

However, for the average conversion rate the concentrations where the actual reactions are taking place are more important, i.e. in the core of the bed - since the catalyst density (1-ε) is higher there compared to close to the membrane wall and the oxygen concentrations are

lower. The average oxygen concentration weighted with the local catalyst concentration is given by:

$$\left\langle y_{O_2} \right\rangle = \frac{1}{\pi R^2 \left(1-\left\langle \varepsilon \right\rangle\right)} \int_{r=0}^{R} 2\pi r \left(1-\varepsilon(r)\right) y_{O_2}(r)\, dr \qquad (46)$$

The average concentration in the catalyst particles is lower, if the radial porosity profile is taken into account, which explains the increased selectivity and the decreased conversion.

However, for the selected model parameter (Table 1, but $d_t/d_p=5$; n=1/m=2) the radial dispersion coefficient is increased by a contribution of turbulent dispersion. When accounting for a porosity profile, the turbulent contribution increases strongly near the membrane wall due to the increased porosity and increased gas velocities.

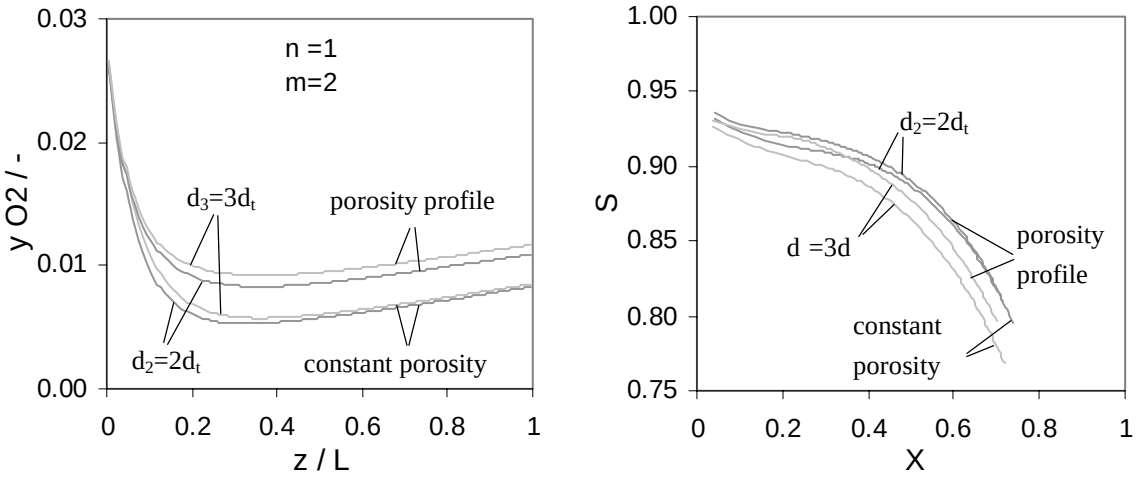

Fig. 15 Influence of the membrane tube diameter on the (a) the axial oxygen concentration profile and (b) selectivity – conversion – plot for kinetics with oxygen reaction orders n=1/m=2; Calculations with radially constant bed porosity (ε=0.448), a porosity profile by Hunt and Tien (1990) for $d_t/d_p=5$.

With a radial porosity profile higher radial dispersion coefficients are calculated, so that the difference in the catalyst phase averaged oxygen concentrations is reduced and thus also the effect on the PBMR performance.

For a PBMR of industrial scale, when radial dispersion is dominated by turbulent transport, the effect of the porosity profile on the integral reactor selectivity and conversion is negligible.

It has to be noted, that this is based on the assumptions made in Section 6.3.2 on the effect of local gas velocity on the radial dispersion. Yet, correlations for the radial dispersion coefficient in packed bed reactors presented in literature were derived for the core of the bed, where porosity and gas velocity are constant. In this studies the radial dispersion near the tube wall was explicitly not taken into consideration.

6.5 Summary and conclusions

In this chapter a two-dimensional, pseudo-homogeneous reactor model was developed to describe the radial and axial concentration and temperature profiles in the PBMR and the local velocity field induced by the distributive membrane flow and a radial porosity profile. With this model the effect of mass transfer limitations from the membrane wall to the center of the packed bed on the integral reactor performance (i.e. conversion and selectivity) was studied for a consecutive reaction system with arbitrary reaction orders in oxygen and the hydrocarbons.

From the calculation results obtained with the 2-dimensional PBMR model the following was concluded:

1. Radial concentration profiles in the concentrations of the hydrocarbons have a considerable adverse effect on the intrinsic selectivity and conversion rates for the assumed first order reaction orders in the hydrocarbons, even in case of very low oxygen concentrations. Due to the higher oxygen concentrations at the membrane wall the concentration of reactant A is decreased, while the concentration of product P is increased, resulting in product selectivity losses.
2. Mass transfer limitations for the oxygen transport from the membrane to the center of the bed increase (n=0.5/m=1) the oxygen concentration level in case of an axially constant membrane flux, which decreases the integral conversion and selectivity of the PBMR.
3. For modified Thiele moduli $\phi"$ >1 radial concentration profiles influence the integral reactor performance. However, for $\phi"$ <1 the effect of radial profiles is marginal, and thus a one-dimensional model can sufficiently describe the PBMR
4. The effects of a radial porosity distribution on the integral reactor performance needs only to be taken into account, if the radial dispersion coefficient is dominated by molecular diffusion, i.e. if it is not influenced by the porosity profile, and then only in case of large modified Thiele moduli $\phi"$ (in the order of 1 or larger).

NOTATION

Latin letters

A,P,W hydrocarbon reactant, target and waste product

a specific surface area per volume packed bed [m^2 / m^3]

c concentration [mol / m^3]

c_p heat capacity [J / kg K]

d diameter [m]

D dispersion coefficient [m^2 / s]

F	factor by which a reaction rate or selectivity is increased due to mass transport limitations
k	rate constant [mol / m^3 s bar^{1+n}], [mol / m^3 s bar^{1+m}]
k^*	rate constant for the packed bed ((1-ε) k $c_{A,P}$) [mol / m^3 s bar^n], [mol / m^3 s bar^m]
k’	rate constant [mol / g_{cat} s bar^{1+n}], [mol / g_{cat} s bar^{1+m}]
L	length of the packed bed [m]
m_{cat}	catalyst mass [kg]
m	reaction order in oxygen of reaction forming the waste product
n	reaction order in oxygen of reaction forming the target product
n_s	interphase mass flow [kg / m^2 s]
nrr	number of reactions
r'_j	rate of reaction j [mol / g_{cat} s]
S	selectivity [-]
u	superficial gas velocity (ε v) [m / s]
v	interstitial gas velocity [m / s]
X	conversion [-]
x	length coordinate in radial direction of the spherical particle [m]
x_F	effective mixing length (=F d_P; F=1.15 for spherical particles) [m]
z	length coordinate in axial direction of the packed bed [m]

Greek letters

α_w	wall heat transfer coefficient [W / m^2 K]
ΔH_j	reaction enthalpy [kJ / mol]
ε	porosity
λ_r	radial conductivity of the packed bed with gas flow [W / m K]
λ_z	axial conductivity of the packed bed with gas flow [W / m K]
λ_g	thermal conductivity of the gas [W / m K]
λ_{bed}	thermal conductivity of the packed bed at no flow [W / m K]
λ_{rad}	contribution of radiation to thermal conductivity of packed bed (no flow) [W / m K]
λ_g	gas bulk viscosity [kg / m s]
μ_g	gas shear viscosity [kg / m s]
ν	stoichiometric coefficient
ρ	density [kg / m^3]
σ	intrinsic selectivity of the target product
$\bar{\bar{\tau}}_g$	gas phase stress tensor [kg / m s]

Φ_m	mass flow [kg / s]
$\phi_{m,distr}$	specific mass flow added per volume packed bed [kg / m^3 s]
ω	mass fraction

Subscripts

0	at the reactor inlet / base case
A,P,W	hydrocarbon reactant, target and waste product
cat	catalyst
distr	distributed
max	maximum value
O_2	oxygen
p	particle
t	tube

Dimensionless numbers

Nu_w	Nusselt number for the wall heat transfer $\left(=\frac{\alpha_w d_P}{\lambda_g}\right)$
Pe_x	Peclet-number $\left(=\frac{u_{sup}\rho_g c_{p,g}}{\lambda_g} x_F\right)$
ϕ"	modified Thiele-modulus $\left(=L\sqrt{\left(\frac{n+1}{2}\nu_1 k_1^* \langle c\rangle^{n-1}+\frac{m+1}{2}\nu_2 k_2^* \langle c\rangle^{m-1}\right)\Big/ D}\right)$
	with $L = R_t/2$ for tubular packed bed
p_{nm}	ratio of reaction rates in the secondary and primary reaction $\left(=\frac{k_2\langle c_P\rangle}{k_1\langle c_A\rangle}\langle c\rangle^{m-n}\right)$
$\langle x\rangle$	represents the spatial average of variable x
$\bar{x}$	represents the vector representation of variable x

References

R.F. Benenati and C.B. Brosilow, 1962, Void fraction Distribution in Beds of Spheres, *A.I.Ch.E. Journal* 8, 359-361

R.B. Bird, W.E. Stewart, E.N. Lightfoot, 1960, Transport phenomena, John Wiley & Sons, New York

D.J. Gunn, 1987, Axial and radial dispersion in fixed beds, *Chem. Eng. Sci*. 42, 363-373

M.L. Hunt and C.L. Tien, 1990, Non-Darcien flow, heat and mass transfer in catalytic packed-bed reactors, *Chem. Eng. Sci.* 45, 55-63

K. Hou, R. Hughes, R. Ramos, M. Menéndez, J. Santamaría, 2001, Simulation of a membrane reactor for the oxidative dehydrogenation of propane, incorporating radial concentration and temperature profiles, *Chem. Eng. Sci.* 56, 57-67

A.E. Kronberg, 1997, Local nonequilibrium approach to chemical reactor modeling, Doctoral Thesis, Twente University, Enschede, the Netherlands

H. Martin, 1977, Low Peclet number particle-to-fluid heat and mass transfer in packed beds, *Chem. Eng. Sci.* 33, 913-919

H. Martin, M. Nilles, 1993, Radiale Wärmeleitung in durchströmten Schüttungsrohren, *Chem.-Ing.-Tech.* 65, 1468-1477

M. Punčochář and J. Drahoš, 1993, The tortuosity concept in fixed and fluidized bed, *Chem. Eng. Sci.* 48, 2173-2175

R. Ramos, M. Menéndez, J. Santamaría, 2000, Oxidative dehydrogenation of propane in an inert membrane reactor, *Catalysis Today 56*, 239-245

R.C. Reid, J.M. Prausnitz, B.E. Poling, 1988, The properties of gases and liquids, McGraw-Hill Book Company, New York, USA

J. Schuster and D. Vortmeyer, 1980, Ein einfaches Verfahren zur näherungsweisen Bestimmung der Porosität in Schüttungen als Funktion des Wandabstandes, *Chem.-Ing.-Tech.* 52, 848

E. Tsotsas and E.U. Schlünder, 1988, Some remarks on channelling and on radial dispersion in packed beds, *Chem. Eng. Sci.* 43, 1200-1203

Mg1-Mb11, VDI-Wärmeatlas, 4th edition 1984

D. Vortmeyer and J. Schuster, 1983, Evaluation of steady flow profiles in rectangular packed beds by a variational method, *Chem. Eng. Sci.* 38, 1691-1699

C.Y.Wen and L.T. Fan, 1975, Models for flow systems and chemical reactors, Marcel Decker, Inc., New York

P. Zehner, E.U. Schlünder, 1970, Wärmeleitfähigkeit von Schüttungen bei mässigen Temperaturen, Chemie-Ing.-Techn.42, 933-941

Appendix A Influence of membrane diameter on PBMR-performance for different sets of reaction orders

A.1 Reaction orders n=0.5/m=1.0 and 0.1 g catalyst

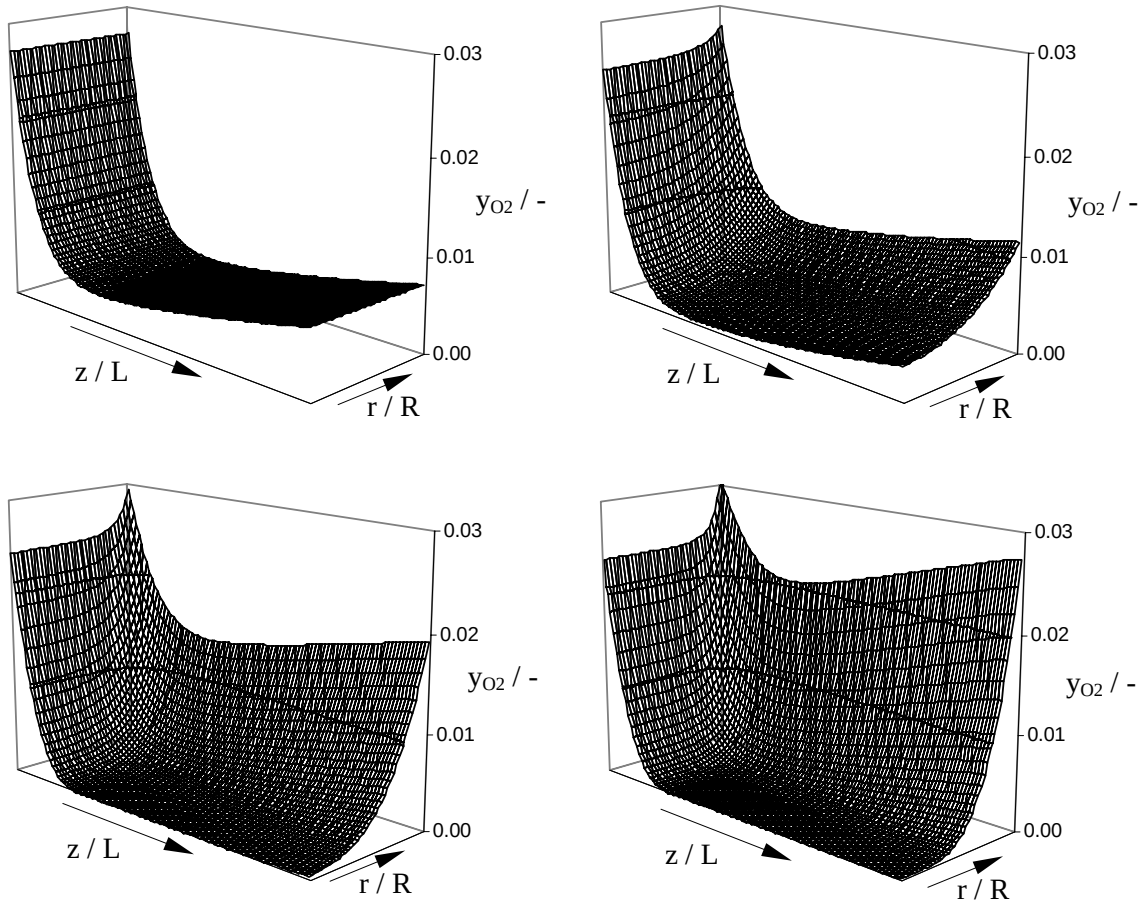

Fig.- A-1 Two-dimensional oxygen concentration profiles for kinetics with oxygen reaction orders n=0.5/m=1 and m_{cat}=0.1 g.

A.2 Reaction orders n=0.5/m=1.0 and 0.32 g catalyst

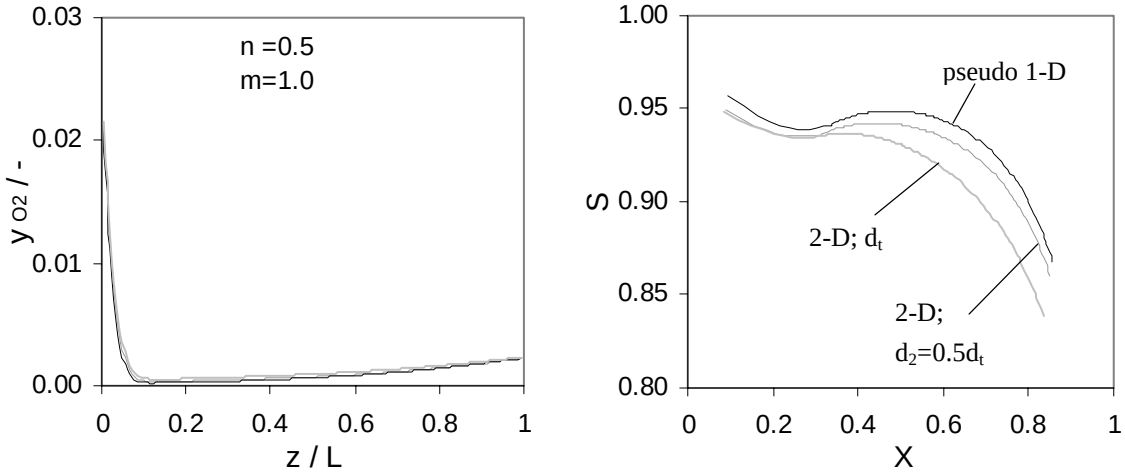

Fig.- A-2 Influence of the membrane tube diameter on the (a) the axial oxygen concentration profile and (b) selectivity – conversion – plot for kinetics with oxygen reaction orders n=0.5/m=1 and m_{cat}=0.32 g.

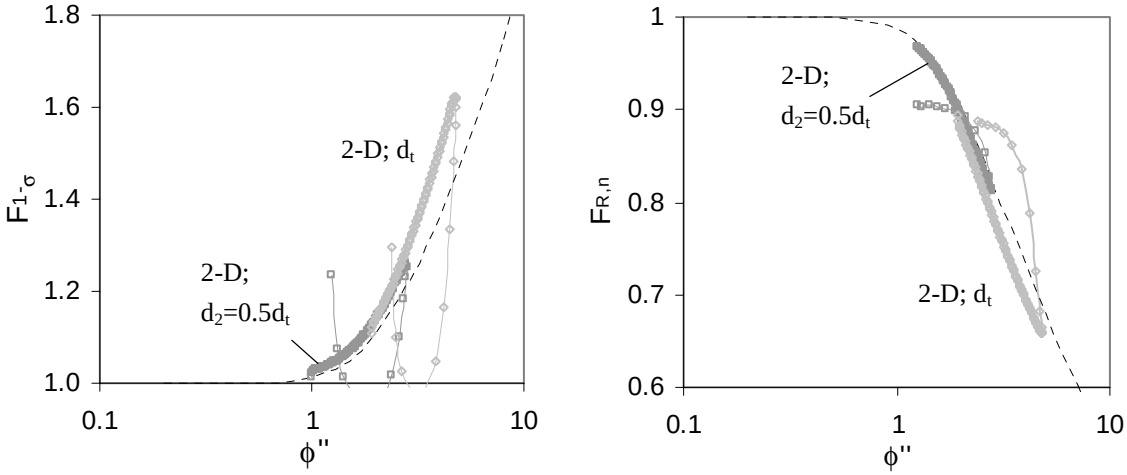

Fig.- A-3 Influence of the modified Thiele modulus (dimensionless membrane tube diameter) on (a) the selectivity loss and (b) the average reaction rate of the primary reaction for kinetics with oxygen reaction orders n=0.5/m=1 and m_{cat}=0.32 g.

A.3 Reaction orders n=1/m=2 and 0.1 g catalyst

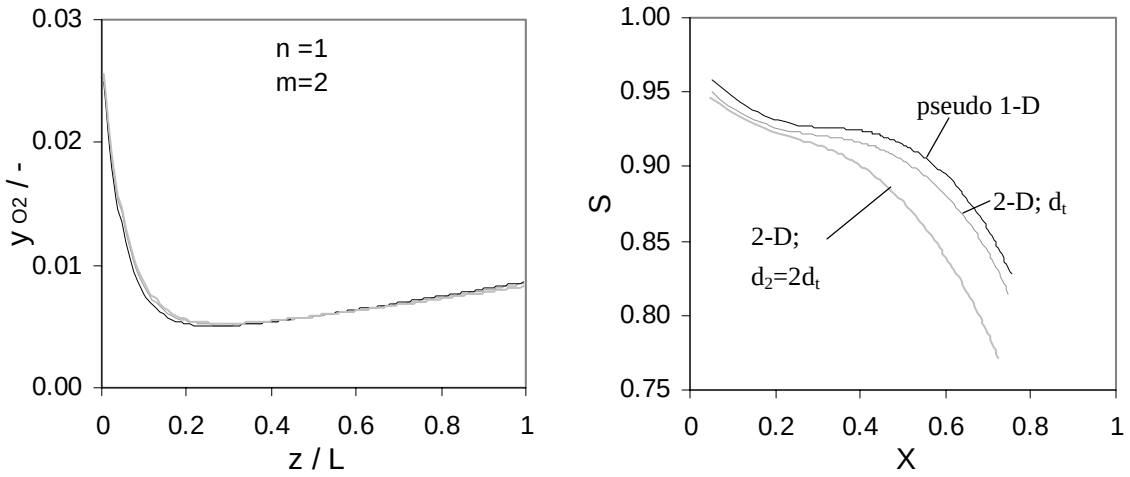

Fig.- A-4 Influence of the membrane tube diameter on the (a) the axial oxygen concentration profile and (b) selectivity – conversion – plot for arbitrary kinetics with oxygen reaction orders n=1/m=2 and m_{cat}=0.1 g.

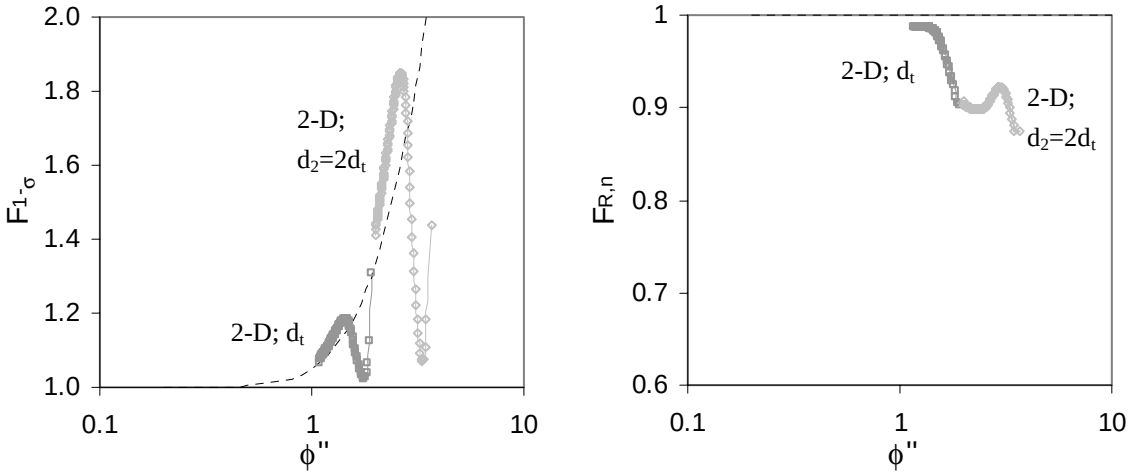

Fig.- A-5 Influence of the modified Thiele modulus (dimensionless membrane tube diameter) on (a) the selectivity loss and (b) the average reaction rate of the primary reaction for kinetics with oxygen reaction orders n=1/m=2 and m_{cat}=0.1 g.

A.4 Reaction orders n=1/m=2 and 0.32 g catalyst

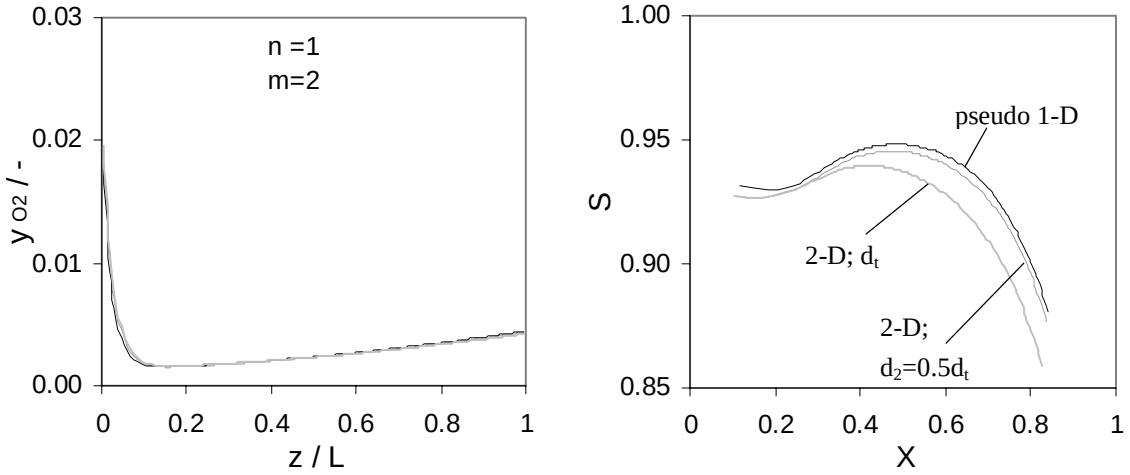

Fig.- A-6 Influence of the membrane tube diameter on the (a) the axial oxygen concentration profile and (b) selectivity – conversion – plot for arbitrary kinetics with oxygen reaction orders n=1/m=2 and m_{cat}=0.32 g.

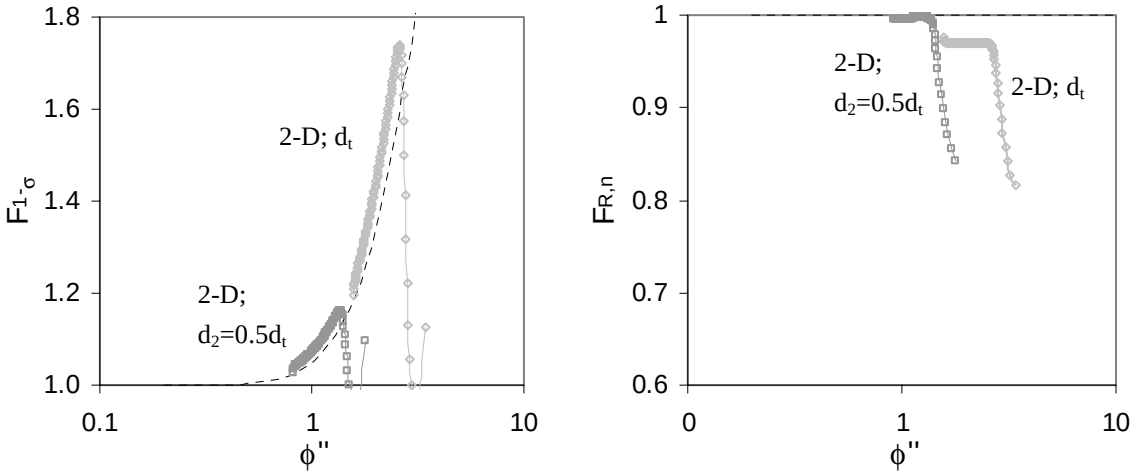

Fig.- A-7 Influence of the modified Thiele modulus (dimensionless membrane tube diameter) on (a) the selectivity loss and (b) the average reaction rate of the primary reaction for kinetics with oxygen reaction orders n=1/m=2 and m_{cat}=0.32 g.

A.5 Reaction orders n=1/m=1 and 0.1 g catalyst

Due to the radial hydrocarbon concentration profiles, the reactor performance is effected by transport limitations from the membrane wall to the center of the bed even if the reaction orders in oxygen for primary and consecutive reaction are equal. This is shown in the next figures for the reaction order n=1/m=1 with the rate constants given in Table- A-1.

Table- A-1 Rate constant for the reaction orders n=1/m=1.

Rate constants: n=1.0/m=1.0	k'_1	0.150 mol / (g s bar^{1+n})
	k'_2	0.045 mol / (g s bar^{1+m})

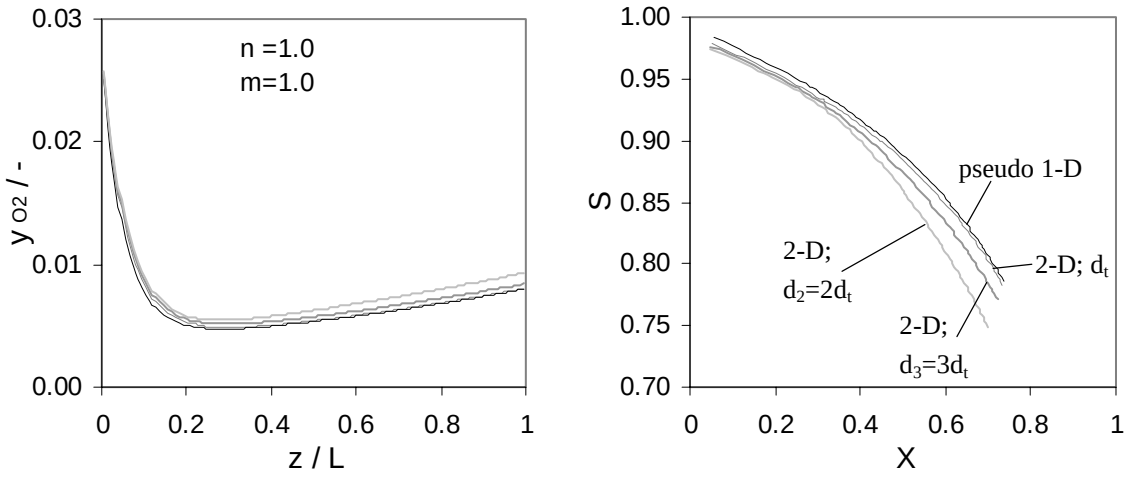

Fig.- A-8 Influence of the membrane tube diameter on the (a) the axial oxygen concentration profile and (b) selectivity – conversion – plot for arbitrary kinetics with oxygen reaction orders n=1/m=1 and m_{cat}=0.1 g.

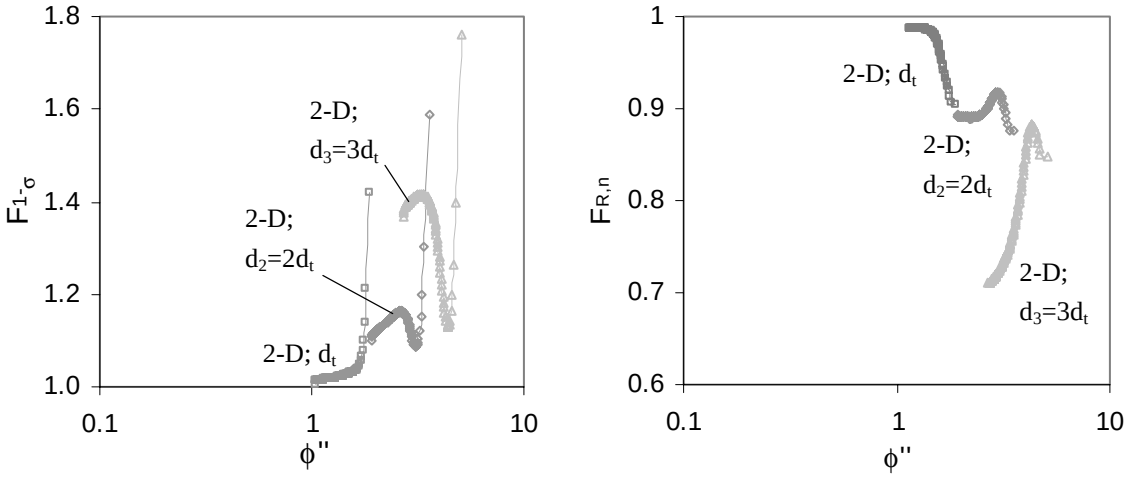

Fig.- A-9 Influence of the modified Thiele modulus (dimensionless membrane tube diameter) on (a) the selectivity loss and (b) the average reaction rate of the primary reaction for kinetics with oxygen reaction orders n=1/m=1 and m_{cat}=0.1 g.

7 The potential of PBMR applications for industrial partial oxidation reactions

Abstract

The different effects of the distribution of oxygen in packed bed membrane reactors (PBMR) have been discussed for three industrially relevant reaction systems, namely the oxidative formation of propene and ethene from propane, the oxidative dehydrogenation (ODH) of ethylbenzene to styrene and the ODH of methanol to formaldehyde, using the different PBMR models derived in the previous chapters. The potentials of distributive feeding of oxygen for the improvement of selectivity or yield of the process have been discussed, and possible effects of mass transfer limitations have been evaluated. While intraparticle mass transfer limitations are stronger, for the design of industrial scale PBMR both intraparticle and membrane-to-center transport effects have to be taken into account.

Two other issues of the PBMR, the diminishing effect of the distribution of oxygen on the temperature hot-spot in the PBMR and the possibility to operate of the PBMR with overall feed compositions within the flammability limits have been demonstrated for the ODH of ethylbenzene and for the ODH of methanol respectively.

7.1 Introduction

In this final chapter the different effects of the distribution of oxygen in packed bed membrane reactors (PBMR) are discussed for three industrially relevant reaction systems, namely the oxidative formation of propene and ethene from propane, the oxidative dehydrogenation (ODH) of ethylbenzene to styrene and the ODH of methanol to formaldehyde. The potentials of distributive feeding of oxygen for the improvement of selectivity or yield of the process are discussed, and possible effects of mass transfer limitations are evaluated. For the ODH of ethylbenzene the positive effect of the distribution of oxygen on the temperature profiles in the PBMR is demonstrated, and for the ODH of methanol the possibility to operate the PBMR with overall feed compositions within the flammability limits is evaluated.

For the evaluation of the particle effects, the heterogeneous, one-dimensional model described in Chapter 5 is used, and for the evaluation of the transport effects from the membrane wall to the center of the packed bed the model presented in Chapter 6. For the latter a constant radial porosity was assumed in the isothermal calculations, and a porosity profile was adapted for the calculations including temperature profiles.

7.2 Selective oxidation of propane

Ethene is produced mainly by thermal cracking of hydrocarbons in the presence of steam, and by recovery from refinery cracked gas, and propene is produced almost entirely as a byproduct because it is obtained in sufficient amounts in ethylene production by steam cracking and in some refinery processes (Ullmann's, 1996).

Predictions of increasing demands for propene were driving intensive research activities in the field of ODHP. Yet, maximum propene yields of about 30 % were achieved (Cavani and Trifirò, 1995a).

At higher reaction temperatures, by homogeneous gas phase reactions or catalyzed, mixed olefin yields of about 50 % can be realized (see Appendix B and Leveles, 2002).

Based on experiments conducted by Leveles (2001, 2002) , a kinetic model was developed (see Appendix A) for the selective propane oxidation over a Mg-Dy-Li-O catalyst at 600°C and atmospheric pressure. This work aims to improve the olefin yield for the selective oxidation of propane using distributive oxygen feed. In Fig. 1 the main products and the proposed main reactions are schematically presented.

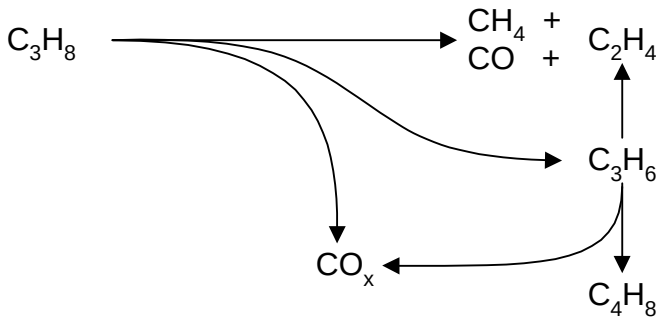

Fig. 1 Model reactions for the selective oxidation of propane over a Mg-Dy-Li-O catalyst at 600°C (Leveles, 2002).

The experimental kinetic data can be described with the reactions and reaction rate expressions listed in Table 1 (see derivation in Appendix A). The kinetic data clearly demonstrate the potential of distributive oxygen feed. Firstly, the combustion reactions show a higher reaction order in the oxygen partial pressure than the oxidative dehydrogenation and cracking reactions, resulting in improved propene stability at lower oxygen concentrations. Secondly, the lower apparent reaction order in the formation of ethene compared to propene shifts the product distribution to the more stable ethene.

Table 1 Model reactions and reaction rate expressions derived from Leveles (2002).

No.	Model reaction	Reaction rate expressions [mol/g s]
1	$C_3H_8 + 0.5\ O_2 \rightarrow C_3H_6 + H_2O$	$r_1 = \left(2.9 \cdot 10^{-5}\, p_{C_3}{}^{3.2} + 4.2 \cdot 10^{-8} \frac{p_{C_3}{}^{0.67}}{p_{CO_2}} \right) p_{O_2}{}^{0.24}$
2	$C_3H_8 \rightarrow C_2H_4 + CH_4$	$r_2 = \left(6.8 \cdot 10^{-6}\, p_{C_3}{}^{2.8} + 1.7 \cdot 10^{-8} \frac{p_{C_3}{}^{0.63}}{p_{CO_2}} \right) p_{O_2}{}^{0.05} \frac{p_{C_3}}{p_{C_3} + p_{O_2}}$
3	$C_3H_8 + 1.5\ O_2 \rightarrow C_2H_4 + CO + 2\ H_2O$	$r_3 = \left(6.8 \cdot 10^{-6}\, p_{C_3}{}^{2.8} + 1.7 \cdot 10^{-8} \frac{p_{C_3}{}^{0.63}}{p_{CO_2}} \right) p_{O_2}{}^{0.05} \frac{p_{O_2}}{p_{C_3} + p_{O_2}}$
4	$1/3\ C_3H_8 + 5/3\ O_2 \rightarrow CO_2 + 4/3\ H_2O$	$r_4 = \left(1 \cdot 10^{-7} + 4.5 \cdot 10^{-8} \frac{1}{p_{CO_2}} \right) p_{C_3}{}^{0.66} p_{O_2}{}^{0.8}$
5	$1/3\ C_3H_6 + O_2 \rightarrow CO + H_2O$	$r_5 = \left(6.6 \cdot 10^{-6} + 7.6 \cdot 10^{-8} \frac{1}{p_{CO_2}} \right) p_{C_{3=}}{}^{0.73} p_{O_2}{}^{0.8}$
6	$1/3\ C_3H_6 + 1.5\ O_2 \rightarrow CO_2 + H_2O$	$r_6 = 1 \cdot 10^{-7} \frac{1}{p_{CO_2}} p_{C_{3=}}{}^{0.73} p_{O_2}{}^{0.8}$
7	$2\ C_3H_6 \rightarrow C_2H_4 + C_4H_8$	$r_7 = \left(5.5 \cdot 10^{-7} + \frac{1.4 \cdot 10^{-8}}{p_{CO_2}} \right) p_{C_{3=}}{}^{0.85} p_{O_2}{}^{0.77}$

In the next sections, firstly, the effect of distributive feeding of oxygen for the ODH of propane is investigated comparing premixed propane/air feed with axially constant oxygen concentrations. Subsequently, the combination of premixed and distributive feeding is studied. Finally, the effects of intraparticle mass transfer limitations and mass transfer limitations from the membrane to the center of the packed bed are discussed.

7.2.1 Premixed propane/air feed

Model calculations with a totally premixed oxygen feed presented in Fig. 2 show that the performance of the Mg-Dy-Li-O catalyst is similar to that of other catalysts and to that produced by gas phase reactions (represented by the dashed line; see Appendix B.1). The maximum olefin yield does not exceed 50 %. Fig. 2b shows that the product distribution shifts towards ethene with increasing conversion, yet at lower oxygen concentrations the propene/ethene ratio increases at high conversions.

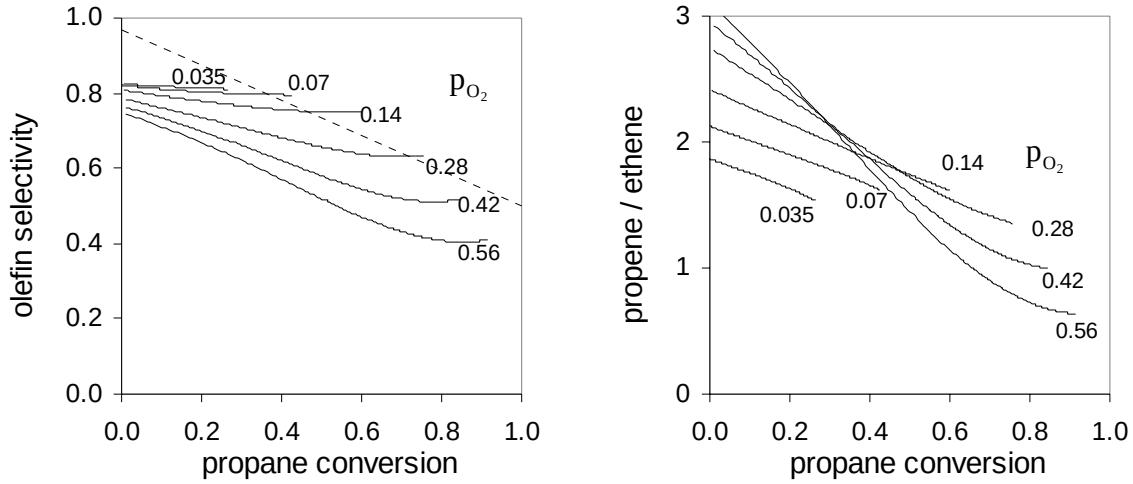

Fig. 2 Influence of propane/air feed composition on the olefin selectivity (a) and propene to ethene selectivity ratio (b) as a function of the propane conversion. The propane partial pressure was set at 0.28 bar, while the oxygen partial pressure was varied between 0.07 and 0.7 bar. (The oxygen partial pressure in bar is indicated in the figure.)

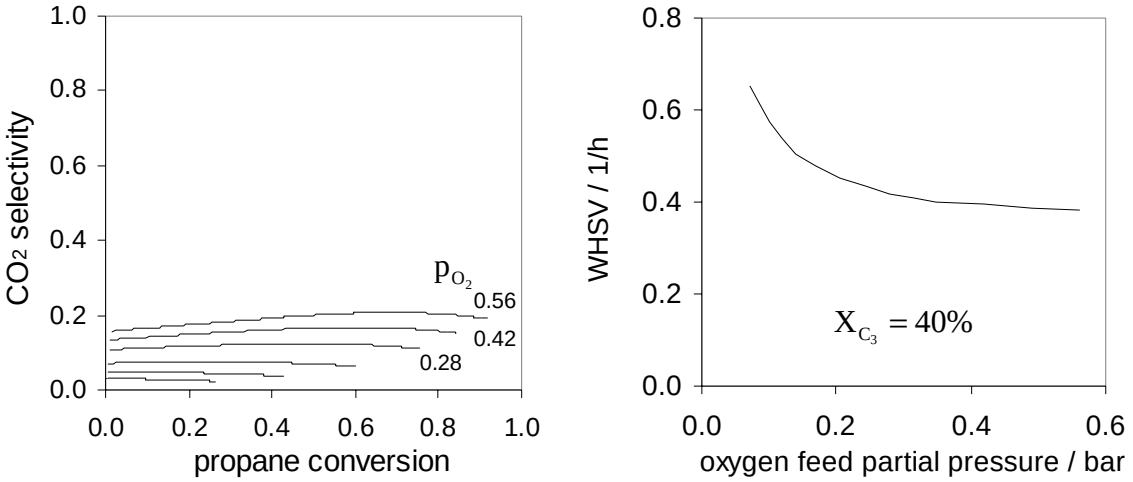

Fig. 3 Influence of the oxygen partial pressure in the premixed propane/air feed on (a) the carbon dioxide formation and (b) the catalyst activity for a constant propane conversion of 40 %, using the same reaction conditions as in Fig. 2.

A positive effect of reduced oxygen concentrations can be discerned from Fig. 3a, namely the reduced selectivity towards carbon dioxide. Carbon dioxide acts as a catalyst inhibitor reducing the reactivity . Therefore, a reduced oxygen level in the FBR results remarkably in an increased productivity. This is illustrated in Fig. 3b, where the WHSV, defined as mass flux of propane per catalyst mass that is converted to 40 %, is shown as function of the partial pressure of oxygen.

7.2.2 Constant oxygen level

The potential of PBMR is evaluated by firstly assuming an axially constant oxygen concentration. For propane conversions above 60 % strong selectivity improvements are predicted for a constant oxygen concentration of p_{O2}=0.035 bar and less (Fig. 4a). According to the kinetic models electivity ratios of propene and ethene above unity can be achieved at low oxygen concentrations even at very high conversions (Fig. 4b).

Note again the remarkable strong increase in the catalyst activity at low oxygen concentrations due to decreased carbon dioxide concentrations (see Fig. 5).

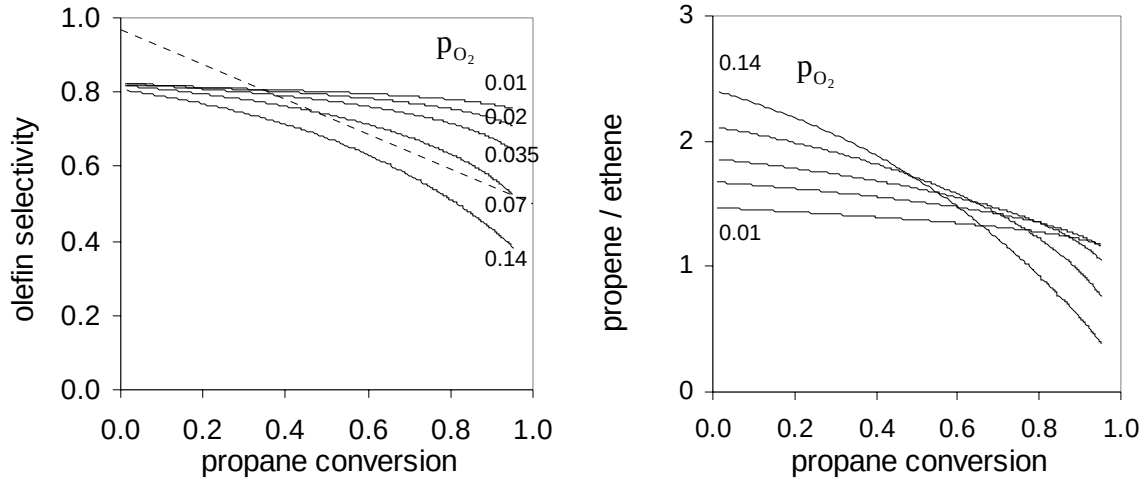

Fig. 4 Influence of the oxygen concentration assumed constant over the entire reactor on the olefin selectivity (a) and the propene / ethene product selectivity ratio (b) as a function of the propane conversion. The propane partial pressure in the feed was set at 0.28 bar, while the oxygen partial pressure was varied from 0.01 to 0.14 bar. (The oxygen partial pressure in bar is indicated in the figure.)

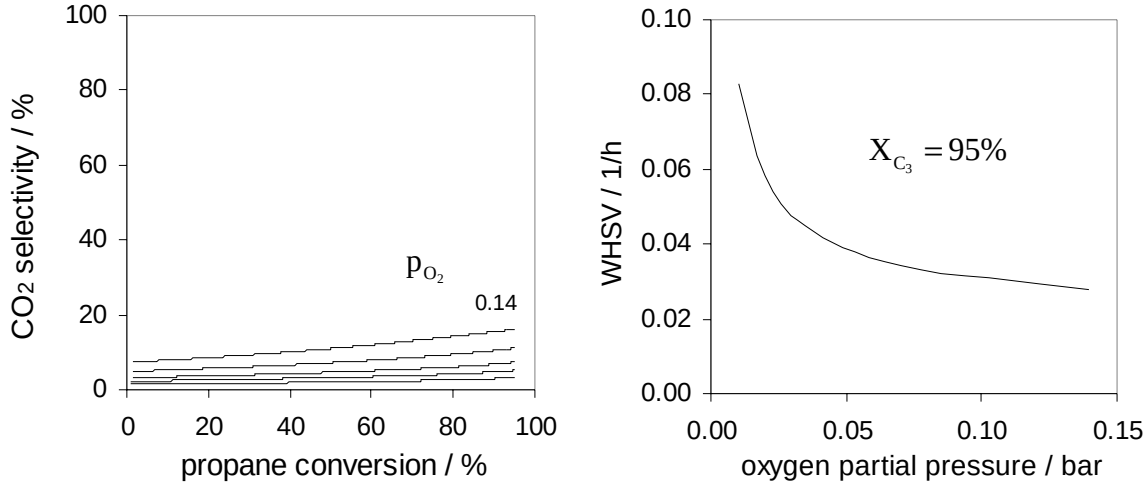

Fig. 5 Influence of the oxygen partial pressure assumed constant over the entire reactor length on the carbon dioxide formation (a) and the catalyst activity (b) at a propane conversion of 95 % for the same reaction conditions as in Fig. 4.

7.2.3 Combination of premixed propane/air feed with distributed oxygen feed

In this section the PBMR performance is assessed by simulating a PBMR operated with a combination of a premixed propane/air feed and a second oxygen containing feed flow $\Phi_{V,distr}$, that is equally distributed over the reactor length (see Fig. 6a). Per mol propane half a mole oxygen is fed to the reactor. The effect of different ratios of the added oxygen between premixed ($\Phi_{V,0}$) and distributive flow ($\Phi_{V,distr}$) is presented in Fig. 6b.

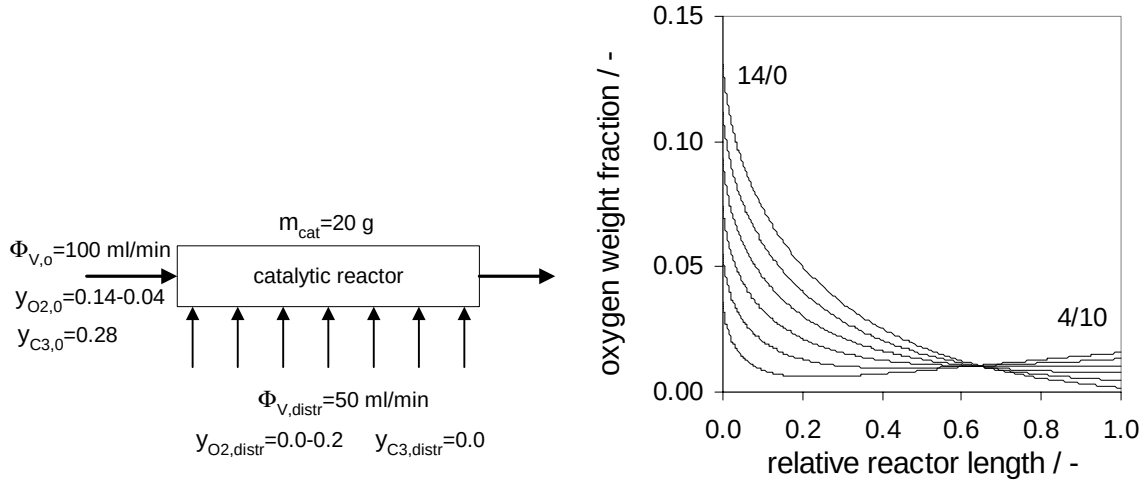

Fig. 6 Schematic drawing of the catalytic reactor with an evenly distributed second reactant feed (a) and calculated oxygen profiles (b), where 14 ml/min oxygen added to the reactor in total in different ratios between premixed and distributed feed (14/0, 12/2, 10/4/ 8/6, 6/8, 4/10).

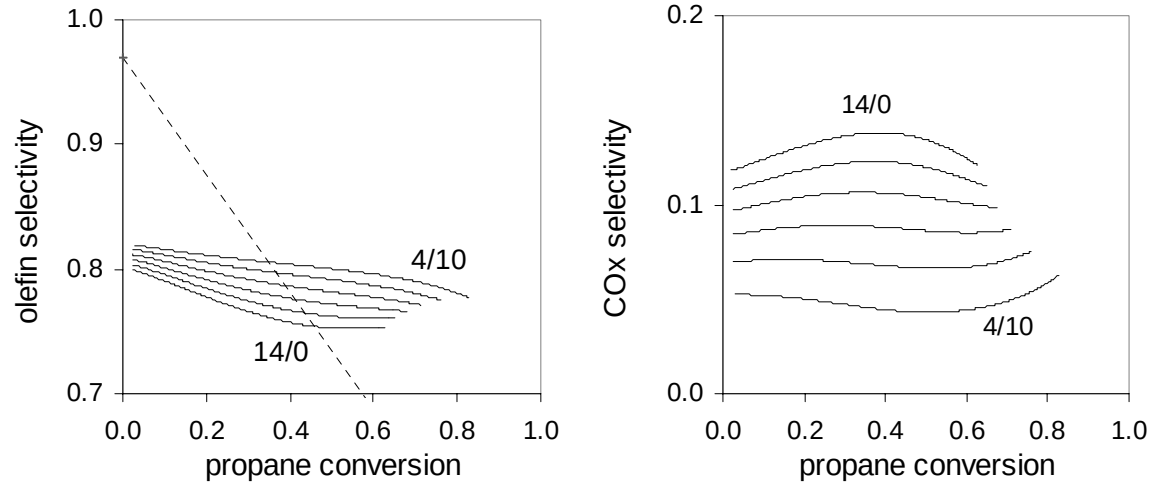

Fig. 7 Influence of the stepwise change from premixed to distributed oxygen feed on the olefin (a) and carbon dioxide (b) selectivity as a function of the propane conversion for the same reaction conditions as listed in Fig. 6. (Ratio of premixed to distributed oxygen feed is indicated in the figures.) (Dashed line reflects the possible olefin selectivity at a certain propane conversion that can be achieved with gas phase reactions.)

With increasing degree of distribution of oxygen along the reactor axis the reactor performance can be significantly improved: Both the olefin selectivity and the catalyst activity is enhanced (see Fig. 7).

Based on the above presented distribution of oxygen $\Phi_{V,O2,0}/\Phi_{V,O2,distr}$=4/10 and a catalyst mass of 20 g, the effect of intraparticle and membrane to centerline mass transport limitations on the performance of the PBMR will be discussed next. Yet, due to the nature of the kinetic scheme, especially the reaction inhibition by carbon dioxide, no meaningful modified Thiele-modulus can be formulated, and therefore it was abstained from.

7.2.4 Effect of intraparticle mass transport limitation

Due to the relative low activity of the catalyst and the assumption that the effective diffusion in the particle is determined by molecular diffusion, the intraparticle mass transfer limitations become apparent only for relatively large particle sizes.

The axial oxygen concentration profiles for catalyst particles of 1, 5 and 10 mm are shown in Fig. 8.

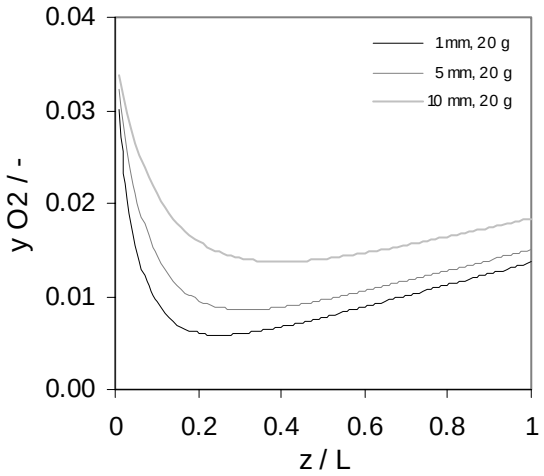

Fig. 8 Axial oxygen concentration profiles for three different catalyst particle diameters.

In Fig. 9 the axial profiles of the selectivity factor (for definition see Section 4.2.2) and the particle effectiveness for oxygen consumption are presented. The influence of the intraparticle mass transport limitations on the olefin selectivity is mostly adverse, and only for d_p=5mm in a small region very small selectivity improvements are obtained, in contrast to theoretical predictions for simple reaction systems discussed in Chapter 4. The explanation for this is that the intraparticle concentration gradients of hydrocarbons are not negligible small compared to that of oxygen, which has several causes. Firstly, in the center of the catalyst particle the catalyst activity is reduced by the increased carbon dioxide concentration. Secondly, the gas phase concentration of propene (or ethene) is not much larger than that of oxygen (maximum factor 6 for d_p=5mm). And thirdly, the conversion of propane to ethene is only slightly effected by the oxygen concentration. Furthermore, ethene was assumed to be stable (no consecutive combustion), so that its production is hardly effected by intraparticle concentration profiles of oxygen.

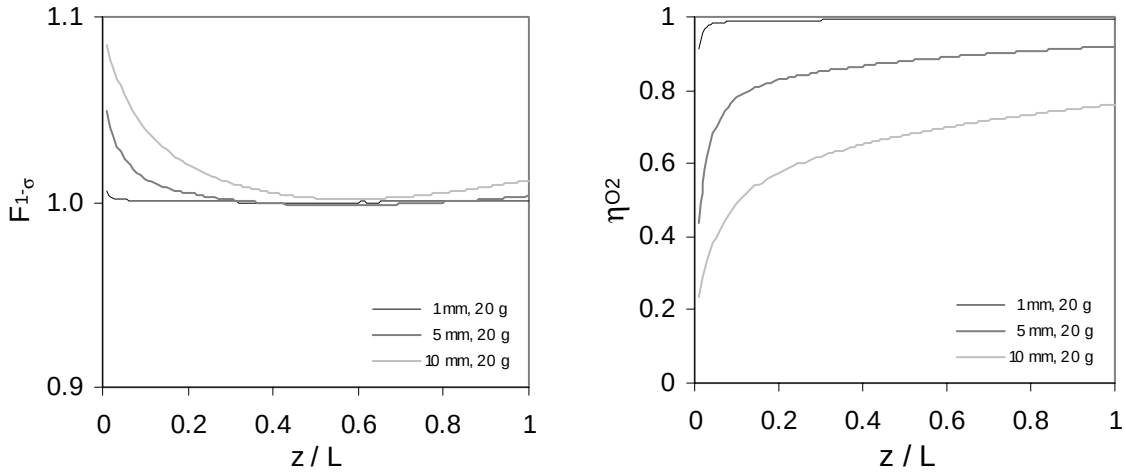

Fig. 9 Axial profile of (a) the selectivity factor and (b) the particle effectiveness for oxygen consumption.

In Fig. 10 the effect of the catalyst particle size on the olefin selectivity and the ratio of propene and ethene selectivities are presented. The intraparticle mass transfer limitations mainly effect the formation of propene, which is reduced, and thus the product distribution shifts to smaller propene/ethene ratios.

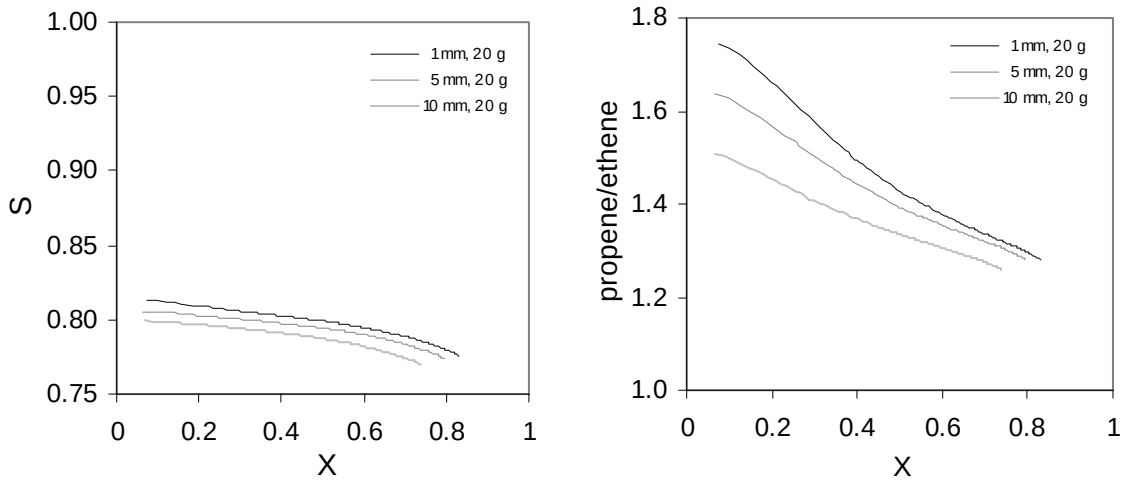

Fig. 10 (a) Olefin selectivity and (b) ration of propene and ethene selectivities as a function of the propane conversion for three different particle sizes.

The reduced catalyst effectiveness in a PBMR with particles of d_p=5mm and larger can be compensated for by an increase of the catalyst mass. However, the integral effect on the propene selectivity remains negative (opposite to the results presented for the model kinetics in Chapter 5), and the propene/ethene ratio actually reduces further (calculations results not shown).

7.2.5 Transport from the membrane

Finally, the effect of mass transport limitations in the PBMR from the membrane wall to the center of the packed bed will be discussed for the ODHP. The selected model parameters are given in Table 2. For the evaluation of the influence of radial mass transport limitations PBMRs with different membrane tube diameters have been simulated. For the larger diameter of $d_2=2d_t$ and $d_3=4d_t$ the volumetric flow rates and the catalyst mass are increased by a factor of 4 or 16 respectively.

Table 2 Model parameters for the study of the effect of radial mass transport limitations.

Reactor length		L	0.24 m
Membrane tube diameter		d_t	0.01 m
Catalyst mass		m_{cat}	20 g
Particle diameter		d_t/d_p	20
Bed porosity		ε	0.389
Catalyst density		ρ_{cat}	1740 kg / m^3
Reactor pressure and temperature		p, T	1.013 bar at outlet, 600°C
Premixed feed:	volumetric flow	$\Phi_{V,0}$	100 ml / min
	mole fraction of reactant A	$y_{C3,0}$	0.28
	mole fraction of oxygen	$y_{O2,0}$	0.04
Distributed feed:	volumetric flow	$\Phi_{V,distr}$	50 ml / min
	mole fraction of oxygen	$y_{O2,distr}$	0.2

In Fig. 11 it can be seen that the effect of radial mass transport limitations on the axial profile of the average oxygen concentration is relatively small, despite the fact that strong radial concentration profiles are established for $d_2=2d_t$ and $d_3=4d_t$. The 2-dimensional oxygen concentration profiles for two different tube diameters are presented in Fig. 12.

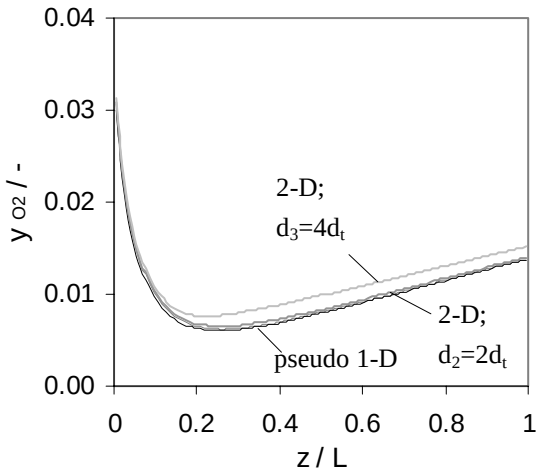

Fig. 11 Influence of the membrane tube diameter on the axial oxygen concentration profile (pseudo-1-D indicates a calculation with infinite radial dispersion coefficient).

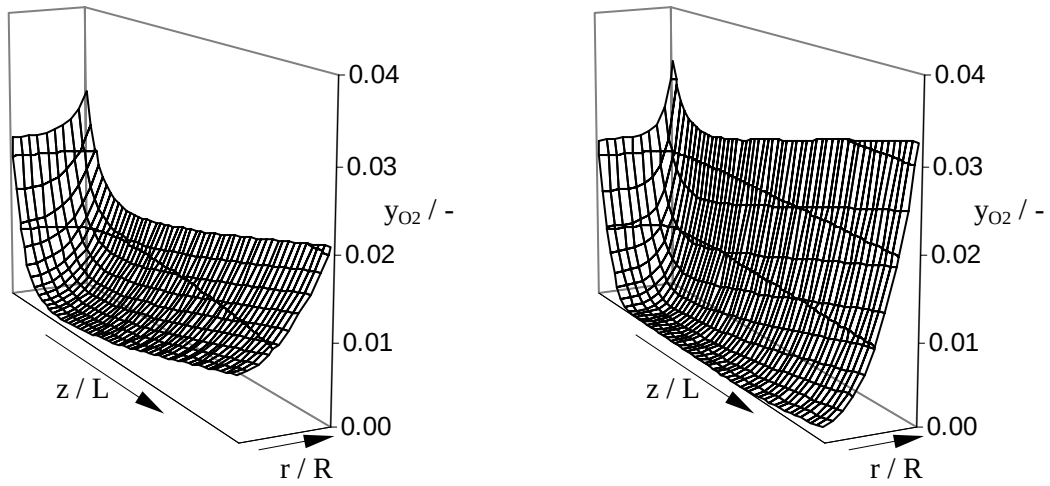

Fig. 12 2-dimensional oxygen concentration profiles for (a) $d_2=2d_t$ and (b) $d_3=4d_t$.

The small effect of radial concentration profiles on the PBMR performance can be explained by the reaction orders of oxygen. The cracking of propane to ethene and methane is hardly effected by the oxygen concentration. The formation and consecutive combustion of propene has reactions orders in oxygen of 0.24 and 0.73 respectively. For these reaction orders the effect of radial concentration profiles is small as was also shown in Chapter 4 (Section 4.3.1). Additionally, the effect on the radially averaged reaction rates for both reaction orders is approximately the same, or –assuming a parabolic profile with a concentration ratio at the wall compared to the center of x- it is even identical for x<10. This explains that the selectivity factor presented in Fig. 13a is only in a small region above unity for $d_2=2d_t$, where strong radial gradients prevail.

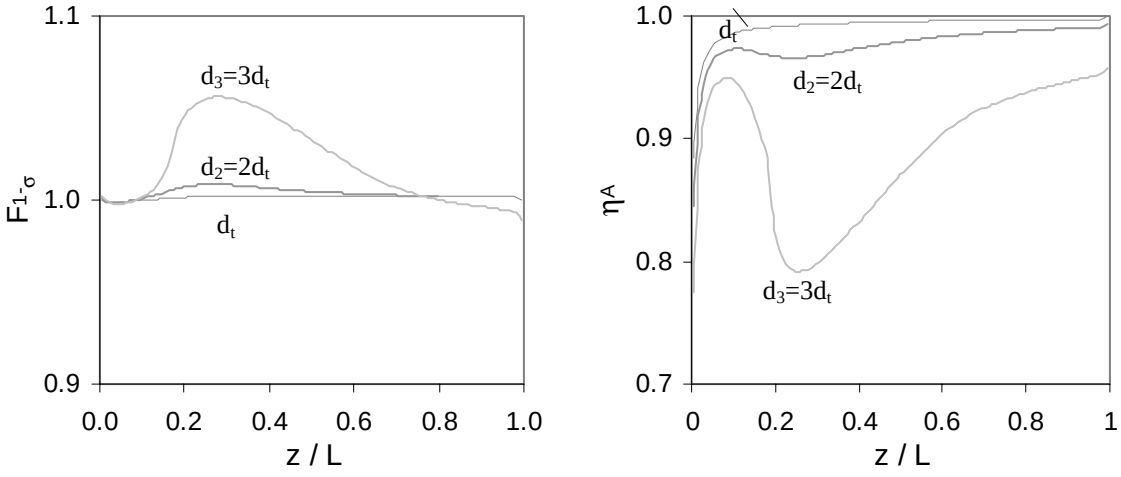

Fig. 13 Axial profile of (a) the selectivity factor and (b) the particle effectiveness for propane consumption.

Only for even larger membrane tube radii ($d_3=4d_t$) significant adverse effects of the olefin selectivity or the product distribution between propene and ethene emerge (Fig. 14).

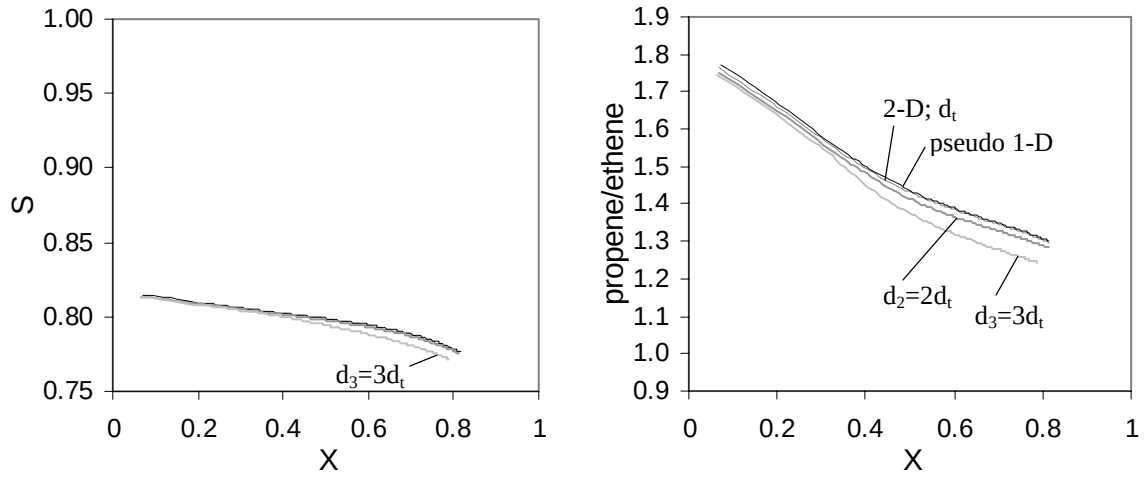

Fig. 14 (a) Olefin selectivity and (b) ration of propene and ethene selectivities as a function of the propane conversion for different membrane tube sizes.

7.2.6 Summary and conclusions

Model simulations based on the kinetic reaction system for the ODHP derived from Leveles (2002) shows a good potential for olefin yield improvements by distributive feeding of oxygen in a PBMR. Effects of mass transfer limitations inside the particle (if governed by molecular diffusion) and from the membrane wall to the center of the packed bed are negligibly small under usual process conditions.

However, it should be noted that the kinetics (Table 1) were based on a limited series of differential measurements (Leveles, 2002). Gas phase and surface reactions were lumped in one correlation. Some remarks on the importance and the possible effect of gas phase reactions can be found in Appendix B. Improved models for the ODHP should account for radical gas phase and surface reactions separately. Surface reactions may act mainly as initiator accelerating gas phase reactions (alternative chain start reactions (and combustion)) The gas phase mechanism may be influenced positively by changing the product distribution.

7.3 Oxidative dehydrogenation of ethylbenzene

Styrene is industrially produced mainly in a two-step process by first alkylating benzene with ethene to form ethylbenzene, which is then dehydrogenated to styrene. Due to thermodynamic limitations only medium ethylbenzene conversions can be achieved in this conventional process. This problem is reduced in the commercial 'SMART' process by sequential combustion of the hydrogen formed via selective catalytic oxidation. Thus, ethylbenzene conversions of about 80 % are achieved at a styrene selectivity of about 95 %.
As an alternative technique the oxidative dehydrogenation has been proposed (see review article of Cavani and Trifirò, 1995b), which however suffers from undesired combustion reactions resulting in too low product selectivities. Two concepts can be followed in order to improve the product yield both as combination of catalyst and reactor development.

Firstly, the development of a redox-type oxide catalyst. Lattice oxygen is expected to be selective, while surface oxygen is held responsible for undesired combustion reactions. The unselective oxygen could be avoided by separation of oxidative dehydrogenation with lattice oxygen and the re-oxidation of the catalyst. Watzenberger et al. (1999) discuss the unsteady-state oxidative dehydrogenation in a fixed bed reactor. The reactor cycle comprises besides ODH and the oxidation of catalyst two intermediate periods of flushing the catalyst with nitrogen. They claimed that the redox-catalyst achieved in lab-scale experiments selectivities of about 95 % at a total conversion of approximately 97 %. Yet, the economic feasibility of this process alternative depends on the oxygen load of the catalyst (8 g active oxygen / kg catalyst = 53 g styrene / kg catalyst) and the cycle times, which determine the required amount of catalyst, i.e. the size of the reactor section.

The second reactor concept combines a catalyst with different reaction orders in oxygen for the target and waste product reactions with distributive feeding of oxygen. For the demonstration of the potential of this concept for the ODH of ethylbenzene, appropriate kinetics were taken from open literature. Shakhnovich et al. (1984) investigated the kinetics of the ODH of ethylbenzene on a zinc oxide modified vanadia/magnesia catalyst in the presence of steam. They investigated the catalyst in steady state after the initial coke formation. The kinetics were studied for the following ranges of experimental conditions:

- Reaction temperature: 420 to 550°C,
- Initial ethylbenzene (EB) concentration $p_{C_8H_{10},0}$: 4.2 to 11.2 kPa,
- Initial oxygen concentration $p_{O_2,0}$: 4.4 to 9.6 kPa,
- Added steam $p_{H_2O,0}$: 10 to 80 kPa.

The following parallel-consecutive scheme for the main products is presented:

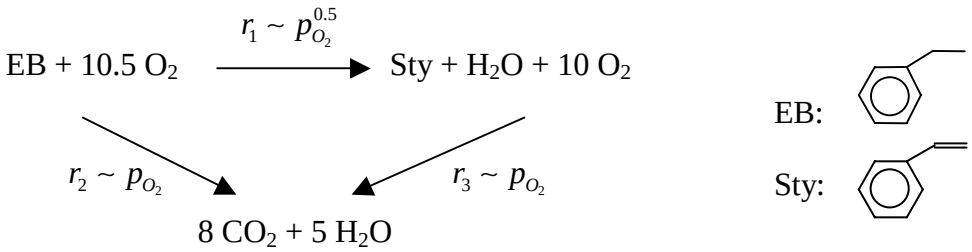

Fig. 15 Model reactions for the ODH of ethylbenzene on a zinc oxide modified vanadia/magnesia catalyst by Shakhnovich et al. (1984).

Table 3 Reaction kinetics by Shakhnovich et al. (1984).

r_i [mol / g s]	$r_1 = K_I \frac{p_{C_3H_{10}} p_{O_2}^{0.5}}{B}$	$r_2 = K_{II} \frac{p_{C_3H_{10}} p_{O_2}}{B}$	$r_3 = K_{III} \frac{p_{C_3H_8} p_{O_2}}{B}$
K_I [mol / g s kPa^{1+n}]	$4.91 \cdot 10^{-2} \exp(-7100/T)$	$6.55 \cdot 10^{-4} \exp(-7050/T)$	$4.55 \cdot 10^{-3} \exp(-7550/T)$
	$B = \left[\left(1 + k_1 p_{C_8H_{10}} + k_2 p_{C_8H_8} + k_3 p_{O_2}\right) \left(1 + x \frac{p_{C_8H_{10}}}{p_{O_2}^{0.5}}\right) \right]^2$ with x=0.04 $kPa^{-0.5}$		
k_i [kPa^{-1}]	$2.31 \cdot 10^{-5} \exp(6300/T)$	$6.72 \cdot 10^{-5} \exp(6300/T)$	$2.62 \cdot 10^{-3} \exp(2500/T)$

Because both combustion reactions show a higher order in oxygen than the styrene formation, a low oxygen concentration improves the selectivity of the target product. In this study it was assumed, that the proposed reaction orders also hold outside the concentration ranges of the kinetic investigation, namely for very low oxygen concentrations.

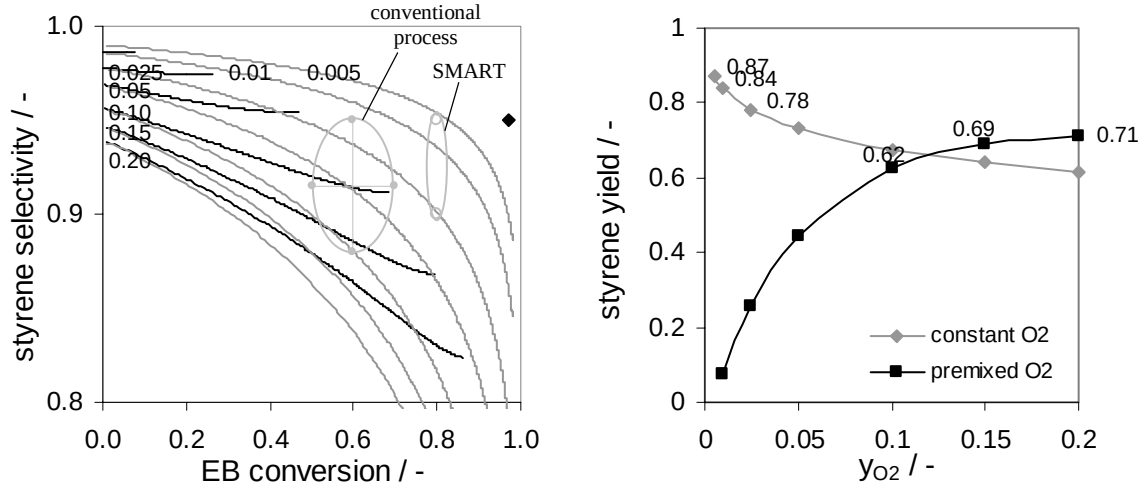

Fig. 16 Influence of the oxygen concentration on (a) the styrene selectivity as a function of the EB conversion, (b) the styrene yield at 550°C. The EB mole fraction for all cases is y_{EB} = 0.1 while that of oxygen is varied from y_{O2} = 0.005 to 0.2. The bold lines represent the model results for premixed oxygen, the thin lines for constant oxygen concentrations. In (a) the performance of the conventional, the SMART process and the unsteady-state oxidation process by Watzenberger et al. (1999) (diamond) are indicated.

In Fig. 16a the influence of the oxygen concentration on the selectivity-conversion-plot is demonstrated for FBRs with premixed oxygen feeding and idealized PBMRs with an axially constant oxygen concentration. For the model calculations a reaction temperature of 550°C, an initial ethylbenzene concentration of y_{EB}=0.1 and a flow rate of 100 ml/min were chosen. The figure clearly demonstrates that the ODH of ethylbenzene with premixed oxygen feeding cannot compete with the standard dehydrogenation process and even less with the SMART process.

The SMART process (conversion of 80 % at a selectivity of 95 %) shall be taken as a target for the investigation of the PBMR. The yield of the SMART process is exceeded by a PBMR with a constant oxygen concentration of y_{O_2}=0.025 (Fig. 16b), but at a low styrene selectivity of only 84 %. Because of the high feed stock costs, such a low selectivity should be avoided. Thus an oxygen concentration of y_{O_2}=0.005 is required. For a catalyst mass of 1.13 g a selectivity of 95.4 % is achieved at 80 % conversion, corresponding to a WHSV of 1.75 kg styrene produced per kg catalyst per hour.
Additional model calculations at 500°C showed a small effect of the reaction temperature on the selectivity-conversion-plot. In this case 3.17 g catalyst were required to achieve a conversion of 80 % and a selectivity of 95.5 %.
Subsequently, the PBMR was not modeled with a constant oxygen concentration, but with a flow of air equally distributed over the length of the reactor. For an increased catalyst mass of 1.5 g the oxygen in premixed and distributive flow was optimized under the constraint of a minimum styrene selectivity of 95 %. The (flat) maximum in the styrene yield was found for an inlet oxygen concentration of y_{O_2}=0.02 of the premixed flow of $\Phi_{V,0}$=100 ml/min and a distributive flow of $\Phi_{V,air,distr}$=35 ml/min with a conversion of 85.4 % and a selectivity of 95.1 %.
In the following sections the effect of intraparticle mass transfer limitations and the transport from the membrane to the core of the packed bed on the PBMR performance will be studied with these optimized model parameters.

7.3.1 Intraparticle transport

In Table 4 the model parameters are listed used for the evaluation of the influence of intraparticle mass transport limitations on the performance of a PBMR for the ODH of ethylbenzene to styrene.
As explained in Section 5.4.3 the effective diffusion coefficients of ethylbenzene and styrene are smaller than that of oxygen, and thus the hydrocarbons are forming relatively strong concentration profiles in the catalyst particles. The ratio of the effective diffusion coefficients of ethylbenzene and oxygen was estimated as:

$$\frac{D_{eff,A}}{D_{eff,O_2}} = \frac{1-y_A}{1-y_{O_2}} \frac{y_A + 0.357\, y_{N_2}}{y_{O_2} + 0.965\, y_{N_2}} = 0.44 \qquad (1)$$

Table 4 Model parameters.

Catalyst mass		m_{cat}	1.5-3 g
Catalyst density		ρ_{cat}	1000 kg / m^3
Particle diameter		d_p	1-5 mm
Interphase mass transfer coefficient		k_s	1 m / s
Reactor pressure and temperature		p, T	1.013 bar, 550 K
Premixed feed:	volumetric flow	$\Phi_{V,0}$	100 ml(STP) / min
	mole fraction of reactant A	$y_{EB,0}$	0.1
	mole fraction of oxygen	$y_{O2,0}$	0.02
Distributed feed:	volumetric flow	$\Phi_{V,distr}$	35 ml(STP) / min
	mole fraction of oxygen	$y_{O2,distr}$	0.2

STP: 1.013 bar and 298 K

7.3.1.1 Increase of the particle size

In Fig. 17 and Fig. 18 the influence of intraparticle mass transfer limitations on the reactor performance is shown for the particle diameters 1, 3 and 5 mm. While the effect is negligible for the smallest particle size, the relative loss in the styrene yield increases from 4 % to 10 % for 3 and 5 mm respectively. For d_p=3mm the modified Thiele-modulus (definition, see Section 4.2) is about ϕ'=0.93, the selectivity reduces to 94.85 % slightly below the target value.

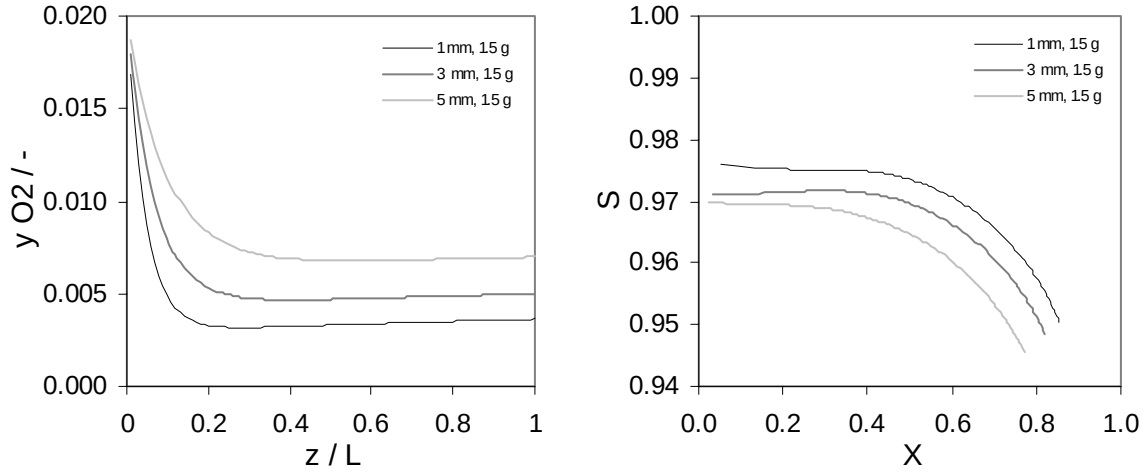

Fig. 17 Influence of the particle size on the (a) the axial oxygen concentration profile and (b) selectivity – conversion – plot.

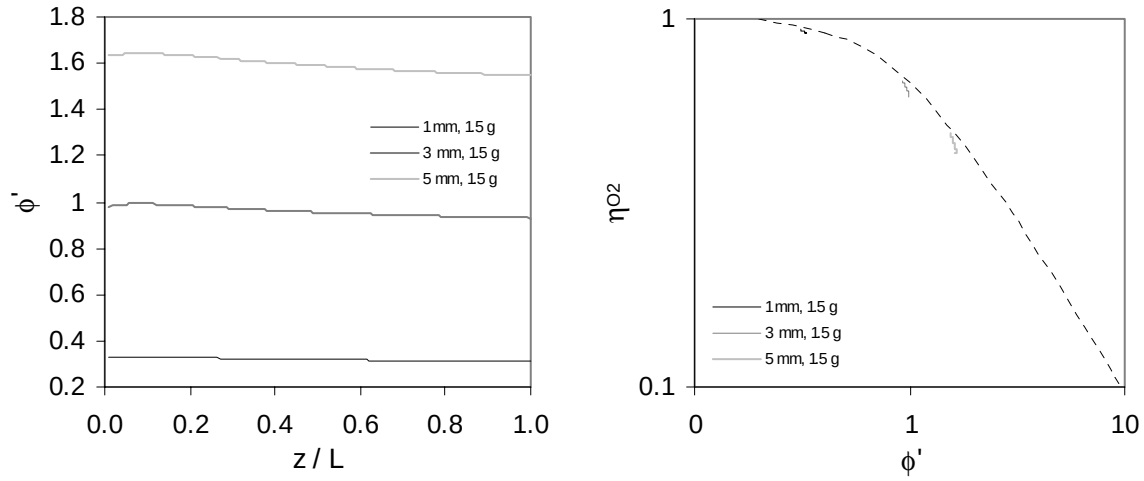

Fig. 18 (a) Axial profile of the Thiele-moduli for the different particle sizes and (b) particle effectiveness as function of the Thiele-modulus (the dashed line represents the results from Chapter 4 assuming model kinetics and a low oxygen concentration compared to the hydrocarbons).

7.3.1.2 Increase of particle size and catalyst mass to account for the reduced activity

If the reduced particle effectiveness is compensated for by an increase of the catalyst mass, such that the axial oxygen concentration profile approaches the values of the original catalyst mass without intraparticle mass transfer limitations, the integral effect of the mass transfer limitations on the styrene selectivity turns out to be slightly positive (Fig. 19b).

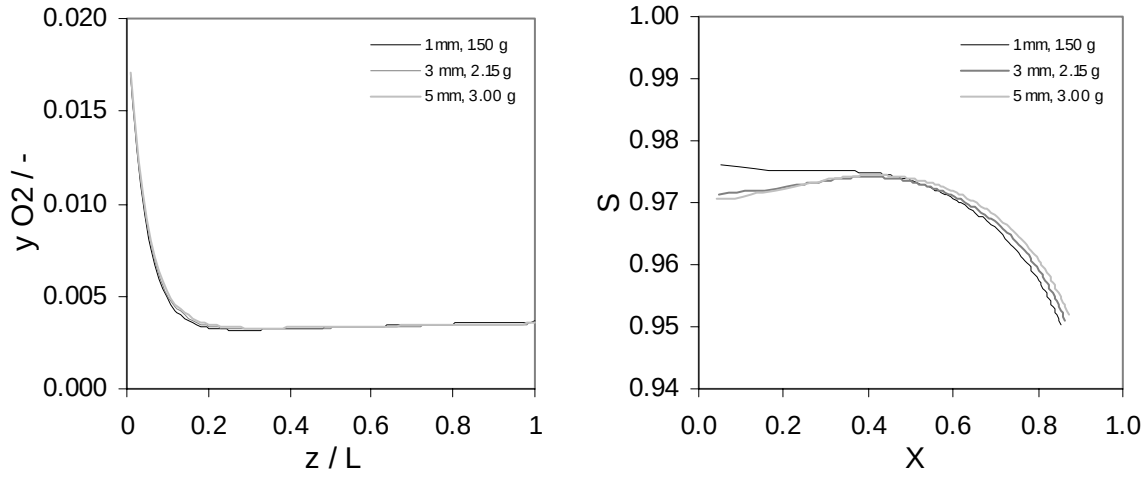

Fig. 19 Influence of the particle size on the (a) the axial oxygen concentration profile and (b) selectivity – conversion – plot.

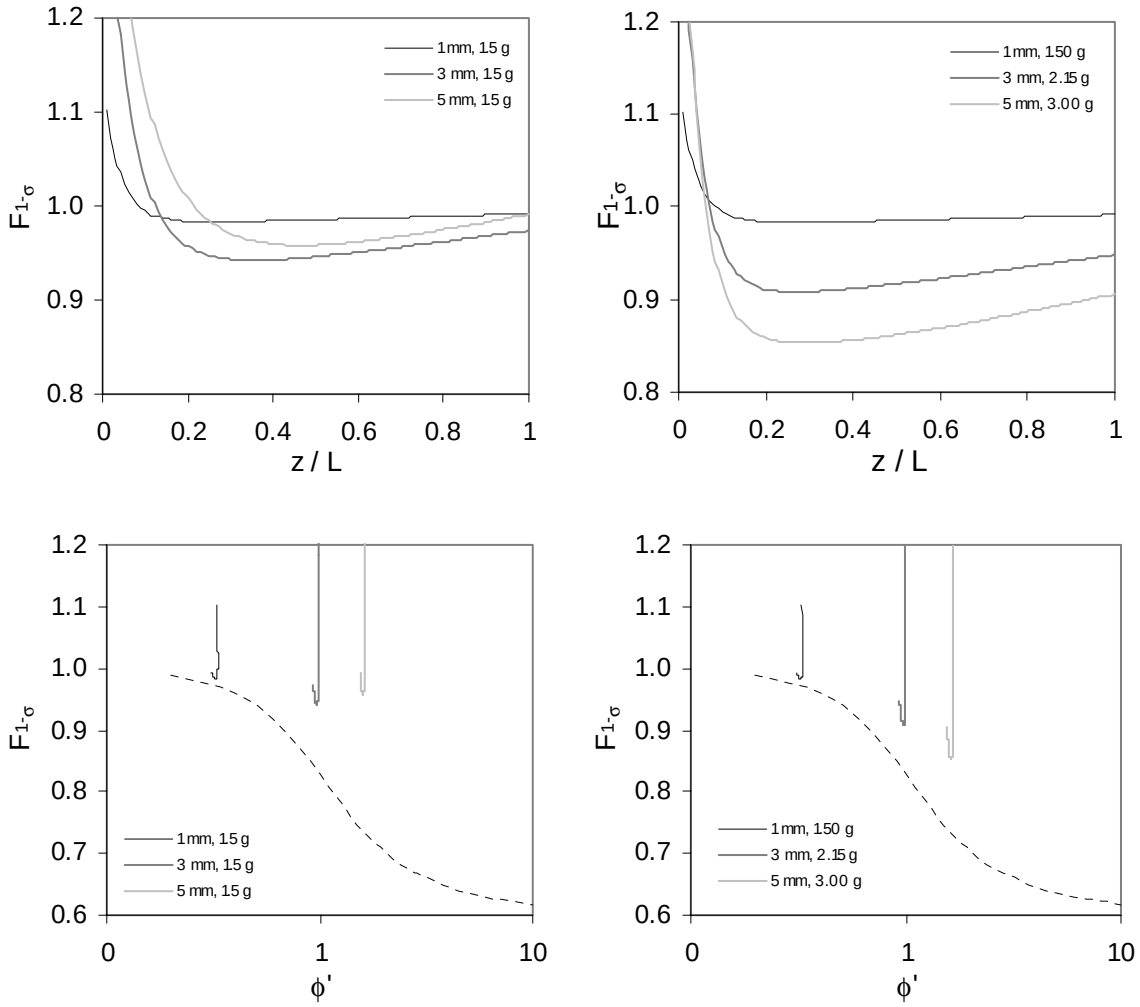

Fig. 20 Comparison of the axial profile of the local selectivity loss for three different particle sizes (a, c) at constant catalyst mass and (b, d) increased catalyst mass to compensate for activity loss (the dashed line represents the results from Chapter 4 assuming model kinetics and a low oxygen concentration compared to the hydrocarbons).

The positive effect of intraparticle oxygen concentrations gradients surpasses the negative effect of the hydrocarbon gradients, such that the selectivity loss ($F_{1-\sigma}>1$) in first 10-20 % of reactor is more than compensated by selectivity improvements in the rest of the reactor.

Fig. 20 shows a comparison of the selectivity factor $F_{1-\sigma}$ as function of the axial position and the modified Thiele-modulus for both situations with a fixed catalyst mass and with catalyst masses increased with the particle diameter. The decrease of the oxygen concentration, i.e. the increase of the ratio of hydrocarbon to oxygen concentrations, results in a decrease of $F_{1-\sigma}$ over the entire length of the reactor. Yet, the influence of the hydrocarbon concentration gradients is still present as can be seen in Fig. 20d in the difference between the actual values and the values calculated in Chapter 4 under the assumption of constant hydrocarbon concentrations (dashed line).

Concluding, it can be stated that the effect of intraparticle mass transfer limitations can be fully compensated for by an - even though significant - increase of the catalyst mass without negative effects on the styrene selectivity.

7.3.2 Transport from the membrane

In the following the influence of mass transfer limitations from the membrane wall to the core of the packed bed on the integral performance of a PBMR of industrial size is evaluated. Intraparticle mass transport effects are neglected here. The selected model parameters are listed in Table 5.

The 2-D model including Navier-Stokes equations was used in this study, where 100 grid cells were used in the axial and 80 in the radial direction, and the time step size was $1 \cdot 10^{-4}$ s for the flow model and $1 \cdot 10^{-2}$ s for the reaction model.

For the selection of the reactor dimensions typical diameters and length of multi-tubular reactors were chosen, i.e. 10-40 mm diameter and 2-12 m length (Ullmann's encyclopedia, 1996). The same ratio of catalyst mass and volumetric flow rates were selected that was used before in the discussion of the intraparticle transport effects.

An important design criterion is the pressure drop over the packed bed of catalyst. Due to the high reactivity of the catalyst at the chosen upper limit of the temperature range, a relative short membrane with a relatively high tube radius should be chosen. Furthermore, selecting large catalyst particles helps to reduce the pressure drop. For the model calculations presented in Fig. 21 and Fig. 22 tube to particle diameter ratios of $d_t/d_p=10$ and $d_t/d_p=5$ were chosen resulting in pressure drops of 0.24 bar and 0.63 bar respectively. This low diameter ratio, i.e. large particle diameter, has a positive effect on the radial mass transport, however, it results in lower particle efficiencies, which was not included in the calculations.

Table 5 Model parameters.

Reactor length		L	2 m
Membrane tube diameter		d_t	0.04 m
Catalyst mass		m_{cat}	1.44 kg
Particle diameter		d_t/d_p	10, 5
Bed porosity		ε	0.389, 0.41, 0.448
Catalyst density		ρ_{cat}	938, 971, 1038 kg / m^3
Reactor pressure and temperature		p, T	1.013 bar at outlet, 550°C
Premixed feed:	volumetric flow	$\Phi_{V,0}$	5.76 m^3 / h
	mole fraction of reactant A	$y_{EB,0}$	0.1
	mole fraction of oxygen	$y_{O2,0}$	0.02
Distributed feed:	volumetric flow	$\Phi_{V,distr}$	2.016 m^3 / h
	mole fraction `of oxygen	$y_{O2,distr}$	0.2

The radial mass transport increases linearly with the particle diameter as can be seen from the turbulent dispersion coefficient as proposed by Tsotsas and Schlünder (1988):

$$D_r^t = \frac{u_c d_p}{8} \qquad (2)$$

Thus, the increase of the particle size in order to reduce the pressure drop, also avoids mass transfer problems from the membrane to the center of the packed bed (Fig. 21b).

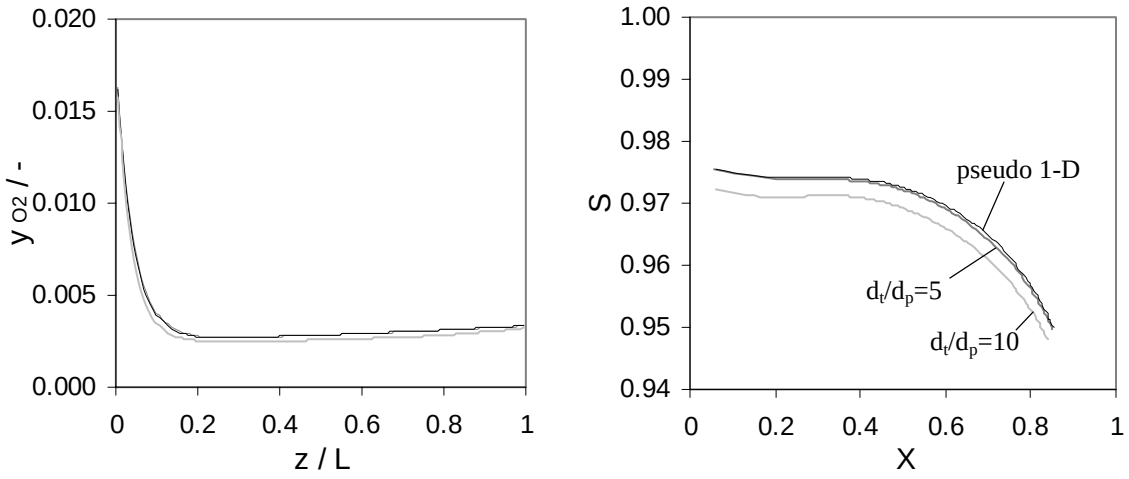

Fig. 21 Influence of the particle diameter on the (a) the axial oxygen concentration profile and (b) selectivity – conversion – plot.

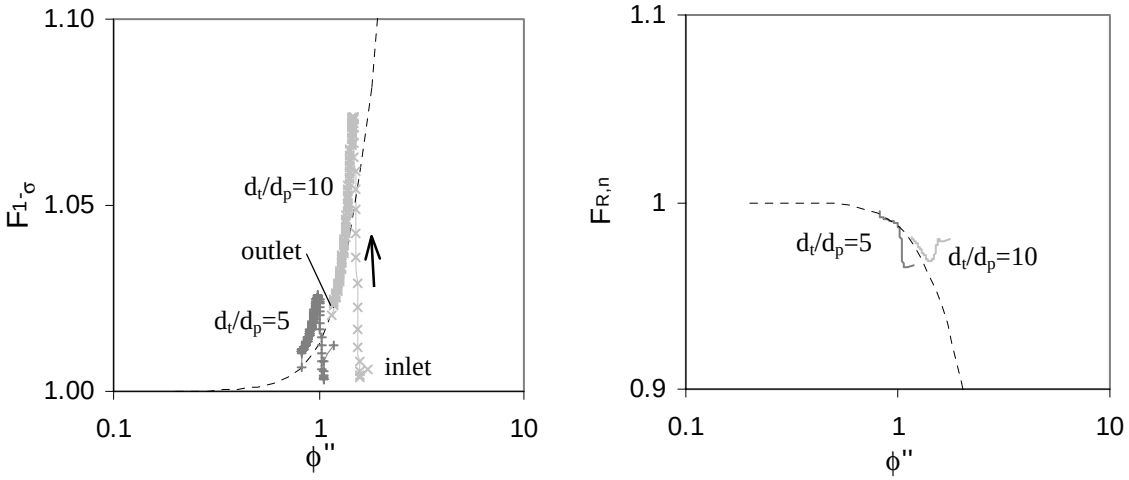

Fig. 22 Influence of the particle diameter on (a) the selectivity loss and (b) the average reaction rate of the primary reaction.

Obviously, the particle effectiveness for catalyst diameters of 4 mm and 8 mm respectively should be considered in the design of the PBMR. As shown in the approximation in Section 4.4.2 for the relative significance of intraparticle and membrane to centerline mass transport limitations, intraparticle mass transport limitations are more severe, due to the high Re-numbers.

Because of the reduced particle efficiencies the PBMR has to be operated at reduced volumetric flow rates of premixed and distributive feed. At lower flow rates the size of the catalyst particles can be reduced at the same pressure drop. Thus, both intraparticle and membrane-to-center mass transfer limitations become significant.
Either way, the ODH of ethylbenzene to styrene cannot be operated in a PBMR at maximal productivity, but will be at least reduced by a half, which is the effectiveness factor of a catalyst particle of d_p=5 mm.

7.3.3 Effect on 'hot spot' temperature and consequence

Up to now isothermity was assumed for the PBMRs, and only the effect of the oxygen distribution on reactant conversion and product selectivity were discussed. However, the manner of the oxygen feeding with the resulting oxygen concentration profiles has an effect on the distribution of the reactivity and thus the distribution of heat formation over the packed bed.
Wall-cooled FBR are known for the development of a strong hot-spot temperature located relatively close to the inlet, where reactant concentrations and reactivity are the highest. With the distributive addition of oxygen to the PBMR the reactivity is (if n>0) distributed more evenly as well.
For the demonstration of the effect of the oxygen distribution on the temperature profiles in the PBMR, a second series of 2-D model calculations was performed at 500°C feed flow and wall temperature with different ratios of premixed and distributive oxygen feed, $\Phi_{V,O_2,0} / \Phi_{V,O_2,distr}$ = 4:3, 2:7, 1:8 and 0:9. The model parameters are listed in Table 6.

Table 6 Model parameters for the study of the effect of oxygen distribution on the temperature profiles for the ODH of EB.

Reactor length		L	2 m
Membrane tube diameter		d_t	0.04 m
Catalyst mass		m_{cat}	1.28 kg
Particle diameter		d_t/d_p	10
Bed porosity		ε	0.41
Catalyst density		ρ_{cat}	863 kg / m^3
Reactor pressure and inlet/wall temperature		p, T	1.013 bar at outlet, 500°C
Premixed feed:	volumetric flow	$\Phi_{V,0}$	1.92 m^3 / h
	mole fraction of reactant A	$y_{EB,0}$	0.1
	mole fraction of oxygen	$y_{O2,0}$	0.04/0.02/0.01/0.0
Distributed feed:	volumetric flow	$\Phi_{V,distr}$	0.48/0.67/0.77/0.86 m^3 / h
	mole fraction of oxygen	$y_{O2,distr}$	0.2

Fig. 23 shows the axial profile of the mole fraction of oxygen. Part of the oxygen is added premixed, part evenly distributed over the length of the packed bed. The fraction of oxygen that is added distributive is given is the figure.

Other model parameters, such as catalyst mass, packed bed dimensions and volumetric flow rates of premixed (EB, O_2, N_2) and distributive (O_2, N_2) flow were kept constant.

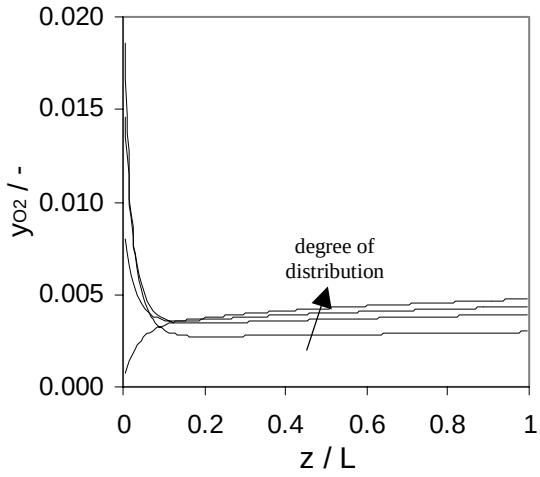

Fig. 23 Axial profile of the (radially averaged) oxygen concentration for different fractions of distributive oxygen addition.

The reduction of the oxygen concentration in the premixed flow clearly results in an improvement of the initial product selectivity (see Fig. 24b). However, distributive addition of oxygen results in the example presented here in an increase of the oxygen concentration in a large part of the reactor. Thus, the selectivity gained at the beginning of the reactor is lost again at the end of the reactor.

Therefore, as far as the styrene yield is concerned it is sufficient to add about 78 % of the oxygen distributively, and no significant improvement can be obtained for a higher fraction – even a slight decrease can be observed for a higher degree of distribution.

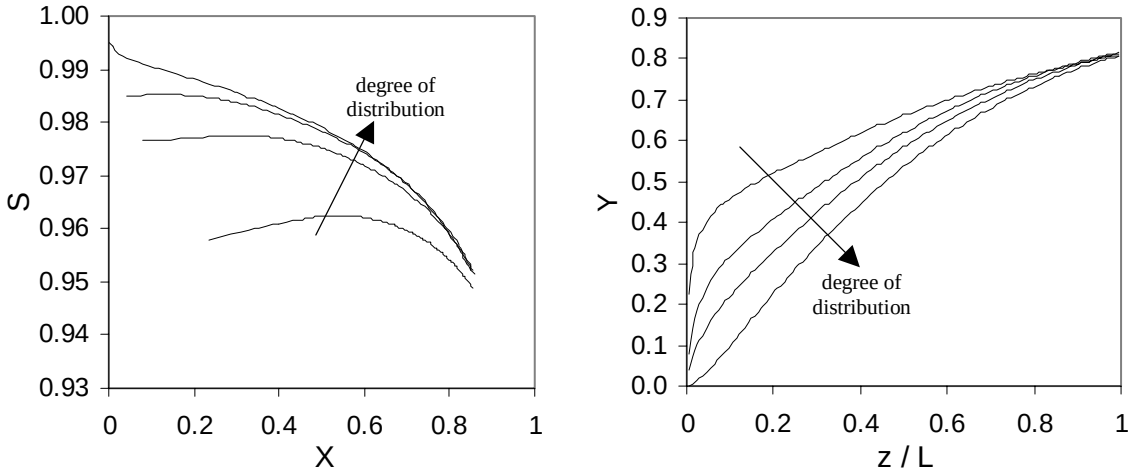

Fig. 24 (a) Selectivity-conversion plot and (b) axial profile of the s yield of styrene for different fractions of distributive oxygen addition.

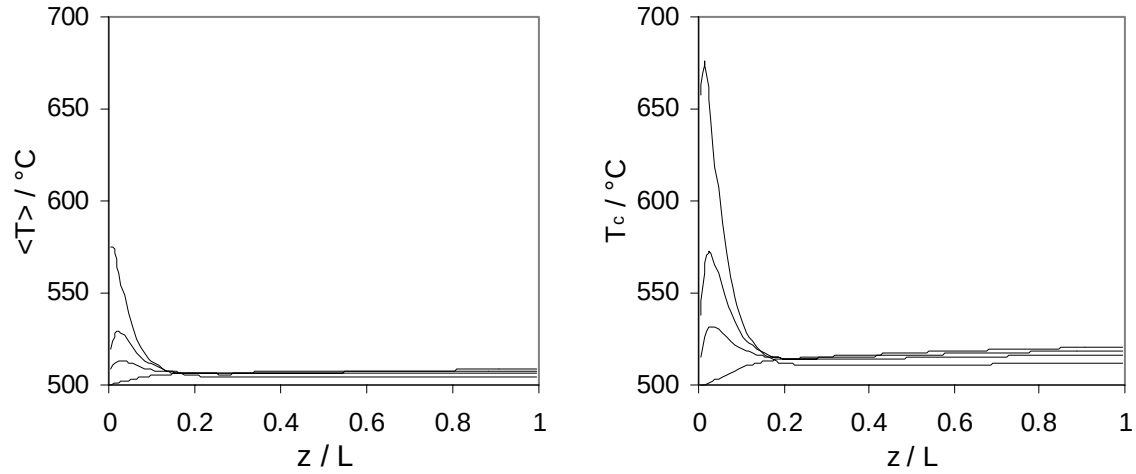

Fig. 25 Axial profile of (a) the radially averaged <T> and (b) the temperature in the center of the bed T_c for different fractions of distributive oxygen addition.

In case of complete distributive addition the product formation is most equally distributed over the reactor length. Conversion and selectivity can be further improved by an increase of the catalyst mass, or the activity of the packed bed.

Distribution of the oxygen considerably reduces the hot-spot temperature as can be concluded from Fig. 25 showing the axial profiles of the radially averaged and the center line temperature.

Two advantages can be obtained from the better temperature control with distributive oxygen feeding:

1. If the product selectivity is temperature sensitive (e.g. low reaction temperature favors the selectivity of the desired product), the PBMR can be operated closer to the optimal reaction temperature. However, in case of the ODH of ethylbenzene the temperature sensitivity of the product selectivity is small.
2. If catalyst or material properties impose a maximum reaction temperature, the PBMR can be operated in large parts much closer at this maximum than the FBR, respectively only 10 % of the oxygen or less should be added in the premixed feed to minimize the hot-spot temperature. The productivity of the PBMR exceeds that of the FBR. Naturally, the design of the FBR can be improved, if the packed bed is divided in zones of different degrees of catalyst dilution.

If the catalyst temperature has to stay below a certain limit, the earlier chosen distribution of $\Phi_{V,O_2,0}/\Phi_{V,O_2,distr}$ =2:7 is not optimal. For $\Phi_{V,O_2,0}/\Phi_{V,O_2,distr}$ =1:8 the reactor throughput can be doubled by an increase of the inlet and wall temperature to 535 °C at the same maximum catalyst temperature.

7.3.4 Summary and conclusions

For the ODH of ethylbenzene to styrene an oxygen concentration of about y_{O2}=0.05 in a PBMR is sufficient to outperform the ODH in a FBR, yet to compete with the SMART process the average oxygen concentration must be an order of magnitude smaller.

Intraparticle mass transfer limitations can be accounted for by an increase of the catalyst mass, i.e. by a factor of about 2 for d_p=5 mm, without a selectivity loss.

In first instance - neglecting the intraparticle effects – the effect of transport limitations from the membrane wall to the center of the packed bed is small in a reactor of industrial scale, if dimensioned under the restriction of a small pressure drop. However, the required particle size is large, so that the catalyst effectiveness is expected to be small. The flow rates have to be reduced and the particle size increased. A heterogeneous, 2-D model is advised for the design of an industrial PBMR.

The temperature rise in a PBMR strongly depends on the degree of oxygen distribution, with a minimum temperature for maximum 10 % of the oxygen in the premixed flow. In case of an constraint of a maximum temperature in the reactor, e.g. induced by increasing contribution of undesired reactions or by material properties, this distribution pattern ensures the optimal productivity of the reactor.

7.4 Oxidative dehydrogenation of methanol

Formaldehyde is one of the most versatile chemicals and is employed by the chemical and other industries to produce a virtually unlimited number of indispensable products used in daily life. It is irreplaceable as a C1 building block and an intermediate in the manufacture of e.g. polyurethane and polyester plastics, resins, resin coatings, dyes, tanning agents, dispersion and plastics precursors, and so on (Ullmann's, 1996).
Formaldehyde is produced industrially from methanol by partial oxidation and dehydrogenation in the presence of air. The reaction can be either catalyzed by MoO_3/Fe_2O_3 (250-400°C) at excess of oxygen, or by silver (600-720°C) under oxygen deficiency (Appendix C). The latter case seems more attractive to test the concept of distributive oxygen addition.

V. Diakov, A. Varma and co-workers investigated the oxidative dehydrogenation of methanol over Fe-Mo oxide catalyst in a packed-bed membrane reactor (Diakov et al. 2001, 2002a, 2002b). The standard composition of the reaction gases was 6 % methanol and 20 % oxygen similar to the composition in industrial processes. Variation of these concentrations showed (Diakov et al. 2001) that high methanol concentrations and low oxygen concentrations favor the selectivity of formaldehyde. Experimental results have been presented that show that at high conversions better selectivities were obtained in a PBMR with distributive addition of oxygen compared with a FBR with the same total feed composition.

Diakov et al. (2002b) presented a kinetic investigation of the oxidative conversion of methanol in the temperature range of 200 to 250 °C. The reaction mechanism is described by a simple consecutive reaction path:

$$CH_3OH \xrightarrow{0.5\,O_2} CH_2O + H_2O \xrightarrow{0.5\,O_2} CO + 2\,H_2O$$

The kinetic investigation involved the variation of feed concentrations of oxygen (5-20 %) and methanol (2-10 %) and the temperature (200-250°C). It can be concluded that the experiments were conducted in most cases with an excess of oxygen. The best fit of the experimental results was achieved with the following rate expressions:

$$r_1 = 0.0048 \exp\left(-17630\left(1/T - 1/485\right)\right) p_{CH_3OH}^{0.5} \qquad [\text{bar}/\text{s}] \qquad (3)$$

$$r_2 = \frac{2.9 \exp\left(-17630\left(1/T - 1/485\right)\right) p_{CH_2O} p_{O_2}}{\left[1 + 3.9 \exp\left(-5920\left(1/T - 1/485\right)\right) p_{O_2}\right]^2} \qquad [\text{bar}/\text{s}] \qquad (4)$$

Diakov at al. performed their kinetic investigation just below the temperature range of industrial practice. Examination of the temperature influence on the reaction order with respect to oxygen for the consecutive reaction gives a possible explanation. With increasing temperature the reaction order decreases, and with it the potential profit of distributive oxygen feeding. For high catalyst temperatures a high reaction order in oxygen for the consecutive reaction can be found only for low partial pressures of oxygen. If the temperature is increased above the range of the kinetic investigation the rate of the undesired combustion reaction decreases with increasing oxygen concentrations (300°C: from p_{O2}=0.04). This could also provide an explanation for the fact that the industrial process is operated at an excess of oxygen.

Table 7 Temperature effect on apparent reaction order for different ranges of oxygen model fractions.

T / °C	*0.002-0.01*	*0.03-0.08*	*0.1-0.2*
200	0.97	0.75	0.40
225	0.95	0.58	0.11
250	0.91	0.36	-0.17

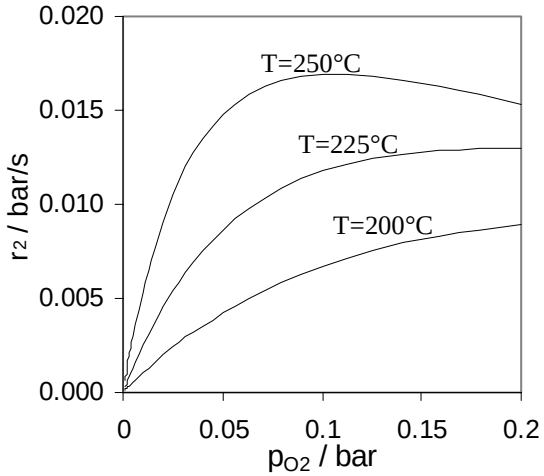

Fig. 26 Reaction rate r_2 for different temperatures as function of the oxygen partial pressure at p_{CH2O}=0.06 bar.

In Fig. 27 the performance of FBR and PBMR with axially constant oxygen concentration are compared under ideal conditions, i.e. no axial mixing and no mass transfer limitations. With increasing reaction temperature the maximum yield improves for both FBR and PBMR. While the absolute value of the yield improvement in the PBMR reduces with increasing temperature, the relative improvement (related to part of methanol not converted to formaldehyde) does not.

Low oxygen concentrations, i.e. below about y_{O2}=0.01, are required to achieve in the PBMR higher formaldehyde yields than in the FBR. Note that the experimental investigation uses inlet oxygen concentrations of y_{O2}=0.05 minimally. The zero order in oxygen of the primary reaction cannot be expected to remain valid at very low oxygen concentrations, but if the reaction rate expression is still valid down to y_{O2}=0.01, sufficient yield improvements can be realized in a PBMR.

In the following section the effect of mass transfer limitations on the performance of the PBMR for the ODH of methanol will be evaluated. Thereby, the primary reaction was rendered to a first order below a concentration of $y_{O2}=10^{-5}$.

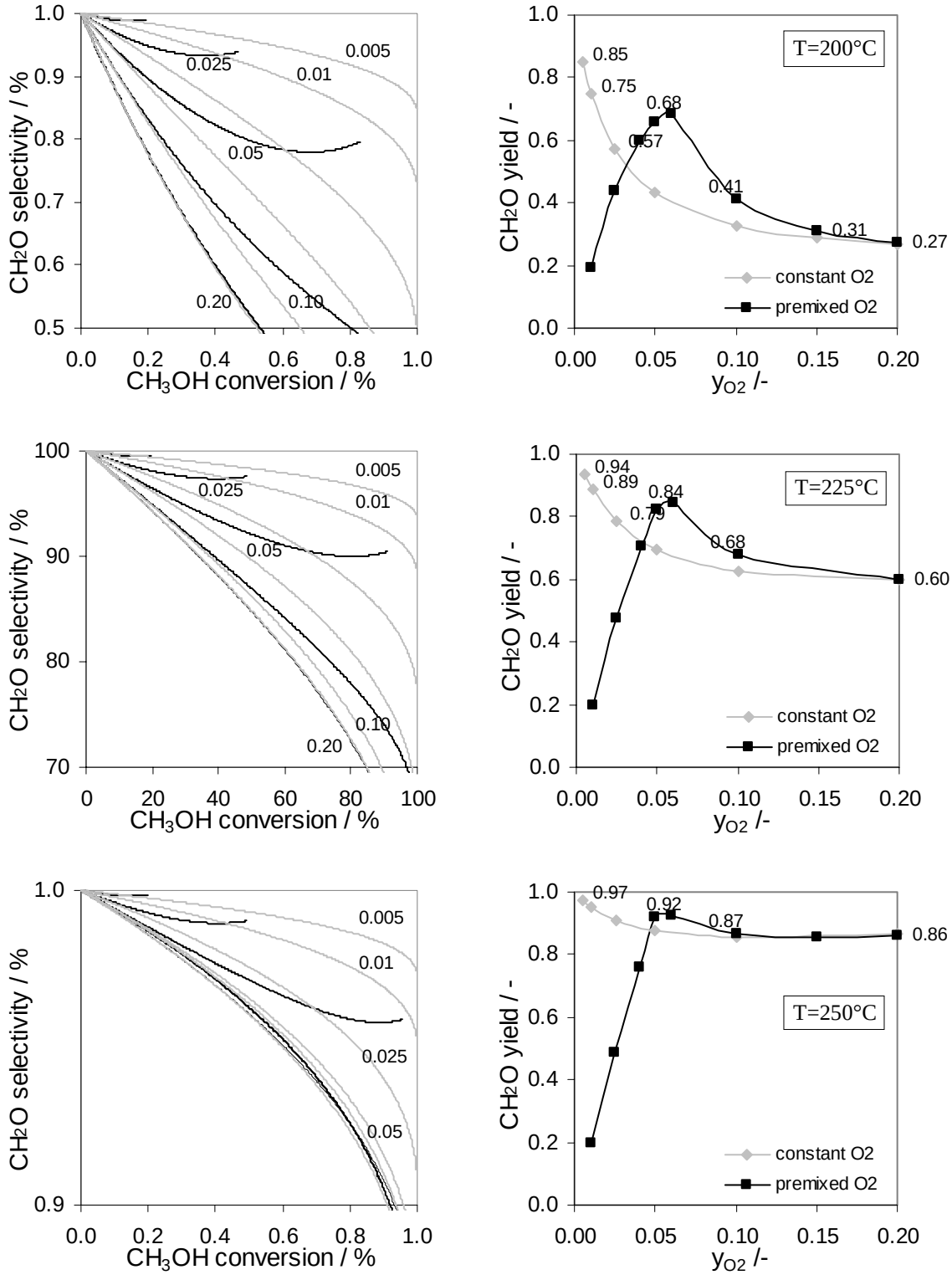

Fig. 27 Comparison of FBR and PBMR (with axially constant oxygen concentration) in (a) selectivity-conversion-plot and (b) maximum formaldehyde yield for the reaction temperatures 200, 225 and 250°C.

7.4.1 Intraparticle transport

The effects of intraparticle mass transfer limitations were studied for the ODH of methanol using the model parameter listed in Table 8.

Table 8 Model parameters for the study of intraparticle mass transfer limitations effects for the ODH of methanol.

Reactor length		L	2.1 m
Membrane tube diameter		d_t	0.04 m
Particle diameter		d_p	1, 3, 5 mm
Reactor pressure and temperature		p, T	1.013 bar at outlet, 250°C
Premixed feed:	volumetric flow	$\Phi_{V,0}$	9 m^3 / hr
	mole fraction of reactant A	$y_{CH3OH,0}$	0.1
	mole fraction of oxygen	$y_{O2,0}$	0.01
Distributed feed:	volumetric flow	$\Phi_{V,distr}$	2.25 m^3 / hr
	mole fraction of oxygen	$y_{O2,distr}$	0.2

Target of the formaldehyde process in a PBMR is a conversion of 98 % and higher and a formaldehyde yield exceeding 92 %. The high methanol conversions make it difficult to obtain oxygen concentrations below that of methanol near the end of the reactor, especially for a constant distribution of the distributed feed. As a consequence of the zero-order in oxygen of the first reaction and the low ratio of the rates of secondary and primary reaction, the oxygen consumption rate is almost exclusively a function of the methanol concentration and decreases continuously over the length of the reactor. This results in strong gradients in the axial concentration profiles of oxygen (see d_p=1mm in Fig. 28).

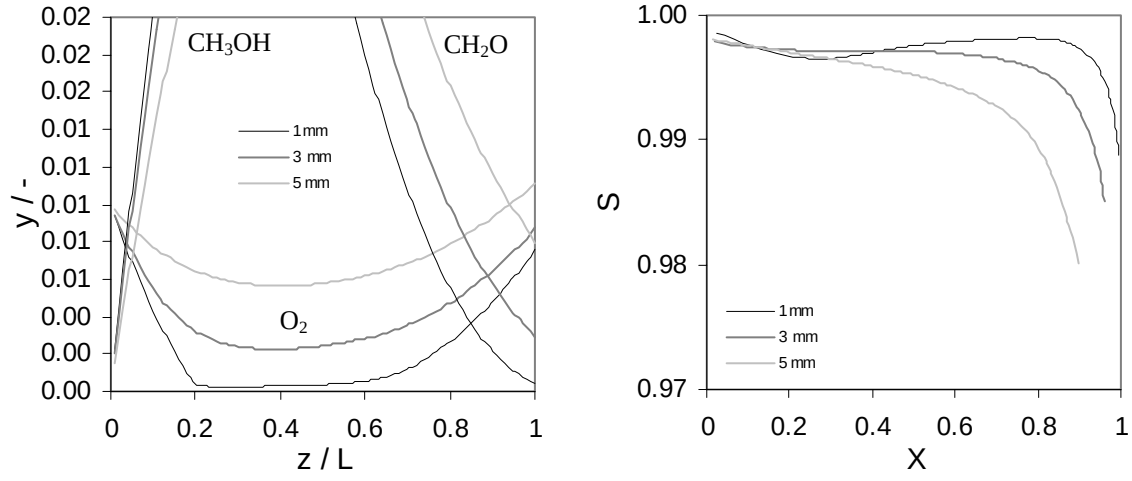

Fig. 28 Influence of the particle size on the (a) the axial concentration profiles and (b) selectivity – conversion – plot at 250°C.

However, while the reaction rate is unaffected, the rate of diffusive transport inside the particle decreases linearly with the oxygen concentration. Therefore, the modified Thiele-modulus ϕ' changes significantly over the reactor length, especially for d_p=1mm, where the oxygen concentration changes over two orders of magnitude very rapidly, as can be seen from the strong drop of $F_{1-\sigma}$ and η_{O2} in Fig. 29ab. Different zones of the PBMR show totally different effects of intraparticle mass transfer limitations on the intrinsic selectivity and particle effectiveness (Fig. 29).

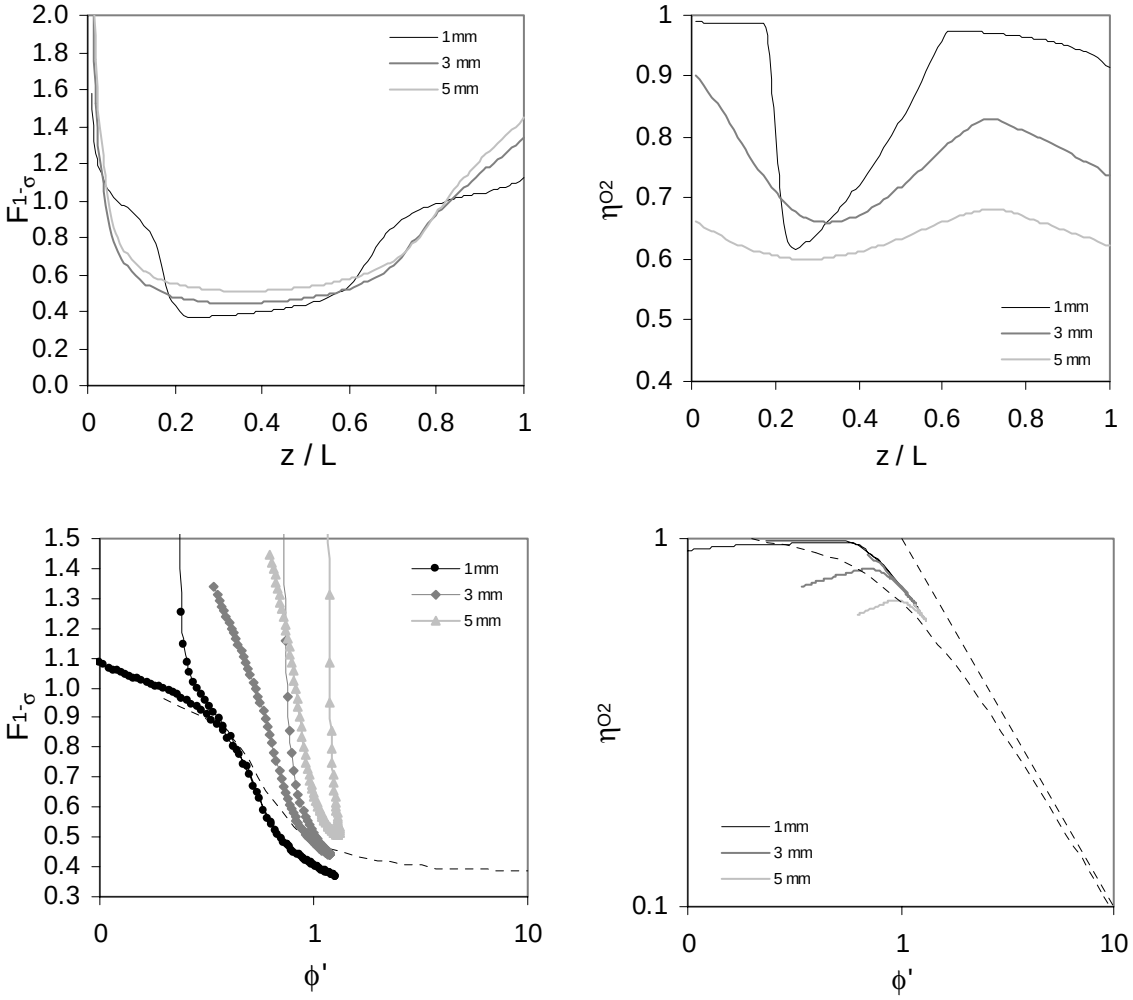

Fig. 29 (a,c) Local selectivity loss and (b,d) local particle effectiveness towards oxygen consumption as functions of (a,b) the axial position of the catalyst particle in the bed and (c,d) the modified Thiele-modulus for three different particle diameters.

The conversion-selectivity plot in Fig. 28b shows that intraparticle mass transfer limitations have a strong effect already for a particle diameter of d_p=3mm for the reaction conditions considered here.

Through an increase of the reactor volume by 35 % (d_p=3mm) and 100 % (d_p=5mm) respectively, the same methanol conversion is obtained as for d_p=1mm, and the integral selectivity loss is reduced.

7.4.2 Transport from the membrane

For the evaluation of the transport effect from the membrane to the center of the packed bed intraparticle effects are neglected. The parameters are the same as in Table 8 besides the particle diameter, which is chosen to obtain the following diameter ratios d_t/d_p=20, 10 and 5 respectively. Fig. 30 shows the effect on the axial oxygen concentration profile and the selectivity-conversion plot. The effect on the formaldehyde selectivity is significant, while the effect on the conversion seems to be negligible. Fig. 31b shows that there is a strong effect of the transport limitations on the average reaction rate of the primary reaction. This apparent discrepancy is simply explained by the difference in the pressure drop resulting from the change in the particle diameter from 1.42 bar (d_t/d_p=20) to 0.68 bar (d_t/d_p=10) and 0.27 bar (d_t/d_p=5).

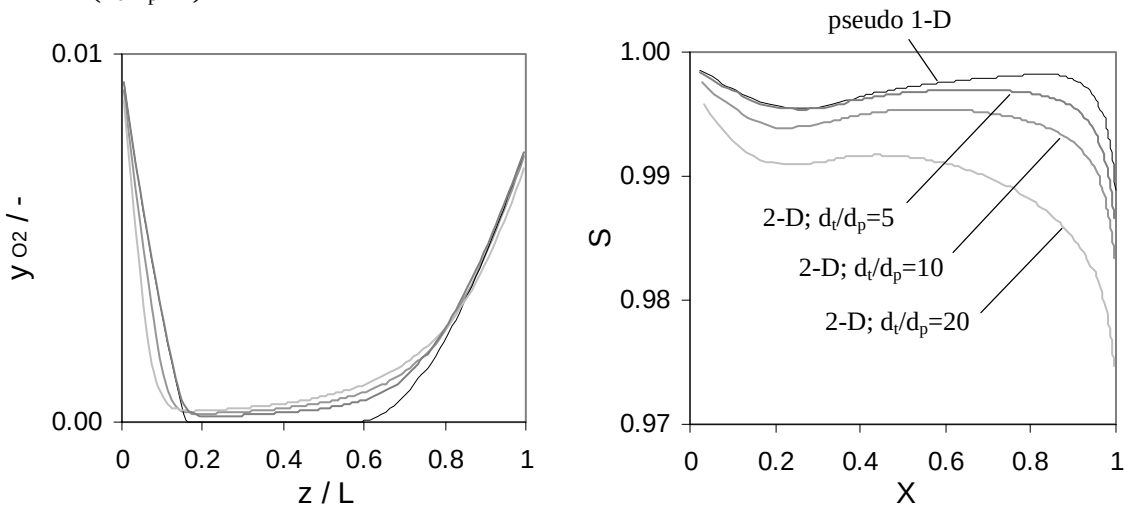

Fig. 30 Influence of the particle diameter on the (a) the axial oxygen concentration profile and (b) selectivity – conversion – plot.

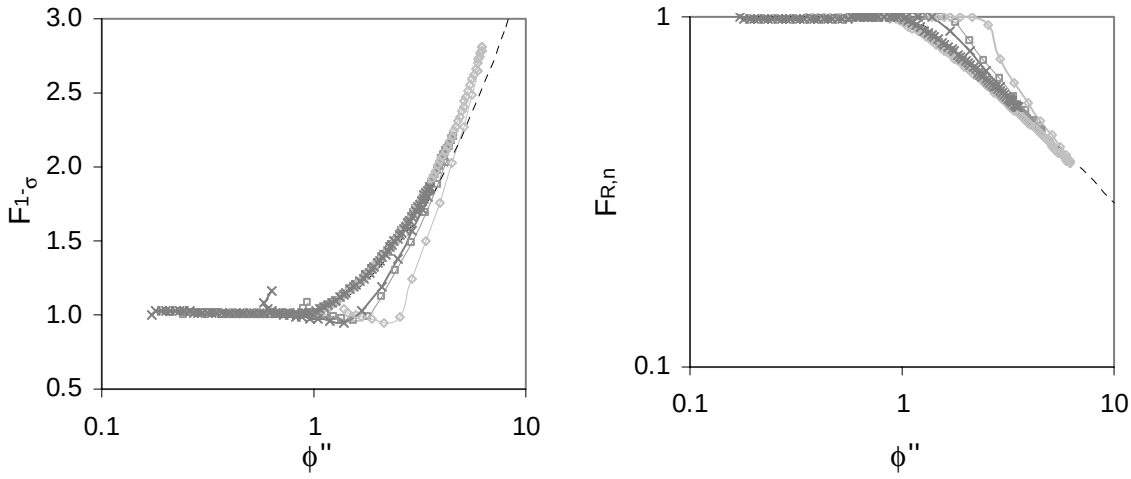

Fig. 31 Influence of the particle diameter on (a) the selectivity loss and (b) the average reaction rate of the primary reaction.

The selectivity decreases for increasing d_t/d_p ratios, showing the negative effect of radial mass transfer limitations.

Note that the oxygen concentration increases strongly towards the reactor end caused by the axially constant permeation flux, while the methanol concentration is small due to the high conversion. This oxygen concentrations increase strongly enhances the consecutive reaction reducing the formaldehyde selectivity. Thus a better PBMR performance is expected with axially decreasing oxygen concentration flux.

7.4.3 PBMR with linearly decreasing membrane flux

In the following the calculations from the intraparticle effects are repeated with a linearly decreasing membrane flux. (Additionally, the distributive flow is reduced to $\Phi_{V,distr}$=1.8 m^3/h.) By this means, it can be avoided that the oxygen concentration exceeds the concentration of methanol near the reactor exit (see Fig. 32b), and consequently the previously observed strong selectivity loss in this region of the reactor is prevented (see Fig. 32b).

The linear decreasing distribution ensures as well that the integral effect of the intraparticle mass transfer limitations on the formaldehyde selectivity is positive, provided that the effectiveness loss is compensated by an increase of the reactor size (see Fig. 33b).

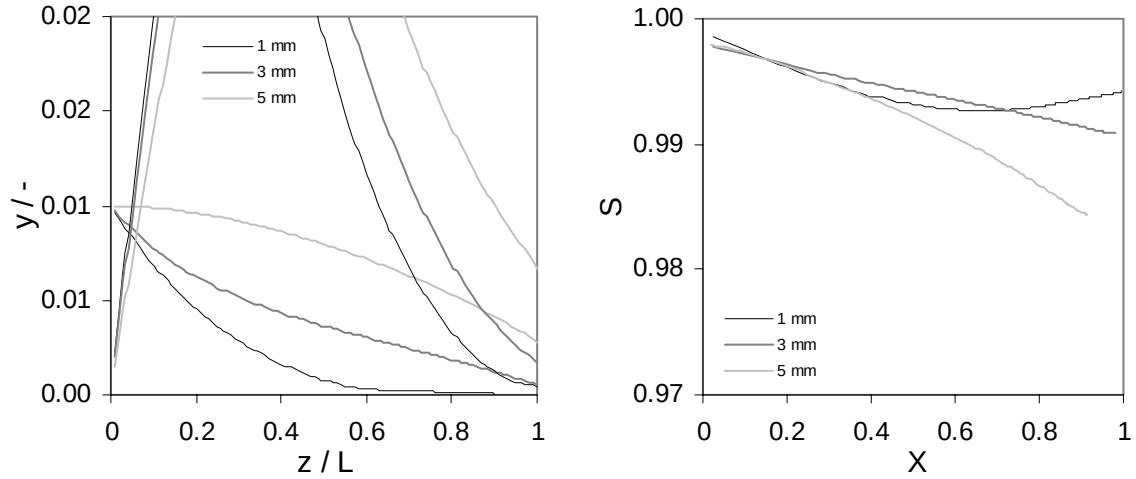

Fig. 32 Influence of the particle size on the (a) the axial concentration profiles and (b) selectivity – conversion – plot for a linearly decreasing membrane flux.

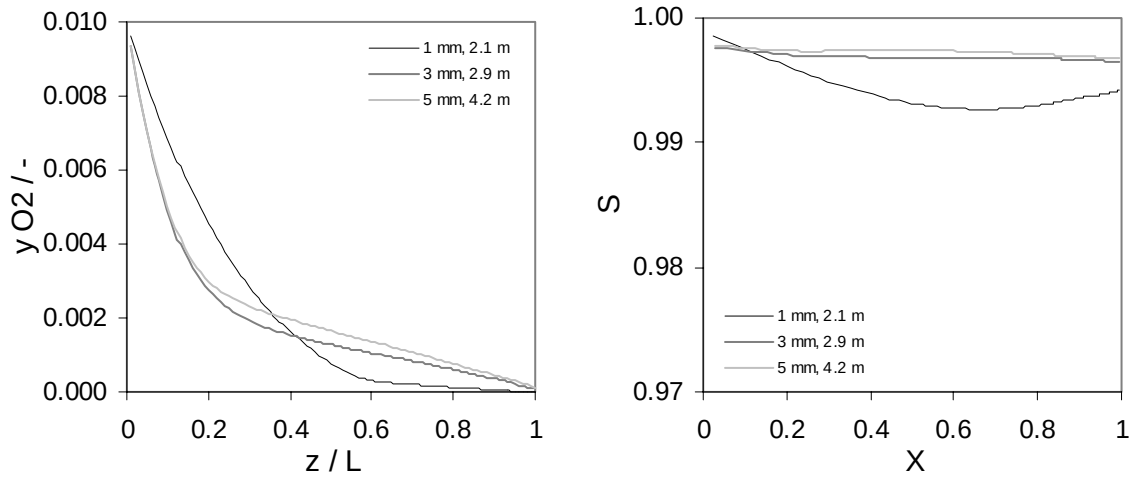

Fig. 33 Influence of the particle size on the (a) the axial concentration profiles and (b) selectivity – conversion – plot for a linearly decreasing membrane flux.

7.4.4 Operation at high methanol concentrations

A PBMR offers the possibility to operate partial oxidation processes at overall feed compositions, which are not feasible in a FBR due to flammability limits. If the industrial process is operated with undiluted feed (y_{O2} about 0.2) the methanol concentration must be limited at about y_{CH3OH}=0.06. The productivity of the process can be almost doubled if the oxygen concentration is reduced below y_{O2}=0.1, e.g. by recycling the reactor outlet flow, which is enriched in nitrogen (Centi et al., 2002), due to the shift in the explosion limits.

In a PBMR the overall concentration of methanol can be doubled. Feed concentrations of $y_{CH3OH,0}$=0.8 (rest air: $y_{O2,0}$=0.04) with a distributive flow of about $\Phi_{V,distr}/\Phi_{V,0}$=2.2 would result in an overall feed composition for a FBR of $y_{CH3OH,0}$=0.267 and $y_{O2,0}$=0.144, which is within the flammability region.

However, the reaction orders in the hydrocarbons are not in favor of an increase of the methanol concentration. The productivity increases only according to a square root function with the methanol concentration, and due to the fact that the consecutive reaction exhibits a first order dependence with respect to the formaldehyde concentration, the maximum product yield (at the same oxygen concentration level) decreases with increasing hydrocarbon concentration. To achieve the same conversion level as for low methanol concentrations (d_t/d_p=5 in Fig. 30b) the volumetric flow of the premixed feed has to be reduced by a factor of 5, which results in a productivity improvement of about 60 % (8:5). Yet, the selectivity is just 95 % compared to above 98 % calculated for the low methanol concentration.

Furthermore, the initial temperature rise increases and the particle effectiveness near the reactor inlet decreases due to the high methanol concentrations, so that an increase of the initial methanol concentrations is not attractive at least for a PBMR. Possibly, it is an promising option to increase the productivity utilizing a fluidized bed membrane reactor (better temperature control and smaller particle size).

7.4.5 Effect of the degree of oxygen distribution on the temperature development

In first instance distributive feeding of oxygen has little effect on the temperature development for ODH of methanol, because the rate of the primary reaction is independent of the oxygen concentration and the contribution of the consecutive reaction is so low. Therefore, even for a relative strong degree of distribution, i.e. $\Phi_{V,O2,distr}/\Phi_{V,O2,0}$ = 5:1 (see Table 8, but d_t/d_p=5), high hot-spot temperatures evolve. With a wall temperature of 245°C and an inlet temperature of the premixed flow of 200°C, model calculations show a maximum average temperature of 275°C and a maximum centerline temperature of 309°C.

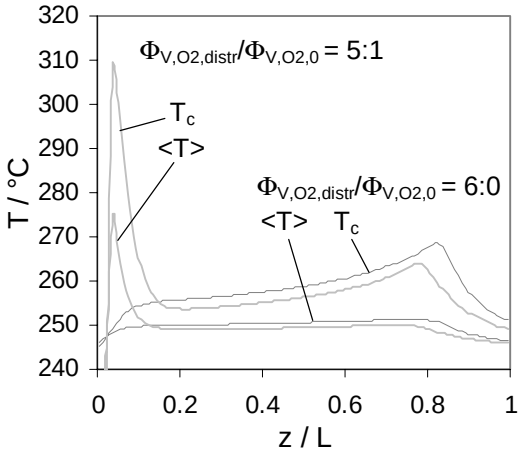

Fig. 34 Axial profiles of average <T> and centerline temperature T_C for $\Phi_{V,O2,distr}/\Phi_{V,O2,0}$ = 5:1 and 6:0 respectively.

Yet, the maximum temperature can be reduced making use of transport limitations, i.e. the inefficient usage of the packed bed, if all oxygen is added distributive and none with the premixed feed. An increase of the distributive flow to $\Phi_{V,distr}$=2.7 m^3/h ensures that the same amount of oxygen is added. With inlet and wall temperature of 245°C a maximum average temperature of 251°C and a maximum centerline temperature of 267°C are calculated.

In Fig. 35 the 2-dimensional oxygen concentration profiles are presented, which have a quite similar shape apart from a short inlet zone.

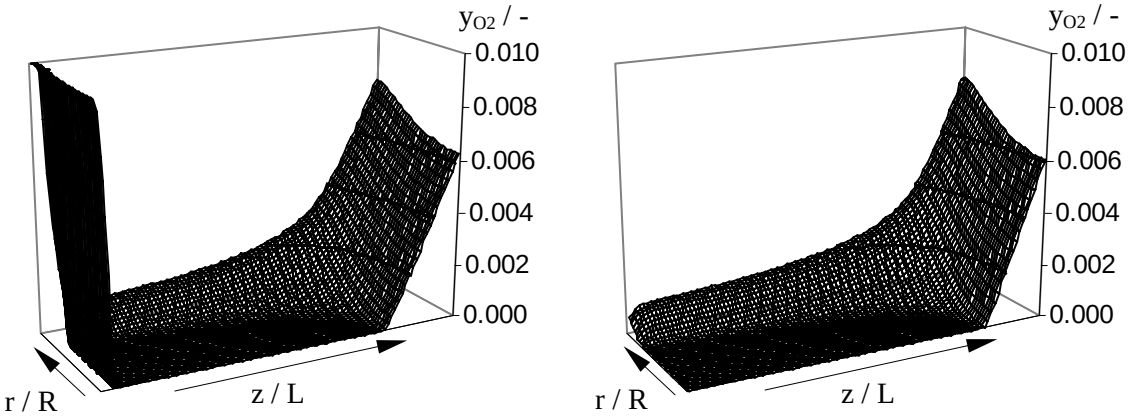

Fig. 35 2-dimensional oxygen concentration profiles for (a) $\Phi_{V,O2,distr}/\Phi_{V,O2,0}$ = 5:1 and (b) 6:0.

7.4.6 Summary and conclusions

It was shown that the ODH of methanol to formaldehyde can be improved in a PBMR resulting in product yields above 92 %. However, due to the low local oxygen concentrations (high modified Thiele-moduli) the effect of mass transfer limitations is considerable. The catalyst particles and the packed bed will locally be used inefficiently with a corresponding reduced productivity of the PBMR.

The model calculations were based on the kinetics of Diakov et al. (2002b), which assumes a zero reaction order in oxygen for the primary reaction. However, the concentrations in the PBMR are locally very low. It is not unlikely that the zero-order in oxygen does not hold at very low oxygen concentrations, but gradually changes to a first order dependence. Yet, very high selectivities can already be realized if the rate of the primary reaction is almost constant down to a oxygen concentration of about y_{O2}=0.01.

NOTATION

Latin letters

D_{eff}	effective mass diffusion coefficient [m^2/s]
D_r^t	radial mass transport coefficient due to turbulent dispersion [m^2/s]
F	factor by which a reaction rate or selectivity is increased due to mass transport limitations
k_s	gas-solid mass transfer coefficient [m / s]
L	length of the packed bed [m]
m_{cat}	catalyst mass [kg]
p	pressure [bar]
r_j	rate of reaction j [mol / g_{cat} s]
R_i	rate of reactive consumption of component i in nr reactions ($=\sum_{j=1}^{nr}\nu_{ij}r_j$) [mol / g_{cat} s]
S	selectivity
T	temperature [K],[°C]
X	conversion
y	molar fraction

Greek letters

ε	porosity
η	effectiveness factor
ρ	density [kg /m^3]

Φ_V volumetric flow [m^3 / s] or [ml / min]

Subscripts

0 at the reactor inlet / base case
cat catalyst
distr distributed
EB ethylbenzene
O_2 oxygen
p particle
t tube

Dimensionless numbers

ϕ' modified Thiele-modulus $\left(= L\sqrt{\left(\frac{n+1}{2}\nu_1 k_1 c_{Ab} c_b^{n-1} + \frac{m+1}{2}\nu_2 k_2 c_{Pb} c_b^{m-1} \right) \Big/ D} \right)$

with $L=R_p/3$ for spherical catalyst particle

ϕ'' modified Thiele-modulus $\left(= L\sqrt{\left(\frac{n+1}{2}\nu_1 k_1^* \langle c \rangle^{n-1} + \frac{m+1}{2}\nu_2 k_2^* \langle c \rangle^{m-1} \right) \Big/ D} \right)$

with $L = R_t/2$ for tubular packed bed

p_{nm} ratio of reaction rates in the secondary and primary reaction

sphere: $= \frac{k_2 c_{Pb}}{k_1 c_{Ab}} c_b^{m-n}$ tube: $= \frac{k_2 \langle c_P \rangle}{k_1 \langle c_A \rangle} \langle c \rangle^{m-n}$

$\langle x \rangle$ represents the spatial average of variable x

References

F. Cavani, F. Trifirò, 1995a, The oxidative dehydrogenation of ethane and propane as an alternative way for the production of light olefins, *Catalysis Today 24*, 307-313

F. Cavani, F. Trifirò, 1995b, Review Alternative processes for the production of styrene, *Applied Catalysis A 133*, 219-239

G. Centi, F. Cavani, F. Trifirò, 2002, Selective Oxidation by heterogeneous catalysis, Kluwer Academic / Plenum Publishers, New York

V. Diakov, D. Larfarga, A. Varma, 2001, Methanol oxidative dehydrogenation in a catalytic packed-bed membrane reactor, *Catalysis Today* 67, 159 - 167

V. Diakov, A. Varma, 2002a, Reactant distribution by inert membrane enhances packed-bed reactor stability, *Chem. Eng. Sci.* 57, 1099 - 1105

V. Diakov, B. Blackwell, A. Varma, 2002b, Methanol oxidative dehydrogenation in a catalytic packed-bed membrane reactor: experiments and model, *Chem. Eng. Sci.* 57, 1563 - 1569

W. Gerhartz, Y.S. Yamamoto, F.T. Chambell, R. Pfefferkorn, J.F. Rounsaville, 1985-1996,'Ullmann's encyclopedia of industrial chemistry', 5th edition, VHC, Weinheim

L. Leveles, 2002, 'Oxidative conversion of lower alkanes to olefins', Doctoral Thesis, Twente University, Enschede, the Netherlands

G.V. Shakhnovich, I.P. Belomestnykh, N.V. Nekrasov, M.M. Kostyukovsky, S.L. Kiperman, 1984, 'Kinetics of ethylbenzene oxidative dehydrogenation to styrene over vanadia/magnesia catalyst', *Applied Catalysis 12*, 23-34

E. Tsotsas and E.U. Schlünder, 1988, Some remarks on channelling and on radial dispersion in packed beds, *Chem. Eng. Sci.* 43, 1200-1203

O. Watzenberger, E. Ströfer, A. Anderlohr, 1999, Unsteady-state oxidative dehydrogenation of ethylbenzene to form styrene, *Chem. Eng. Technol. 21*, 659-662

Appendix A Kinetics of the selective oxidation of propane over Mg-Dy-Li-O catalyst and its side-reactions

The reaction scheme and associated kinetics developed here are based on the interpretation of experiments performed by L.Leveles, which are partially presented in his thesis (Leveles, 2002), and on mutual discussions on the reaction mechanism and kinetics. The kinetic experiments were carried out only at 600°C, so that activation energies could not be determined.

A.1 Primary reactions

The conversion rate of propane on Li/MgO catalysts is influenced by the partial pressures of propane (C_3H_8; C3), oxygen and carbon dioxide. The research of Swaan (1992) on the oxidative dehydrogenation of ethane on promoted lithium doped magnesia oxide catalysts showed a strong reaction inhibition by co-adsorption of carbon dioxide at the active sites of the catalyst. Leveles (2002) performed three series of experiments in order to evaluate the influence of each of these components on the production rates of the main products.

Differential conditions were aimed at for the kinetic measurements. The concentrations were considered to be constant over the length of the reactor. The conversion of propane is below 2 % (except for the two lowest CO_2 concentrations). The conversions of oxygen vary between 4 and 16 %. Yet, the reaction orders of oxygen are small which reduces the inaccuracies induced by the assumption of constant reactant concentrations, so that the average of inlet and outlet concentration could be used. The catalyst activity turned out to be inversely proportional to the CO_2 partial pressure (see Fig.- A-1). It is therefore not possible to perform differential measurements with a carbon dioxide free feed stream, because even very small amounts of CO_2 formed cause a strong decrease in the catalyst activity. For a reaction order of –1 the average reaction rate is the same as the rate of the arithmetic averaged concentration.

The standard composition is 0.28 bar propane, 0.14 bar oxygen, and 0.02 bar carbon dioxide.

The experiments were carried out in quartz tube with an inner diameter of 4 mm. 100 mg of the catalyst (sieve fraction 300÷500 μm) was fixed inside the tube by two plugs of quartz wool. The quartz tube was placed in an oven.

Main primary products of ODHP were propylene (C_3H_6; C3=) and ethylene (C_2H_4; C2=), methane and carbon oxides. C4 components were formed with selectivity between 0.5 and 1.8 %, ethane amounts up to 1.7 %. In the present study these side reactions will be neglected. The reaction rates are expressed in mol/g s, and the partial pressures in bar are used to express their dependence on the reactant concentrations.

Table- A-1 Model reactions.

No.	*Model reaction*
1	$C_3H_8 + 0.5\ O_2 \rightarrow C_3H_6 + H_2O$
2	$C_3H_8 \rightarrow C_2H_4 + CH_4$
3	$C_3H_8 + 1.5\ O_2 \rightarrow C_2H_4 + CO + 2\ H_2O$
4	$1/3\ C_3H_8 + 5/3\ O_2 \rightarrow CO_2 + 4/3\ H_2O$
5	$1/3\ C_3H_6 + O_2 \rightarrow CO + H_2O$
6	$1/3\ C_3H_6 + 1.5\ O_2 \rightarrow CO_2 + H_2O$
7	$2\ C_3H_6 \rightarrow C_2H_4 + C_4H_8$

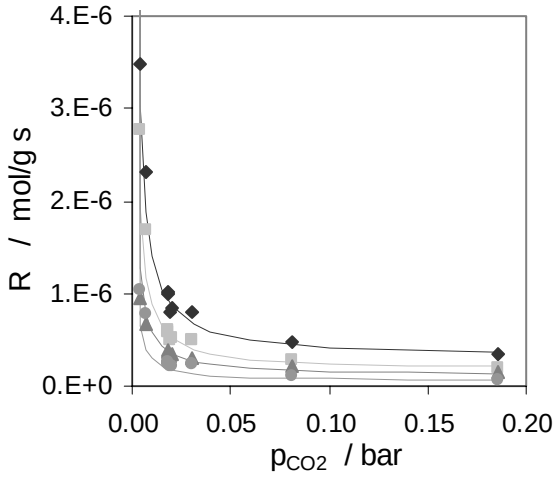

Fig.- A-1 Influence of the partial pressure of carbon dioxide on the formation rates of propene, ethene, methane and carbon (symbols as in Fig.- A-2).

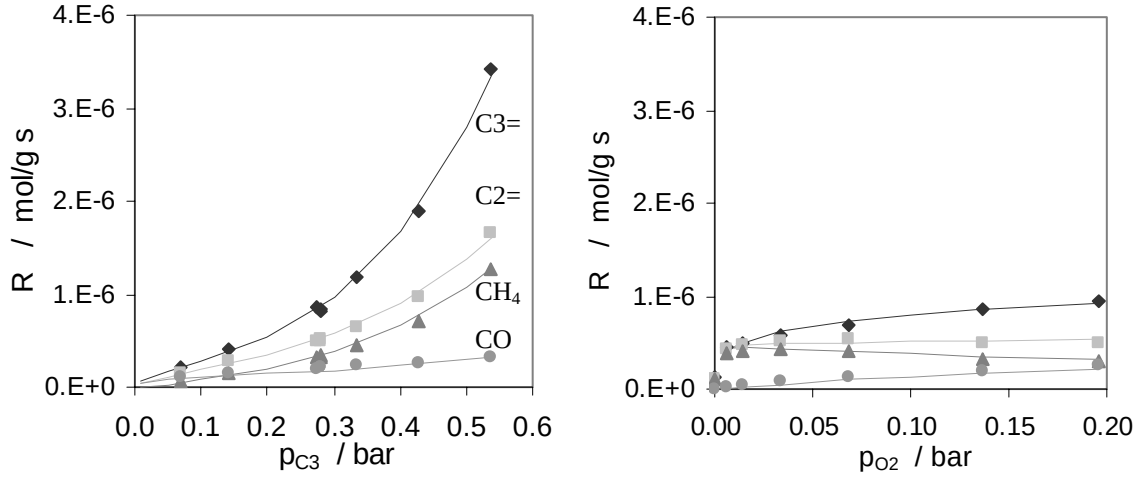

Fig.- A-2 Influence of the partial pressure of (a) propane and (b) oxygen on the formation rates of propene, ethene, methane and carbon monoxide from propane on the Dy-Li/MgO catalyst. Comparison of experimental data by Leveles (points) and model equation (lines).

A.1.a Formation of propene

In the experiments where the partial pressures of propane and oxygen were varied, propene was formed in larger quantities than hydrogen. The ratio of propene and hydrogen formation was less dependent on the oxygen concentration (at 0.006 bar: ratio=2.2; from 0.03 to 0.2 bar: about 3.3) than on the propane concentration (0.07-0.56 bar: ratio increasing from 2.5 to 6.5). In the present kinetic model the formation of hydrogen will be neglected, and thus also the possibility of hydrogenation reactions of the olefins.

According to the reaction mechanism presented by Leveles (2002), propane is activated via formation of a propyl-radical on the active sites on the catalyst surface (dominantly at low concentrations of propane and CO_2) and by homogeneous gas phase reactions. The active

sites of the catalyst are deactivated by CO_2, which results in an –1 reaction order in CO_2. The contribution of the homogeneous activation increases with a high reaction order with the partial pressure of propane and becomes dominant at high propane concentrations.

Propene is formed in the gas phase from the (i-)propyl-radical via cleavage of a second hydrogen radical. This cleavage is promoted by the presence of oxygen. The following rate expression was chosen, and the parameters were fitted minimizing the sum of the squares of the relative deviation.

$$r_1 = R_{C_3=} = \left(k_{11} {p_{C_3}}^{a11} + k_{12} \frac{{p_{C_3}}^{a12}}{p_{CO_2}} \right) {p_{O_2}}^{n1} = \left(2.9 \cdot 10^{-5} {p_{C_3}}^{3.2} + 4.2 \cdot 10^{-8} \frac{{p_{C_3}}^{0.67}}{p_{CO_2}} \right) {p_{O_2}}^{0.24} \quad \text{(A.1)}$$

A.1.b Formation of ethene

Under cleavage of a methyl-radical from the (n-)propyl-radical ethene is formed. The ethene formation rate hardly depends on the oxygen concentration, but decreases when the oxygen partial pressure becomes negligibly small.

$$r_2 + r_3 = R_{C_2=} = \left(k_{21} {p_{C_3}}^{a21} + k_{22} \frac{{p_{C_3}}^{a22}}{p_{CO_2}} \right) {p_{O_2}}^{n2} = \left(6.8 \cdot 10^{-6} {p_{C_3}}^{2.8} + 1.7 \cdot 10^{-8} \frac{{p_{C_3}}^{0.63}}{p_{CO_2}} \right) {p_{O_2}}^{0.05} \quad \text{(A.2)}$$

A.1.c Formation of methane and carbon monoxide

Besides a mole ethene, an equivalent mole of a C1-molecule has to be formed from propane. Methane as well as CO are identified as primary C1-products, which are formed together in about the same amount as ethene. The formation rates of these products can satisfactorily be described by a statistical approach proposing that methane is formed, if the methyl-radical first interacts with a propane molecule, and carbon monoxide, if the first interaction proceeds is with an oxygen molecule.

$$r_2 = R_{CH_4} = R_{C_2=} \frac{p_{C_3}}{p_{C_3} + p_{O_2}} \qquad r_3 = R_{CO} = R_{C_2=} \frac{p_{O_2}}{p_{C_3} + p_{O_2}} \qquad \text{(A.3-4)}$$

By this approach the CO formation is slightly underestimated. C1 (CO and CH_4) is produced in slightly larger quantities compared with ethene, probably caused by an additional formation reaction, e.g. $H_2 + CO_2 = H_2O + CO$, which is neglected in the present study.

A.1.d Formation of carbon dioxide

Carbon dioxide is formed in a comparable amount as carbon monoxide. However, the experimental data show a strong variation indicating a larger experimental error, due to the fact that quite a large amount of CO_2 was added with the feed in these experiments (the CO_2 concentration increases only by about 1 to 10 % due to the reactions). The formation rates of CO_2 were higher in the series of variation in the oxygen concentration compared to the series for propane.

Nevertheless, a primary formation of carbon dioxide is considered with the following approximate rate expression.

$$r_4 = R_{CO_2} = \left(k_{41} + k_{42} \frac{1}{p_{CO_2}} \right) {p_{C_3}}^{a4} {p_{O_2}}^{n2} = \left(1 \cdot 10^{-7} + 4.5 \cdot 10^{-8} \frac{1}{p_{CO_2}} \right) {p_{C_3}}^{0.66} {p_{O_2}}^{0.8} \qquad \text{(A.5)}$$

A.2 Consecutive reactions

The consecutive reactions of propene under ODHP reaction conditions were also investigated by Leveles. The experimental procedure was similar to the one described before for propane. The standard composition is 0.33 bar propane, 0.08 bar oxygen, and 0.01 bar carbon dioxide. Ethene was assumed to be a stable product at the reaction temperature of 600°C.

Main products besides carbon oxides (60-80 %) are methane, ethene and several butanes (including butadiene). Many more products were formed in the experiments, but these will be neglected here, as well as the formation of methane (selectivities around 5 %) as the neglected product with the highest selectivity.

The formation rates of the consecutive products do not increase with increasing partial pressures of propene as was found for the primary reactions as a function of the propane partial pressure – at least not up to a partial pressure of propene of 0.35 bar. Therefore, the same propane reaction order was assumed for both catalytic and gas phase initiated reactions.

A.2.a Formation of carbon oxides

The formation rates of carbon monoxide and carbon dioxide differ in their dependence on the partial pressure of carbon dioxide. While the formation of CO shows a similar form as the primary products, the formation of CO_2 seems to be predominately initiated by the catalyst surface. For high partial pressures of carbon dioxide, the formation rate of carbon dioxide approaches zero (see Fig.- A-3a).

$$r_5 = R_{CO} = \left(k_{51} + \frac{k_{52}}{p_{CO_2}} \right) {p_{C_3=}}^{a5} {p_{O_2}}^{n5} = \left(6.6 \cdot 10^{-6} + 7.6 \cdot 10^{-8} \frac{1}{p_{CO_2}} \right) {p_{C_3=}}^{0.73} {p_{O_2}}^{0.8} \qquad \text{(A.6)}$$

$$r_6 = R_{CO_2} = \frac{k_6}{p_{CO_2}} {p_{C_3=}}^{a6} {p_{O_2}}^{n6} = 1 \cdot 10^{-7} \frac{1}{p_{CO_2}} {p_{C_3=}}^{0.73} {p_{O_2}}^{0.8} \qquad \text{(A.7)}$$

For the formation of carbon monoxide the reaction orders in propene and oxygen were found by minimization of the standard deviation (the minimum standard deviation was doubled, if the reaction order in oxygen was set to 1).

For the formation of carbon dioxide the experimental data (see Fig.- A-4a and Fig.- A-5a) do not allow for a determination of the reaction orders. Therefore, the same reaction orders were chosen as for the formation of carbon monoxide.

A.2.b Recombination to ethene and butene

Leveles identified butanes (trans/cis-2-butene, 1-butene, iso-butene) and butadiene. Together they were formed with (almost) the same rate as ethene. Therefore, a recombination reaction is supposed as model equation (see no.5 in

Table- A-1). The effect of carbon dioxide on this reaction rate indicates that the catalyst is involved in this consecutive reaction as well. However, in this study it will not speculated on the mechanism. A power-law reaction rate expression is proposed for the influence of the partial pressure of propene.

$$r_7 = R_{C4=} = \left(k_{71} + \frac{k_{72}}{p_{CO_2}} \right) p_{C_3=}{}^{a7} p_{O_2}{}^{n7} = \left(5.5 \cdot 10^{-7} + \frac{1.4 \cdot 10^{-8}}{p_{CO_2}} \right) p_{C_3=}{}^{0.85} p_{O_2}{}^{0.77} \qquad \text{(A.8)}$$

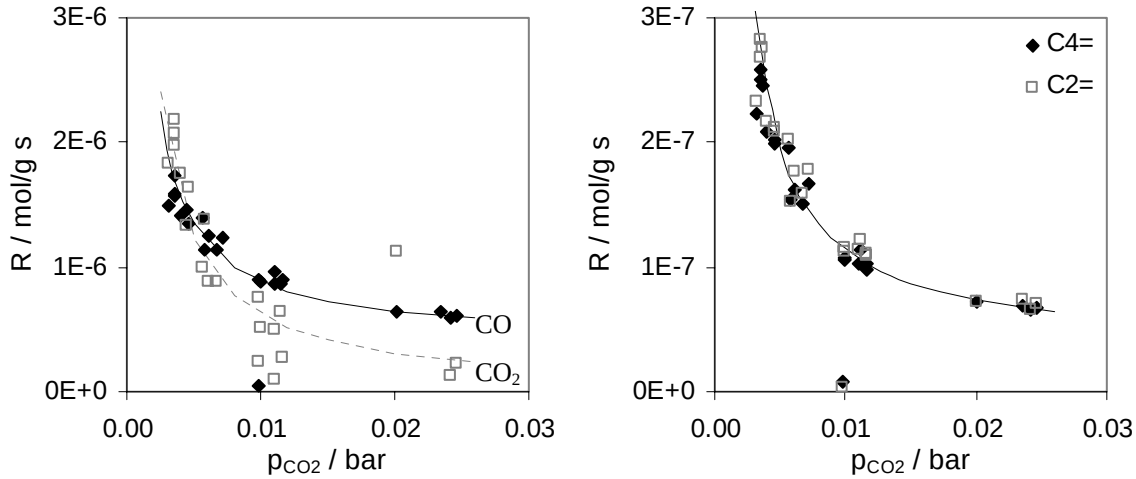

Fig.- A-3 Influence of the partial pressure of carbon dioxide on the formation rates of (a) CO and CO_2 and (b) butene and ethene from propene on the Dy-Li/MgO catalyst. Comparison of experimental data by Leveles (2001) (squares and diamonds) and model equations (lines).

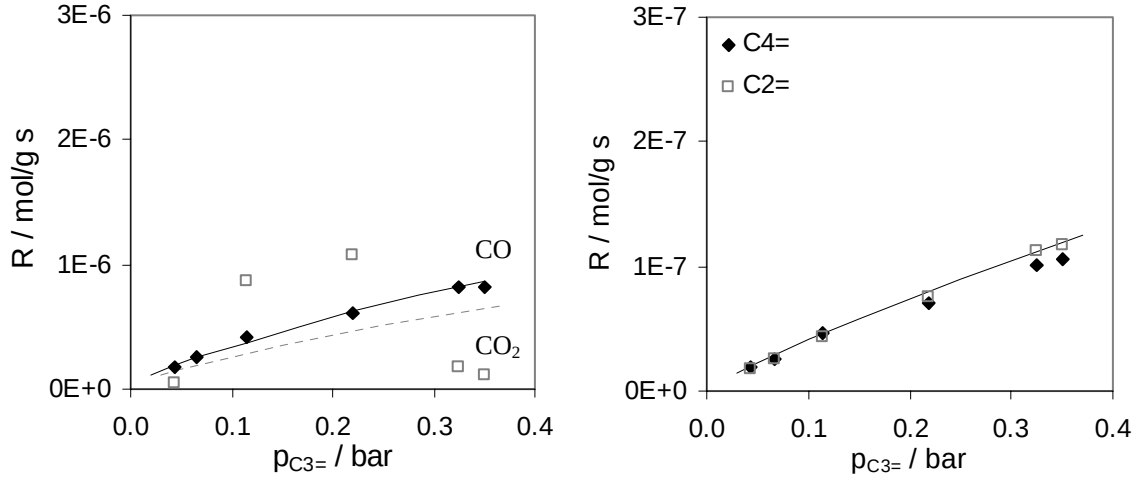

Fig.- A-4 Influence of the partial pressure of propene on the formation rates of (a) CO and CO_2 and (b) butene and ethene from propene on the Dy-Li/MgO catalyst. Comparison of experimental data by Leveles (2001) (squares and diamonds) and model equations (lines).

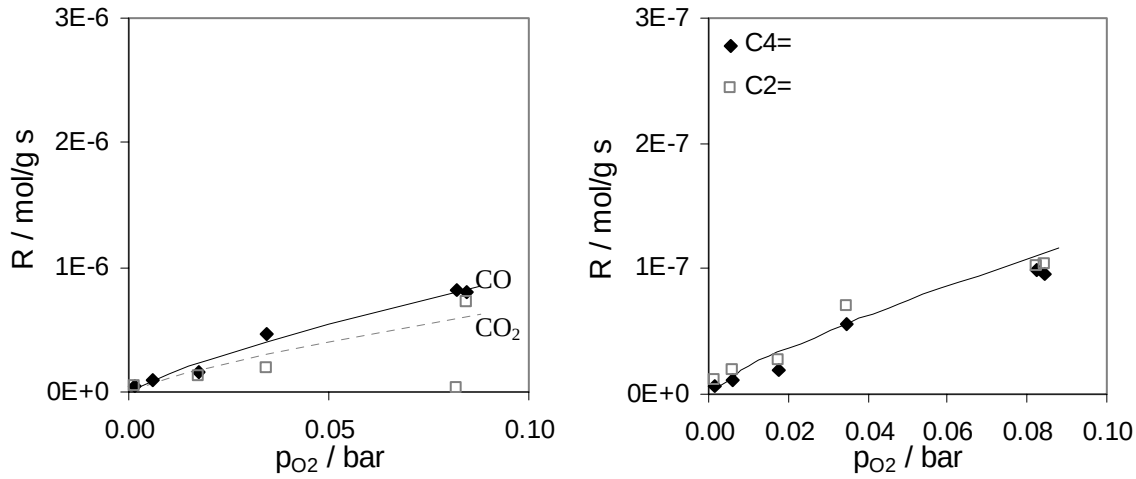

Fig.- A-5 Influence of the partial pressure of oxygen on the formation rates of (a) CO and CO2 and (b) butene and ethene from propene on the Dy-Li/MgO catalyst. Comparison of experimental data by Leveles (2001) (squares and diamonds) and model equations (lines).

Acknowledgement

Dr. L. Leveles for his efforts investigating the reaction kinetics and the mutual exchange regarding the mechanism.

References

L. Leveles, 2001, internal communication

L. Leveles, 2002, Oxidative conversion of lower alkanes to olefins, Doctoral Thesis, Twente University, Enschede, the Netherlands

H.M. Swaan, 1992, The oxidative dehydrogenation of ethane using promoted lithium doped magnesia oxide catalysts, Doctoral Thesis, Twente University, Enschede, the Netherlands

Appendix B Homogeneous oxidation of propane

B.1 Experimental studies from literature

Several authors investigated the non-catalytic ODH of light paraffins. The non-catalytic, gas-phase ODH of propane is very selective with olefin yields as high as 50 % at high conversions. A catalyst can be used effectively for igniting the gas-phase reactions.

Burch and Crabb (1993) compared the ODH of propane on V-Mg-O catalysts with the non-catalytic, homogeneous ODH in an open tube. At the same conversion, the propene selectivity of the non-catalytic ODH is at least as high as that of the catalyzed reaction. This also holds for other catalysts. Only by Dahl et al. (1991) higher selectivities were reported, using salt melts.

Xu and Lunsford (1996) investigated the ODH of propane over a bed of Dy_2O_3/Li^+-MgO-Cl^- catalyst between two beds of quartz chips and a non-catalytic bed solely filled with quartz chips. By use of the catalyst, the reaction rate is slightly increased. However, the selectivity for olefins (propene + ethene) of the non-catalyzed reaction is the same at the same extent of conversion.

Similar results were reported by Beretta et al. (1999) and Lødeng et al. (1999) for a Pt/γ-Al_2O_3 and a Pt/Rh gauze catalyst respectively at short contact times. Homogeneous ODH yields up to about 50 % olefins at high conversion were reported. Beretta et al. used the catalyst for igniting and thermally supporting the gas-phase reaction. Lødeng et al. (1999) report superior selectivities for the homogeneous ODH up to about 70 % conversion. At higher conversions, the catalyzed ODH is slightly more selective. The maximum olefin yield is about 50 % for the homogeneous and 53 % for the catalyzed ODH. (In the homogeneous ODH no carbon dioxide is formed. For the catalyzed reaction, the carbon dioxide content decreases with increasing conversion.)

Choudhary et al. (1998) describe the advantages of the combination of (endothermic) thermal cracking and (exothermic) non-catalytic oxidative conversion, the oxycracking process. By addition of oxygen, propane can be thermally activated at lower temperatures (700°C→635°C). Oxycracking shows higher conversions, is very energy efficient, and coke formation is drastically reduced. The olefin yield reaches about 50 %. The propane-oxygen ratio of $C_3H_8/O_2=2$ is applied, and water is added in a ratio of $H_2O/C_3H_8=0.5$. Furthermore, the gas-phase reactions are supported by sulfur additives, as e.g. thiophene (thiophene/C_3H_8 $=10^{-4}$), resulting in a higher conversion.

In Fig.- B-1 the selectivity–conversion relation is illustrated for the described gas phase reactions with and without catalytic activation / ignition. It can be seen that the non-catalytic ODH is at least as selective as the catalytic up to very high conversions.

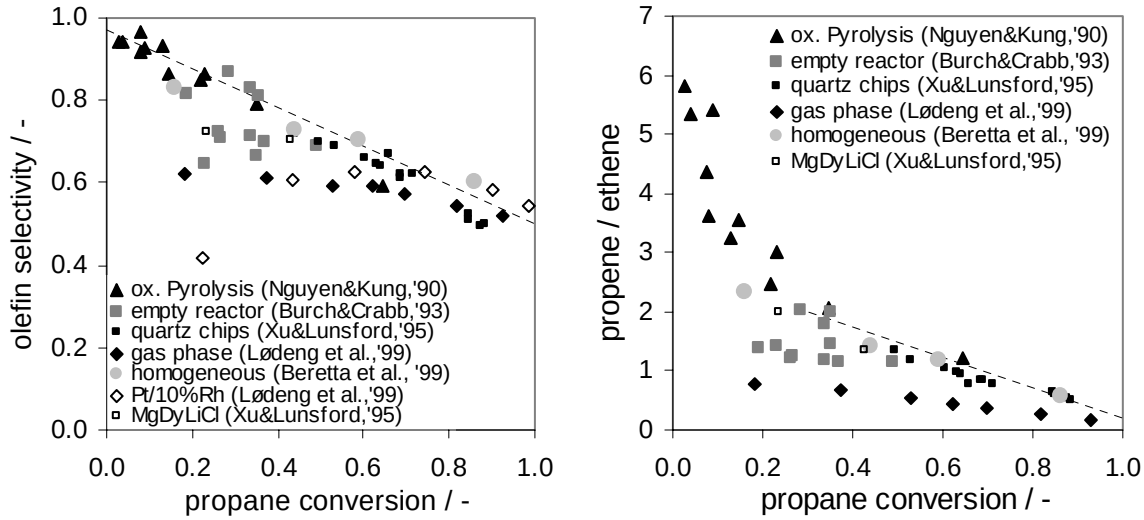

Fig.- B-1 (a) Olefin selectivity and (b) propene/ethene selectivity ratio as function of the propane conversion reported in literature for gas phase processes with and without catalytic initiation.

Sinev et al. (1995) published a review on the interaction of heterogeneous and free-radical reactions in oxidation processes. Among other things they state that in oxidation reactions of C1-C3 hydrocarbons heterogeneous chain initiation was proven in a quartz reactor. They finally concluded:

Analysis of the literature data shows that it is difficult to find examples of purely homogeneous oxidation processes in the gas phase, which are not influenced by heterogeneous factors. On the other hand, the reactions on heterogeneous catalysts are frequently accompanied by the release of free radials into the gas phase and this is not a side process in relation to the main reaction pathway in the adsorbed layer but is an essential stage leading to the formation of the final products in homogeneous or secondary heterogeneous stages.

B.2 Radical gas phase mechanism

To test the possible benefit of distributive oxygen feeding on the olefin selectivity in the gas phase oxidation of propane a relatively simple radical mechanism was taken from literature and implemented in the reactor model. The mechanism of Westbrook and Pitz (1984) consists of 163 elementary reactions between 41 chemical species. A series of model calculations were carried out, where an axially constant oxygen concentration was assumed.

From Fig.- B-2 the relative small influence of the oxygen concentration on the selectivity can be discerned, with selectivity improvements only for propane conversions above 80 %. The calculated selectivities are below that reported in the experimental studies (represented by the dashed line in Fig.- B-2). The model calculations performed with radical gas phase mechanism by Westbrook and Pitz (1984) shows that olefin yields above 50 % cannot be reached with homogeneous ODHP even at constant low oxygen concentrations.

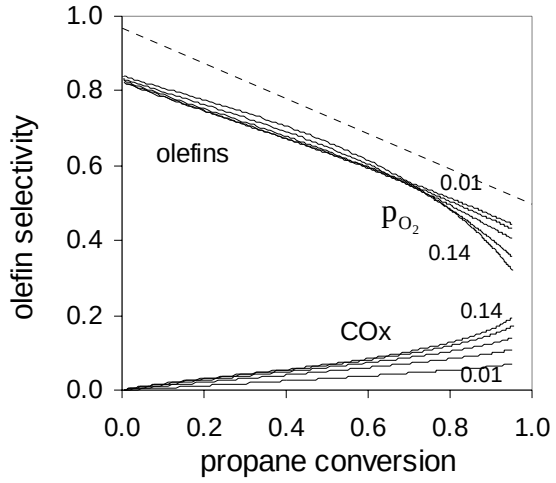

Fig.- B-2 Olefin Selectivity – propane conversion plot calculated with the radical mechanism

References

A. Beretta, P. Forzatti, E. Ranzi, 1999, Production of Olefins *via* Oxidative Dehydrogenation of Light Paraffins, *4th European Congress on Catalysis*, Book of Abstracts, O/01/10, 10

R. Burch, E.M. Crabb, 1993, Homogeneous and heterogeneous contributions to the oxidative dehydrogenation of propane on oxide catalysts, *Appl. Catal. A 100*, 111

V.R. Choudhary, V.H. Rane, A.M. Rajput, 1998, Simultaneous Thermal Cracking and Oxidation of Propane to Propylene and Ethylene, *AIChE J. 44(10)*, 2293

I.M. Dahl, K. Grande, K.-J. Jens, E. Rytter, Å. Slagtern, 1991, Oxidative dehydrogenation of propane in lithium hydroxide/lithium iodide melts, *Appl. Catal. 77*, 163

R. Lødeng, O.A. Lindvåg, S. Kvisle, H. Reiner-Nielsen, A. Holmen, 1999 ,Oxidative dehydrogenation of propane over gauze catalysts, *4th European Congress on Catalysis*, Book of Abstracts, O/01/11, 11

K.T. Nguyen, H.H. Kung, 1990, Generation of Gaseous Radicals by a V-Mg-O Catalyst during Oxidative Dehydrogenation of Propane, *J. Catal. 122*, 415

C.K. Westbrook, W.J.Pitz, 1984, A comprehensive chemical kinetic reaction mechanism for oxidation and pyrolysis of propane and propene, *Combustion Science And Technology 37*, 117-152

M. Xu, J.H. Lunsford, 1996, Oxidative dehydrogenation of propane, *React. Kinet. Catal. Lett. 57 (1)*, 3

Appendix C Comparison of different industrial formaldehyde processes

Different industrial processes have been developed for the oxidative dehydrogenation of methanol to formaldehyde. They mainly differ in the applied catalyst and the composition of the feed gas with methanol in excess for the silver process and oxygen in excess for the redox-catalyst.

Table- C-1 comparison of different industrial formaldehyde processes (taken from Ullmann's, 1996).

	BASF process	*ICI, Borden, Degussa*	*Formox process*
catalyst	silver crystals; Regeneration every 3-4 month	silver crystals or silver gauze	Mo-Fe oxide (small amounts of V and other components)
excess of	methanol	methanol	air
reactor	Fixed bed, length: 25-30 mm; diameter: up to3.2 m; adiabatic	Shallow bed or layer of gauze ; adiabatic	Multiple tubes, length: 1-1.5 m; shell diameter: 2.5 m; isothermal;
TR	680-720°C	590-650°C, suppressed secondary reactions	250-400°C; rate of consecutive reaction increases considerably
X	97-98 %	77-87 % distillative recovery;	98-99 %
product	40-55 wt.% CH_2O, 1.3 wt.% methanol, 0.01 wt.% formic acid	50-55 wt.% CH_2O, < 1.5 wt.% methanol	55 wt.% FA, 0.5-1.5 wt.% methanol
process yield	89.5-90.5 %	91-92 %	88-91 %
economics	higher capacities are in favor of the silver processes		can be built on very small size of few thousand tons.

Raw material costs account for > 80 % of total production costs

Summary

In heterogeneously catalyzed partial oxidation systems where the reaction order in oxygen for the formation of the target product is lower than the reaction order in oxygen for the formation of waste products, low oxygen concentrations can significantly enhance the product selectivity. A decrease in the oxygen concentration is beneficial for the product selectivity for both consecutive and parallel reaction schemes. If the main by-product is formed via a consecutive reaction, the reactor must possess low back-mixing characteristics in order to limit the product losses. A packed bed membrane reactor (PBMR) combines the features of distributive oxygen feeding and low axial back-mixing of a packed bed reactor. For a parallel reaction scheme high conversions can be achieved with low oxygen concentrations without the application of membranes and without loss of selectivity in a well-mixed reactor (e.g. fluidized bed). Therefore, in the evaluation of the benefits and disadvantages of distributive oxygen feeding the following reaction scheme of the partial oxidation of a hydrocarbon is studied in this thesis:

target product formation: $A + \nu_1 O_2 \rightarrow P$ $r_1 = k_1 c_A c^n$

waste product formation: $P + \nu_2 O_2 \rightarrow W$ $r_2 = k_2 c_P c^m$

where A represents the hydrocarbon reactant, P the target product, W the waste product and ν_i the stoichiometric constants and k_i the reaction rate constants. The reaction rates of both reactions have been assumed first order in the hydrocarbons. The reaction orders of oxygen for the target product formation and for the waste product formation are indicated with n and m, respectively.

In the PBMR air or oxygen permeates through the membrane due to pressure or concentration gradients. From the membrane surface the oxygen penetrates into the packed bed perpendicular to the main flow direction of the reaction mixture, and radial concentrations profiles may emerge. These concentrations profiles can effect the performance of the PBMR.

In addition, intraparticle transport limitations can play an important role, since often in these reactors porous catalysts are employed. However, the standard approach of effectiveness factors cannot be applied for this special type of reaction system. Due to the fact that oxygen is consumed in both reactions the particle effectiveness factors of the main and consecutive reactions are correlated (for $m>0$). Thus, even if the consecutive reaction rate is small, the effectiveness of that reaction can be reduced by the consumption of oxygen by the primary reaction. The consecutive reaction could even be stronger effected by oxygen concentration gradients than the primary reaction due to the higher reaction order in oxygen ($m>n$). While in usual consecutive reactions of the type $A \rightarrow B \rightarrow C$ the selectivity of the intermediate product is negatively effected by intraparticle mass transport limitations, the reaction systems discussed in this thesis show a selectivity improvement, if the oxygen concentration is small compared to the concentrations of the hydrocarbons, as is the situation in the PBMR.

The main objective of this thesis is to elucidate the effects of the oxygen distribution in

- the axial distribution over the reactor length,
- the radial distribution from the membrane wall towards the center of the packed bed
- intraparticle concentration gradients.

In this thesis the focus is on the effect of the oxygen distribution on the performance of the PBMR in terms of conversion and selectivities. A detailed description of the oxygen transport through the membrane is not considered in this work. Here, the membrane is considered as an ideal distributor with a fixed membrane flow, independent from the reaction conditions inside the packed bed. This assumption enables an independent discussion of the influence of the oxygen distribution on the performance of the PBMR.

A literature study is presented with two main objectives. Firstly, industrially relevant partial oxidation systems and the oxidative dehydrogenation are screened, if they could benefit from distributive oxygen feeding. Surprisingly few partial oxidation systems show the required characteristics, namely a consecutive reaction exhibiting a higher reaction order in oxygen than the formation of the target product. Especially in the selective oxidation of propane to propene and ethene, the oxidative dehydrogenation (ODH) of the ethylbenzene to styrene and the ODH of methanol to formaldehyde distributive oxygen feeding in a PBMR could enhance the product selectivity. Secondly, a short literature overview on experimental and modeling studies on packed bed membrane reactors is presented focusing on the incentives to study the application of PBMRs and on the type of models used to describe these reactors. In the literature often 1D-pseudo-homogeneous models are used to describe PBMRs. Although for laboratory scale reactors mass transfer limitations inside the catalyst particles and across the radius of the packed bed can indeed often be neglected, for industrial scale PBMRs strong effects of mass transport limitations can be envisaged, which is studied in this thesis.

Firstly, potential yield improvements of PBMRs were illustrated comparing the maximal product yield in a PBMR with a constant oxygen concentration level with the optimal yield of a FBR with premixed oxygen feed. The influence of the difference in the oxygen reaction orders (m-n) and the ratio of the reaction rates of consecutive and primary reaction (k_2/k_1) was elucidated. Secondly, the effect of the axial oxygen concentration profile was investigated for PBMRs operated with different amounts of catalyst mass. Four different axial oxygen distribution patterns were tested. It was found that for small catalyst masses complete premixed feeding can result in the maximum product yield, but with further increase of the catalyst mass, an increasing part of the oxygen should be added distributively to the PBMR to achieve maximum product yield. For medium catalyst masses the combination of premixed and constant distributed oxygen feeding is best, but for high catalyst masses, membranes with an axially decreasing permeation profile produce better results.

Two disadvantages emerge when decreasing the oxygen concentration level in the reactor. Firstly, a decrease in the oxygen concentration causes a decrease in the activity of the packed bed (for n>0), which requires an increased reactor size to obtain the same conversion, i.e. increase of investment costs. Secondly, at lower oxygen concentrations possible problems with the distribution of oxygen from the membrane wall to the centerline of the packed bed as well as from the bulk of the gas phase to the interior of the particle may become important. If the reaction order in oxygen of the main reaction is smaller than 1, mass transfer limitations become more pronounced when the oxygen concentration level decreases. The effect of mass transfer limitations on the intrinsic product selectivity and the intrinsic activity of a catalyst particle and a slab of the PBMR at low oxygen concentrations were investigated.
If the oxygen concentration is small compared to those of the hydrocarbons ($c \leq 0.1 \cdot \max\{\nu_1 c_A, \nu_1 c_P, \nu_2 c_P\}$), intraparticle mass transport limitations result in an increase in the intrinsic product selectivity. This effect has been quantified for different combinations of reaction orders of the target and waste product formation rates as a function of the characteristic numbers ϕ' and p_{nm}, representing the modified Thiele-modulus for oxygen transport and consumption and the ratio of the consecutive and main reaction rates.
In contrast, transport limitations from the membrane to the center of the packed bed decrease the intrinsic product selectivities for most sets of relevant reaction orders, especially at high values of the modified Thiele-modulus ϕ''. The modified Thiele modulus ϕ'' characterizes the radial transport and the consumption of oxygen in a slab of the PBMR, defined analogously to the Thiele modulus ϕ' for oxygen transport and consumption inside a particle. For PBMRs the radial transport is dominated by dispersion, and the contribution of the radial convective flow to the radial distribution of oxygen is negligible. For ϕ''<1 the distribution of oxygen from the membrane to the center of the packed bed is sufficiently fast to avoid a negative effect of radial concentration profiles on the product selectivity and conversion rate.

On the basis of the results on the intrinsic activity and selectivity of a catalyst particle and a slab of the PBMR, the effects on the integral activity and selectivity were studied. The effect of intraparticle mass transfer limitations on the integral reactant conversion and selectivity of the intermediate product in a PBMR were investigated using a one-dimensional, heterogeneous reactor model. Two opposing effects influence the integral selectivity of the target product. The intrinsic selectivity increases with particle size for a given gas phase composition with a low oxygen concentration. However, the resulting increased oxygen concentration level in the PBMR will result in a selectivity loss that will exceed the gain produced by concentration gradients inside the catalyst particles. If the design of the PBMR necessitates the use of large catalyst particles, e.g. because of pressure drop limitations, an adverse integral effect of intraparticle mass transfer limitations on the integral selectivity can

be avoided, provided that the reduced particle effectiveness factor due to the lower activity is compensated for by an increase of the catalyst mass.

Furthermore, a two-dimensional, pseudo-homogeneous model has been developed to describe the radial and axial concentration and temperature profiles in the PBMR, including the two-dimensional flow field induced by the distributive membrane flow and a radial porosity profile. For the model reaction scheme the effects of mass transfer limitations from the membrane wall to the center of the bed on the integral performance of the PBMR were investigated. The calculation results revealed that radial mass transfer limitations deteriorate the integral conversion and selectivity of the PBMR due to its combined effect on both the oxygen and the hydrocarbon concentration profiles. For modified Thiele moduli $\phi'' > 1$ radial concentration profiles influence the integral reactor performance and a two-dimensional modeling is required to quantify the effects of mass transfer limitations, but for $\phi'' < 1$ a one-dimensional model can sufficiently accurate describe the performance of a PBMR. The effects of a radial porosity distribution on the integral reactor performance needs only to be taken into account, if the radial dispersion coefficient is dominated by molecular diffusion, i.e. if the radial dispersion coefficient is not influenced by the porosity profile, and then only in case of large modified Thiele moduli ϕ'' (in the order of 1 or larger). In case the radial dispersion coefficient is independent of the porosity, the effect of the radial porosity profile on the product selectivity is positive due to the fact that the radial oxygen concentration profile is hardly effected, but at the membrane wall where the highest oxygen concentrations prevail less catalyst is present resulting in higher product selectivities. In case the turbulent contribution to the radial dispersion is dominant, as usual for industrial scale PBMRs, the effect of the radial porosity profile is negligible due to the increased radial dispersion coefficient near the wall.

Finally, the different effects of the distribution of oxygen in PBMRs have been studied for three industrially relevant processes, namely the oxidative formation of propene and ethene from propane, the oxidative dehydrogenation (ODH) of ethylbenzene to styrene and the ODH of methanol to formaldehyde. The potentials of distributive feeding of oxygen for the improvement of selectivity or yield of the processes have been discussed, and possible effects of mass transfer limitations have been evaluated. While intraparticle mass transfer limitations are more important, for the design of industrial scale PBMR both intraparticle and membrane-to-center transport effects have to be taken into account. Furthermore, two additional issues of the PBMR, the reducing effect of the distribution of oxygen on the temperature hot-spot in the PBMR and the possibility to operate the PBMR with overall feed compositions within the flammability limits have been demonstrated for the ODH of ethylbenzene and for the ODH of methanol respectively.

Samenvatting

In heterogeen gekatalyseerde partiële oxidatie systemen, waar de reactie-orde in zuurstof voor de vorming van het doelproduct lager is dan die van het bijproduct, kan bij lage zuurstof-concentratie een significant hogere selectiviteit van het doelproduct gerealiseerd worden. Dit geldt voor zowel volgreacties als nevenreacties. Als de bijproducten voornamelijk gevormd worden via volgreacties, moet de reactor weinig axiale menging vertonen om productverliezen te minimaliseren. Een gepakt-bed-membraanreactor (PBMR) combineert de distributieve toevoer van zuurstof met de geringe axiale menging van een gepakt bed reactor. Voor een parallelle nevenreactie kunnen hoge conversies ook zonder de toepassing van membranen bij lage zuurstofconcentratie bereikt worden in een goed gemengde reactor (bijvoorbeeld in een wervelbed-reactor) zonder verlies aan product-selectiviteit. Daarom wordt in dit proefschrift het volgende reactiesysteem bestudeerd voor de evaluatie van de voor- en nadelen van distributieve voeding van zuurstof:

vorming doelproduct: $A + \nu_1 O_2 \rightarrow P$ $\quad r_1 = k_1 c_A c^n$

vorming bijproduct: $P + \nu_2 O_2 \rightarrow W$ $\quad r_2 = k_2 c_P c^m$

waar A voor de koolwaterstof-reactant staat, P voor het doelproduct, W voor het bijproduct, ν_i de stoïchiometrische reactiecoëfficiënt en k_i de reactiesnelheidsconstante. Voor de reactiesnelheid van beide reacties wordt een eerste orde afhankelijkheid in de koolwaterstoffen verondersteld. De reactieordes in zuurstof voor de vorming van het doelproduct en het bijproduct worden respectievelijk weergegeven met n en m.

In een PBMR wordt lucht of zuurstof met behulp van een druk of concentratie-gradiënt door het membraan getransporteerd. Vanuit het membraanoppervlak dringt de zuurstof het gepakte bed binnen loodrecht op de hoofdstromingsrichting van het reactiemengsel, waardoor radiale concentratieprofielen kunnen ontstaan, die de prestaties van de PBMR kunnen beïnvloeden.

Daarnaast kunnen inwendige diffusielimiteringen in het katalysatordeeltje een belangrijke rol spelen, aangezien vaak poreuze katalysatoren worden gebruikt in deze reactoren. Berekening van de mate van inwendige transportlimiteringen met behulp van de standaard benuttingsgraad is echter niet mogelijk voor dit speciale type van reactiesystemen, want zuurstof wordt in zowel de hoofdreactie als de volgreactie omgezet, waardoor de benuttingsgraden van beide reacties gecorreleerd zijn (voor m>0). Zo wordt de benuttingsgraad van de volgreactie verlaagd door de consumptie van zuurstof in de hoofdreactie, zelfs als de reactiesnelheid van de volgreactie laag is. Vanwege de hogere reactieorde in zuurstof (m>n) wordt de volgreactie zelfs sterker beïnvloed door gradiënten in de zuurstofconcentratie dan de primaire reactie. Terwijl in gewone volgreactie-systemen van het type A→B→C de selectiviteit van het tussenproduct negatief door inwendige diffusielimiteringen in het katalysatordeeltje wordt beïnvloed, laten het reactiesysteem dat in dit proefschrift bestudeerd is juist een selectiviteitsverbetering zien, mits de zuurstof-

concentratie klein is in vergelijking met de concentraties van de koolwaterstoffen, zoals gebruikelijk in de PBMR.
De hoofddoelstelling van dit proefschrift is de modelmatige bestudering van de consequenties van distributieve zuurstof-toevoer. De invloed van de volgende concentratie-gradiënten zijn beschouwd op het reactor gedrag van de PBMR:

- de axiale verdeling over de reactor lengte,
- de radiale verdeling van het membraanoppervlak naar het midden van het gepakt bed,
- concentratiegradiënten in een katalysatordeeltje.

De nadruk ligt hierbij op het effect van de zuurstofdistributie op de prestaties van de PBMR in termen van conversie en selectiviteit. Een gedetailleerde beschrijving van het zuurstoftransport door het membraan is hier niet nagestreefd. Het membraan is eenvoudigweg beschouwd als een ideale verdeler, waarbij de membraanflux onafhankelijk is verondersteld van de reactieomstandigheden in het gepakt bed. Deze aanname maakt een onafhankelijke discussie van het effect van de zuurstofverdeling op het gedrag van de PBMR mogelijk.

Een literatuurstudie is gepresenteerd met twee hoofddoelen. Eerst is onderzocht of industrieel relevante reactiesystemen van partiële oxidaties en oxidatieve dehydrogeneringen kunnen profiteren van distributieve zuurstofvoeding. Verassend weinig reactie systemen blijken het noodzakelijke patroon van een volgreactie met een hogere zuurstof reactieorde dan de vormingsreactie van het doelproduct te vertonen. In het geval van de selectieve oxidatie van propaan naar propeen en etheen, de oxidatieve dehydrogenering (ODH) van ethylbenzeen naar styreen en de ODH van methanol naar formaldehyde kan de distributieve voeding van zuurstof in een PBMR de selectiviteit van het doelproduct verhogen. Ten tweede is een kort literatuuroverzicht gegeven over experimentele en modellering studies van gepakt bed membraan reactoren, dat zich met name richt op enerzijds de motieven die ten grondslag lagen aan de bestudering van PBMR's en anderzijds het type model dat gebruikt is om deze reactoren te beschrijven. In de literatuur worden vaak een-dimensionale, pseudo-homogene reactormodellen gebruikt. Hoewel inderdaad voor reactoren op laboratoriumschaal massatransportlimiteringen in het katalysatordeeltje en over de radius van het gepakte bed vaak verwaarloosd kunnen worden, kunnen voor PBMR's van industriële schaal sterke effecten van massatransportlimiteringen worden voorzien, die in dit proefschrift zijn bestudeerd.

Als eerste zijn mogelijke opbrengstverbeteringen in kaart gebracht door de maximale opbrengst aan doelproduct in een PBMR met een constante zuurstofconcentratie te vergelijken met de maximale opbrengst van een gepakt bed reactor met voorgemengde zuurstofvoeding. De invloed van het verschil in de zuurstof-reactieorde (m-n) en de verhouding van de reactiesnelheden van de volgreactie en de hoofdreactie (k_2/k_1) is

toegelicht. Ten tweede is het effect van het axiale concentratieprofiel van zuurstof onderzocht voor PBMR's met verschillende hoeveelheden aan katalysatormassa. Vier verschillende axiale zuurstofdistributie-verdelingen zijn getest. Er is geconstateerd dat voor kleine katalysatormassa's de volledig voorgemengde voeding de hoogste opbrengst kan opleveren, maar dat met een verdere toename van de katalysatormassa een stijgend aandeel van het zuurstofdebiet distributief aan de PBMR toegevoegd moet worden om de maximale opbrengst te kunnen realiseren. Met een gemiddelde katalysatorhoeveelheid is de combinatie van deels voorgemengd en deels constant verdeelde zuurstofvoeding optimaal, maar met grotere katalysatorhoeveelheden leveren membranen met een axiaal afnemend permeatie-profiel betere resultaten.

Twee nadelen zijn verbonden aan een verlaging van het zuurstofniveau in de PBMR. Het eerste nadeel is de verlaagde activiteit van het gepakte bed (als n>0), waardoor een groter reactorvolume vereist is om dezelfde conversie te kunnen bereiken, resulterend in hogere investeringskosten. Ten tweede kunnen bij verlaagde zuurstofconcentraties problemen met de verdeling van zuurstof van het membraanoppervlak naar het midden van het gepakte bed en ook van de bulk van de gasfase naar het midden van een katalysatordeeltje belangrijk worden. Als de reactieorde in zuurstof in de hoofdreactie kleiner is dan 1, worden massatransportlimiteringen versterkt door het verlagen van het zuurstofniveau. De invloed van massatransportlimiteringen op de intrinsieke activiteit van een katalysatordeeltje en van een differentieel gedeelte van de PBMR zijn onderzocht bij lage zuurstofconcentraties.
Als de zuurstofconcentratie klein is in vergelijking met die van de koolwaterstoffen ($c \le 0.1 \cdot \max\{\nu_1 c_A, \nu_1 c_P, \nu_2 c_P\}$), resulteren massatransportlimiteringen in een verbetering van de intrinsieke selectiviteit van het doelproduct. Deze invloed is gekwantificeerd voor verschillende combinaties van reactieordes van de gewenste en ongewenste reacties met behulp van de karakteristieke kengetallen ϕ' and p_{nm}, die respectievelijk staan voor de gemodificeerde Thiele-modulus voor zuurstoftransport en -consumptie in een katalysatordeeltje en voor de verhouding van de reactiesnelheden van de volgreactie en de hoofdreactie.
In tegenstelling tot inwendige diffusielimiteringen verlagen massatransportlimiteringen van het membraanoppervlak naar het midden van het gepakte bed de intrinsieke selectiviteit van het doelproduct voor de meeste relevante combinaties van reactieordes, vooral bij hoge waardes van de gemodificeerde Thiele-modulus ϕ''. De gemodificeerde Thiele-modulus ϕ'' beschrijft het radiale transport en consumptie van zuurstof in een differentieel gedeelte van de PBMR, en is analoog gedefinieerd met de gemodificeerde Thiele-modulus ϕ' voor zuurstof transport en consumptie in een katalysatordeeltje.
Het radiale transport in een PBMR wordt gedomineerd door dispersie en de bijdrage van de radiale convectie aan de radiale distributie van zuurstof is verwaarloosbaar klein. Voor ϕ''<1

is de distributiesnelheid van zuurstof van het membraan naar het midden van het gepakte bed toereikend om een negatief effect van radiale concentratieprofielen op de product-selectiviteit en de conversiesnelheid te vermijden.

Voortbouwend op de resultaten voor de intrinsieke activiteit en selectiviteit, zijn de effecten van distributieve zuurstoftoevoer op de integrale activiteit en selectiviteit bestudeerd. De invloed van inwendige massatransportlimiteringen in het katalysatordeeltje op de integrale conversie en selectiviteit van het tussenproduct is onderzocht met een een-dimensionaal, heterogeen reactor model. Twee tegengestelde effecten beïnvloeden de integrale selectiviteit van het tussenproduct. De intrinsieke selectiviteit stijgt met de deeltjesgrootte voor een gegeven gasfase samenstelling met lage zuurstofconcentratie. De veroorzaakte hogere zuurstofconcentratie resulteert vervolgens echter weer in een verlies aan selectiviteit, die de selectiviteitswinst door concentratiegradiënten in het katalysatordeeltje overschrijden. Echter, indien volgens het PBMR ontwerp het gebruik van grote katalysatordeeltjes nodig is, bijvoorbeeld om de drukval over het bed te beperken, kan het negatieve integrale effect van massatransportlimiteringen op de selectiviteit worden vermeden, mits de gereduceerde activiteit van de katalysator met een verhoogde katalysatormassa wordt gecompenseerd.

Vervolgens is een twee-dimensionaal, peudo-homogeen reactormodel ontwikkeld om de radiale en axiale concentratie en temperatuur profielen in de PBMR te beschrijven, inclusief het twee-dimensionale stromingsveld veroorzaakt door de distributieve membraanflux en het radiale porositeitsprofiel in het gepakte bed. Voor het gekozen model-reactiesysteem zijn de effecten van massatransportlimiteringen van het membraan naar het midden van het gepakte bed op de integrale prestaties van de PBMR in kaart gebracht. De modeleringsresultaten hebben verduidelijkt dat radiale massatransportlimiteringen de integrale conversie en selectiviteit van een PBMR verslechteren als gevolg van een gecombineerde invloed op de zuurstof en koolwaterstof-concentraties. Voor gemodificeerde Thiele-moduli $\phi'' > 1$ vereisen de ontstane radiale concentratieprofielen het gebruik van een twee-dimensionaal model om de integrale effecten op de PBMR resultaten te kunnen kwantificeren, maar voor $\phi'' < 1$ is een een-dimensionaal model toereikend. Met de invloed van een radiaal porositeitsprofiel op het integrale reactorgedrag hoeft alleen rekening gehouden te worden, als de radiale dispersiecoëfficiënt door moleculair diffusie wordt gedomineerd, d.w.z. als de radiale dispersiecoëfficiënt niet door het radiale porositeitsprofiel wordt beïnvloed, en dan alleen in het geval van hoge gemodificeerde Thiele-moduli ϕ'' ($\geq$ 1). Als de radiale dispersiecoëfficiënt onafhankelijk is van de locale porositeit, heeft het radiale porositeitsprofiel een positief effect op de product-selectiviteit, doordat het radiale zuurstofconcentratieprofiel nauwelijks wordt beïnvloed, maar dicht bij het membraanoppervlak, waar de zuurstofconcentratie het hoogst is, minder katalysator aanwezig

is. Als de turbulente bijdrage aan de radiale dispersie overheersend is, zoals te verwachten is voor een PBMR van industriële schaal, is het effect van het radiale porositeitsprofiel te verwaarlozen vanwege de verhoogde radiale dispersiecoëfficiënt nabij het membraan.

Tenslotte zijn de verschillende effecten van de zuurstofverdeling in PBMR's bestudeerd voor drie industrieel relevante processen: de oxidatieve vorming van propeen en etheen uit propaan, de oxidatieve dehydrogenering (ODH) van ethylbenzeen naar styreen en de ODH van methanol naar formaldehyde. Het potentieel van distributieve voeding van zuurstof voor het verbeteren van de selectiviteit of de opbrengst van deze processen is bediscussieerd, en de mogelijke effecten van massatransportlimiteringen zijn in kaart gebracht. Terwijl inwendige massatransportlimiteringen in het katalysatordeeltje belangrijker zijn, moet bij het ontwerp van een PBMR van industriële schaal ook met transportlimiteringen van het membraan-naar-midden van het gepakte bed rekening gehouden worden. Daarnaast zijn twee additionele voordelen van de PBMR gedemonstreerd, namelijk het reducerende effect van de zuurstofdistributie op de hot-spot temperatuur bij de ODH van ethylbenzeen en de mogelijkheid de reactor met een overall voedingssamenstelling binnen de explosiegrenzen te bedrijven voor de ODH van methanol.

Dankwoord

Allereerst wil ik mijn promotoren prof. Hans Kuipers en prof. Geert Versteeg bedanken voor de mogelijkheid die zij mij hebben geboden te promoveren en het in mij gestelde vertrouwen. Geert was het die mij aanbood, om een post-doc positie te beginnen met de optie naar twee jaren te besluiten of ik er een proefschrift van wilde maken. Kort na dit besluit verloren we het geloof in een experimentele realisatie van het concept van een gepakt bed membraan reactor, en we besloten ons op de numerieke studie van de PBMR te concentreren, met name de distributie van zuurstof. Bij het ontwikkelen van zowel de reactor modellen als ook de nieuwe richting van mijn onderzoek was de expertise van Hans onmisbaar. Maar ook de ondersteuning door dr. Martin van Sint Annaland, die als begeleider bij het project bijkam, stel ik zeer op prijs. De talloze discussies met Martin hebben de vorm en de inhoud van dit proefschrift maatgevend beïnvloed. Hartelijk dank voor het grondig lezen van mij conceptversies en het gedetailleerd commentaar. Bedankt voor de motivatie die ik door jullie heb ervaren.

De Nederlandse Organisatie voor Wetenschapelijk Onderzoek (NWO) ben ik erkentelijk voor de beschikbaar gestelde financiële middelen voor dit onderzoek. En natuurlijk ook de CPM groep van prof. Lercher en later prof. Lefferts, die het project initieerde. De samenwerking en de discussies met dr.K. Seshan en dr.L. Leveles heb ik heel aangenaam in herinnering. Dank aan László bovenal voor die extra inspanning om de kinetiek van de volgreacties te bepalen, en voor zijn les in zake positivisme.

Heel veel dank gaat uit naar Benno Knaken voor de uitstekende reactor die hij voor mij heeft gebouwd (sorry, dat ik er zo weinig gebruik van heb kunnen maken), en natuurlijk ook aan de andere technici van OOIP en FAP, Henk-jan Moed, Wim Leppink en Gerrit Schorfhaar, die altijd een helpende hand boden. Robert Meijer dank ik dat problemen met de computer nooit lang voortduurden en voor de CD-brander, die me in Duitsland voor data-verlies behoedde. Dank aan Gerrit Mollenhorst voor zijn inbreng bij het ontwerp van de PBMR en voor het verglazen van de membranen. Ook aan Bert Kamp, Harry Olde Veldhuis, Benny Hövels en al die anderen die het experimentele werk mogelijk gemaakt hebben.

Dank aan Nicole Haitjema, Ria Hofs-Winkelman en de andere secretaresses van beide werkgroepen. Nicole’s vriendelijke geest was vele jaren een belangrijke morele ondersteuning en in de laatste tijd in Duitsland was zij een grote hulp bij de informatietransfer met Enschede en bij de promotieformaliteiten.

Een speciale dank gaat uit naar mijn enige afstudeerder Esther van den Hengel, omdat zij het met mij aandurfde. Al mijn collega's –present and past – van FAP en OOIP wil ik bedanken voor de gezelligheid rond de koffiebar en de prettige werksfeer. Het was leuk met jullie te voetballen. Toine Cents en Mark Meerdink, een collega uit mijn TwAIO tijd, ben ik dankbaar dat zij mij als paranimfen gaan seconderen.
Liesbeth Kuipers wil ik hartelijk danken voor haar werk om de FAP-groep samen te laten groeien, voor de leuke skivakanties en de pan-feesten, maar een karaokeliefhebber heb je van mij niet kunnen maken.

Een van de grootste plus van een studie aan de Universiteit Twente is de internationale sfeer. TwAIOs en AIOs uit verschillende landen te leren kennen is een privilege waarvan ik in de laatste jaren heb genoten. Vooral de Indische (Pranay, Kapil, Senthil, Vishwas, Salim, ...) en Bulgaarse (Nikolay, Lora, Stanislav en Vania, ...) 'familie' zal voor altijd in mijn herinnering blijven. Bedankt voor de feesten die ik met jullie heb mogen vieren. Ook vrienden en collega's die voor mij hebben gekookt en die met mij een avondje 'Siedler' gespeeld hebben of een glas nieuwe wijn hebben gedeeld wil ik hierbij bedanken.

Tenslotte, wil ik mijn ouders bedanken, die mij nu al zo vele jaren steunen, en Ivayla voor haar onvoorwaardelijke liefde.

Tot kijk, misschien im schönen Heidelberg.

Ulrich